

**Republic of Iraq  
Ministry of Higher Education & Scientific Research  
University of Kerbala  
College of Engineering  
Department of Civil Engineering**



# **APPLICATION OF DYNAMIC MEASUREMENTS FOR QUALITY ASSESSMENT OF SUBGRADE STRENGTH AND COMPACTION**

---

A Thesis Submitted to the Department of Civil Engineering, University of Kerbala in Partial Fulfillment of the Requirements for the Degree of Master of Science in Civil Engineering/ Civil Engineering

By  
**Nada Amer Yousif**  
BSc. in Civil Eng. / University of Kerbala (2018)

Supervised by  
Assist. Prof. Dr. Alaa M. Shaban  
Dr. Raid R. Almuhanha

June 2021

Zul-Qadah 1442

بِسْمِ اللَّهِ الرَّحْمَنِ الرَّحِيمِ

يَرْفَعِ اللَّهُ الَّذِينَ آمَنُوا مِنْكُمْ وَالَّذِينَ أُوتُوا

الْعِلْمَ صَرَجَاتٍ

صَطَقَ اللَّهُ الْخَالِيَّ الْعَظِيمِ

سورة المجادلة - الآية ١١

## ABSTRACT

---

Subgrades provide structural stability to pavements by transmitting superimposed traffic loads safely to underneath soil strata. The density and strength of subgrade soil layers are main parameters for the most pavement layers that used in quality assessments. For evaluating density and strength properties of subgrade soils, several conventional testing methods were developed. Among these tests methods are sand cone test density test and CBR test methods which are carried out to determine density and strength of subgrade layer. However, there are several limitations associated with using these old testing techniques including: complicated testing procedure, laborious, time consuming, does not reflect or represent actual soil properties.

Therefore, there is a necessarily demand to use more effective tools that can be considered as in place quality control test for pavement materials strength. The main aim of this work is to develop an alternative testing protocol which involves the use of the dynamic measurements to evaluate in-situ compaction level and strength of subgrade soils through computing the dry density and California bearing resistance.

In this work, two testing methods were used for three different roadway subgrade soils to evaluate dynamic properties of subgrade soils. These testing methods are [1]: light weight deflectometer (LWD) and dynamic cone penetrometer (DCP). Three highway projects in Karbala were selected to test their subgrade soils. These projects are located at Al-Intifada, Al-Fares, and Al-Tahady district in all of which the subgrade was classified a poorly graded sand soil (i.e., type A-3). Three dynamic measurements were obtained from LWD test: surface deflection, degree of compatibility, and dynamic modulus with typical range values (0.701-0.383) mm, (4.25-2.936) ms, and (38.18-60.04) MPa, respectively. Two parameters were obtained from DCP test including: dynamic cone penetration index (DCPI) with typical range values (25.833-15.89) mm/blow, in-situ CBR with typical range values (8.77-19.206) %. In addition, dry density and moisture content were also measured using sand cone method (SRM).

Statistical analysis was carried out to predict strength and degree of compaction of subgrades. The strength was defined in terms of California bearing ratio (CBR), and degree of compaction were evaluated in terms of dry density. For determining dry density, three groups of regression models were developed based on independent variables: LWD measurements data, DCP measurements data, both LWD and DCP measurements data. Similarly, three groups of regression models were developed to predict CBR based on measurements of LWD, basic soil

## ABSTRACT

---

parameters, both LWD and basic soil characterise.

The results of statistical analyses showed that there is a good correlation between dry density and LWD and DCP measurements. Several theoretical models (i.e., single and multiple regressions) were developed. A single exponential model in which LWD degree of compatibility (Dc) was utilized as an independent parameter provides the best dry density estimation with  $R^2$  equal to 0.80. While, the dynamic cone penetration index (DCPI) model gives a best dry density prediction with  $R^2$  equal to 0.87.

For evaluating strength of subgrades, three groups of regression models were established based on independent variables: LWD measurements data, basic soil properties, both LWD and basic soil properties. The results exhibited that LWD dynamic modulus is a best independent parameter to estimate CBR using a single nonlinear exponential model with  $R^2$  values equal to 0.84. The results also showed acceptable relation between strength and basic soil properties, whereas a nonlinear regression model with value of  $R^2=0.90$  were proposed to predict strength as a (dry density, water content). Additionally, a multiple nonlinear regression model in which LWD dynamic modulus and dry density were used as independent parameters was established to provide a good CBR estimation with  $R^2$  equal to 0.86.

Finally, the results of this study showed the efficiency and possibility of using the dynamic measurements obtained from LWD device, and DCP device to rapidly and easily predict the density and strength of subgrade soils.

## SUPERVISOR CERTIFICATE

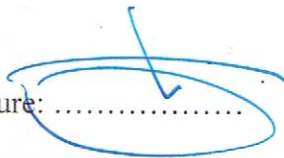
---

I certify that this thesis entitled "Application of Dynamic Measurements for Quality Assessment of Subgrade Strength and Compaction", which is prepared by Engineer "Nada Amer Yousif", is under our scientific supervision at the University of Kerbala in partial fulfilment of the requirements for the degree of Master of Science in Civil Engineering (Civil Engineering).

Signature: ..... 

Name: Assist. Prof. Dr. Alaa M. Shaban  
(Supervisor)

Date: .... / .... / 2021

Signature: ..... 

Name: Dr. Raid R. Almuhanha  
(Supervisor)

Date: .... / .... / 2021

## LINGUISTIC CERTIFICATE

---

I certify that this thesis entitled “**Application of Dynamic Measurements for Quality Assessment of Subgrade Strength and Compaction**” which is prepared by Engineer "Nada Amer Yousif" was under my linguistic supervision, and it was amended to meet the English requirements.

Signature:  .....

(Linguistic Supervisor)

Name: Assist. Lec. Noor Hussam Jabir

Date: 4 / 11 / 2021

## Examination Committee Certification

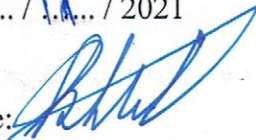
We certify that this thesis entitled "Application of Dynamic Measurements for Quality Assessment of Subgrade Strength and Compaction" and as an examining committee, we examined engineer "Nada Amer Yousif" in its content and in what is connected with it, and that in our opinion it is adequate as a thesis for degree of Master of Science in Civil Engineering (Civil Engineering).

Signature: 

Name: Assist. Prof. Dr. Alaa M. Shaban

(Member)

Date: ..2.. / ..1.. / 2021

Signature: 

Name: Assist. Prof. Dr. Khawla Hammoudi Hassan

(Member)

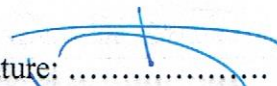
Date ..2.. / ..1.. / 2021

Signature: 

Name: Assist. Prof. Dr. Shakir Al-Busaltan

(Chairman)

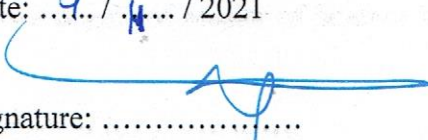
Date: ...2 / ..1.. / 2021

Signature: 

Name: Dr. Raid R. Almuhanha

(Member)

Date: ...4.. / ..4.. / 2021

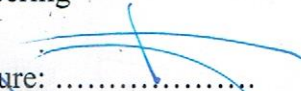
Signature: 

Name: Assist. Prof. Dr. Wajde Shober Saheb

(Member)

Date ..2.. / ..1.. / 2021

Approval of the Department of Civil Engineering

Signature: 

Name: Dr. Raid R. Almuhanha  
(Head of Civil Engineering Dep.)

Date: 4 / ... / 2021

Approval Deanery of the College of Engineering- University of Kerbala

Signature: 

Name: Assist. Prof. Dr. Laith Sh. Rasheed  
(Dean of College of Engineering)

Date: ..... / ..... / 2021

## DEDICATION

---

This thesis is dedicated to my parents and my family, my husband, my  
unique girl, for every one helps me



## **ACKNOWLEDGEMENTS**

---

I would like to take this opportunity to first and foremost thank Almighty Allah for being my strength and guide to complete this work. Without him, I would not have the wisdom or the physical ability to do so.

I express my gratitude to my thesis advisor Assist. Prof. Dr. Alaa M Shaban and Dr. Raid R. Al muhanna for their valuable assistance, suggestions, advise, continuous guidance and encouragement throughout the research. Also, I would like to thank all the team of highway laboratory/Karbala University/College of Engineering. Department of project management and direct implementation of Karbala city for raw materials supplementation.

I thank my parents for always being supportive of my education. I also take this opportunity to acknowledge everyone in my large extended family.

# CONTENTS

---

ABSTRACT.....	I
SUPERVISOR CERTIFICATE.....	III
LINGUISTIC CERTIFICATE.....	IV
EXAMINATION COMMITTEE CERTIFICATION.....	V
ACKNOWLEDGMENTS.....	VII
CONTENTS.....	VIII
LIST OF FIGURES.....	XI
LIST OF TABLES.....	XIV
ABBREVIATIONS.....	XVI
<b>CHAPTER One.....</b>	<b>1</b>
INTRODUCTION.....	1
1.1 General .....	1
1.2 Problem Statement .....	2
1.3 Research aim and objectives .....	3
1.4 Scope of the Research Work .....	3
1.5 Thesis Layout .....	4
<b>CHAPTER Two.....</b>	<b>5</b>
LITERATURE REVIEW.....	5
2.1 Introduction .....	5
2.2 Strength Characteristics of Subgrade Soils.....	6
2.2.1 California Bearing Ratio (CBR) .....	6
2.2.2 Resilient Modulus (Mr).....	9
2.3 Compaction Characteristics of Subgrade Soils .....	11
2.3.1 Purpose of Compaction.....	11
2.3.2 Compaction Theory.....	14
2.3.3 Factors Affecting Compaction .....	16
2.4 Light Weight Deflectometer (LWD).....	16
2.4.1 Historical Development of LWD.....	17
2.4.2 Theoretical Basis of LWD .....	18
2.4.3 Factors Affecting LWD Measurements .....	21

# CONTENTS

---

2.4.4	Correlation between LWD and soils properties.....	23
2.5	Dynamic Cone Penetrometer (DCP).....	25
2.5.1	Historical Development of DCP.....	25
2.5.2	Theoretical Basis of DCP.....	26
2.5.3	Types and Uses of DCP.....	27
2.5.4	Factors Affecting DCP Measurements.....	28
2.5.5	Correlation Between DCP and Soil Properties.....	30
2.6	Summary.....	31
<b>CHAPTER Three.....</b>		<b>32</b>
LABORATORY TESTING PROGRAM.....		33
3.1	Introduction.....	32
3.2	Test Materials.....	32
3.2.1	Soil Types and Locations.....	32
3.2.2	Physical and Chemical Properties of Subgrade soils.....	33
3.3	Experimental Work.....	38
3.3.1	Laboratory Testing Setup.....	38
3.3.2	Soil Preparations and System Layout.....	39
3.4	Experimental Research Methodology.....	42
3.5	Test Methods.....	45
3.5.1	Light Weight Deflectometer (LWD).....	45
3.5.2	Dynamic Cone Penetrometer (DCP).....	47
3.5.3	Sand Replacement Method (SRM).....	50
<b>CHAPTER Four.....</b>		<b>52</b>
LABORATORY TESTING RESULTS.....		53
4.1	Introduction.....	52
4.2	SRM Data results.....	53
4.3	DCP Data results.....	56
4.4	LWD data results.....	65

# CONTENTS

---

<b>CHAPTER Five</b> .....	<b>70</b>
STATISTICAL ANALYSIS.....	71
5.1 Introduction .....	70
5.2 Exploratory Data Analysis .....	72
5.2.1 Outliers Test.....	71
5.2.2 Normality Test .....	73
5.2.3 Correlations Between Variables .....	76
5.2.4 Regression Analysis.....	78
5.3 Developing Statistical Models .....	79
5.3.1 Developing dry density Model.....	79
5.3.1.1 Developing dry density-LWD Model.....	79
5.3.1.2 Developing dry density-DCP Model .....	82
5.3.1.3 Developing dry density with (LWD-DCP) Model .....	85
5.3.2 Developing CBR Model.....	86
5.3.2.1 Developing CBR-LWD Model.....	86
5.3.2.2 Developing CBR-Basic soil properties Model .....	89
5.3.2.3 Developing CBR with (LWD and Basic soil properties) Model.....	92
<b>CHAPTER Six</b> .....	<b>94</b>
CONCLUSIONS AND RECOMMENDATIONS.....	95
6.1 Summary and Conclusions.....	94
6.2 Recommendations and Further works.....	95
 <b>Appendix A: LWD Testing Curves</b>	
<b>Appendix B: DCP Testing Curves</b>	

## LIST OF FIGURES

---

Figure 2-1: Deformation soil behavior under a sequence of repeated load (Sheng, 2016) .....	9
Figure 2-2: Schematic representation of compaction and the corresponding zero air voids curves for a typical soil. ....	15
Figure 2-3: Schematic representation of four possible types of compaction curves. (Akr &e and Suedkmp, 1972).....	15
Figure 2-5: Typical time history data from LWD Test.....	20
Figure 2-6: (a) Stock Prima 100 LWD, .....	22
Figure 2-7: Dynamic Cone Penetrometer Index .....	28
Figure 2-8: Trend among the trends obtained from Laboratory summary (Harison, 1987) .....	29
Figure 3-1: Aerial Photo of Three Field Sites in Karbala.....	32
Figure 3-2: Grain Size Distribution of (a) Al-Faris, (b)Al-Tahadi , (c) Al-Intifadah sites.....	34
Figure 3-3: Proctor Test Curves of (a) Al-Faris, (b) Al-Tahadi , (c) Al-Intifadah sites.....	35
Figure 3-4: Soak CBR Test Curves of (a) Al-Faris, (b)Al-Tahadi, (c) Al-Intifadah sites.....	37
Figure 3-5: Unsoak CBR Test Curves of (a) Al-Faris, (b)Al-Tahadi , (c) Al-Intifadah sites .....	38
Figure 3-6: steel box .....	39
Figure 3-7: Electrical mixer .....	40
Figure 3-8: shows first subgrade layer, (b) Show final subgrade layer .....	41
Figure 3-9: Layout of Testing Points.....	42
Figure 3-10: Research methodology .....	44
Figure 3-11: Components of LWD field test equipment .....	45
Figure 3-13: Schematic diagram of DCP device (ASTM D 6951-03, 2009) .....	48
Figure 3-14: Photos of the dynamic cone penetrometer .....	49
Figure 3-15: Typical summary of DCP. ....	50
Figure 3-16: SRM Apparatus.....	51
Figure 4-1: Relationship between dry density and moisture content. ....	55
Figure 4-2: Relationship between dry density and compaction effort.....	58
Figure 4-3: Average time deflection curve for Al-Faris site .....	60
Figure 4-4: Average time deflection curve for Al-Intifada site.....	62

## LIST OF FIGURES

---

Figure 4-5: Average time deflection curve for Al-Tahady site .....	63
Figure 4-6: Relationship between dry density and LWD parameters obtained from three locations .....	63
Figure 4-7: Relationship between compaction effort and LWD measurements .....	63
Figure 4-8: Relationship between DCPI and DD obtained from three locations ..	66
Figure 4-9: Relationship between CBR and DD obtained from three locations....	67
Figure 4-10: Relationship between compaction effort and DCP .....	68
Figure 5-1: Outliers test for LWD parameters.....	72
Figure 5-2: Outliers test for DCP parameters .....	73
Figure 5-3: Q-Q plots for LWD parameters. ....	75
Figure 5-4: Normal Q-Q plots for DCP parameters .....	76
Figure 5-7: Comparisons between LWD parameters and dry density.....	80
Figure 5-8: Predicted dry density verse measured dry density (LWD-DD) Model	81
Figure 5-9: Residuals verse DD model.....	82
Figure 5-10: Comparisons between DD parameters and dry density .....	83
Figure 5-11: Predicted dry density verse measured dry density (DCP-DD) Model	84
Figure 5-12: Residuals verse DD model.....	85
Figure 5-13: Predicted dry density verse measured dry density (DCP-LWD) Model.....	86
Figure 5-14: Residuals verse DD model.....	86
Figure 5-15: Comparisons between CBR parameters and LWD .....	88
Figure 5-16: Predicted CBR verse measured CBR (CBR-LWD) Model.....	89
Figure 5-17: Residuals verse CBR model.....	89
Figure 5-18: Comparisons between CBR parameters and Basic soil properties....	90
Figure 5-19: Predicted CBR verse measured CBR (LWD-basic soil properties) Model .....	91
Figure 5-20: Residuals verse CBR model.....	92
Figure 5-21: Predicted CBR verse measured CBR (CBR- (LWD. Basic soil properties)) Model.....	93
Figure 5-22: Residuals verse CBR model.....	93

## LIST OF TABLES

---

Table 2-1: A Summary of Mr and CBR Correlations .....	10
Table 2-2: Various associations for fine-grained soil compaction parameter .....	13
Table 2-3: Physical Characteristics of Typical LWD Devices.....	21
Table 2-4: Correlation Between LWD and soil properties .....	24
Table 2-5: Potential energy per drop for different DCP design .....	27
Table 2-6: Relationships between the CBR and the DCPI .....	30
Table 3-1 Summarizes summary of laboratory tests that were carried out to determine basic soil properties.....	33
Table 3-2: Summary of total numbers of laboratory tests .....	43
Table 4-1: Summary of SRM test results of subgrade soils at: Al- Fares, Al- Intifada, and Al-Tahady sites, (10,14,18) NOP.....	54
Table 4-2: LWD test summary of subgrade soil A-3, location at Al- Fares.....	57
Table 4-3: LWD test summary of subgrade soil A-3, location at Al- Intifada.....	58
Table 4-4: LWD test summary of subgrade soil A-3, location at Al- Tahady .....	60
Table 4-5: Summary of DCP test results of subgrade soils at: Al- Fares, Al- Intifada, and Al-Tahady sites, (10,14,18) NOP .....	65
Table 5-1: Correlation between variables .....	77
Table 5-2: Summary of models and coefficients for Nonlinear CBR, LWD parameter .....	79
Table 5-3: Statistical models based on LWD data are summarized in this table. ...	81
Table 5-4: Summary of statistical models based on DCP data.....	82
Table 5-5: Statistical models based on LWD data are summarized in this table. ...	84
Table 5-6: Summary of statistical models based on LWD-DCP data .....	85
Table 5-7: Summary of models and coefficients for Nonlinear CBR, LWD parameter .....	87
Table 5-8: Summary of statistical models based on CBR-LWD data.....	88
Table 5-9: Summary of models and coefficients for Nonlinear CBR, LWD parameter.....	90
Table 5-10: Summary of statistical models based on CBR-basic soil properties data .....	91
Table 5-11: Summary of statistical models based on CBR- (LWD-basic soil properties) data.....	92

## ABBRAVIATIONS

---

AASHTO	American Association of State Highway and Transportation Officials.
AISC	American Institute of Steel Construction and European standard.
ARRB	Australian Road Research Board.
ASTM	American Society for Testing and Materials.
CBR	California Bearing Ratio.
CCM	Core Cutter Method.
CIH	Clegg Impact Hammer.
CIV	Clegg Impact Values.
CH	High Plasticity Inorganic Clay.
C <sub>c</sub>	Coefficient of Curvature.
C <sub>u</sub>	Coefficient of Uniformity.
D <sub>c</sub>	Degree of Compatibility.
DCP	Dynamic Cone Penetration.
DCPI	Dynamic Cone Penetration Index.
DOC	Degree of Compaction.
E	Modulus of Elasticity.
E <sub>d</sub>	Dynamic Modulus.
ELWD	Dynamic LWD soil Modulus.
EPFWD	Dynamic PFWD soil Modulus.
FWD	Falling weight deflectometer.
GC	Gravel with Inorganic Clay.
GM	Gravel with Inorganic Silt.
GP	Poorly Graded Gravel.
GS	Specific Gravity.
GW	Well Graded Gravel.
K <sub>s</sub>	Modulus of Subgrade Reaction.
LL	Liquid Limit.
Loi	Loss of Ignition.
LVDT	Linear Variable Differential Transformer.
LWD	Light Weight Deflectometer.
MC	Moisture Content.
MDD	Maximum Dry Density.



## ABBRAVIATIONS

---

MH	High plasticity inorganic silt.
MI	Silt of intermediate compressibility.
ML	Low plasticity inorganic silt.
MLRA	Multiple linear regression analysis.
MPMT	Miniaturized Pressure Meter Test.
Mr	Resilient Modulus.
NDT	Non Destructive Test .
NOP	Number of passes.
OH	High Plasticity Organic Silt or Clay.
OL	Low Plasticity Organic Silt or Clay.
OMC	Optimum Moisture Content.
PBT	Plate Bearing Test.
PFWD	Portable Falling Weight Deflectometer.
PI	Plasticity Index.
PL	Plastic Limit.
PLT	Plate Loading Test.
RMSE	Root Mean Square Error .
SC	Sandy soil with inorganic clay.
SDG	Soil Density Gauge.
S <sub>d</sub>	Surface Deflection.
SLRA	Simple Linear Regression Analysis.
SM	Sandy Soil With Inorganic Silt.
SO <sub>3</sub>	Sulfur Trioxide.
SP	Poorly Graded Sand.
SPSS	Statistical Package For the Social Science.
SRM	Sand Replacement Method.
SSE	Residual Sum of Square.

## ABBRAVIATIONS

---

SSG	Soil Stiffness Gauge.
SW	Well Graded Sand.
TRRL	Transportation and Road Research Laboratory.
USACE	US Army Corps of Engineers.
W.C	Water content.

## **Chapter One**

### **INTRODUCTION**

#### **1.1 General**

Subgrade is a vital component of a pavement system, as all adverse overlying loads are transmitted through the subgrade. It does provide a main support to foundation structures and stability to embankments. The subgrade soil works as the foundation that supports the road. The success or failure of any pavement system is more often dependent upon the strength of the underlying subgrade upon which the pavement structure is built. The main functions of subgrade soils are principally based on several parameters, such as density, strength, and moisture content. The evaluation of the subgrade is an essential step that must be considered in analysis and design process of pavement systems. This step also allows for the proper selection of materials for the pavement to carry out expected traffic load **Madhira and Abhishek, (2015)**.

Soil compaction is one of the most critical task in the construction process of roads, airfields, embankments, and foundations. The durability and stability of a structure are related to achieving a proper soil compaction. Consequently, the compaction control of different soils used in the construction of highways and embankments is needed for enhancing their engineering properties. The current methods for assessing the quality control for construction of highways is based on determining the field unit weight and comparing that to the maximum dry unit weight obtained in a lab using standard or modified Proctor tests **Nazzal, (2003)**.

Traditionally, subgrade strength is measured by California bearing ratio (CBR). Empirical pavement design methods are based on CBR value. The CBR test is a laborious testing method that determines bearing resistance of tested materials and

compare to resistance of well-graded crushed stone material **Gabr, (2000)**.

Many non-destructive testing (NDT) tools are available to measure in-situ strength and stiffness of subgrade (i.e., nuclear density gauge, portable falling weight deflectometer, light weight deflectometer, and dynamic cone penetrometer). The LWD is widely used for construction quality control of soil layers in highway construction, because of ease of use and portability **bin Arshad,( 2007)**. The DCP is an effective tool in assessment of subgrade pavement conditions and strength because of its portability, simplicity, and ability to provide rapid measurements of in-situ strength of subgrades **Stamp, (2013 )**.

## **1.2 Problem Statement**

The density and strength of subgrade soil layers are main parameters which are often used in quality assessments of any roadway projects. The characteristic of subgrade effect mainly on the structural performance of the pavement system. In general, subgrade layer presents primarily as a platform to support others provided pavement layers. For evaluating density and strength properties of subgrade soils, several conventional and testing methods were developed. Among these tests methods are sand cone test density test and CBR test methods which carried out to determine density and strength of subgrade layer. However, there are several limitations associated with using these old testing techniques including: complicated testing procedure, laborious, time consuming, does not reflect or represent actual soil properties.

At present, most of international highway agencies resort to involve new non-destructive characteristics of subgrade and unbound pavement layers. However, those testing techniques are still unpopular in Iraq, and all Iraqi highway agencies merely depend on conventional supplementary destructive tests appraise the quality of pavement materials based on density and moisture content measurement.

Therefore, there is a necessary demand to use more effective tools that can be considered as in-place quality control test for pavement materials

### **1.3 Research Aim and Objectives**

The main aim of this research is to develop an alternative quality assessment of testing protocol to identify density and strength of subgrades using the modern, simple and reliable dynamic-based testing methods. This aim will be achieved through conducting the following objectives:

- Evaluating selected local subgrade soils, and identifying their physical and chemical properties.
- Use light weight deflectometer test and dynamic cone penetrometer test to predict density and strength of subgrade soil by obtaining dynamic measurements such as dynamic modulus, CBR, and dynamic cone penetration index.
- Correlating the dynamic measurements from LWD and DCP with conventional subgrade soils characteristics such as dry density and CBR.

### **1.4 Scope of Research Work**

This research was completed within the following parameters:

- 1- All subgrade soils used in this research were collected from three roadway project sites at Karbala, Iraq. The dominant soil type in Karbala is a poorly graded sand soil type (A-3). Thus, only A-3 subgrade soils were examined in this work.
- 2- Selected subgrade soils were evaluated in the lab in terms of basic physical and chemical properties.

- 3- All tests were performed at the laboratory, some testing device has locally manufactured, including loading frame, and steel box. This manufactured apparatus provides a similar environment for sites and conducting field tests.
- 4- The efficiency (i.e., compaction effort) of the compactor used in the lab was less efficient than the one used in the site work.

## 1.5 Thesis Layout

This thesis is presented in six chapters, which are outlined as follows:

**Chapter One:** introduces the background of the research, problem statement, aim and objectives, and scope of the research work.

**Chapter Two:** reviews previous research works to discuss the current understanding of the strength properties, compaction characteristic, and description of LWD and DCP.

**Chapter Three:** presents the experimental work details, which include the description of soil samples and identified their physical and chemical properties and describe testing procedure of LWD, DCP, sand replacement test.

**Chapter Four:** illustrates and discusses the results of the laboratory tests including dry density, LWD, and DCP.

**Chapter Five:** presents the statistical analyses of the summary, and theoretical model developed by using SPSS software.

**Chapter Six:** presents conclusions obtained from the experimental and statistical work and recommendations for future studies.

## CHAPTER TWO

### REVIEW OF LITERATURE

#### 2.1 Introduction

The majority of highway designs codes use soil and aggregate materials as base layers. Some laboratory tests are needed before soils can be compacted in the field to assess their engineering properties. The optimal dry density and the optimum moisture content are the most two essential properties that determine the density that must be compacted in the region. The standard and modified Proctor tests are commonly used and have remained unchanged for decades as the first standardized laboratory procedure for soil compaction **Andrew,( 2012)**.

Compaction effort, on the other side, is unlike any other forms of field compaction. In certain cases, these laboratory effect techniques tend to be incapable of reflecting the maximum feasible field density of soil due to the development of heavier modern rollers **Andrew,( 2012)**.

It is important to use proper quality control procedures when placing granular base course materials in road construction in the United States, this is usually done with a nuclear density gauge (NDG), which measures the moisture and wet density of the sand before calculating the dry density. The goal maximal dry density obtained from the Proctor test in the laboratory is then compared to this dry density that reflects field conditions **Xiaoyang, J (2019)**.

Dynamic cone penetrometers (DCP), surface stiffness gauges (SSG), and light weight deflectometers (LWD) are the most commonly used tools for construction quality control. The current understanding of the strength characteristic, compaction characteristic, LWD, and DCP are defined in this chapter, which includes a summary of published literature **Emre, (2020)**.

## 2.2 Strength Characteristics of Subgrade Soils

The subgrade is the material that exists when the pavement base is constructed. Despite the fact that it is normal to think of pavement efficiency exclusively in terms of pavement design and mix design, the subgrade is still the most important factor. The most common characteristics that need to be considered in pavement design and study are the resistance to deformation under load (stiffness) and the bearing potential of subgrade materials (i.e., strength) **Roy, (2013)**.

The strength characteristics of soils are influenced by a variety of factors, including the soil type, moisture content, dry density, and the type and mode of stress application. There are three basic subgrade stiffness/strength characterizations in pavement design requirements: CBR (California Bearing Ratio), Resistance value (R-Value), and Resilient modulus (MR).

### 2.2.1 California Bearing Ratio (CBR)

The California bearing ratio (CBR) is a strength index measure that is often used in pavement layer thickness design. CBR test has been and still the most commonly tool for evaluating soil subgrades under rigid and flexible pavement thickness design, and it is a key component of many pavement thickness design methods **Yavuz, G( 2020)**.

The CBR of a soil is measured by dividing the stress needed to penetrate 2.54, 5.08, 7.62, 10.16, and 12.70 mm into the soil by the normal penetration stress at each depth of penetration ASTM D1883, (2014). The California State Highways Department developed the CBR test at the early 1930s to measure the mechanical properties of subgrades and base courses under lab conditions. Following the CBR efficiency of the pavement, numerous countries have established or introduced pavement construction methods depending on the CBR performances of the pavement **Abbas, M(2017)**.



The CBR test is time-consuming and complex in the field due to the equipment used and the fact that the moisture content of the field varies over time. In recent years, there appears to have been an increasing trend toward obtaining CBR values through indirect non-destructive testing methods such as the Dynamic cone penetrometer (DCP), Falling Weight Deflectometer (FWD), and Light Weight Deflectometer (LWD) **Thomas, (2007).**

The CBR value of soil is determined by a variety of factors, includes physical features of the soil, like maximum dry density (MDD), optimum moisture content (OMC), liquid limit (LL), plastic limit (PL), plasticity index (PI), grain size distribution, and soil permeability, among others **Shirur, hirematth, (2014).**

Simple linear regression analysis (SLRA) of subgrade soils with an overall liquid limit compared with experimental summary and SLRA of subgrade soils with an annual liquid limit (20 % to 70 %), there is no important relationship between liquid limit and plastic limit in predicting CBR value, but there is a strong relationship between MDD and OMC in predicting CBR value **Shirur, hirematth, (2014):**

$$\text{CBR}=4.99 \text{ MDD}- 5.711(R^2=0.78) \quad (2.1)$$

$$\text{CBR}=-0.2443 \text{ OMC}+7.5264 (R^2=0.71) \quad (2.2)$$

Although the CBR value of fine-grained silty soils of low compressive strength (ML) and medium compressibility (MI) has a meaningful correlation with PI, MDD, and OMC; the identified CBR value decreases by increasing the plasticity index and optimum moisture content of soil, and therefore increases with increasing the maximum dry density **Shirur, and Hiremath, (2014).**

The CBR obtained value in the lab varies significantly from the CBR value calculated using a multiple linear regression model (MLR) that includes LL, PL, PI, MDD, and OMC **Talukdr, (2014):**

$$\text{CBR soaked} = 0.127(\text{LL}) + 0.00 (\text{PL}) - 0.1598(\text{PI}) + 1.405 (\text{MDD}) - 0.259 (\text{OMC}) + 4.618 \quad (2.3)$$

Another proposed empirical relationship derived from fine-grained soils multiple

linear regression analysis (MLRA) presents a clear association between MDD and OMC in predicting CBR value **Talukdr, (2014)**:

$$\text{CBR} = -4.8353 - 1.56856(\text{OMC}) + 4.6351(\text{MDD}) \quad (R^2 = 0.82) \quad (2.4)$$

According to research observations and simple linear regression analysis (SLRA), there is no substantial association between liquid limit and plastic limit in predicting CBR value Shirur, hirematth, (2014), but there is a small discrepancy between the CBR value calculated in the laboratory and the CBR value computed using a multiple linear regression model involving LL, PL, PI, MDD, and OMC **Talukdr, (2014)**.

The DCP values are typically compared with the CBR of the pavement subgrade in order to determine the structural properties of the pavement subgrade. Both CBR and DCP tests were performed in the laboratory on a wide range of undisturbed and compacted fine-grained soil samples, with and without saturation, during the establishment of this relationship **John, (2001)**.

In the flexible molds, compacted granular soils were tested with variable controlled lateral pressures. Natural and compacted layers representing a wide variety of possible pavement and subgrade materials were tested within the field. The subsequent quantitative relationship between the CBR and its DCP value was discovered as a result of the study **Das, (2010)**:

$$\text{Log CBR} = 2.2 - 0.71 * (\text{DCP})^{1.5} \quad R^2 = 0.95, N=74 \quad (2.5)$$

where the DCP is in millimeters per blow.

### 2.2.2 Resilient Modulus ( $M_r$ )

The resilient modulus is that the coefficient of elasticity that was utilized in elastic theory rather than being absolutely elastic, the majority of pavement materials, principally soils, have an elastic-plastic behavior. That is, they are partially elastic under a static load but are permanently deformed. They can, however, exhibit different critical properties once subjected to repetitive masses. They behave even as they were going to underneath a static load initially **Reyn, (2005)**.

However, after a certain amount of repetition, the permanent deformation caused by each load is almost entirely reversible. If the repetitive load is small enough in relation to its strength, it can almost be called elastic at this stage; otherwise, the soil structure would be weakened **Richard,J(2013)**. The action of unbound material under different conditions is depicted in Figure (2.1).

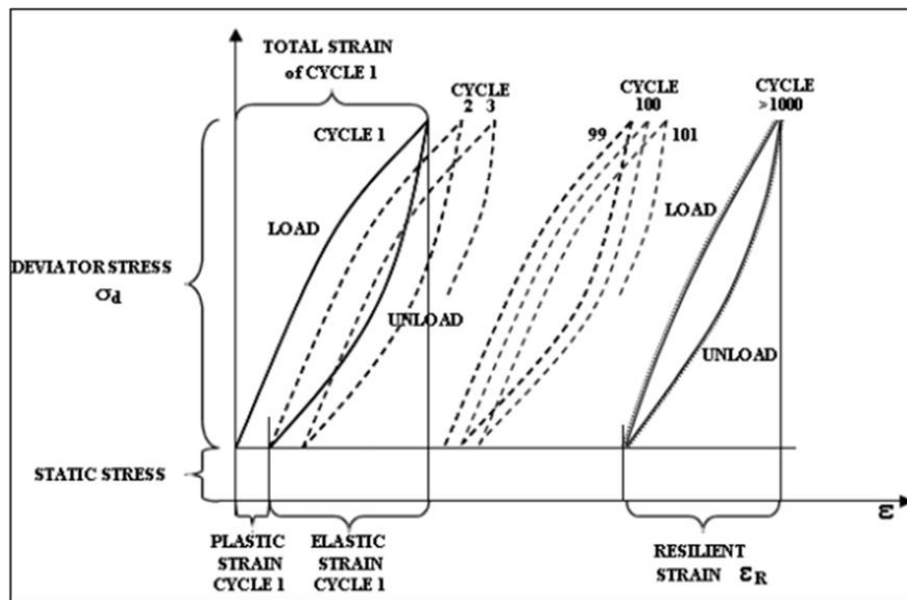


Figure 2-1: Deformation soil behavior under a sequence of repeated load **Sheng, (2016)**

The resilient modulus is a measurement of a soil elasticity that takes into account nonlinear characteristics. It was the ratio of axial deviator stress to revocable axial pressure, and it was written like this **Reyn, (2005)**:

$$M_R = \sigma_d / \varepsilon_r \quad (2.6)$$

Where  $\sigma_d$  =axial deviator stress

$\varepsilon_r$ = axial revocable

The resilient modulus of soils is influenced by a number of factors including soil type, soil properties, dry unit weight, strain and stress levels, and test procedures. The resilient modulus test protocol and the selection of a suitable specification resilient modulus for pavement subgrades have both been improved. The resilient modulus test technique, as well as choosing a suitable specification resilient modulus for pavement subgrades, have proven to be extremely difficult, time-consuming, and expensive AASHTO T307-99, (2000). Many researchers have developed various Mr empirical models to predict Mr as a function of other soil characteristics, as shown in Table (2.1) **Sheng, (2020)**.

Table 2-1: Summary of Mr and CBR Correlations **Sheng, (2020)**

Relationship proposal	Citation	Observations
Mr (MPa) = 16.2 CBR <sup>0.7</sup>		For CBR less than 5
Mr (MPa) = 22.4 CBR <sup>0.5</sup>	NAASRA (1950)	For CBR more than 5
Mr (Psi) = 1500 × CBR	Heukelom and Klomp (1962)	Only fine-grained non-expanding soils with a soaked CBR of 100 percent are included in this correlation.
Mr (MPa) = 10.34 × CBR	Heukelom and Klomp (1962)	/
Mr (MPa) = 38 CBR <sup>0.711</sup>	Green, J.L. and Hall (1975)	/
Mr (MPa) = 17.58 × CBR <sup>0.64</sup>	Powell et al. (1984)	/
Mr (MPa) = 18 CBR <sup>0.64</sup>	Lister and Powell (1987)	/
Mr (MPa) = 21 CBR <sup>0.65</sup>	Ayres (1997)	/
Mr = 5.00535CBR + 2.95173	Razouki and Kuttah (2004)	For CBR ≥ 1
Mr = 810 CBR (kPa)	Putri et al.(2012)	MR = 863.82 CBR, v = 0 MR = 840.53 CBR, v = 0.3 MR = 751 CBR, v = 0.4
Mr = 8.795(CBR) – 0.972	George and Kumar (2018)	The cyclic triaxle test is used to determine the resilient modulus.

## 2.3 Compaction Characteristics of Subgrade Soils

Laboratory compactions experiments are often used to prepare criteria for borrow material compaction in field construction projects. The modified proctor compaction test is also known as the standard proctor compaction test ASTM 1557.

### 2.3.1 Purpose of Compaction

The aim of compacting earth fills soils, such as fills in earth dams and embankments of (highway, railway, and corn railway anal, and subgrades), is to create a soil mass that meets two basic criteria: settlement reduction and increased shear strength **Ramaswami, (2004)**. As a result, compaction was needed for many other engineering structures built on soils, such as highways, railway subgrade and airfield pavements, tunnels, and overpasses. Compaction increases the strength of soils, thus increasing the bearing ability of foundations built on top of them **Patel, (2019)**.

Laboratory testing of soil properties such as permeability, compaction, consolidation, strength, and compressibility is critical for understanding and interpreting how soils will behave in the field. Under these test conditions, the behavior of soil is determined by the amount of moisture absorbed.

As a result, several researchers have attempted to build a prediction model for fine-grained soil that is both naturally available and artificially. As time passed, researchers attempted to link soil index properties to compaction parameters **Das, and Sobhan,( 2013)**.

Tables (2.2) show the established models and their coefficients of determination ( $R^2$ ) for fine-grained soil. The investigation of statistical and numerical methods has also been discussed. A variety of researchers have used the statistical program which provides the option of linear or multiple regression, and significant correlations have been found. between compaction characteristics and soil classification properties, the researcher developed the correlation equations from the results of two studies.

For the first study, the compaction data were correlated with LL and PL, from which the approximate MDD and OMC of soil could be determined. In the second study, the correlation equations (1) and (2) were developed to predict MDD and OMC, respectively, from LL, PL, PI, approximate average particle diameter (D50), the content of particles finer than 0.001 mm (F 0.001) and fineness average (FA) **Verma, (2019)**. Wang, Huang (1984) developed the two sets of correlation equations (3) to (6), one each for MDD and OMC by statistical analyses. Each set of equations contain two different prediction models. The soil samples were prepared artificially from four different components of soil, i.e. bentonite, lime stone dust, sand and gravels, 57 different mixes were prepared by blending these materials in different proportions.

Al-Khafaji (1993) presented few empirical relationships as shown in equations (7) through (10), for MDD and OMC from LL and PL. He had also prepared some charts using curve fitting technique from soil compaction and Atterberg limits data.

Table 2-2: Various associations for fine-grained soil compaction parameter Verma, (2019).

Author	Predetection method type	Compaction type	No. of soil samples	Equation	R <sup>2</sup>
Ring, Sallberg, and Collins(1962)	MRA	NA	NA	MDD=147.525-0.02 LL-1.195PL- 0.198 FA (1) OMC=1.427LL-0.815PL-1.373PI-0.0007D50+0.062FA +0.035(0.001fraction)-1.312 (2)	NA
Wang and Hang(1984)	SAS	SP	57	(MDD/ $\gamma_s$ ) $\times$ 100 = 45.6-1.28FMlog <sub>10</sub> (D <sub>10</sub> )-0.0464FM $\times$ PL+ 1.43MF (3) (MDD/ $\gamma_s$ ) $\times$ 100 = 45.9- 7.5FM- 0.45log <sub>10</sub> C <sub>u</sub> -0.0754FM $\times$ B (4)	0.95
Al-khafaji (1993)	Curve fitting technique	SP	88	OMC $\times$ 100 =2614 + 12.7 PL -95 FM <sup>2</sup> - 88.1(log <sub>10</sub> C <sub>u</sub> ) <sup>2</sup> (5) OMC $\times$ 100 =1035 -905 log <sub>10</sub> (D <sub>50</sub> )+0.22 B <sup>2</sup> + 106 FM log <sub>10</sub> (D <sub>50</sub> ) (6) MDD=2.44-0.02 PL- 0.008 LL Iraqi soil (7) OMC=0.24 LL+0.63 PL- 3.13 (8) MDD=2.27 – 0.019 PL – 0.003 LL US Ssoil (9) OMC= 0.14 LL + 0.54 PL (10)	0.88 0.8 NA NA
Bera and Ghosh (2011)	Log linear regression through MRA	5 different energy	5	MDD= -66.8798+ 2.75298 log E- 0.03585 LL+28.60931 Gs – 121.2903 D50 (11) OMC= 226.0947 – 7.000262 log E – 70.3473 Gs + 0.097542 LL – 459.492 D50 (12)	0.98 0.95
Gurtug, Sridharan, and Lkizler (2018)	Curvilinear Regression analysis	SP, RMP and MP	4+123	MDD = 0.98 MDD <sub>PL</sub> (13) OMC = 0.943 PL (14)	

MDD: Maximum dry density;NA: Not available; OMC: Optimum moisture content; LL: liquid limit; PL: plastic limit; PI: plasticity index;  $\gamma_s$  : density of solid phase FA: fineness average; ; D50: mean particle size (mm); FM: fineness modulus; Cu: uniformity coefficient; B: bentonite content in % by weight; E: compaction energy (kJ/m<sup>3</sup>);SP:standard proctor(592.55kj/m<sup>3</sup>) ;RMP:reduced modified proctor (1616Kj/m<sup>3</sup>) ; MP: modified proctor(2693.35Kj/m<sup>3</sup>) ; SAS: statistical analysis system; SRA: simple regression analysis; MRA: multiple regression analysis; SP:

### 2.3.2 Compaction Theory

The fundamental of compaction of cohesive soils are relatively new. R.R. Proctor in the early 1930 built dams for an old bureau of waterworks and supply in Los Angeles, and he developed the principles of compaction in a series of articles in Engineering News-Record (procter,1933). In his honor, a standard laboratory compaction test was developed and called the Proctor test **William, (1980)**.

Compaction is a function of four variables, according to Proctor: dry density, water content, compactive effort, and soil. Compaction effort is a measure of the mechanical energy applied to a soil mass. The composition of the bearing soil limits the ability of any rational design approach to predict the compression and strength behavior of soil deposits. To ensure the fill's consistency and efficiency, the density of fills put around and underneath foundations of structures must also be managed **Tascon, and Andres (2011)**.

Impact or kneading compaction is often used in the laboratory to achieve specific densities. Impact compaction is achieved by repeatedly striking a soil sample in a mold of known volume with a hammer. The soil is divided into multiple layers, each of which is struck with a hammer of known weight that falls a predetermined distance. The compactive effort (CE) is then measured as follows: **Günaydn, (2008)**

$$CE = \frac{W_h H_d N_l N_d}{V} \quad (2.7)$$

Where  $W_h$ , is the weight of hammer,  $H_d$  is the height of hammer fall,  $N_l$  is the number of soil layers,  $N_d$  is the number of hammer drops per layer, and  $V$  is the volume of the mold.

Figure (2.2) shows how a soil sample was compacted using two different compactive attempts at different water contents. The compactive commitment used



to compact curve 2 is greater than that required to compact curve 1. It is worth noting that as the compactive effort rises, the optimum dry unit weight rises and the optimum water content decreases. The assumption is that less water is needed to reach the same level of dehydration required to achieve a denser soil mass.

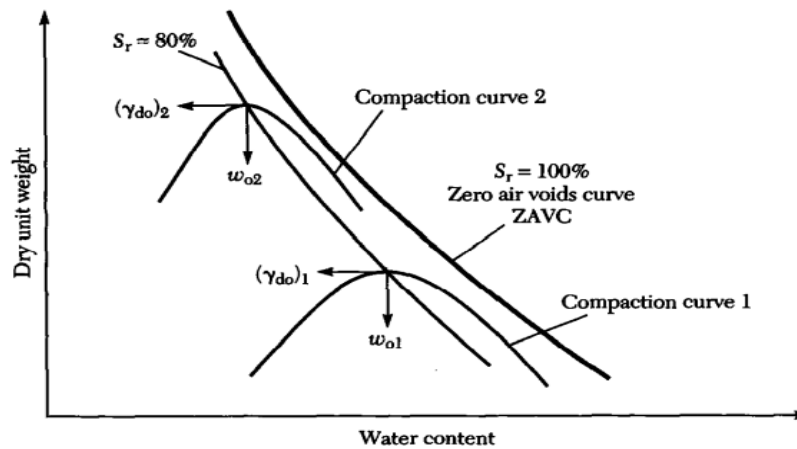


Figure 2-2: Schematic representation of compaction and the corresponding zero air voids curves for a typical soil **Günaydın, O (2008)**.

Lee and Suedkamp , (1972) Discovered that four different types of compaction curves exist: (a) a single peak, (b) an irregular peak, (c) a double peak, and (d) a nearly straight line with no clear optimum dry unit weight. Figure (2.3) illustrate these kinds of compaction curves.

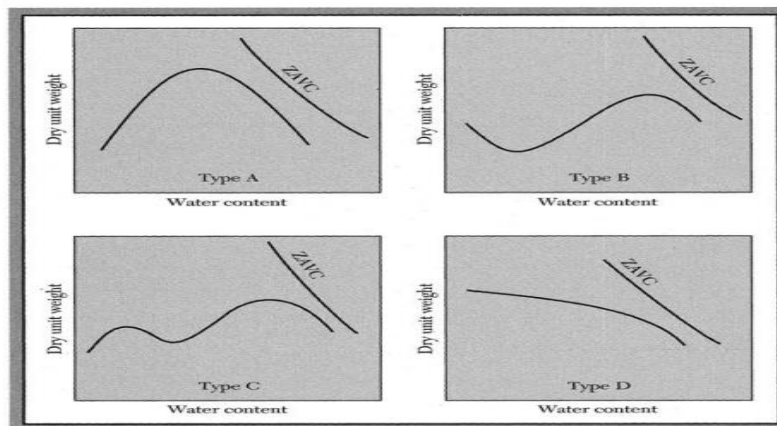


Figure 2-3: Schematic representation of four possible types of compaction curves **Akr and Suedkmp, (1972)**.

### 2.3.3 Factors Affecting Compaction

Whether in the lab or out in the field, a variety of factors affect compaction, the amount of compactive energy used, the water content of the soil, and the grain size distribution are all factors that influence compaction **Ahmet, (2005)**.

**Bloomfield, (2004)** the degree of compaction is inversely proportional to the layer thickness. For a given compactive energy, a thicker layer will be less compacted as compared to a thin layer. The reason is, for thicker soils, the energy input per unit weight is less. Therefore, it is very important to decide the right thickness of each layer to achieve the desired density.

**Kim, and Sagong, (2004)** Proper control of moisture content in soil is necessary for achieving desired density. Maximum density with minimum compacting effort can be achieved by compaction of soil near its optimum moisture content.

**Sivakugan, (2011)** the effects of median grain size, as well as other influences, on the density of packing of granular soils were investigated. **Patra , 2010** tested 55 clean sand samples and found that the void ratio and relative density were related to the compaction energy (CE) and median grain size.

### 2.4 Light Weight Deflectometer

The Light Weight Deflectometer (LWD) is a portable and non-destructive device. The LWD which is used to measure the in-situ elastic modulus of subgrade pavement layers was developed as an alternative field test to many other tests such as Field Dry Density (FDD), and California Bearing Ratio (CBR) **Akbariyeh, (2015)**.

The benefits of using the LWD are: It is a non-destructive testing equipment, the deflection measurements are repeatable and accurate, the equipment is durable and inexpensive compared to other complicated testing systems, small and Easy to operate any place **Hossain, (2010)**.

LWD works by lowering a known weight from a predetermined height onto a circular plate over the soil and calculating the vertical surface deflection under the plate. Surface soil stiffness can be also determined using LWD. The LWD modulus for a given soil ( $E_{LWD}$ ) is calculated using the measured deflection. The elastic half-space principle is used to measure  $E_{LWD}$ , which assumes that all underlying soil layers were made of a uniform elastic substance.

The LWD data obtained during development is typically used in two ways:  
**Ebrahimi, (2013)**

- 1- Compaction quality control, which involves compacting pavement materials so the LWD deflection was equal to or less than a set target value; this approach is solely analytical and has been extensively used by the Minnesota Department of Transportation.
- 2- Determining the resilient modulus ( $M_r$ ) of pavement materials from the  $E_{LWD}$ .

#### **2.4.1 Historical Development of LWD**

Over the past 15 years, the UK Highways Agency has sponsored extensive investigations into the development and use of a range of portable falling weight deflectometers (PFWDs). One of the key aims has been to establish a specification for such PFWD devices to be used as a field compliance tool within a performance-based specification for pavement foundation construction, aimed to optimize the use of materials **Fleming, (2007)**.

(LWD) is a hand-held falling weight gadget that was developed as an in-situ measuring device by the Federal Highway Research Institute and the HMP Company in Germany in 1980 **Elhakim, (2013)**.

The LWD device provides a time-deflection curve which is utilized to measure the in-situ maximum vertical surface deflection and elastic modulus of pavement

layers. The maximum vertical deflections are measured by integrating the geophone (velocity transducer) signal. This has two important divisions; the peak deflection may not occur instantaneous under the peak load due to dynamic effects, and the peak deflection may include both plastic and elastic deflection that depends on the strength of testing materials and proper contact between material and geophone **Fleming, (2007)**.

The peak deflection was a measure either to degree of compaction or stiffness of soil, or both together with the peak force. to calculate the elastic modulus based on the well-known Boussinesq elastic half – space theory by the following expression:

**Moony, (2013)**

$$E_{LWD} = \frac{(1-\nu^2)\sigma \cdot a}{\delta} \cdot f \quad (2.8)$$

Where:

$E_{LWD}$ : Dynamic LWD soil modulus

$\sigma$ : Applied dynamic stress (MPa)

$\delta$ : Soil surface deflection (mm)

$a$ : Radius of the loading plate (mm)

$\nu$ : Possion ratio in range (0.3-0.45) depending on the type of test material

$f$ : Shape factor depending on stress distribution under a plate

## 2.4.2 Theoretical Basis of LWD

The light Weight Deflectometers are the most precise and effective way to evaluate the structural integrity of pavements. The layers' moduli, which can be used in pavement construction, are the most significant parameter obtained from the LWD test. Since deriving the modulus from LWD field data is difficult and demands strong engineering decisions, boussinesq theory was hired to measure modulus **Sanjeev, (2020)**.

Boussinesq devised a series of equations for calculating stress, strain, and displacement at a depth 'z' below the center line of a uniform circular load with a radius 'a' from the loading center in a homogeneous, isotropic, linear elastic, semi-infinite vacuum.

Many automated programs have used Boussinesq's equations to calculate the moduli of pavement layers; they use the equations iteratively to find moduli values that are accurate for the input pavement parameter combinations **kessler, (2012)**.

Elastic moduli of the pavement layers can be calculated using back calculation and other techniques from the deflection basin formed by adding a load to the pavement surface with the NDT unit. When a LWD test is performed on a surface (subgrade or pavement), the pavement deflects when the load is lowered.

The load-induced deflection is extended in the form of a bowl, which is referred to as the deflection bowl. The load magnitude, pavement layer structure, layer hardness, loading plate size, load impulse, length, temperature, and other factors can influence the size and shape of the deflection bowl. Since the deflection bowl parameters are very closely linked to the structural strength and characteristics of the pavement.

During operation, it requires a flat surface to function properly and three seating drops are performed to ensure close contact. Then another three drops are performed, and the deflection corresponding to each blow and the soil's dynamic modulus were calculated by the data acquisition system. An important insight into the soil property can be obtained by a typical output from acquisition system of LWD, which show time history data **Moony, (2013)**.

In traditional LWD analysis, the peak applied force (F) peak and displacement (w) peak are extracted from the measured time histories to determine E hereafter called ELWD. The load cell and geophone measure the applied force and velocity time histories, respectively, whilst the displacement time history was produced by

numerically integrating the velocity. The trapezoid method was utilized for the integration with a time step of 0.02 ms, corresponding to the sampling frequency. Using error propagation techniques to account for the numerical integration, the accuracy of the maximum displacement was estimated to be 0.005 mm. This was verified by repeatability assessment of the calculated displacement from multiple drops at the same location. The corresponding error in ELWD was determined to be < 4%. Figure (2.5) illustrates typical time histories from LWD testing on compacted clay using both 200 and 300 mm plate diameters and a drop height of 0.9 m. (F) peak was found to be independent of plate diameter. As expected, for the same (F) peak, the measured plate velocity and integrated plate displacement were greater for the smaller plate **Moony, (2013)**.

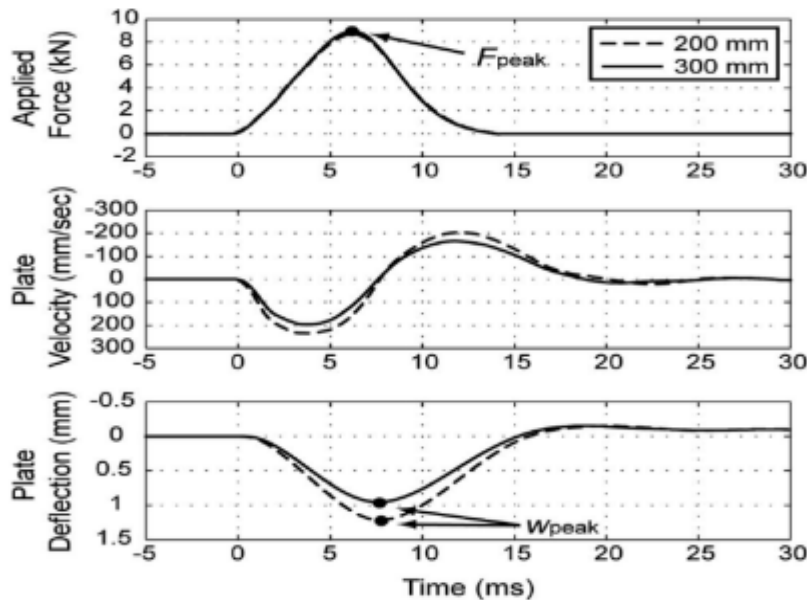


Figure 2-4: Typical time history data from LWD Test **Moony, (2013)**.

### 2.4.3 Types and Uses of LWD

There were some various kinds of LWDs. Table (2.3) summarizes the features offered by five different LWD manufacturers. In terms of falling weight and height,

impulse time, plate diameter and design, touch strength, and sensor styles, each unit is special (**Burhani, 2016**).

Table 2-3: Physical Characteristics of Typical LWD Devices (**Burhani, 2016**).

Manufacturer	CSM	Zorn	Prima	Load man	TFT
Plate style	Solid	Solid	Annulus	Solid	Annulus
Plate diameter (mm)	200, 300	150, 200,300	100, 200, 300	130, 200, 300	100, 150, 200, 300
Plate mass (kg)	6.8, 8.3	15	12.0	6.0	Variable
Drop mass (kg)	10.0	10	10, 15, 20	10.0	10, 15, 20
Drop height (m)	Variable	0.72	Variable	0.80	Variable
Damper	Urethane	Steel spring	Rubber	Rubber	Rubber
Force measured	Yes	No	Yes	Yes	Yes
Plate response Sensor	Geophone	Acceleromet Er	Geophone	Accelerometer	Geophone
Impulse time (ms)	15 – 20	18 ± 2	15 – 20	25 – 30	15 – 25
Max load (KN)	8.8 <sup>a</sup>	7.07 <sup>a</sup>	1 - 15 <sup>a</sup>	20 <sup>a</sup>	1 - 15 <sup>a</sup>
Contact stress	User def.	Uniform	User def.	Rigid	User def.
Poisson's ratio	User def.	0.50	User def.	0.50	User def.

#### 2.4.4 Factors Affecting LWD Measurements

The measurements of LWD test are influenced by several factors including:

- 1) **Bearing plate size:** the size of loading plate was the most significant factor that changed the LWD test condition. The diameter of plate effects on the amount of pressure, as it reduces as it transfers from top down through pavement layers **lin , (2006)**.
- 2) **Types and location of deflection sensor:** The type and position of the deflection sensors were different with various manufacturers, for example, the Zorn LWD reads the vertical surface deflection using an accelerometer built into the solid plate, as shown in Figure (2.6 c). The other types like Prima, TFT, Keros /Dynatest LWD devices estimate

vertical surface deflection using a spring-loading geophone in direct contact with the ground surface through a (40 mm) diameter hole in the center of plate as shown in Figure (2.6 a, b, c) **Mooney, (2009)**.

- 3) **Plate contact stress:** the effect of this factor depends on the type of layers underneath, **Vennapusa, and White, (2013)** explained that for dense and granular materials increasing contact stress lead to increase in the elastic modulus, while the materials with cementitious properties will not influenced by changes in contact stress.

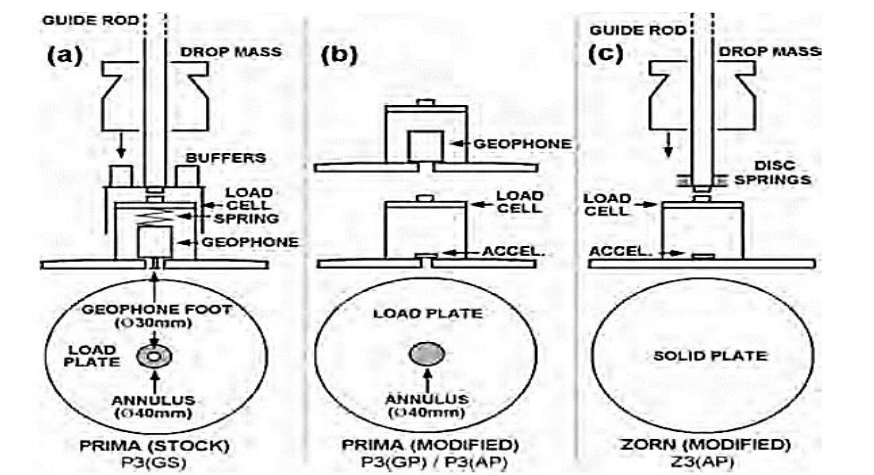


Figure 2-5: (a) Stock Prima 100 LWD, (b) Modified configurations of Prima LWD with geophone (top) or accelerometer (bottom) fixed rigidly to the load plate, and (c) Zorn LWD showing modification to include load cell. **Mooney(2009)**.

- 4) **Plate Rigidity:** This factor is important for estimating the distribution of stress under the plate and for selecting the shape factor (f).
- 5) **Loading rate and buffer stiffness:** The elastic modulus (ELWD) that measured by using elastic half – space theory influences by the rate of loading which can be controlled by changing the stiffness of buffer



placed between the contact plate and drop weight **Vennapusa and White, (2013)**.

- 6) **Proper contact between the loading plate and the tested surface:** The **ASTM E 2835, (2011)** recommended that the test surface should be clean and smooth to obtain a uniform contact between the surface and load plate, thus it recommended to place a thin layer of fine sand over the test point for a gravel surface.

### **2.4.5 Correlation between LWD and soils properties**

(LWD) was created as a top management tool for assessing the performance characteristics of pavement layers. The LWD would be a non - destructive testing instrument used to determine the in-place stiffness qualities of unbound pavement materials under the effect of a dynamic impact load **Mehran, (2019)**.

Experimental work was conducted by **Hossain, (2010)** to study the possibility of employing the LWD as a field-testing method to evaluate unbound granular materials for Virginia's roads instead of conventional density and moisture content tests. It was observed that the soil modulus obtained from the LWD increases with increasing density. In addition, the study found a significant effect of moisture content on decreasing LWD stiffness. This behavior may be attributed to high pore water pressure that develops when a soil is subjected to a high dynamic impact load during the LWD testing procedure.

**Emre, (2020)** made an attempt to correlate the LWD modulus values obtained from the field and from the mold for subgrade and base layers. The results showed strong correlation for the subgrade but poor correlations for the base course strong relation, but the base course had a low correlation (granular material).

**Nazzle, (2004)** Studied the relationship between LFWD (mainly Prima 100) and plate load test measurements for subgrade materials which contains volcanic soil,

and silty sand, and mechanically stabilized crushed stone. They suggested the following correlation based their results:

$$\text{Log} \left( \frac{k_{LFD}}{K_{30}} \right) = 0.0031 \log (k_{LFD}) + 1.12 \quad (2.9)$$

Where:

$k_{LFD}$ : is the ratio of stress on loading plate of the LFD to the measured deflection at this stress.

$K_{30}$ : is the ratio of stress on plate with a diameter of 300 mm for a PLT to the measured deflection at this stress.

A number of comparative work were carried out by several researchers to correlate LWD with other field tests, establishing the in-situ elastic modulus of pavement foundations in various transportation projects. These correlations were summarized in Table (2.4): **Ahela, (2017)**

Table 2-4: Correlation Between LWD and soil properties

Reference	Suggested formula	$R^2$
<b>(Rao et al, 2008).</b>	$E_{LWD} = \left( \frac{CBR+2.754}{0.2867} \right)$	0.9
<b>(Louay et al, 2009)</b>	$E_{LWD} = \left( \frac{M_r}{27.75} \right)^{-0.18}$	0.54
<b>(Zhang, 2010)</b>	$E_{LED} = \frac{E_{FWD} - 8.1}{0.4}$ $E_{LWD} = \frac{E_{BCD} - 29}{0.3}$	0.35
<b>(Shaban, 2016)</b>	$E_{LWD} = 4.22 + 3.36 E_i(\text{MPMT}) + 0.04 E_i(\text{MPMT})^2$ For Subgrade Coarse $E_{LWD} = 7.07 + 0.66 E_r(\text{MPMT}) - 0.001 E_r(\text{MPMT})^2$	0.84 0.79
	For base coarse $E_{LWD} = 34.48 + 3.34 E_r(\text{MPMT}) - 0.01 E_i(\text{MPMT})^2$	0.94
	For base coarse $E_{LWD} = 50.93 + 0.34 E_r(\text{MPMT}) - 4.2 \times 10^{-4} E_r(\text{MPMT})^2$	0.77
<b>(Nazzle, 2016)</b>	$E_{LWD} = \frac{CBR+14}{0.66}$ For subgrade coarse $E_{LWD} = 4.22 + 3.36 E_i(\text{MPMT}) + 0.04 E_i(\text{MPMT})^2$ For subgrade coarse	0.83 0.84

---

Where:

$E_{LWD}$ : Dynamic LWD soil Modulus

$M_r$ : Resilient modulus of pavement materials

$E_{FWD}$ : Dynamic FWD soil Modulus

$E_{BCD}$ : Modulus of the compacted material obtained from Briaud Compaction

$E_{i(MPMT)}$ : Initial Elastic Modulus (MPa) obtained from MPMT tests

$E_{r(MPMT)}$ : Reload Elastic Modulus (MPa) obtained from the MPMT tests

---

## 2.5 Dynamic Cone Penetrometer (DCP)

In 1998, Minnesota Department of Engineering (Mn/DOT) adopted a DCP aggregate base quality assurance specification. The cone was driven into the pavement base material by the DCP's dropping mass, which drops from a given height. The DCP penetration index was the DCP penetration distance per drop (DPI). Using analytical relationships, the DPI was used to measure the shear strength and modulus of unbound components.

(DCP) is a simple field test device that saves time, low maintenance cost, and provides with a more exact continuous profile of the pavement layers. The DCP's function eliminates the need for manual driving. DCP has a huge advantage over other in-situ pavement measurement systems since it can locate weak spots fast. **Ahsan, (2014).**

### 2.5.1 Historical Development of DCP

Scala in South Africa was the first to establish the Dynamic Cone Penetration test (DCP) as an in-situ pavement measurement technique for assessing pavement layer ability Scala, (1956). The early development of the DCP was reported by Scala from Australia in 1959 as an in situ geotechnical assessment technique for evaluating the strength of subgrade soils and base and sub-base materials, of new and existing flexible pavement structures Scala (1959). DCP is also used for quality control of compaction of some soils and also in shallow subsurface investigation as an alternative to other expensive and time-consuming approaches **Rodrigo, (2003).**

Since a soil's shear resistance is its ability to withstand load, the Dynamic Cone Penetrometer (DCP) has been used to test its in-situ shear resistance. In 1969, van, (2015) engineered a newer version of the Dynamic Cone Penetrometer with a 30° cone.

DCP was widely used in South Africa, the United Kingdom, Australia, and New Zealand, as well as many states in the United States, including California, Florida, Illinois, Minnesota, and Kansas. The pavement layers and subgrades were characterized in Mississippi and Texas. DCP has also been used by the US Corps of Engineers for in-situ research. DCP has been shown to be a reliable method for determining pavement layer and subgrade intensity parameters **Ahsan, (2014)**.

### **2.5.2 Theoretical Basis of DCP**

Many experiments were conducted on the theoretical analysis of the DCP system. During the 1988 Symposium on Penetration Testing, a review of the summary of the committee on the dynamic cone penetrometer testing indicated that evaluating the DCP protocol on a merely empirical or scientific basis was questionable, and many others felt that analyzing the stress condition at the cone tip was a difficult task **Nazzle, (2004)**. A review of literature reveals that considerable research was conducted investigating the stresses induced by static cone penetration in soil. For granular materials, the advancement of a static cone was investigated by **Meier, and Baladi, (1988)**. A cone penetration model was developed and was partly verified by laboratory studies. A practical relationship between DCP index (or cone index, CI) and soil properties  $c$  and  $\phi$  was derived. Since the equations developed and reported by **Meier, and Baladi, (1988)** were derived for a static cone penetrometer, they are not directly applicable to dynamic cone testing.

In a study conducted by Allersma , (1988) an optical stress/strain analysis in granular material was performed based on the advancement of a static cone

penetrometer Salgado , (1997) presented a theory based on cavity expansion analysis for determining static cone tip resistance in sands including the relative density and stress state as input parameters.

### 2.5.3 Types and Uses of DCP

The DCP apparatus developed by Scala has a cone point angle of  $60^\circ$ , a drop mass of 8.0 kg and a falling height of 575 mm. The parameters of the DCP such as the drop mass, the falling height and the cone tip design are varied with the testing method from different investigators and organizations **Jones, (2006)**.

**van, (2015)** from South Africa developed and proposed a new DCP device with 10 kg mass and 460 mm drop. Van Vuuren also indicated that his DCP is applicable for soil materials with CBR values ranging from 1 to 50. The DCP design of the ASTM D6951-03 uses an 8-kg hammer dropping through a height of 575 mm and a 608 cone. However, the Australian standard DCP (AS 1289.6.3.2) uses a 9-kg hammer with the falling height of 510 mm. The potential energy per drop for these DCP apparatus is represented in Table (2.5) **Van, (2015)**.

Table 2-5: Potential energy per drop for DCP apparatus **Van, (2015)**.

DCP design	Drop mass (Kg)	Falling Hight (m)	Potional energy per drop (J)
Scala 1959	8	0.575	45.1
Van Vuuren 1969	10	0.46	45.1
ASTM D6951-03	8	0.575	45.1
AS 1289.6.3.2	9	0.51	45

The kinetic energy per drop for whatever and all penetrometers listed in Table (2.5) would be similar to that of Scala's first model. As illustrated in Figure (2.7), DCP device was designed in almost the same way for multiple kinds and testing

operations.

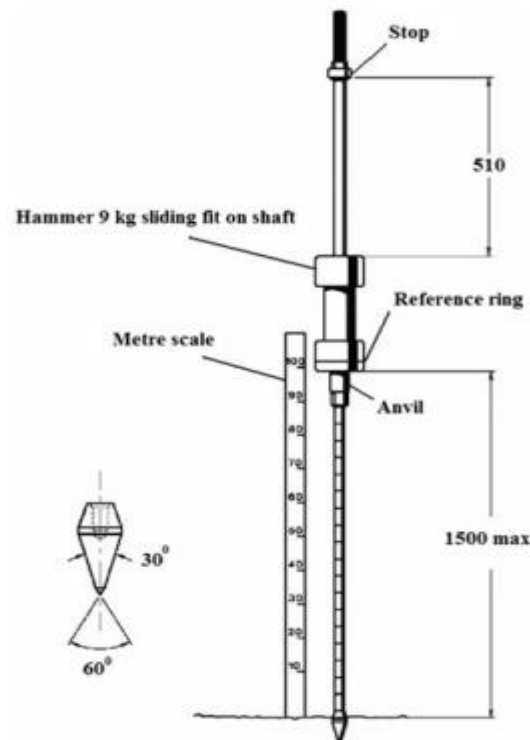


Figure 2-6: Dynamic Cone Penetrometer Index **Jones, (2006)**

The DCP was created in response to a number of issues and uncertainties associated with in-situ assessments, especially when working with difficult-to-sample soils. The DCP test can be used on any form of soil to validate a stratification around a site that has already been calculated by other methods.

### 2.5.4 Factors Affecting DCP Measurements

#### 1) Material Effects

Many researchers have conducted studies to determine how factors such as soil type, gradation, moisture content, density, plasticity, and maximum aggregate size can influence measurements taken with the Dynamic Cone Penetrometer. Plasticity, density, moisture content, and gradation all influence measurements taken with the DMM, according to (**Savage, 2012**) DCP measurements are greatly influenced by moisture content, AASHTO soil classification, confining stresses,

and dry density for fine grained soils, according to **Hassan, (1996)**, whereas **George, (2000)** indicated that the maximum aggregate size and the coefficient of uniformity affect DCP data. **Harison (1987)** discovered a correlation between DCPI, moisture content, and dry unit weight, as seen in Figure (2.9).

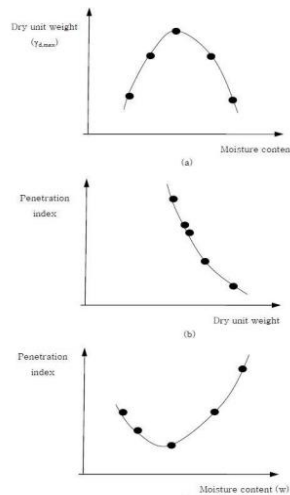


Figure 2-7: correlation between dry unit weight, moisture content, penetration index **Harison, (1987)**.

## 2) Vertical Confinement Effects

**Liven (1995)** investigated the impact of vertical confinement on the strength of soil derived from DCP measurements, and located no impact of vertical confinement by rigid pavement structures or higher cohesive layers on the DCP information of lower cohesive subgrade layers. However, the higher asphaltic layers have a vertical confinement impact on the DCP information of the granular pavement layers. This impact could also be caused by friction generated within the DCP shaft by leaning penetration or by the granular material on the shaft surface collapsing throughout penetration.

## 3) Side Friction Effect

The non-vertical penetration of the DCP shaft into the soil causes side friction, which is frequently produced while penetrating. It may also be generated when a collapsible granular substance was penetrated. In cohesive soils, however, the

amount of side friction produced was always minimal. A correction factor could be used to adjust the DCP value for the side friction effect, according to **Livneh (2000)**.

### 2.5.5 Correlation Between DCP and Soil Properties

Assessment of structural properties of the pavement layers by using of DCP test that required the development of reliable correlations with conventional methods such as the CBR test. A number of researchers were performed the development of empirical relationship between dynamic cone penetration resistance (DCPI) and CBR measurements Kleyn, (1975), Smith and Pratt, (1983), Harrison, (1986), Livneh and Ishai, (1987), and Livneh (1994). According to the summary of past studies, Numerous correlations were developed between the DCP test summary and CBR values. Table (2.6) summarizes the theoretical models that were developed for numerous soil types.

Table 2-6: Relationships between the CBR and the DCPI **Jameson, (2010)**.

References	Correlation equation	Conditions for research	R-Squared
Kleyn (1975)	$\text{Log CBR} = 2.620 - 1.270 \log (\text{DCPI})$	CBR: Lab, DCP: Field	Un available
Smith and Pratt (1983)	$\text{Log CBR} = 2.555 - 1.450 \log (\text{DCPI})$	CBR: Lab, DCP: Field	0.85
Harison (1989)	$\text{Log CBR} = 2.560 - 1.160 \log (\text{DCPI})$	CBR: Lab, DCP: Field	0.97
Livneh (1987)	$\text{Log CBR} = 2.20 - 0.7 [\log (\text{PR})]^{1.5}$	CBR: Lab, DCP: Field	0.93
Livneh et al. (1992)	$\text{Log CBR} = 2.450 - 1.120 \log (\text{DCPI})$	CBR: Lab & Field, DCP: Field	Un available
Continued. Relationships between the CBR and the DCPI ( Jameson, 2010)			
Coonse (1999)	$\text{Log CBR} = 2.530 - 1.140 \log (\text{DCPI})$	CBR: Lab, DCP: Field	This item is not available
Gabr et al. (2000)	$\text{Log CBR} = 1.550 - 0.550 \log (\text{DCPI})$	CBR: Lab, DCP: Field	This item is not available



\*where PR is the penetration through the layer in millimeters.

## 2.6 Summary

From the extensive literature review that was achieved, the following points can be highlighted:

- Subgrade strength and compaction were a very important factor for evaluation airfield and highway pavement design, whereas, under limited lab facilities, this property can be determine using LWD and DCP.
- As the laboratory tests are costly, time consuming, need to sample and considered as a destructive test, the field tests were suggested to evaluate the strength and compaction of pavement layers.
- Due to the simplicity and rapidity, recently conducting field test by LWD was widely used to evaluate the subgrade strength of subgrade soils.
- However, in this research, the quality assessment by using LWD was suggested to extend the current knowledge regarding the prediction of subgrade compaction values from advanced techniques.
- The DCP device was used for evaluation of in-situ subgrade strength, recently DCP used by geotechnical and pavement engineers due to their simplicity and low operation cost.

However, in this research, the correlation between the density, strength, and dynamic measurements were suggested to extend the current knowledge regarding the prediction of subgrade density and strength values from advanced techniques.

## CHAPTER THREE

### LABORATORY EXPERIMENTAL PROGRAM

#### 3.1 Introduction

This chapter provides a comprehensive presentation of the laboratory testing procedures that were carried out to determine the density, and strength of subgrade soils. It goes also over the experimental research methodology that were adopted to achieve the objectives of this work.

#### 3.2 Test Materials

Subgrade soils collected from three different roadway projects were tested in the lab for quality assessment evaluation. The following subsections presents soils selections and their geotechnical characteristics.

##### 3.2.1 Soil Types and Locations

In this research three types of soil were excavated and collected from different locations in Karbala city and tested in the laboratory. The standard A-3 subgrade materials were evaluated. Three roadway projects were located in (1) Al- Tahadi site, (2) Al-Fares site, and (3) Al- Intifada site. Figure 3.1 illustrates an aerial view of the three locations in Karbala city.

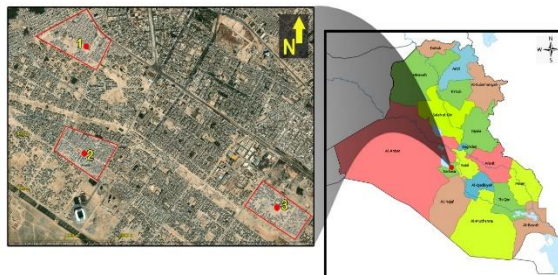


Figure 3-1: Aerial photo of three field sites in Karbala.

### 3.2.2 Physical and Chemical Properties of Subgrade soils

The basic properties of each soil selected in this work were assessed in the laboratory. The soil was classified as (A-3) soil classifications, and poorly graded sand (SP) according to American Association of State Highway and Transportation Officials (AASHTO M145-91, 2012) and the American Society for Testing and Materials (ASTM D 2487). Figure (3.2) shows grain-size distribution curves of the selected soils. Table (3.1) summarizes results of laboratory tests that were carried out to determine basic soil properties.

Table (3.1): Basic Physical and Chemical Properties of Subgrade Soils

Property	Test Result			Specification
	Soil Location	Al-Fares	Al-Tahadi	
AASHTO Classification	A-3	A-3	A-3	AASHTO M 145
USCS Classification	Poorly graded sand (SP)	Poorly graded (SP)	Poorly graded sand (SP)	ASTM D 2487
Max.Dry Unit Weight	2.105	1.83	1.975	ASTM D 1557
OMC	7.8	9.5	7.8	ASTM D 1557
D10,D30,D60	0.126, 0.208, 0.406	0.196, 0.331, 0.584	0.195, 0.276, 0.548	ASTM D2487
Specific Gravity	2.6	2.6	2.6	ASTM D 854
Uniformity Coefficient (Cu)	3.215	2.817	2.973	ASTM D 2487
Curvature Coefficient (Cc)	0.844	0.715	0.953	ASTM D 2487
Gravel Fraction (GF)	0	0	0	ASTM D2487
Sand Fraction (SF)	3	1.9	1.5	ASTM D2487
CBR Soaked	19.21	20	19.8	ASTM D 1883
CBR Unsoaked	68	60	40	ASTM D 1883
Chemical characteristics				
Location	Al-Intifadah	Al- Tahadi	Al- Fares	
SO3	2.915	3.807	2.726	
Gypsum	5.862	6.268	8.185	

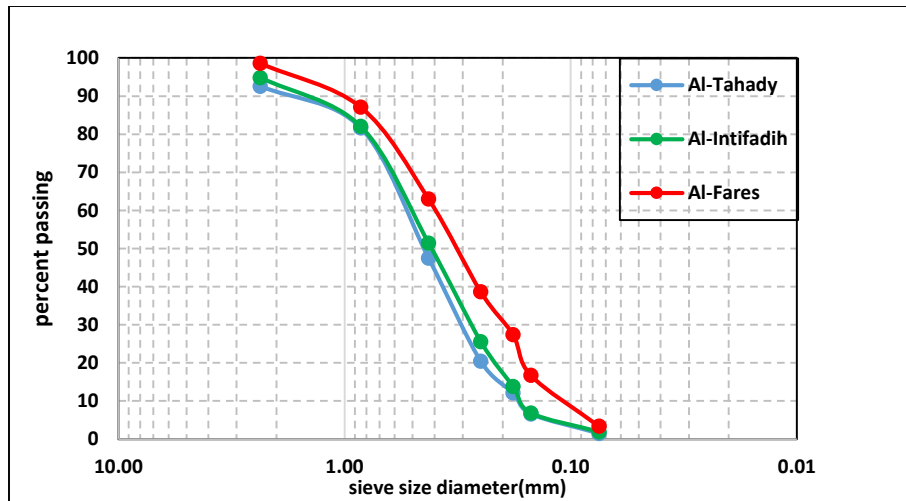
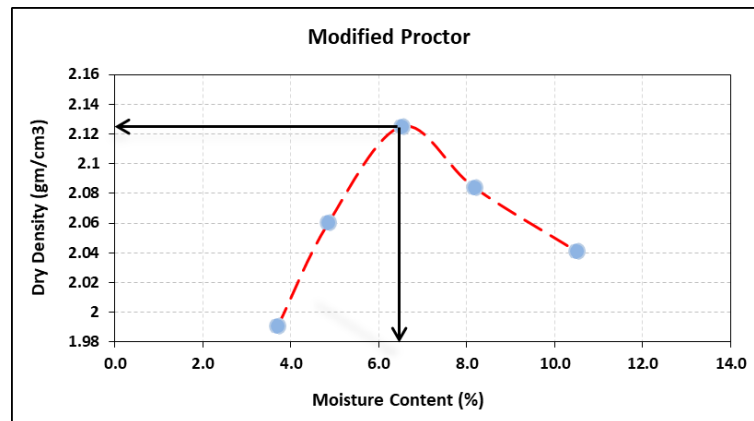
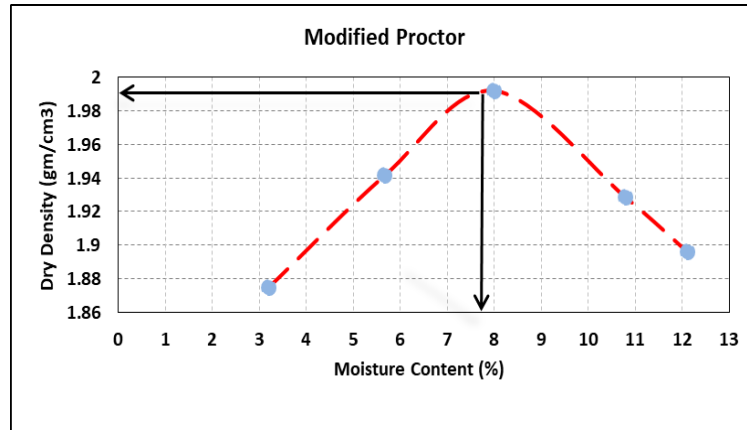


Figure 3-2: Grain Size Distribution of Al-Faris, Al-Tahadi, Al-Intifadah sites

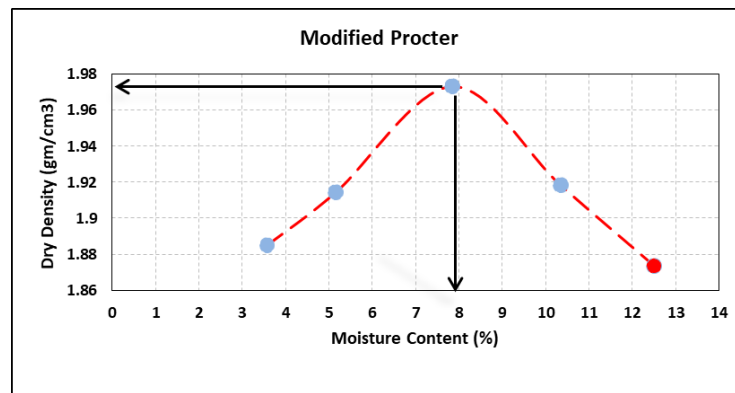
The proctor test described conformed with the (ASTM) requirements in most respects. ASTM D 1557 currently specifies the procedures and equipment requirements for the modified Proctor compaction test. The Proctor compaction test was a laboratory procedure for evaluating the optimal moisture content at which a particular soil type become densest and reach it is maximum dry density. The result of modified proctor shown in Figure (3.3).



(a)



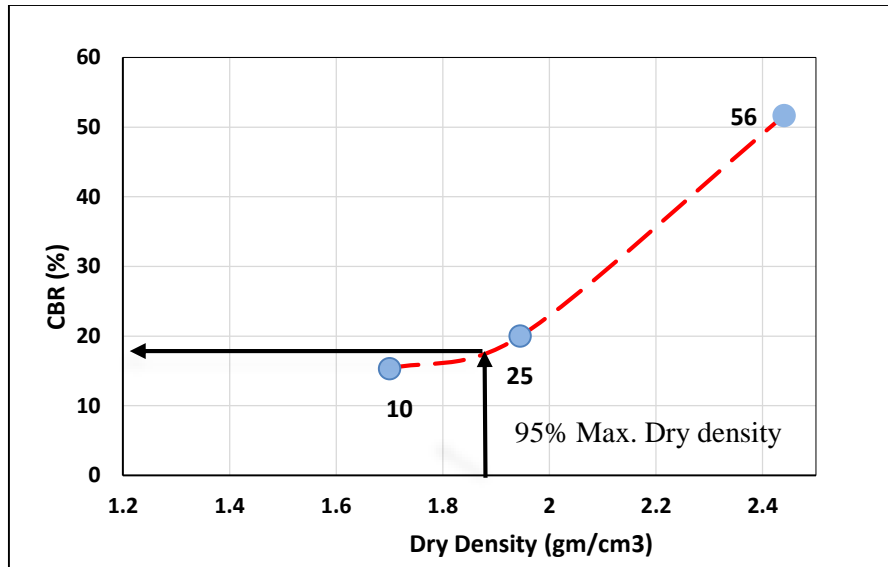
(b)



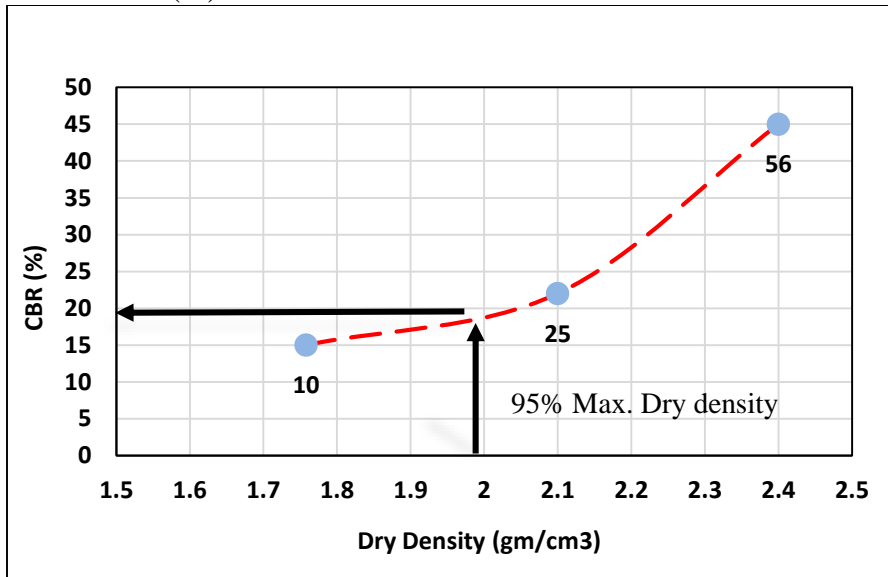
(c)

Figure 3-3: Proctor Test Curves of (a) Al-Faris, (b) Al-Tahadi , (c) Al-Intifadah sites

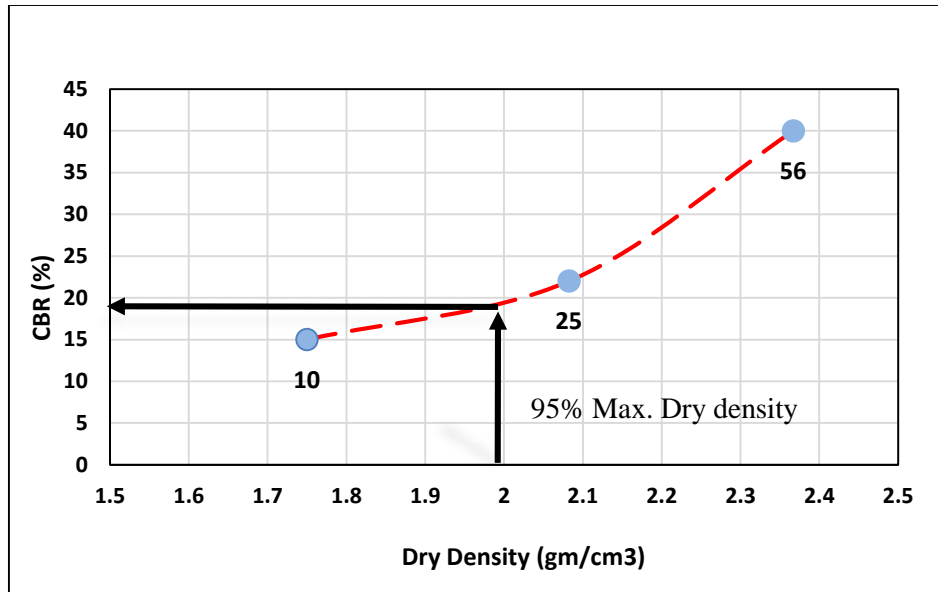
Samples taken from test sections were also subjected to CBR laboratory examinations. All samples were prepared in compliance with ASTM D1883-99 using soaked and unsoaked CBR, and all samples were prepared at the wet content specified in the research. The summary of the CBR tests were conferred in Figure (3.4) and (3.5). (Nazzal, 2003)



(A) Soaked CBR Test Curves of Al-Faris site

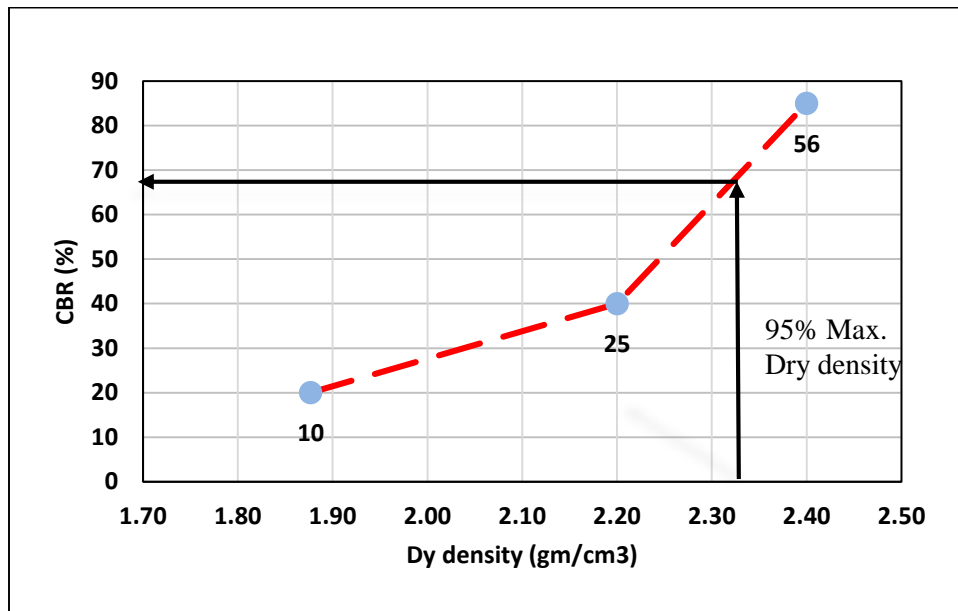


(B) Soaked CBR Test Curves of Al-Intifada site

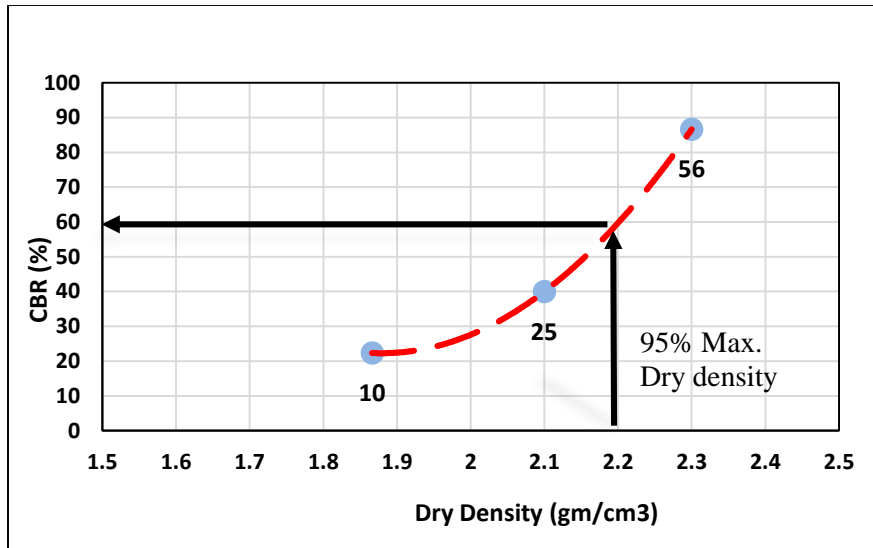


(C) Soaked CBR test curve of Al-Tahady site.

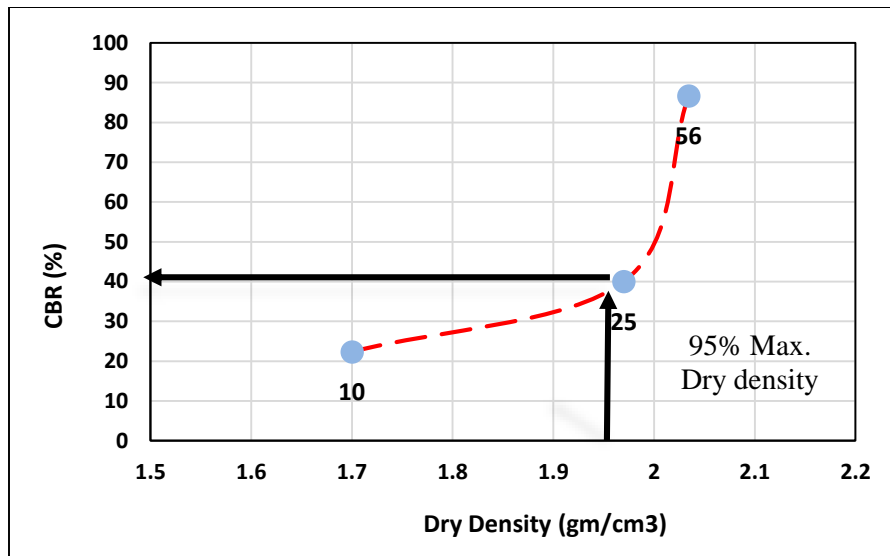
Figure 3-4: Soaked CBR Test Curves of (a) Al-Faris, (b) Al-Tahadi, (c) Al-Intifadah sites.



(A) Unsoaked CBR test for Al-Faris site.



(B) Unsoaked CBR test for Al-Intifada site.



(C) Unsoaked CBR test for Al-Tahady site.

Figure 3-5: Unsoaked CBR Test Curves of (a) Al-Faris, (b) Al-Tahadi, (c) Al-Intifadah sites

### 3.3 Experimental Work

#### 3.3.1 Laboratory Testing Setup

The main goal of the field experimentation program was to determine the degree of in-situ compaction and strength of subgrades pavement layers by computing dry density and California bearing resistance, and dynamic stiffness characteristics.



Special test method and various accessories were designed and manufactured to achieve this goal. As shown in Figure (3.6), a steel box with dimensions (length = 2.4m, height = 1.25, width = 1.2m) were used to simulate in-situ subgrade conditions. The function of the steel box was to represent the subgrade layer in order to perform compaction and other tests. The height of the steel box was identified depending on the deformation zone of the light weight deflectometer (LWD) test. The total deformation influence is  $(1.5-2) B$  from LWD diameter ( $D=300$  mm.), so that zone of influence depth = 0.6m The following factors were considered when determining the box dimensions: The thickness of the actual road layers that can be represented in the laboratory, the Zone of influence of the Plate tests, depth of influence of Plate tests. steel box and data acquisition system, this manufactured apparatus was considered the first device that was designed by the University of Karbala to provide a similar environment for sites and conducting field tests

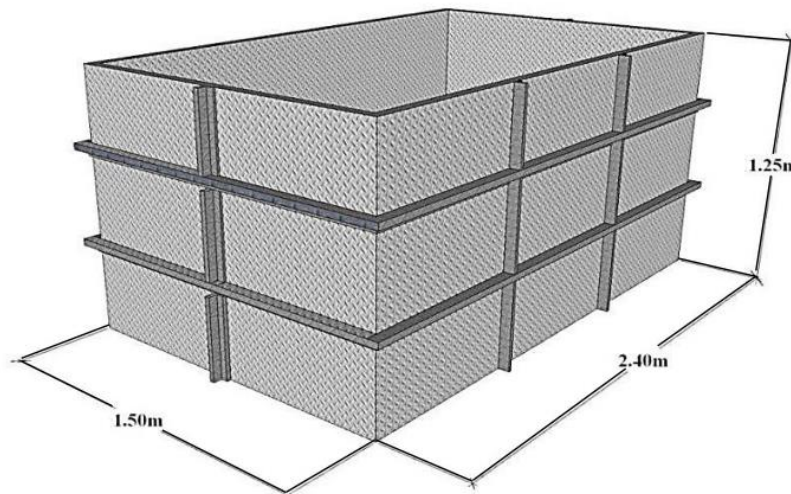


**Figure 3-6: Steel Box**

### **3.3.2 Soil Preparations and System Layout**

Soils were excavated and collected from three locations in Karbala city at depth 0.5m below the surface. Each subgrade soil was tested and compacted in the laboratory,

and the performance of the subgrade layer structure was evaluated using three in-situ testing method: (LWD) test, (DCP) test, and sand replacement method (SRM) to measure density and water content.

To build a (0.6 m) thick compacted subgrade layer, approximately( $3 \text{ m}^3$ ) of each soil was needed. The subgrade was prepared by achieving the optimum water content using an electrical mixer, as shown in Figure (3.7). During compaction, the water content and dry unit weight of each soil layer were registered.

The subgrade was then compacted as layers by (15 cm per layer) within the measuring steel box until it reached the desired height (60 cm). Figure (3.8) shows first and final subgrade layers in laboratory during compacted.



**Figure 3.7: Electrical Mixer**



Figure 3-8: Illustrate Soil Preparation of Subgrade Soils.

Each soil layer was compacted, a compactor (design: petrol engine with 6 (KW) of power, 160 (Kg) of weight, and 4000 (VPM) of frequency) was used to achieve the compacted effort. For each soil type, three compaction efforts were considered based on the number of compactor passes (NOP) performed to each layer. Compaction effort was divided into three categories: ten number of passing (10 NOP), fourteen number of passing (14 NOP), and eighteen number of passing (18 NOP) (18 NOP).

As shown in Figure (3.9), the soil surface was divided into six testing areas, each of which was subjected to a variety of tests, including the 1) (LWD) test, 2) (DCP) test, and 3) (SRM) test.

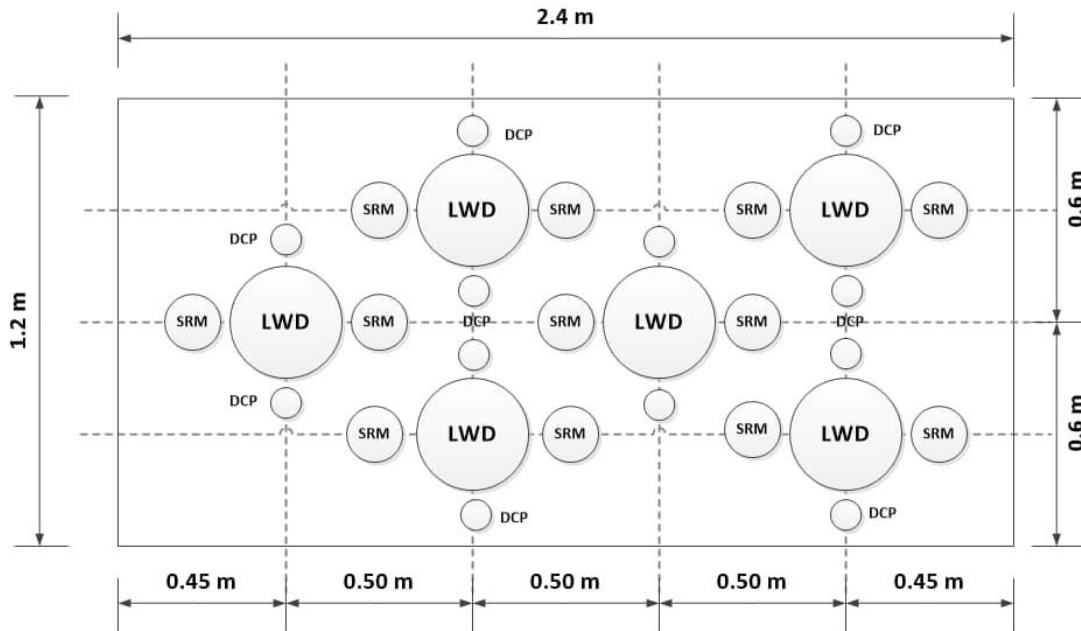


Figure 3-9: Layout of Testing Points.

### 3.4 Experimental Research Methodology

Various highway parts in Karbala were chosen for the experimental research program. The selection of highway projects has been based on covering as much as possible the predominant soil types that were available in Karbala.

Soil samples collected from fields were tested in the lab to assess their basic engineering properties. Different laboratory tests were implemented including: grain size distribution, CBR test, Proctor test, specific gravity test. Table (3.2) summarizes total number of laboratory tests performed in this work. Three test methods: [1] light weight deflectometer (LWD), [2] dynamic cone penetrometer (DCP), and [3] sand replacement testing methods (SRM) were used to obtain inclusive measurements about in-situ strength and compaction characteristics of subgrade layers. The soil

would be first tested in laboratory, then it would be subject to several compaction level to examine the effect of degree of compaction on soil properties.

Table 3-2: Summary of Total Numbers of Laboratory Tests

Tests Type		Soils Type and Locations			Complete No. of Tests
Physical Properties		Al-Fares (A-3)	Al-Tahadi (A-3)	Al-Intifada (A-3)	
CBR	Soaked	8	8	8	24
	Unsoaked	8	8	8	24
Proctor	Standard	8	8	8	24
	Modified	8	8	8	24
Grain Size Distribution		1	1	1	3
Specific Gravity		3	3	3	9
Chemical Test		2	2	2	6
Laboratory Tests	LWD	18	18	18	54
	DCP	36	36	36	108
	SRM	36	36	36	108

Three field measurements were be obtained from (LWD): surface deflection, degree of compatibility, and dynamic modules. Two field measurements can be obtaine from (DCP): dynamic penetration index, in-situ CBR. Additionally, density and moisture content will be determined in the field use (SRM). Methodology stages can be seen in Figure (3.10).

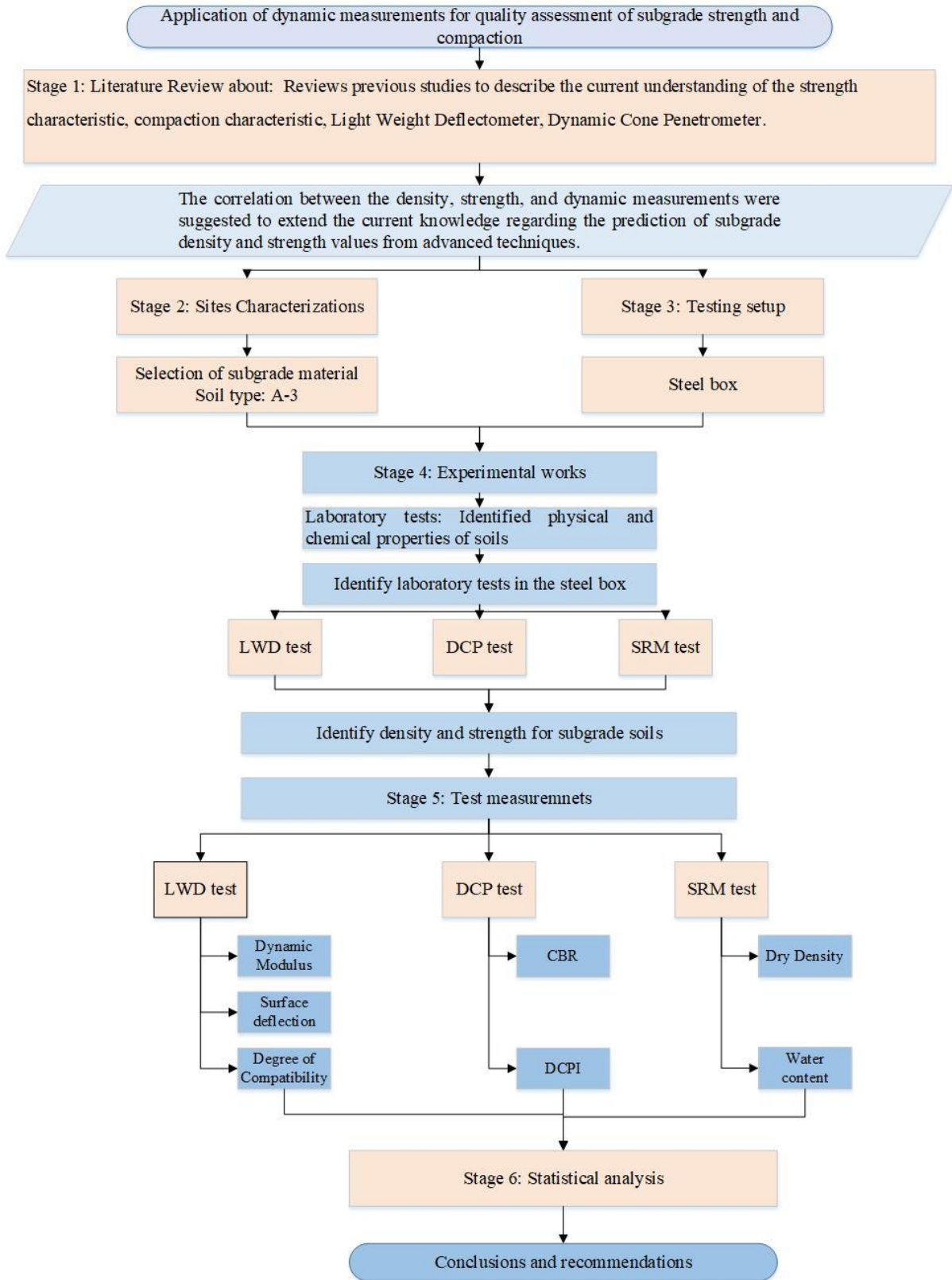


Figure 3-10: Research Methodology

### 3.5 Test Methods

#### 3.5.1 Light Weight Deflectometer (LWD)

The light weight deflectometer (LWD) was a portable, scaled-down version of the falling deflectometer, as shown in Figure (3.11). The model of LWD device used in this study was Zorn ZFG3. The LWD outline as a nondestructive testing device accustomed verify in-situ stiffness properties of pavement materials underneath the impact of dynamic impact loads at in- situ conditions. This device provides one dynamic stiffness back-calculated supported actual wave rate propagated within a pavement layer (**Rayden and Mooney, 2009**). The influence depth of LWD pulse was at vary (1.5 - 2.0) times of loading plate diameter. For this reason, the LWD device is taken into account as not appropriate device to evaluate in-situ stiffness for depth was usually larger than 50.8 cm (20 inches).



Figure 3-11: Components of LWD Field Test Equipment

Three in-situ measurements were produced by the LWD: vertical surface deflection ( $\delta$ ) and dynamic modulus ( $E_d$ ), and degree of compatibility. Additionally, this device provides soil deflection response with time. Integrating impulse velocity readings from an accelerometer mounted within a circular loading plate is used to calculate surface deflections. Then, using Boussineq elastic half-space theory, the vertical deflections calculated from accelerometer readings are used to calculate surface soil modulus. The following expression represents the Boussineq elastic theory, which relates displacements to applied dynamic pressure for a rigid or flexible foundation **Shaban, (2016)**.

$$E_d = \frac{(1-v^2)\sigma_0 a}{\delta} \cdot f \quad (3.1)$$

Here  $E_d$  has been the dynamic soil modulus (MPa),  $\delta$  seems to be the soil surface deflection (mm),  $\sigma_0$  is really the applied dynamic stress (MPa),  $a$  is radius of the loading plate (mm), and  $f$  is the plate rigidity factor which is typically assumed ( $f=2$ ), and  $v$  is Poisson's ratio.

The LWD measurement technique used in this research can be explained simply as follows:

- 1) A loading plate with a diameter of 300 mm that is placed in contact with the testing surface to conduct a uniform distribution load.
- 2) A 10-kg dropping weight falls from a height of 116 cm, built to be powered by one person with minimal resistance or friction. According to ASTM E2583, (2007), three drops were made on each testing point when the dropping weight reached the loading plate, resulting in a half sine formed load on the testing surface, to reduce the impact of loose soil particles that might cause unfavorable



plastic deformations. Dynamic modulus, vertical surface deflection, and degree of compatibility were amongst the test parameters. The vertical deflections created by accelerometer readings are used to obtain surface soil modulus based on Boussinesq elastic half-space theory. The surface deflections are determined by integrating impulse velocity readings of an accelerometer fixed within a circular loading plate.

- 3) The load was uniformly transferred to the plate using a buffer system, explained that increasing the amount of buffers causes the device to stiffen and the pulse length to shorten.
- 4) A dynamic parameter is measured using deflection sensors such as an accelerometer.

### **3.5.2 Dynamic Cone Penetrometer (DCP)**

This test method covers the calculation of the Dynamic Cone Penetrometer's penetration rate through undisturbed soils or compacted materials, or both, using an 8-kg [17.6-lb] hammer. The penetration rate may be linked to in situ soil strength (i.e., CBR value).

The DCP structure is made up of two vertical shafts that are joined at the anvil (ASTM D 6951-03, 2009):

1. Both handle and hammer are located upon this higher shaft. The handle is used to give the hammer a consistent drop height of 575 mm and also to allow the user to just hold the DCP vertical. The hammer weighs 8 kg and has a constant force of impact.
2. The bottom shaft features a degree anvil at the top and a pointed cone at the bottom. The anvil prevents the hammer against dropping below the standard drop height. The anvil keeps the hammer from falling below the recommended

drop height. As once hammer was born and hits the anvil, the cone was driven into the ground. Schematic diagram of the DCP are shown in Figure (3.13).

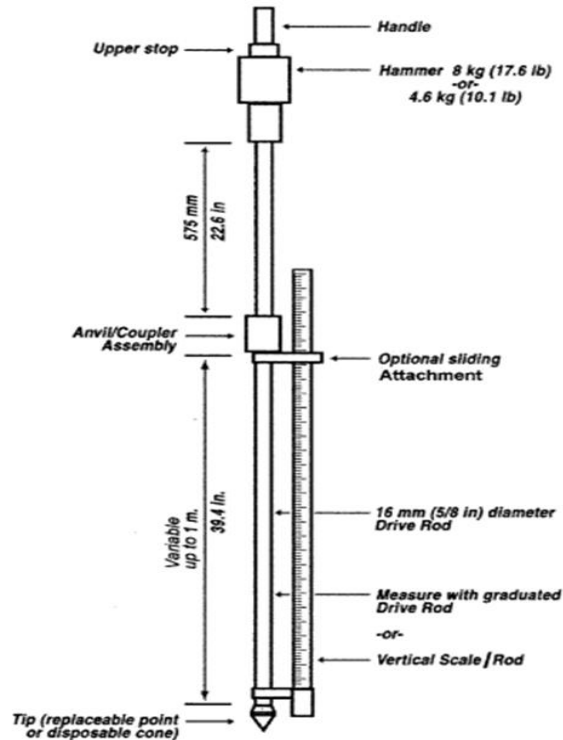


Figure 3-12: Schematic diagram of DCP Device **ASTM D 6951-03, (2009)**.

The DCP test protocol is defined by ASTM D 6951-03 and the Minnesota Department of Transportation (Mn/DOT). The test procedure used during this project is described briefly below:

1. Make sure the equipment is free of fatigue and broken parts, and that all links are firmly fastened.
2. The device is kept vertically by the handle on the top shaft by the user.
3. The operator elevates the hammer from the anvil towards the handle and releases after a second person estimates the distance between the bottom of the anvil as well as the ground.

4. At the bottom of the anvil, the second person reports the new height. An extraction jack should be used to remove the DCP from the newly created cavity. If the tip is disposable, a gentle tap on the handle with the hammer is appropriate. Figures (3.14), (3.15) show DCP in laboratory and typical results.



Figure 3-13: Dynamic Cone Penetrometer

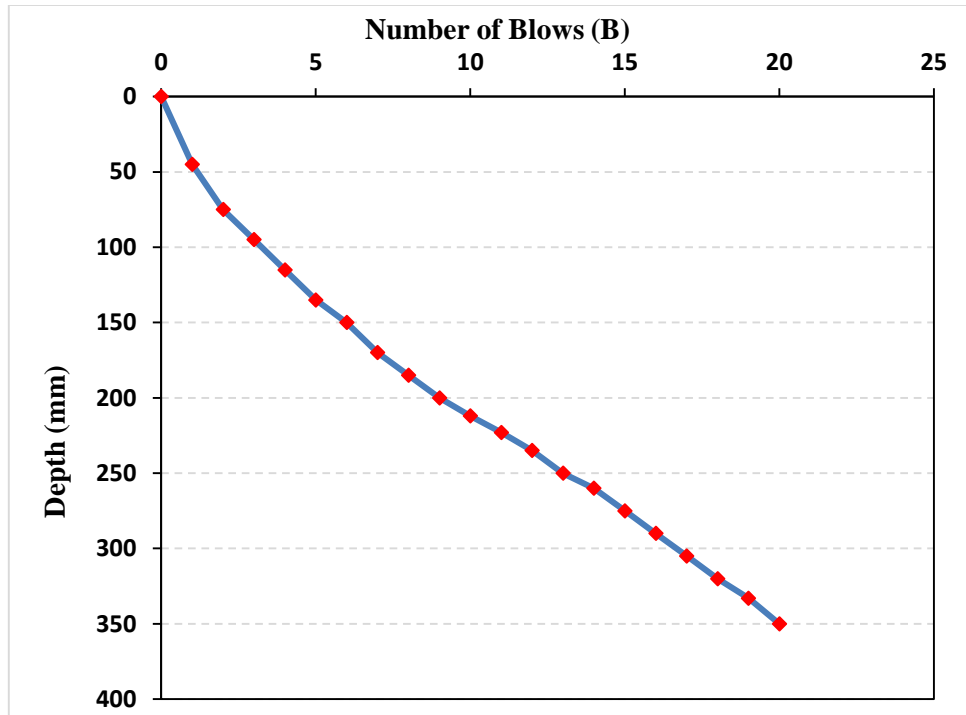


Figure 3-14: Typical Results of DCP.

### 3.5.3 Sand Replacement Method (SRM)

According to (ASTM D1556, 2015), this test is used to assess the field density and moisture content of soil. SRM is ideal for natural, saturated, or highly plastic soils that will deform or compress during the excavation of the test hole, but it is also suitable for soils with appreciable quantities of rock or coarse materials that exceed 1.5 in. (38 mm).

A test hole is hand excavated in the soil to be tested and all the material from the hole is saved in a container. The hole is filled with free flowing sand of a known density, and the volume is determined. The in-place wet density of the soil is determined by dividing the wet mass of the removed material by the volume of the hole.

The water content of the material from the hole is determined and the dry mass of the material and the in-place dry density are calculated using the wet mass of the

soil, the water content, and the volume of the hole. Figure (3.15) shows SRM apparatus.



Figure 3-15: SRM Apparatus.

## **CHAPTER FOUR**

### **EXPERIMENTAL TESTS RESULTS**

#### **4.1 Introduction**

This chapter presents and discusses the results of the experimental works carried out for three subgrade soils located at: Al-Fares, Al-Intifada, Al-Tahady. Total number of LWD, DCP, and SRM tests performed on subgrade soils were: 54 LWD tests, 108 tests results were collected by for each DCP and SRM to obtain the dry density and moisture content, respectively.

#### **4.2 Results of SRM Test**

The water content and dry density measurements of subgrade soils are summarized in Table (4.1). The densities were determined based on how many times the compacting device passed over the soil layers. The results revealed that when increasing the number of passes, the dry density increases.

For Al-Faris subgrade soils, the results illustrate that the dry density varied from  $1.698 \text{ gm/cm}^3$  to  $2.02 \text{ gm/cm}^3$ , and moisture content varied from 7.146 % to 7.844%, while the results for Al-Intifada subgrade soil illustrate that the dry density varied from  $1.712 \text{ gm/cm}^3$  to  $1.942 \text{ gm/cm}^3$ , and moisture content varied from 9.275 % to 9.867%. Finally, the results for Al-Tahady subgrade soil illustrate that the dry density varied from  $1.689 \text{ gm/cm}^3$  to  $1.981 \text{ gm/cm}^3$ , and moisture content varied from 9.719 % to 10.10%.

Table 4-1: Summary of SRM test results of subgrade soils at: Al- Fares, Al- Intifada, and Al-Tahady sites, (10,14,18) NOP.

Test Points		Al-Fares		Al-Intifada		Al-Tahady	
		W.C (%)	Dry Density (gm/cm <sup>3</sup> )	W.C (%)	Dry Density (gm/cm <sup>3</sup> )	W.C (%)	Dry Density (gm/cm <sup>3</sup> )
1	A1	7.514	1.698	9.429	1.739	9.527	1.808
	B1	7.246	1.789	8.291	1.777	10.100	1.689
2	A2	7.773	1.771	8.187	1.724	9.654	1.735
	B2	7.844	1.821	9.500	1.742	10.100	1.810
3	A3	7.710	1.804	9.278	1.741	10.210	1.784
	B3	7.743	1.765	9.867	1.744	9.422	1.752
4	A4	7.750	1.806	8.108	1.787	10.087	1.760
	B4	7.248	1.755	9.091	1.712	9.639	1.696
5	A5	7.367	1.788	8.235	1.771	9.583	1.766
	B5	7.548	1.783	9.722	1.751	9.885	1.780
6	A6	7.490	1.719	9.643	1.748	9.698	1.702
	B6	7.672	1.727	9.248	1.731	9.868	1.797
	Average	7.575	1.769	9.050	1.747	9.789	1.757
	STD	0.198	0.036	0.631	0.021	0.221	0.041
	COV	2.607	2.050	6.977	1.197	2.255	2.338
1	A1	7.774	1.931	9.589	1.822	9.448	1.867
	B1	7.911	1.956	9.825	1.792	9.765	1.833
2	A2	7.579	2.017	9.231	1.811	10.198	1.808
	B2	7.413	1.935	9.538	1.776	9.512	1.826
3	A3	7.759	1.927	9.394	1.822	9.963	1.829
	B3	7.63	1.934	9.333	1.78	9.867	1.841
4	A4	7.661	1.948	9.244	1.766	9.661	1.797
	B4	7.492	1.909	9.355	1.797	9.809	1.828
5	A5	7.659	1.915	9.846	1.816	10.37	1.813
	B5	7.889	1.904	9.333	1.809	9.741	1.76
6	A6	7.752	1.939	9.778	1.789	10.077	1.789
	B6	7.877	1.936	9.841	1.833	9.944	1.812
	Average	7.700	1.938	9.526	1.801	9.863	1.817
	STD	0.150	0.028	0.232	0.020	0.257	0.026
	COV	1.954	1.444	2.436	1.114	2.610	1.442
1	A1	7.478	2.017	9.275	1.889	10.200	1.876
	B1	7.784	2.033	9.286	1.863	9.686	1.855
2	A2	7.313	2.061	9.867	1.875	9.890	1.879
	B2	7.966	2.001	9.383	1.891	10.300	1.871
3	A3	7.146	2.026	9.697	1.877	9.589	1.896
	B3	7.555	2.01	9.508	1.903	9.904	1.914
4	A4	8.36	2.016	9.5	1.895	9.763	1.910
	B4	7.475	1.98	9.859	1.942	9.719	1.912
5	A5	7.677	2.008	8.955	1.93	9.882	1.921
	B5	7.726	1.981	9.804	1.864	9.231	2.112
6	A6	7.287	2.019	9.643	1.941	9.583	1.981
	B6	7.314	2.02	8.197	1.904	9.577	1.891
	Average	7.758	2.014	9.415	1.898	9.735	1.915
	STD	0.235	0.021	0.450	0.026	0.212	0.063
	COV	3.024	1.039	4.782	1.391	2.182	3.307

For Al-Faris subgrade soils, the percent of increase in dry density due to compaction is 19%, but the percent of decrease in water content is 9%, while for Al-Intifada subgrade soils the percent of increase in dry density due to compaction is 13%, but the percent of decrease in water content is 6%. Finally, for Al-Tahady subgrade soils the percent of increase in dry density due to compaction is 17%, but the percent of decrease in water content is 7%

The ratio of the standard deviation to the average value (i.e., coefficient of variance(COV)) was calculated for SRM measurements to examine the variation of determined SRM. The lower the value of the coefficient of variation, the more precise the data were measured. As listed in table (4.1), the results of COV were approximately less than 10% which reflects an acceptable variation (i.e., high consistent measurements).

The results of dry density and moisture content which determined by SRM methods for three locations of soil shown in Figures (4.1). This figure showed that there is significant relationship between dry density and moisture content.

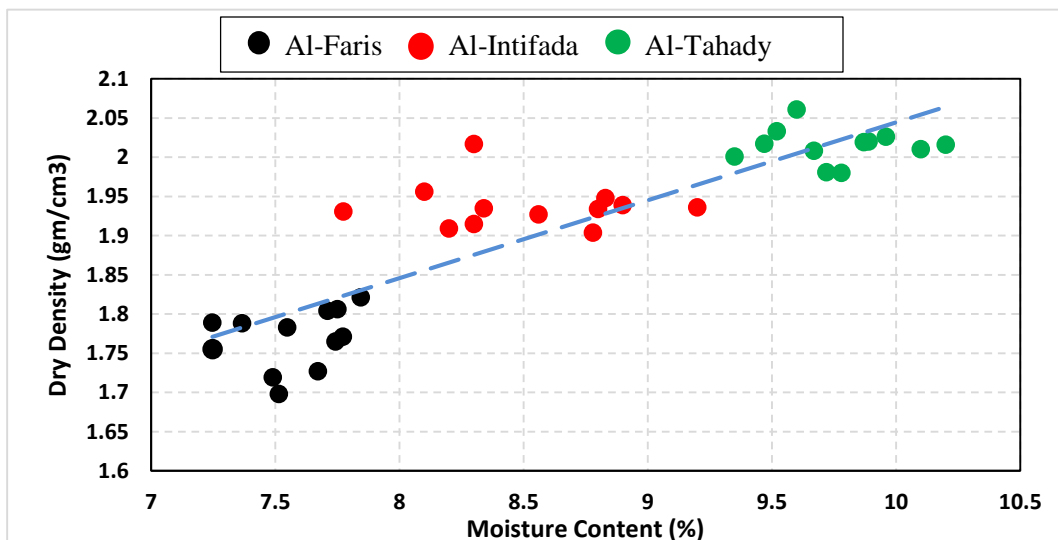


Figure (4.1): Relationship between dry density and moisture content



Figure (4.2) show that the increase in compaction effort from 10 to 14 then to 18, lead to an increase in the dry density. Al-Faris subgrade soil shows more influence in increasing in compaction effort than Al-Intifada and Al-Tahady. The increment in dry density for Al-Faris subgrade soils might be further to physical characteristics, is due to: different in grain size distribution, water content, compaction effort, and percentage of fine content, that agreed completely with **Kuttah, (2019)** reported that dry density value for sandy soil varied from  $1.72 \text{ gm/cm}^3$  to  $1.89 \text{ gm/cm}^3$  with moisture content 12%

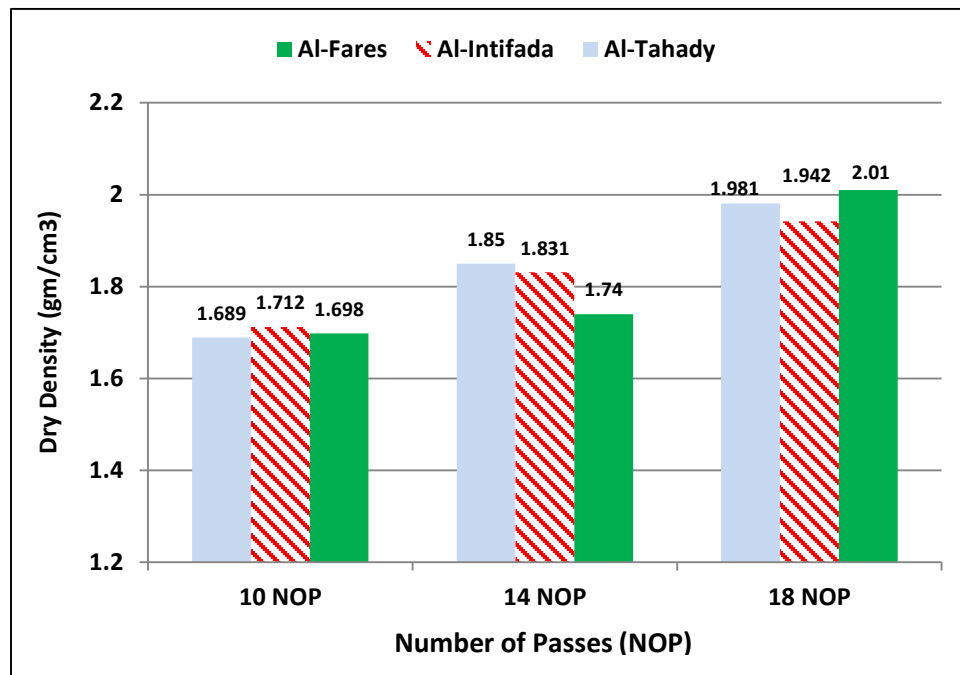


Figure (4-2): Relationship between dry density and number of passes

### 4.3 Results of LWD Test

The results of the 54 LWD testing points test from three locations with different NOP are presented in Tables (4.2) through (4.4). The LWD parameters measured throughout this study include: surface deflection ( $S_d$ ), dynamic modulus (Ed), and degree of compatibility (Dc). The results of LWD test are summarized in following sub sections.

For Al-Fares subgrade soil, the results of different number of passes (i.e., 10, 14, and 18) indicated that the values of  $S_d$  varied from 0.365 mm to 0.701 mm. Figure (4.3) illustrate average time deflection curve for subgrade soil. The results also showed that the values of  $E_d$  varied from 32.124 MPa to 61.640 MPa, and  $D_C$  ranged from 2.981ms to 4.250ms. Table (4.2) lists LWD results for three number of passes (NOP) performed for Al-Fares subgrade. As summarized in Table (4.1). The percent of increase in  $E_d$  due to compaction is 92%, but the percent of decrease in  $S_d$  is 48%, and  $D_C$  is 30%.

The ratio of the standard deviation to the average value (i.e., coefficient of variance(COV)) was calculated for all LWD measurements to examine the variation of determined LWD. The lower the value of the coefficient of variation, the more precise the data were measured. As listed in table (4.2), the results of COV were approximately less than 10% which reflects an acceptable variation (i.e., high consistent measurements).

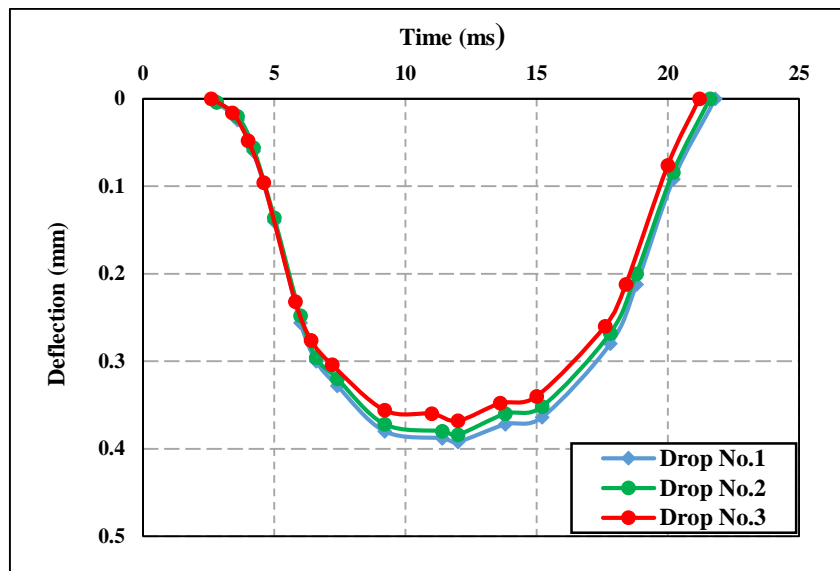


Figure 4-3 : Average time deflection curve for Al-Fares site.

Table 4-2: Summary of LWD test results for subgrade soil, at Al- Fares site.

No. of passes	Points	Surface Deflection (mm)			Mean	$E_d$ (MPa)	$D_c$ (ms)
		$\delta_1$	$\delta_2$	$\delta_3$			
10	1	0.662	0.643	0.626	0.644	34.941	3.890
	2	0.636	0.630	0.609	0.625	36.421	3.730
	3	0.675	0.637	0.595	0.636	35.380	3.640
	4	0.66	0.650	0.670	0.660	33.741	3.810
	5	0.712	0.701	0.691	0.701	32.124	3.900
	6	0.563	0.600	0.645	0.602	41.590	4.250
	Average	0.651	0.644	0.639	0.645	35.625	3.868
	STD	0.046	0.030	0.033	0.031	2.950	0.193
	COV	6.999	4.690	5.229	4.777	8.282	4.985
14	1	0.527	0.521	0.516	0.521	43.19	2.876
	2	0.465	0.462	0.449	0.459	49.02	3.332
	3	0.476	0.458	0.452	0.462	48.7	3.113
	4	0.48	0.466	0.459	0.468	48.08	3.475
	5	0.506	0.498	0.475	0.493	45.64	3.154
	6	0.415	0.428	0.416	0.42	53.57	2.936
	Average	0.478	0.472	0.461	0.470	48.033	3.147
	STD	0.034	0.029	0.030	0.031	3.195	0.208
	COV	7.310	6.321	6.550	6.618	6.652	6.625
18	1	0.564	0.524	0.508	0.532	56.160	2.981
	2	0.394	0.385	0.370	0.383	58.750	3.135
	3	0.45	0.441	0.455	0.449	50.110	3.059
	4	0.465	0.473	0.465	0.468	48.080	3.180
	5	0.503	0.496	0.481	0.493	45.640	3.012
	6	0.361	0.370	0.363	0.365	61.640	3.102
	Average	0.456	0.448	0.440	0.448	53.396	3.078
	STD	0.066	0.055	0.054	0.058	5.823	0.068
	COV	14.667	12.492	12.433	13.067	10.906	2.233

For subgrade soil from Al-Intifada site, the data extracted from the integration process indicate that values of  $S_d$  varied from 0.360 mm to 0.771 mm. Figure (4.4) illustrate average time deflection curve for subgrade soil. The results also showed that the values of  $E_d$  varied from 39.400 MPa to 64.500 MPa, and  $D_c$  ranged from 2.06ms to 4.01ms. Table (4.3) lists LWD results for three number of passes (NOP) performed for Al-Intifada subgrade. As summarized in Table (4.3). The percent of increase in  $E_d$  due to compaction is 74 %, but the percent of decrease in  $S_d$  is 53

%, and  $D_C$  is 49 %.

The ratio of the standard deviation to the average value (i.e., coefficient of variance (COV) was calculated for all LWD measurements to examine the variation of determined LWD. The lower the value of the coefficient of variation, the more precise the data were measured. As listed in table (4.3), the results of COV were approximately less than 10% which reflects an acceptable variation (i.e., high consistent measurements).

Table 4-3: LWD test results for subgrade soil A-3, at Al- Intifada site.

No. of passes	Points	surface deflection (mm)			Mean	Evd (MPa)	Dc (ms)
		$\delta_1$	$\delta_2$	$\delta_3$			
10	1	0.680	0.657	0.606	0.648	39.400	3.890
	2	0.610	0.563	0.540	0.571	41.590	4.010
	3	0.608	0.615	0.605	0.609	42.300	3.530
	4	0.610	0.620	0.640	0.623	38.180	4.060
	5	0.786	0.793	0.734	0.771	40.100	4.030
	6	0.636	0.604	0.600	0.613	39.780	3.600
	Average	0.655	0.642	0.620	0.639	40.225	3.853
STD	0.064	0.073	0.059	0.063	1.369	0.212	
COV	9.737	11.362	9.441	9.887	3.403	5.490	
14	1	0.559	0.530	0.503	0.531	42.370	3.035
	2	0.418	0.403	0.390	0.404	55.690	3.178
	3	0.610	0.570	0.546	0.572	48.755	3.608
	4	0.566	0.533	0.516	0.538	41.820	3.043
	5	0.766	0.719	0.710	0.732	49.030	3.755
	6	0.541	0.565	0.534	0.672	45.287	3.156
	Average	0.575	0.553	0.533	0.574	47.158	3.295
STD	0.102	0.092	0.094	0.105	4.721	0.280	
COV	17.855	16.729	17.650	18.329	10.012	8.525	
18	1	0.533	0.533	0.518	0.528	58.731	2.834
	2	0.361	0.357	0.363	0.360	61.640	2.982
	3	0.556	0.449	0.402	0.536	62.100	2.871
	4	0.558	0.448	0.344	0.480	64.501	2.141
	5	0.680	0.624	0.600	0.635	58.110	2.062
	6	0.487	0.452	0.433	0.457	60.041	2.781
	Average	0.529	0.477	0.443	0.499	60.851	2.610
STD	0.095	0.083	0.089	0.083	2.168	0.366	
COV	17.989	17.407	20.228	16.785	3.564	14.051	

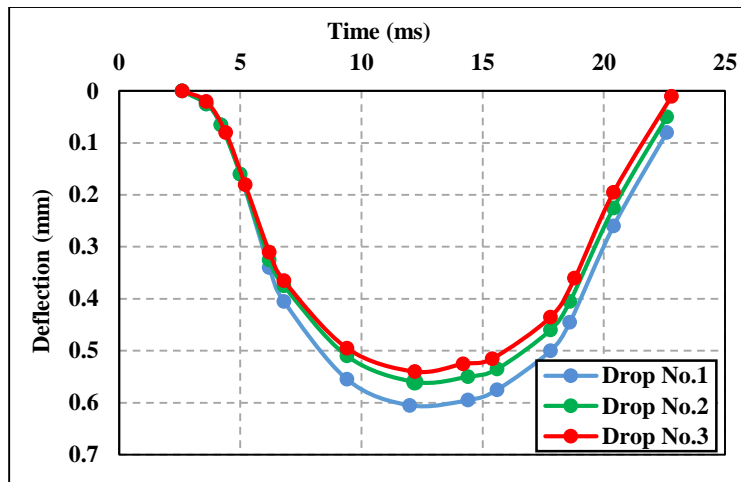


Figure 4-4: Average time deflection curve for Al-Intifada site.

For subgrade soil from Al-Tahady site, the results of the 18 LWD tests conducted on different compacted subgrade are given in table (4.4). These results exhibited that the  $S_d$  varied from 0.480 mm to 0.889 mm, Figure (4.5) illustrate average time deflection curve for subgrade soil,  $E_d$  varied from 40.16 MPa to 64.570 MPa, and  $D_C$  varied from 2.05ms to 4.060ms. As summarized in Table (4.4). The percent of increase in  $E_d$  due to compaction is 61%, but the percent of decrease in  $S_d$  is 46 %, and  $D_C$  is 50 %.

The ratio of the standard deviation to the average value (i.e., coefficient of variance (COV) was calculated for all LWD measurements to examine the variation of determined LWD. The lower the value of the coefficient of variation, the more precise the data were measured. As listed in table (4.4), the results of COV were approximately less than 10% which reflects an acceptable variation (i.e., high consistent measurements).

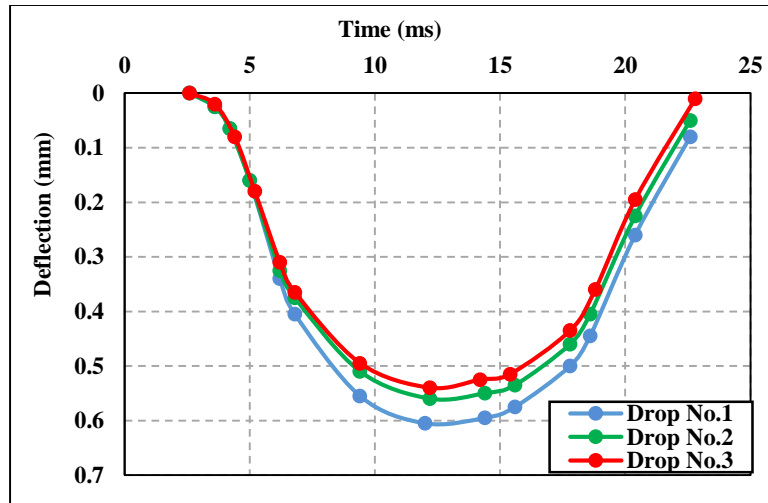
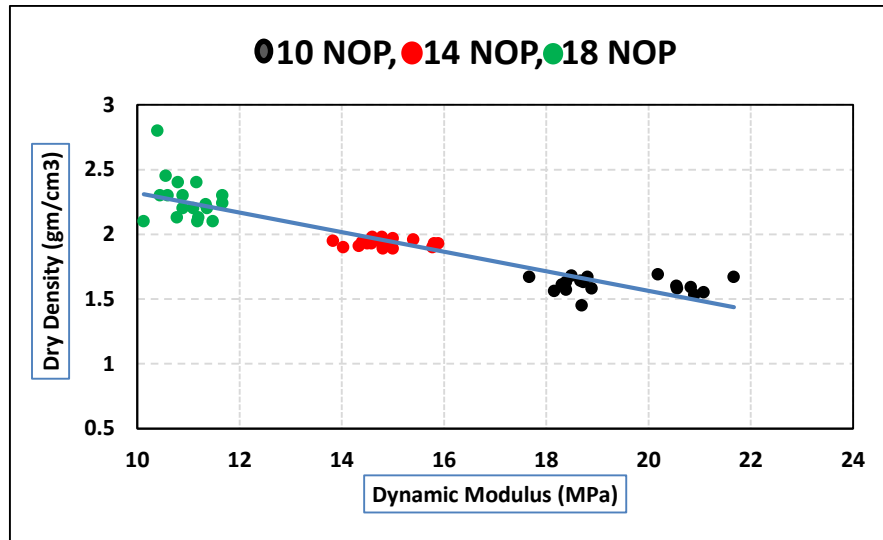


Figure 4-5: Average time deflection curve for Al-Tahady site.

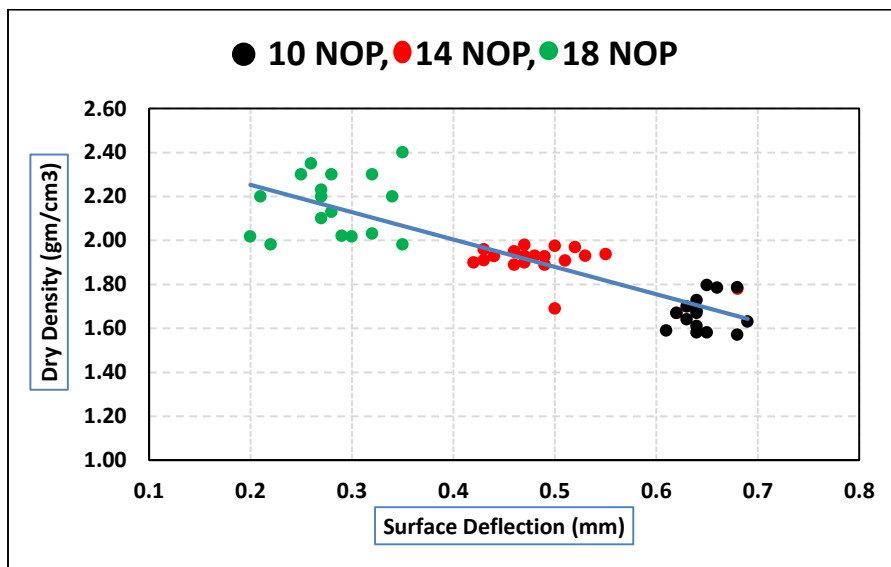
Table 4-4: LWD test results for subgrade soil A-3, at Al- Tahady site.

No. of passes	Points	surface deflection (mm)			Mean	Ed Mpa	Dc (ms)
		$\delta_1$	$\delta_2$	$\delta_3$			
10	1	0.576	0.571	0.523	0.557	40.200	3.891
	2	0.679	0.637	0.626	0.647	43.100	4.013
	3	0.787	0.777	0.744	0.769	45.120	3.530
	4	0.544	0.514	0.524	0.527	41.100	4.062
	5	0.915	0.883	0.869	0.889	42.3	4.038
	6	0.678	0.671	0.649	0.666	40.16	3.601
	Average	0.696	0.675	0.655	0.675	41.960	3.853
STD	0.125	0.123	0.121	0.123	1.728	0.211	
COV	18.004	18.317	18.588	18.254	4.118	5.490	
14	1	0.549	0.541	0.537	0.542	50.112	2.705
	2	0.524	0.495	0.488	0.502	50.080	3.202
	3	0.550	0.525	0.508	0.528	52.370	3.006
	4	0.496	0.484	0.483	0.488	53.891	2.844
	5	0.762	0.713	0.699	0.725	54.380	3.445
	6	0.852	0.777	0.759	0.796	51.400	3.261
	Average	0.622	0.589	0.579	0.596	52.038	3.077
STD	0.134	0.113	0.108	0.118	1.682	0.252	
COV	21.613	19.225	18.801	19.904	3.233	8.206	
18	1	0.663	0.652	0.635	0.65	61.700	2.549
	2	0.548	0.510	0.489	0.516	64.011	2.936
	3	0.49	0.485	0.466	0.48	60.100	2.050
	4	0.533	0.544	0.511	0.529	62.700	2.240
	5	0.534	0.497	0.487	0.506	64.570	2.340
	6	0.545	0.541	0.529	0.538	63.101	2.100
	Average	0.552	0.538	0.519	0.536	62.695	2.369
STD	0.053	0.055	0.055	0.053	1.477	0.301	
COV	9.615	10.266	10.645	10.061	2.357	12.726	

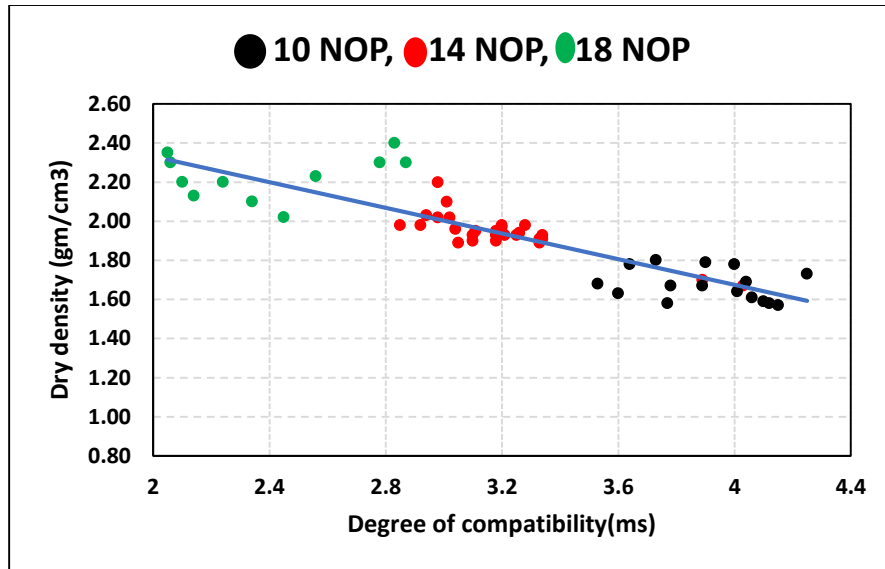
The variations of LWD measurements with dry density obtained from using three different NOP (i.e., 10, 14 and 18) are illustrated in Figure (4.6). Figure (4-6: a) shows that each the DD and Ed increase with increasing the compactive effort (i.e., NOP). While, Figures (4.6b) and (4.6c) illustrate that the values of Sd and Dc decreases with increasing DD of the soils.



(A) Relationship between DD and Ed obtained from three locations



(B) Relationship between Sd and DD obtained from three locations

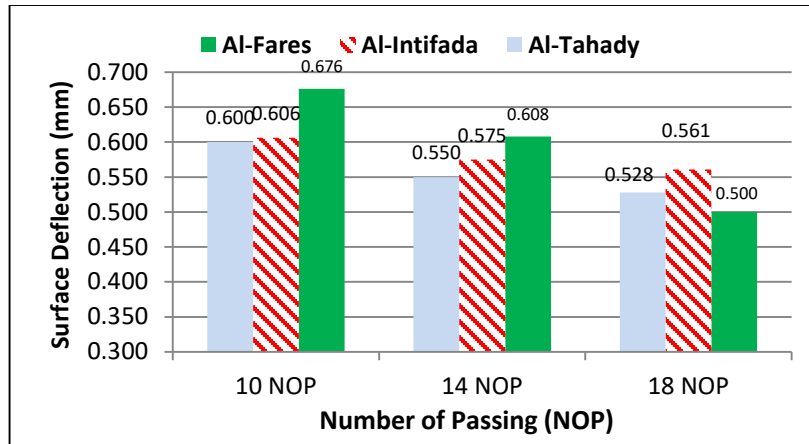


(C) Relationship between Dc and DD obtained from three locations

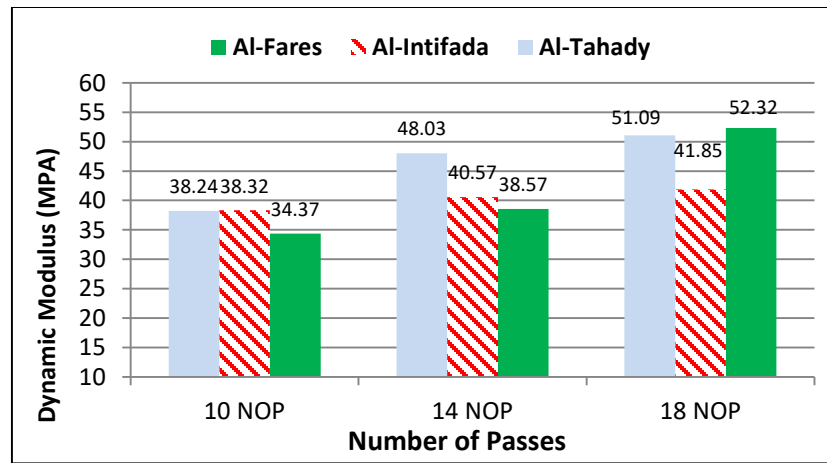
Figure (4-6): Relationship between DD and LWD parameters obtained from three locations.

In general, figure (4.7) below show Al-Faris subgrade soil shows more influence in increasing in compaction effort for each parameter (i, e., Sd, Ed, Dc) than Al-Intifada and Al-Tahady. The increment in (i, e., Sd, Ed, Dc) for Al-Faris subgrade soils is due to grain size distribution, the degree of compaction, the dry density, and the moisture content, and that agreed completely with **Rawaq, (2017)** reported that Ed value for sandy soil varied from 49.67 MPa to 53.57 MPa, Sd varied from 0.391mm to 0.453mm, Dc varied from 2.829ms to 3.241ms for 16 NOP.

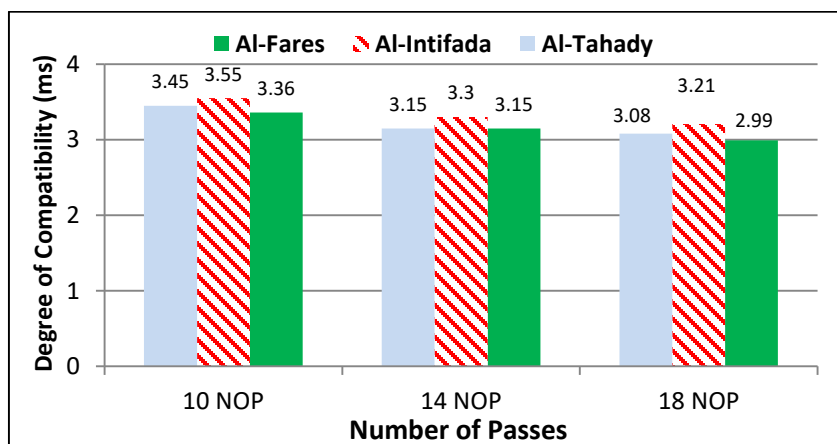




(A) Relationship between compaction effort and surface deflection



(B) Relationship between compaction effort and dynamic modulus



(C) Relationship between compaction effort and degree of compatibility

Figure (4.7): Relationship between compaction effort and LWD measurements.

### 4.3 Result of DCP Test

The DCP test was carried out to determine bearing resistance of subgrades. Total number of DCP testing points are equal to 108. The DCP parameters determined during this study include: dynamic cone penetrometer index (DCPI), California bearing ratio (CBR). The (CBR) has been determined according to the Kelyn, (1975), which was recommend and used by US army crop of engineering:

$$CBR = \frac{292}{(DCPI)^{1.12}} \quad (4.1)$$

The DCP was additionally calculated in keeping with Minnesota Department of Transportation (Mn/DOT) by averaging the five drops that occurred after three sitting drops. As a result, three seating drops with granular material should be used during the LWD procedure. The DCPI was additionally calculated by averaging the five drops that occurred after three seating drops.

The results of the 108 LWD testing points test from three locations with different NOP are presented in Tables (4.5). The DCP parameters measured throughout this study include: California bearing ratio (*CBR*), dynamic cone penetrometer index (DCPI). The results of DCP test are summarized in following sub sections.

For Al-Fares subgrade soil, the results of different number of passes (i.e., 10, 14, and 18) indicated that the values of CBR varied from 10.951% to 17.824%, and the values of DCPI varied from 12.214mm/blow to 25.067mm/blow. The percent of increase in CBR due to compaction is 63%, but the percent of decrease in DCPI is 35%, for Al-Intifada subgrade soil, the values of CBR varied from 9.030% to 18.344%, and the values of DCPI varied from 15.10mm/blow to 23.125mm/blow. The percent of increase in CBR due to compaction is 63%, but the percent of decrease in DCPI is 34%, and for Al-Tahady subgrade soil, the values of CBR varied from 10.328% to 18.7%, and the values of DCPI varied from 13.822mm/blow to

22.854mm/blow.

Table 4-5: DCP test results for subgrade soil A-3, at Al-Fares, Al-Intifadha, Al-Tahady site, (10,14,18) NOP.

Test Points	Al-Fares		Al-Intifadha		Al-Tahady		
	DCPI (mm/blow)	CBR (%)	DCPI (mm/blow)	CBR (%)	DCPI (mm/blow)	CBR (%)	
1	A1	16.181	15.315	17.167	13.191	18.053	12.934
	B1	16.856	14.280	21.167	11.428	19.533	11.649
2	A2	20.903	10.085	21.667	9.587	22.021	10.409
	B2	23.627	12.562	22.583	9.300	20.583	10.291
3	A3	17.389	13.331	19.917	10.927	18.133	12.523
	B3	25.067	8.770	23.125	9.441	22.854	9.205
4	A4	22.347	9.924	20.646	10.761	17.667	12.934
	B4	22.700	11.075	23.167	9.801	20.333	11.173
5	A5	21.200	10.950	20.833	10.553	20.142	10.328
	B5	20.547	12.807	22.750	9.030	20.167	10.854
6	A6	22.233	9.763	18.500	11.766	18.633	11.695
	B6	21.080	11.152	19.708	11.097	21.750	9.495
	Average	20.844	11.667	20.935	10.573	19.989	11.124
	STD	2.631	1.908	1.806	1.165	1.596	1.202
	COV	12.622	16.354	8.626	11.020	7.988	10.811
1	A1	18.587	16.851	16.400	13.765	22.690	26.518
	B1	16.900	13.851	15.967	15.574	14.025	17.518
2	A2	21.400	10.002	19.667	11.368	17.667	13.079
	B2	26.330	14.872	20.229	14.722	18.333	12.939
3	A3	18.400	11.965	17.367	12.749	16.806	13.860
	B3	21.266	15.981	20.250	16.490	17.667	12.996
4	A4	19.160	11.707	17.733	12.554	17.283	13.378
	B4	23.850	13.680	21.067	17.793	18.467	14.378
5	A5	21.600	9.753	18.833	16.456	16.278	13.579
	B5	25.833	14.687	20.500	14.246	19.500	12.529
6	A6	22.833	13.780	16.813	14.409	14.917	15.454
	B6	21.667	9.654	16.867	17.567	17.867	12.003
	Average	21.485	13.065	18.474	14.807	17.625	14.853
	STD	2.802	2.332	1.739	1.944	2.108	3.789
	COV	13.042	17.851	9.416	13.132	11.961	25.513
1	A1	18.329	18.540	15.722	18.344	14.722	16.754
	B1	15.252	16.581	15.867	22.56	13.833	18.35
2	A2	17.429	13.306	18.667	12.596	18.063	13.039
	B2	16.295	22.425	17.267	18.789	16.000	15.645
3	A3	16.200	15.462	16.883	14.008	16.750	15.140
	B3	17.824	18.780	17.603	18.678	15.100	12.825
4	A4	15.529	19.206	15.556	14.729	15.400	14.947
	B4	15.908	14.712	15.933	20.678	16.866	18.700
5	A5	17.114	18.453	17.467	12.342	18.333	16.973
	B5	17.257	14.218	17.933	18.727	16.753	13.178
6	A6	15.958	15.060	15.100	16.454	13.822	16.581
	B6	16.821	18.895	15.722	24.875	15.500	14.322
	Average	16.643	17.136	16.635	17.731	15.920	15.538
	STD	0.922	2.553	1.098	3.723	1.419	1.908
	COV	5.541	14.900	6.606	20.996	8.9175	12.281

The lower the value of the coefficient of variation, the more precise the data were measured. As listed in table (4.5), the results of COV were approximately less than 10% which reflects an acceptable variation (i.e., high consistent measurements).

It was clear for all testing sections that CBR increases with increasing NOP, however the DCPI results exhibited a significant reduction with increasing number of passes. Figures (4.8) and (4.9) show that as density increase, CBR increases as well, but DCPI decrease.

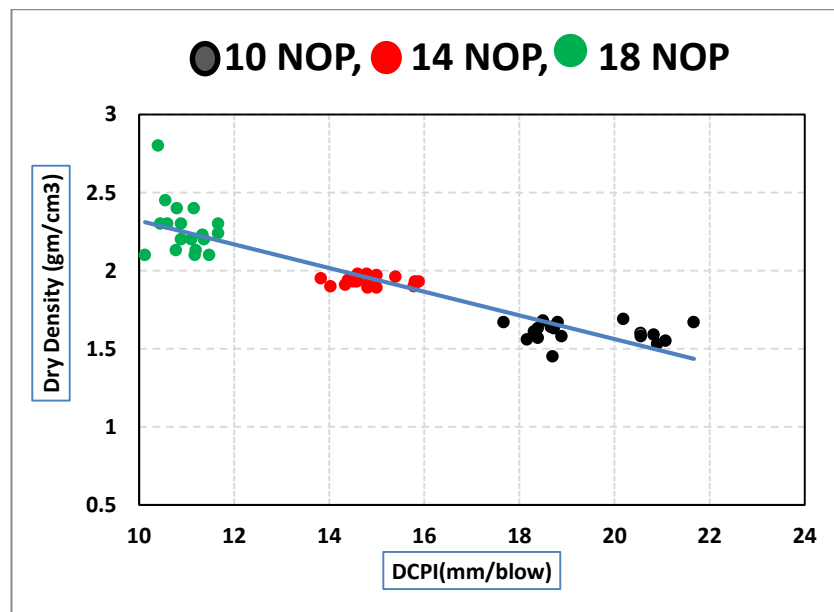


Figure 4-8: Relationship between DCPI and DD obtained from three locations

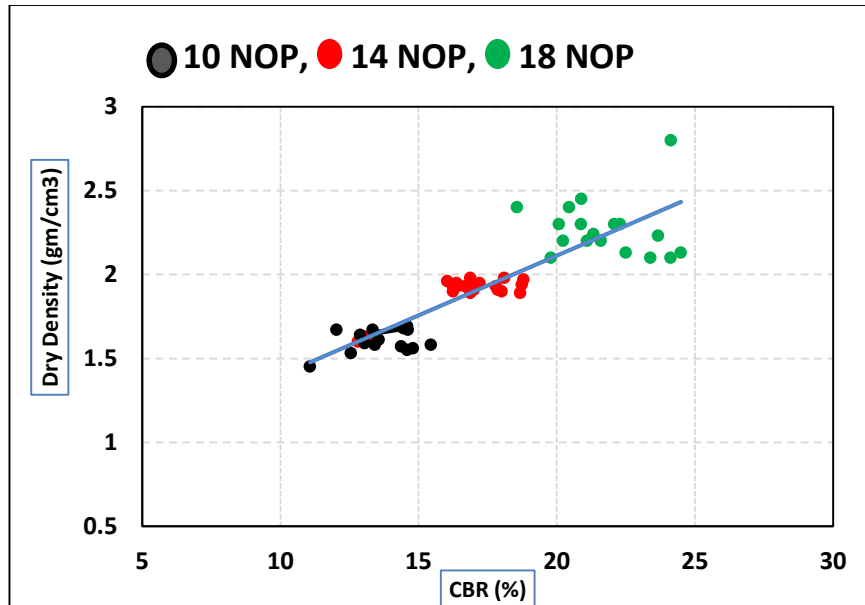
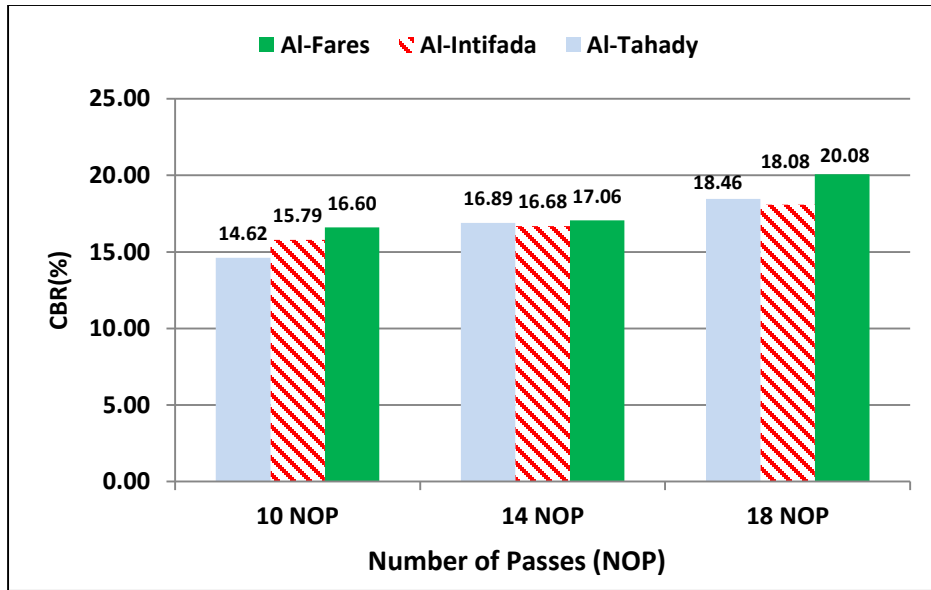
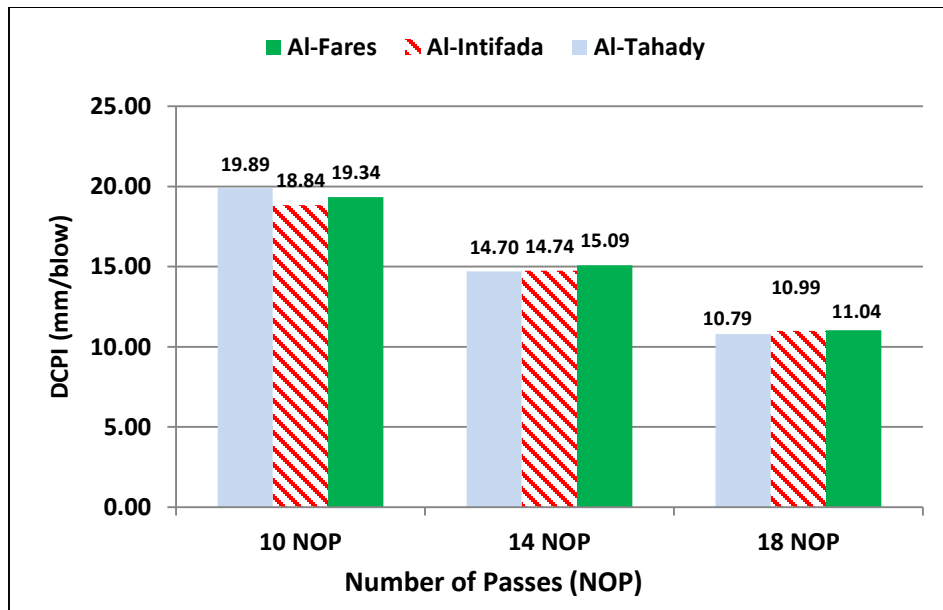


Figure 4-9: Relationship between CBR and DD obtained from three locations

Figure (4.10) show Al-Faris subgrade soil shows more influence in increasing in compaction effort for each parameter (i, e.,  $S_d$ ,  $E_d$ ,  $D_c$ ) than Al-Intifada and Al-Tahady. The increment in (i, e.,  $S_d$ ,  $E_d$ ,  $D_c$ ) for Al-Faris subgrade soils is due to grain size distribution, the degree of compaction, the dry density, and the moisture content. The results indicate that the CBR value which obtained in laboratory remolded samples is higher than the results obtained in steel box. The difference between these results is due to difference in site condition, that agreed with **Mousavi, (2016)** reported that CBR value for sandy soil varied from 13% to 24%, and DCPI varied from 14mm/blow to 26mm/blow, and **George, (2009)** reported that CBR value for sandy soil varied from 15% to 23%, and DCPI varied from 18mm/blow to 25mm/blow.



(A) Relationship between compaction effort and CBR



(B) Relationship between compaction effort and CBR

Figure 4-10: Relationship between compaction effort and DCP measurements

#### **4.4 Summary**

The results of the conducted testing program for evaluating subgrade soils using different sites and different tests, can be summarized in the following points:

1. Dry density of subgrade soil was influenced with their basic physical properties such as different in grain size distribution, water content, compaction effort, and percentage of fine content.
2. LWD parameters include surface deflection, dynamic modulus and degree of compaction influenced with the basic physical properties and degree of compaction for subgrade soils.
3. DCP parameters include California bearing ratio, and dynamic cone penetrometer index influenced with grain size distribution, the degree of compaction, the dry density, and the moisture content.
4. The results indicate that the CBR value which obtained in laboratory remolded samples is higher than the results obtained in steel box. The difference between these results is due to difference in site condition.

## Chapter Five

### Statistical Analysis

#### 5.1 Introduction

A statistical model could be defined as a mathematical equation that formalizes the connections between variables. It describes the connection between one or a lot of random variables and one or a lot of different variables. Statistical techniques are used to enhance experimental techniques, in which, instead of selecting one starting mix proportion and then modifying by trial and error to get the best solution, statistical methods are used to improve the experimental techniques. The general goal of this section of the research is to create a prediction equation that connects a dependent variable to an independent variable **Santner, (2003)**.

To determine subgrade strength and dry density, the experimental research program used three testing devices: the light weight deflectometer (LWD), the dynamic cone penetrometer (DCP) and sand replacement method (SRM). To evaluate any correlations between DCP, LWD, and basic soil properties data, the testing measures collected from these two devices were compared and statistically evaluated using regression analysis.

A Statistical Package for the Social Science (SPSS) software (Version 26) was used to undertake data input, analysis, and the creation of tables and graphs in this study. It can handle a vast amount of data and do all of the analyses discussed in the next paragraphs. As a result, the next part covered the fundamentals of statistical analysis, and discloses the analysis process for building and validating the prospective models and explains how the future models were built and validated through analysis **George, (2019)**.



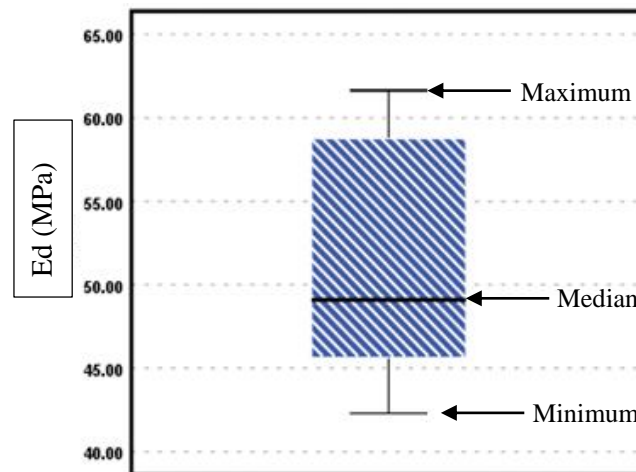
## 5.2 Exploratory Data Analysis

Many statistical principles are available in SPSS applications. The main concepts and their definitions are demonstrated below.

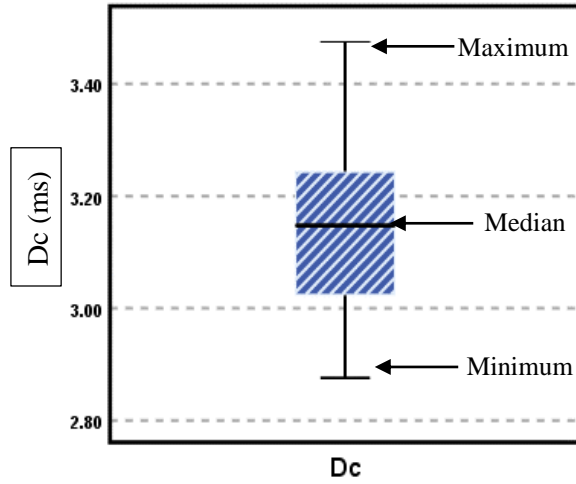
### 5.2.1 Outliers Test

An outlier in static is an observation that differ greatly from the majority of a set of data. Outliers can affect the normality of data; an outlier may be due to variability in the measurement or it may indicate experimental error **Zhang, (2007)**.

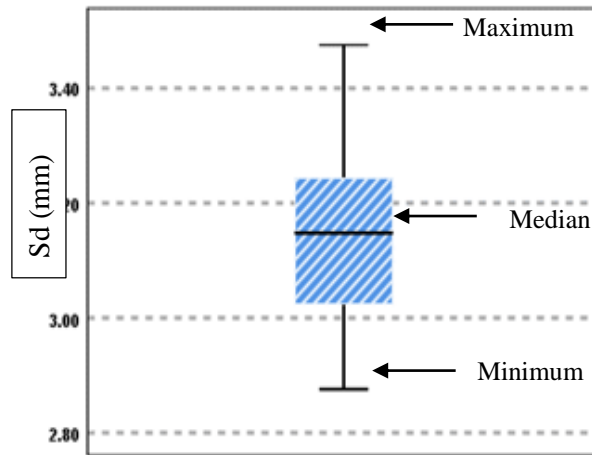
Box plots method were used to find outliers in the results. LWD, DCP, SRM tests parameters were checked using the boxplots method, if there are no circles or asterisks on either end of the box plot, this is an indication that no outliers are present. The results showed that there were no outliers in the LWD and DCP data, as shown in figures (5.1) and (5.2).



(A) Dynamic modulus.

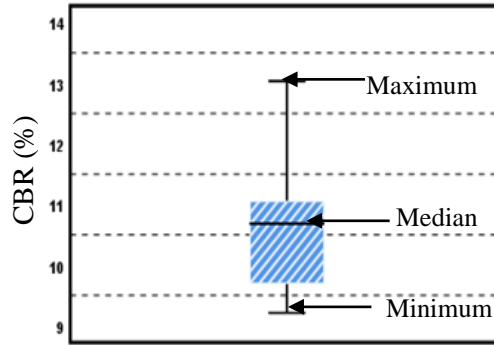


(B) Degree of compatibility

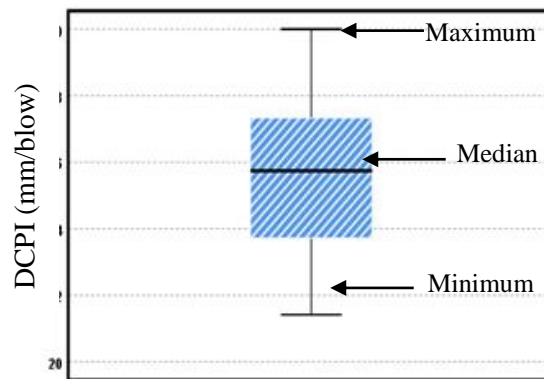


(C) Surface deflection

Figure 5-1: Outliers test for LWD parameters



(A) California bearing ratio



(B) Dynamic cone penetrometer index

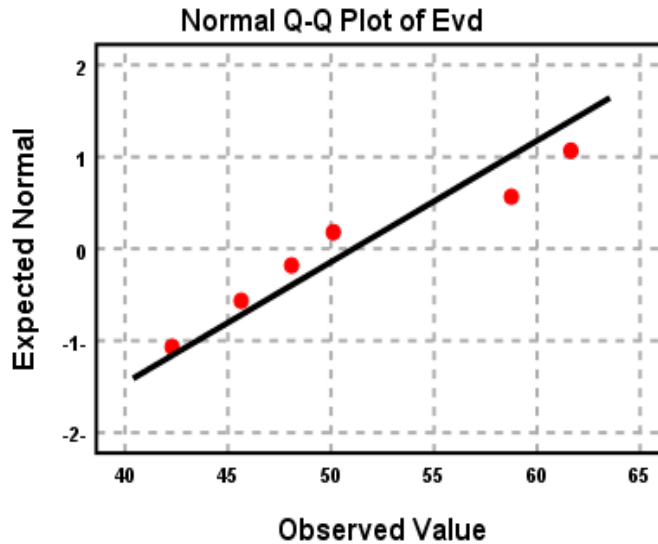
Figure 5-2: Outliers test for DCP parameters

### 5.2.2 Normality Test

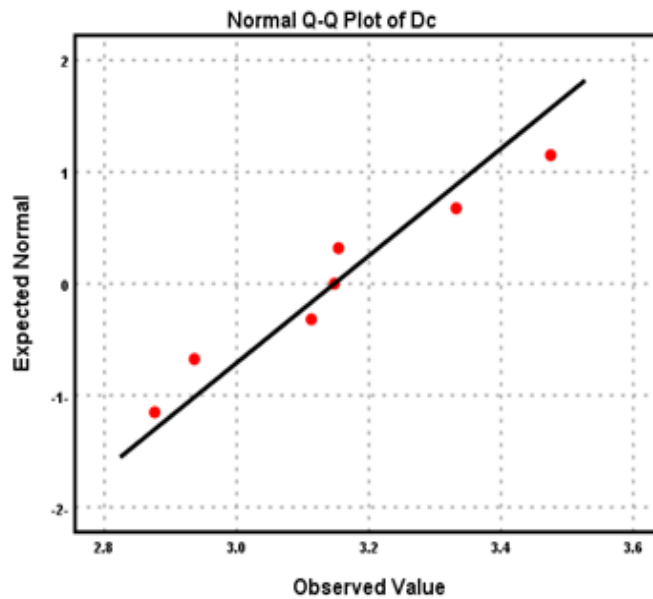
Normality test is a statistical method used to ensure if the data have a normal distribution. A normal distribution is a symmetric bell shaped curve, if the data is not normal, then you should consider using non-parametric. There are also many ways to test normality of the data: **George, (2009)**

1. Shapiro-wilk test is considered by some authors to be the best test of normality, if the test is significant (more than 0.05), then the data are normally distributed. The significant value ranges for LWD parameters were from (0.192) to (0.21), and for DCP data ranges from (0.187) to (0.91) that mean the data are normally.

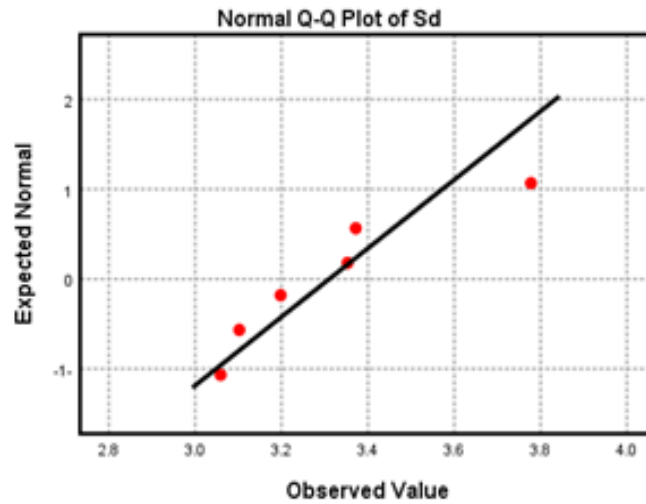
2. Normal Q-Q plot is a scatterplot created by plotting two sets of quantiles against one another. If both sets of quantiles came from the same distribution, we should see the points forming a line that's roughly straight, as shown in figures (5.3) and (5.4) all the data for LWD and DCP test are near the line.



(A) Dynamic modulus

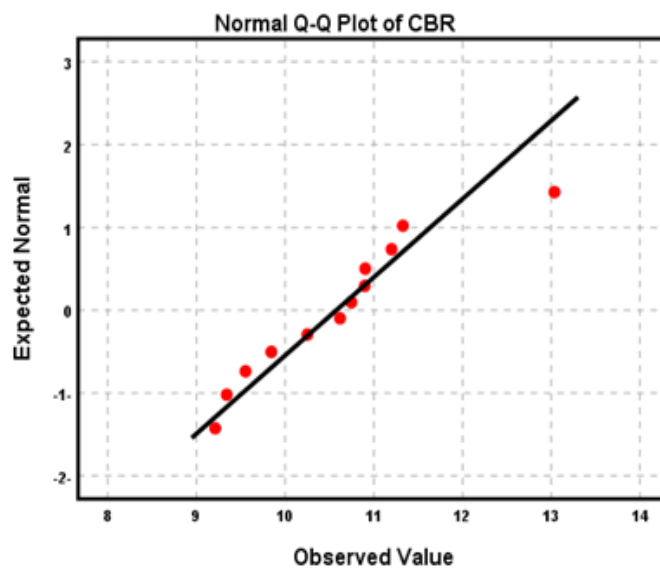


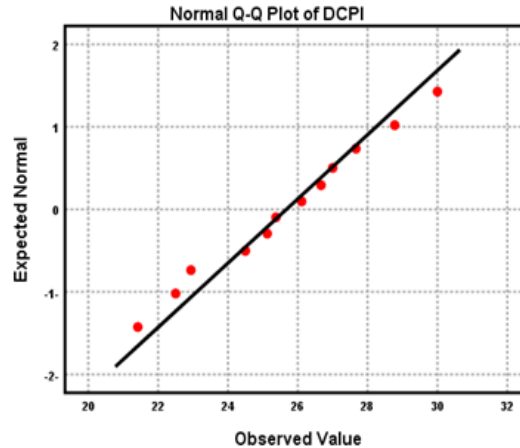
(B) Degree of compatibility



(C) Surface deflection

Figure 5-3: Q-Q plots for LWD parameters.





(B) Dynamic cone penetrometer index

Figure 5-4: Normal Q-Q plots for DCP parameters

### 5.2.3 Correlations Between Variables

Correlation is a statistical approach for displaying the relationship between two variables or the strength of the relationship. Positive correlation happens when variables move in the same direction; otherwise, negative correlation occurs. The correlation coefficient varies from -1 to 1. Based on the magnitude of the coefficient, the degree of correlation is divided into five categories: Shipley, (2016)

1. When the coefficient value is more than 0.75, there is a high degree of correlation.
2. Moderate degree of correlation, when the coefficient ranges between 0.50 to 0.75.
3. Low degree of correlation occurs when the value of coefficient ranges from 0.25 to 0.5
4. Lack of presence of correlation when the value is less than 0.25.

The correlation between the variables is determined using SPSS Pearson's matrix which is considered as the first analytical step in developing statistical models. Table (5.1) summarizes the Pearson correlation coefficients.

Table 5-1: Pearson correlation coefficients.

		<i>Sd</i>	<i>Ed</i>	<i>Dc</i>	CBR	DD	DCPI
<i>Sd</i>	Pearson Correlation	1	-.924 <sup>**</sup>	.869 <sup>**</sup>	-.902 <sup>**</sup>	-.901 <sup>**</sup>	.929 <sup>**</sup>
	Sig. (2-tailed)		.000	.000	.000	.000	.000
	N	54	54	54	54	54	54
<i>Ed</i>	Pearson Correlation	-.924 <sup>**</sup>	1	-.885 <sup>**</sup>	.905 <sup>**</sup>	.903 <sup>**</sup>	-.929 <sup>**</sup>
	Sig. (2-tailed)	.000		.000	.000	.000	.000
	N	54	54	54	54	54	54
<i>Dc</i>	Pearson Correlation	.869 <sup>**</sup>	-.885 <sup>**</sup>	1	-.862 <sup>**</sup>	-.867 <sup>**</sup>	.885 <sup>**</sup>
	Sig. (2-tailed)	.000	.000		.000	.000	.000
	N	54	54	54	54	54	54
CBR	Pearson Correlation	-.902 <sup>**</sup>	.905 <sup>**</sup>	-.862 <sup>**</sup>	1	.877 <sup>**</sup>	-.916 <sup>**</sup>
	Sig. (2-tailed)	.000	.000	.000		.000	.000
	N	54	54	54	54	54	54
DD	Pearson Correlation	-.901 <sup>**</sup>	.903 <sup>**</sup>	-.867 <sup>**</sup>	.877 <sup>**</sup>	1	-.919 <sup>**</sup>
	Sig. (2-tailed)	.000	.000	.000	.000		.000
	N	54	54	54	54	54	54
DCPI	Pearson Correlation	.929 <sup>**</sup>	-.929 <sup>**</sup>	.885 <sup>**</sup>	-.916 <sup>**</sup>	-.919 <sup>**</sup>	1
	Sig. (2-tailed)	.000	.000	.000	.000	.000	
	N	54	54	54	54	54	54

\*\* . Correlation is significant at the 0.01 level (2-tailed).

This table shows:

1. The LWD measurements (i.e., *Ed*,  $\delta d$ , and *Dc*) have high correlation with each other. It was noted that there is a negative high correlation between *Ed* and ( $\delta d$ , and *Dc*). Whereas the correlation between ( $\delta d$ ) and (*Dc*) is positive correlation, which means that the surface deflection increases with increasing degree of compatibility.
2. The correlations between the CBR and LWD measurements, and DCPI have high correlation. High positive correlation with *Ed*, negative correlation with

- Dc, and surface deflection ( $\delta d$ ), and DCPI.
3. The correlation between the dependent variable dry density (DD) and some independent variables like LWD surface deflection ( $\delta d$ ), degree of compatibility (Dc), and dynamic cone penetrometer index (DCPI) is negative high correlation, which indicates that any decrease in these values leads to increase DD, and vice versa. Also, this degree of correlation can develop an acceptable theoretical model between DD and any one of these variables.
  4. The DCPI has the most significant correlation to surface deflection ( $\delta d$ ), degree of compatibility (Dc), it has a high positive correlation, while with CBR and dry density has negative high correlation.

#### 5.2.4 Regression Analysis

Regression analysis is a statistical process for determining whether or not there is a relationship between an independent and a dependent variable in order to predict the dependent variables' future values. Linear regression analysis, multiple regression analysis, and nonlinear regression analysis are the three primary forms of regression analysis. R-squared is a statistic index that indicates how near the data are to the fitted regression line. For multiple regression, it's also known as the coefficient of multiple determination. R-squared has a value that is always between 0% and 100%. R-squared equals 0% when the model does not show any variability in the response data around its mean, While R-squared will equal 100 % if the model shows all of the variability of the response data around its mean. The greater the R-squared, the better the model fits your data in general. Adjusted R-square compares the explanatory power of regression models that contain different number of predictors Santner, (2003)



### 5.3 Developing Statistical Models

The SPSS software was used to examine and constructed predictive models. To predict strength and density of subgrade soil, six sets of nonlinear models were correlated: 1) dry density (DD) with LWD parameters, 2) dry density (DD) with DCP parameters, 3) dry density (DD) with LWD and DCP, 4) CBR with LWD parameters, 5) CBR with basic physical soil properties, 6) CBR with LWD parameters and basic physical soil properties.

#### 5.3.1 Developing DD Model

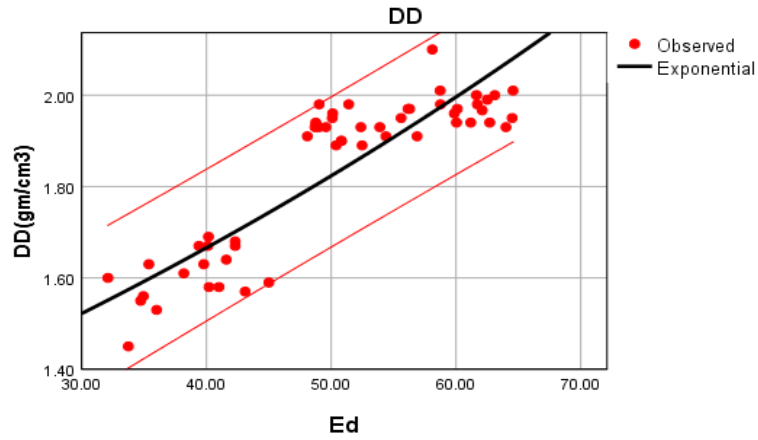
##### 5.3.1.1 Developing DD-LWD Model

For subgrade granular soil (A-3), it was assumed that the DD is influenced by three LWD variables: surface deflection (Sd), dynamic modulus (Ed) and degree of compatibility (Dc).

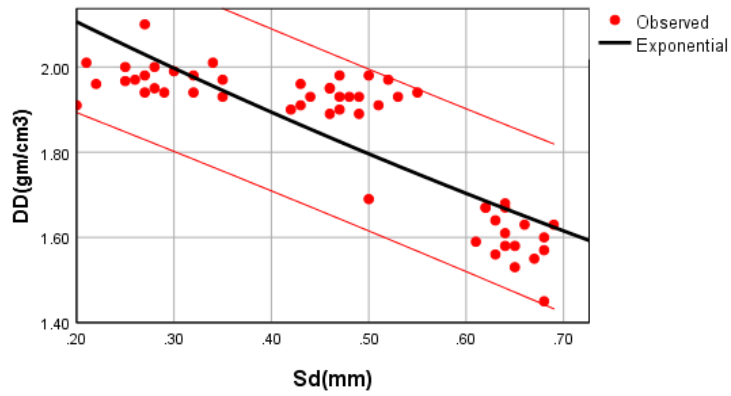
Three simple non-linear regression models were developed to predict dry density (DD) as a function of LWD parameters (Ed, Sd, Dc). Three nonlinear correlations were developed using the principles of selected regression model where this model represented higher  $R^2$  value among other models such as (linear, inverse, logarithmic, quadratic, cubic, exponential, power, ... etc.) as shown in Table (5.2) and models' expression for these relations were shown in Figure (5.5).

Table 5-2: Summary of statistical models based on LWD parameters.

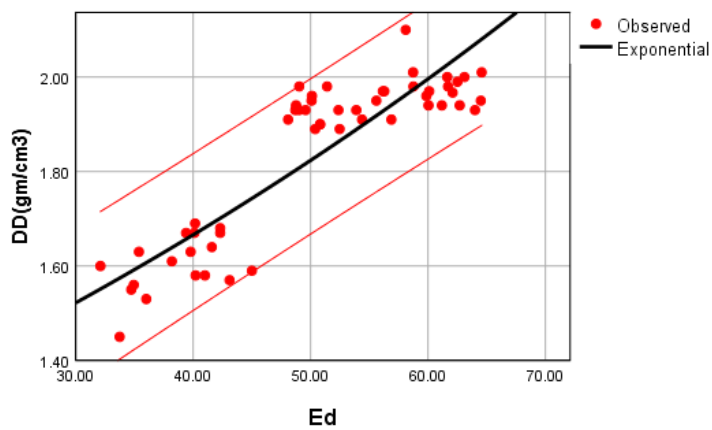
Ind. Variable	D. variable	Models expression	$R^2$	Std. Error	Estimated parameters
DD	Ed	$DD = B_1 e^{B_0 Ed}$	0.810	0.056	$B_0 = -0.011$ $B_1 = 1.093$
	Sd	$DD = B_1 e^{B_0 Sd}$	0.752	0.057	$B_0 = -0.648$ $B_1 = 2.584$
	Dc	$DD = B_1 e^{B_0 D}$	0.764	0.052	$B_0 = -0.175$ $B_1 = 3.371$



(A) Exponential relation between DD-Ed



(B) Exponential relation between DD-Sd



(C) Exponential relation between DD-Dc

Figure 0-5: Correlations between LWD parameters and dry density

A multiple non-linear regression model was developed to predict the dry density (DD) as a function of LWD parameters, Table (5.3) presents the statistical model with  $R^2 = 85.57\%$ , which indicate a strong correlation between DD and LWD parameters.

For ensuring the accuracy of information entered, the results of models were validated using previous experimental data.

Figure (5.6) explains the adequacy of the model and the acceptability of scattered between the predicted and measured dry density (DD). From the figure it can be recognized that all values are within the significant level boundaries with  $R^2 = 0.909$ . A figure (5.7) shows the scatter of residual points around the mean zero. In this Figure the residuals are plotted against the dependent variable dry density (DD) to check the normality assumption.

Table 5-3: Summary of statistical models based on LWD parameters.

Predictors	Model	$R^2$	Adjusted $R^2$	Std. Error
Ed	DD=2.077-0.716 Sd+0.011 Ed-0.1113 Dc	85.57%	85.56%	0.041
Sd				
Dc				

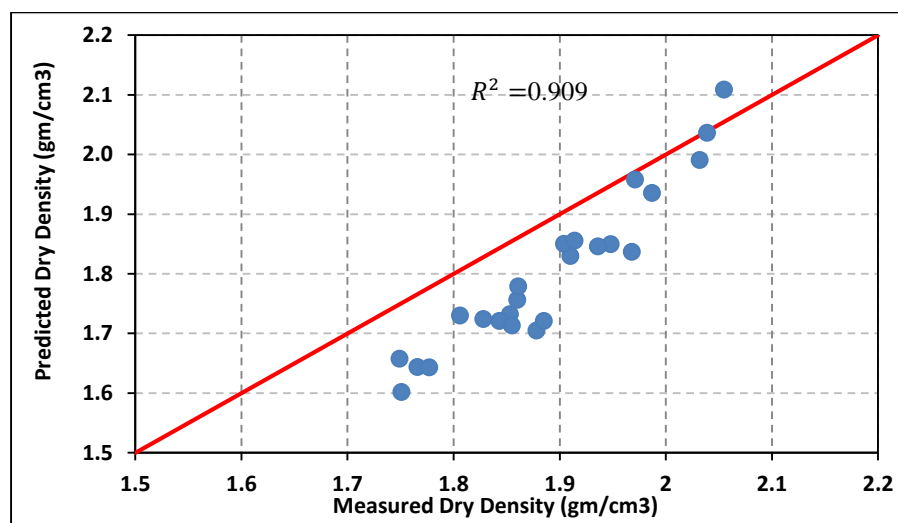


Figure 5-6: Predicted dry density vs. measured dry density (LWD-DD) Model

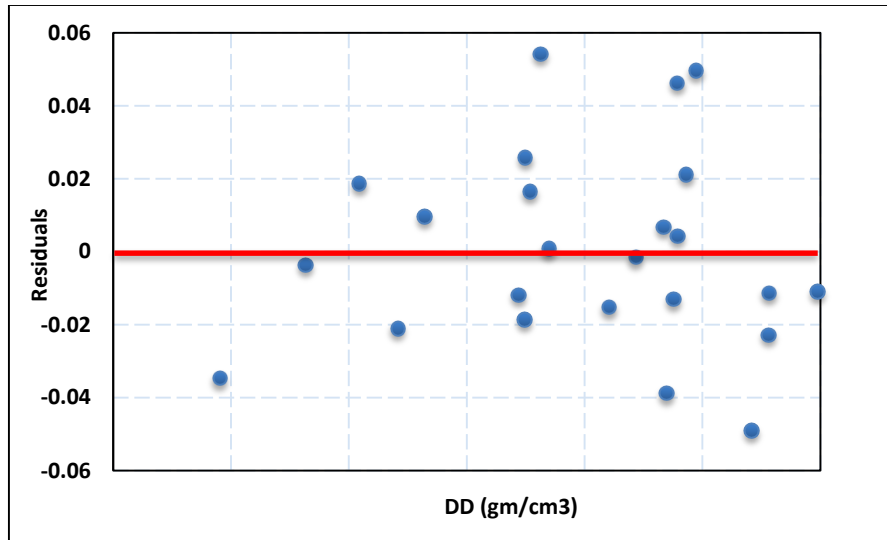


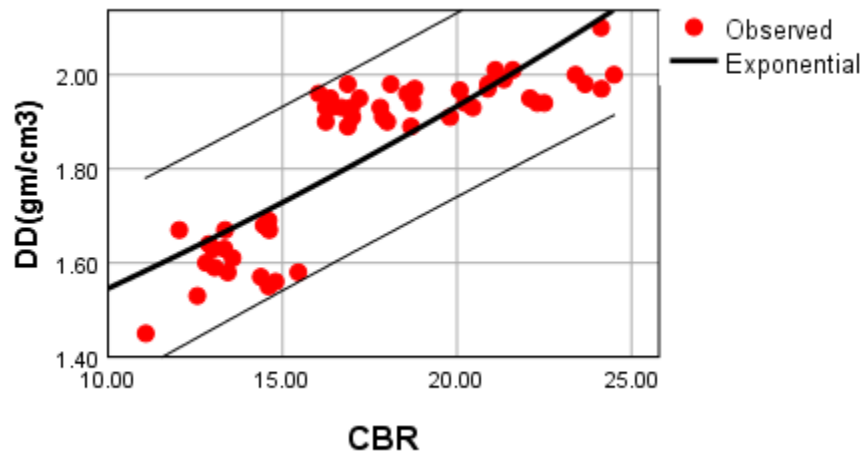
Figure 5-7: Residuals vs. DD model

### 5.3.1.2 Developing DD-DCP Model

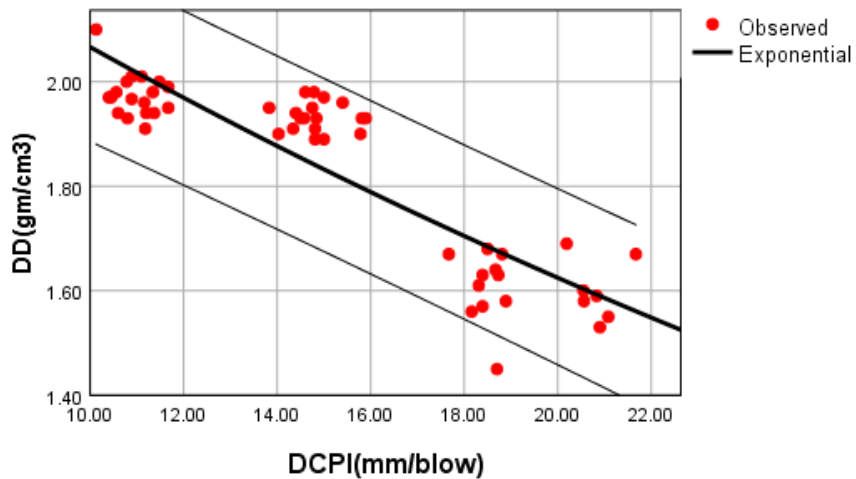
Three simple non-linear regression models were developed to predict dry density (DD) as a function of DCP parameters (DCPI, CBR). Three nonlinear correlations were developed using the principles of selected regression model where this model represented higher  $R^2$  value among other models such as (linear, inverse, logarithmic, quadratic, cubic, exponential, power, ... etc.) as shown in Table (5.5) and models' expression for these relations were shown in Figure (5.8).

Table 5-4: Summary of statistical models based on DCP parameters

Ind. variable	D. variable	Models expression	$R^2$	Std. Error	Estimated parameters
DD	DCPI	$DD = B_1 e^{B_0 DCPI}$	0.872	0.054	$B_0 = -0.039$ $B_1 = 3.461$
	CBR	$DD = B_1 e^{B_0 CBR}$	0.778	0.07	$B_0 = 0.037$ $B_1 = 1.004$



(A) Exponential relationship between DD-CBR



(B) Exponential relationship between DD-DCPI

Figure 5-8: Correlations between DD parameters and DCP

A multiple non-linear regression model was developed to predict the dry density (DD) as a function of LWD parameters, Table (5.6) presents the statistical model with  $R^2 = 85.57\%$ , which indicate a strong correlation between DD and LWD parameters.

For ensuring the accuracy of information entered, the results of models were validated using previous experimental data.

Figure (5.9) explains the adequacy of the model and the acceptability of scattered between the predicted and measured dry density (DD). From the figure it can be recognized that all values are within the significant level boundaries with  $R^2 = 0.812$ . A figure (5.10) shows the scatter of residual points around the mean zero. In this figure the residuals are plotted against the dependent variable dry density (DD) to check the normality assumption.

Table 5-5: Summary of statistical models based on DC parameters.

Predictors	Model	$R^2$	Adjusted $R^2$	Std. Error
CBR	DD=3.227- 0.2345 DCPI +0.104 CBR + 0.00538 (DCPI) <sup>2</sup> - 0.00271 (CBR) <sup>2</sup>	88.01%	88.00%	0.063
DCPI				

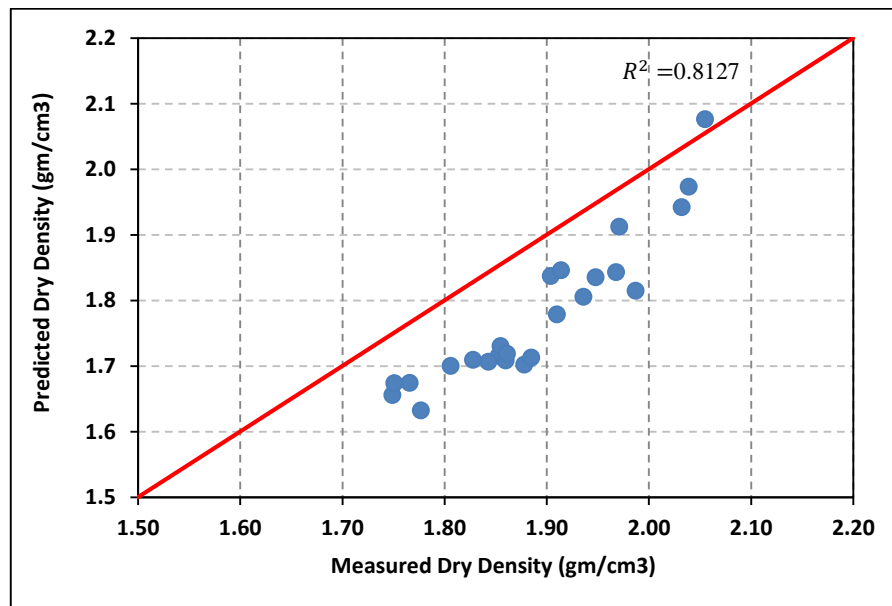


Figure 5 0-9: Predicted dry density verse measured dry density (DCP-DD) Model

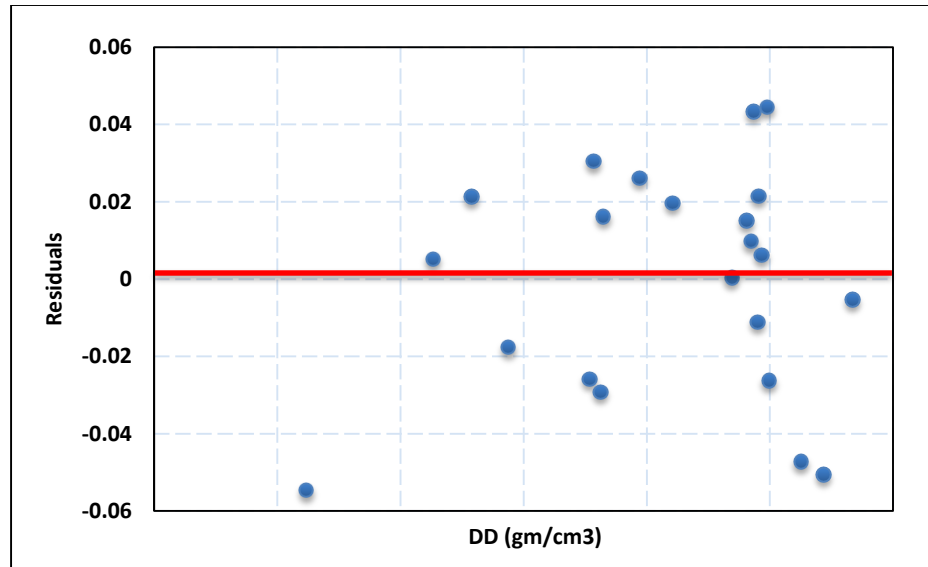


Figure 5-10: Residuals verse DD model

### 5.3.1.3 Developing DD with (LWD-DCP) Model

A multiple non-linear regression model was developed to predict the dry density (DD) as a function of LWD parameters, Table (5.6) presents the statistical model with  $R^2 = 84.67\%$ , which indicate a strong correlation between DD and LWD parameters.

For ensuring the accuracy of information entered, the results of models were validated using previous experimental data.

Figure (5.11) explains the adequacy of the model and the acceptability of scattered between the predicted and measured dry density (DD). From the figure it can be recognized that all values are within the significant level boundaries with  $R^2 = 0.8147$ . A figure (5.12) shows the scatter of residual points around the mean zero. In this Figure the residuals are plotted against the dependent variable dry density (DD) to check the normality assumption.

Table 5-6: Summary of statistical models based on LWD – DCP parameters.

Predictors	Model	$R^2$	Adjusted $R^2$	Std. Error
Ed DCPI	$DD = 3.074 - 0.1622 DCPI + 0.00914 Ed + 0.00353 (DCPI)^2$	84.67%	84.62	0.068

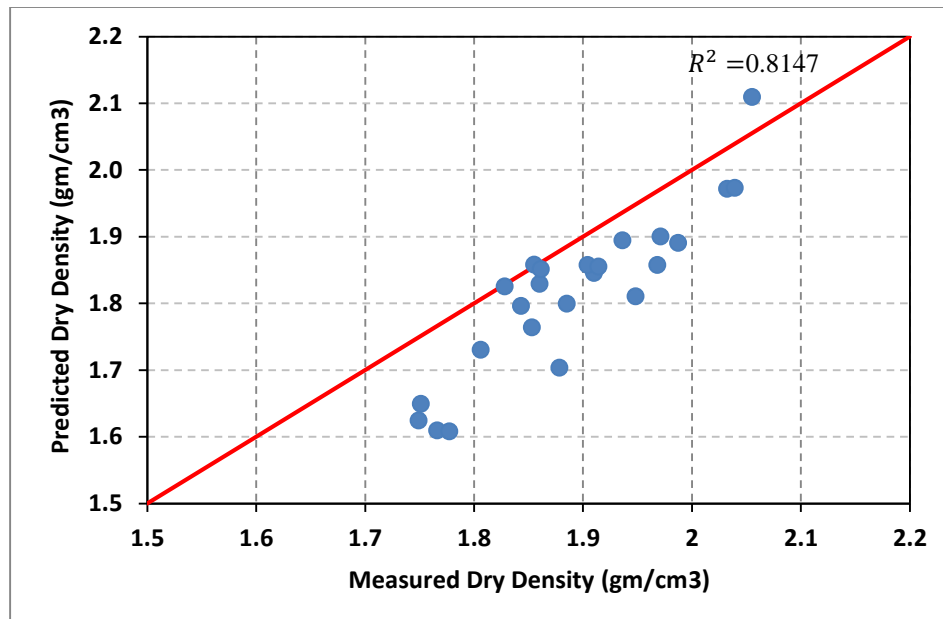


Figure 5-11: Predicted dry density verse measured dry density (DCP-LWD) Model

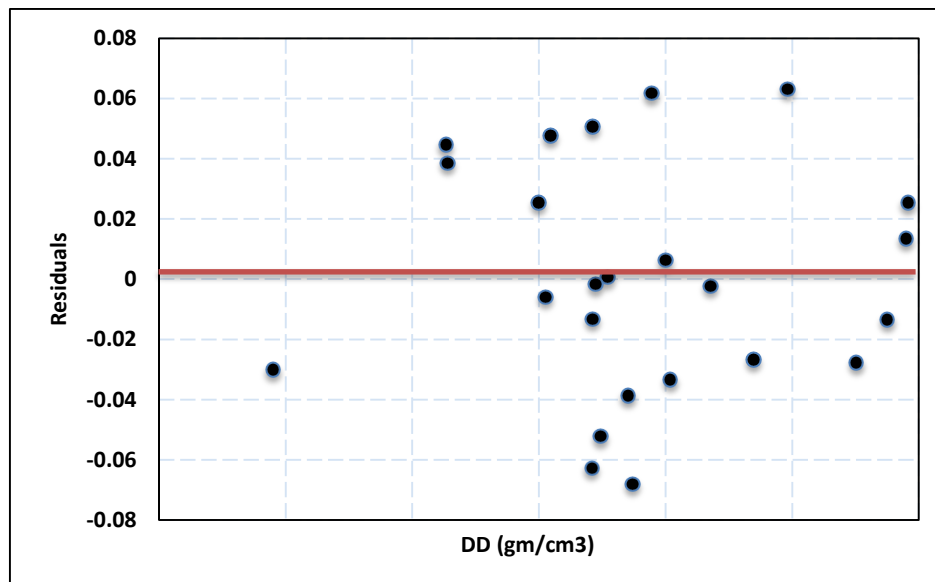


Figure 5-12: Residuals vs. DD model

### 5.5.1 Developing CBR Model

#### 5.3.2.1 Developing CBR-LWD Model

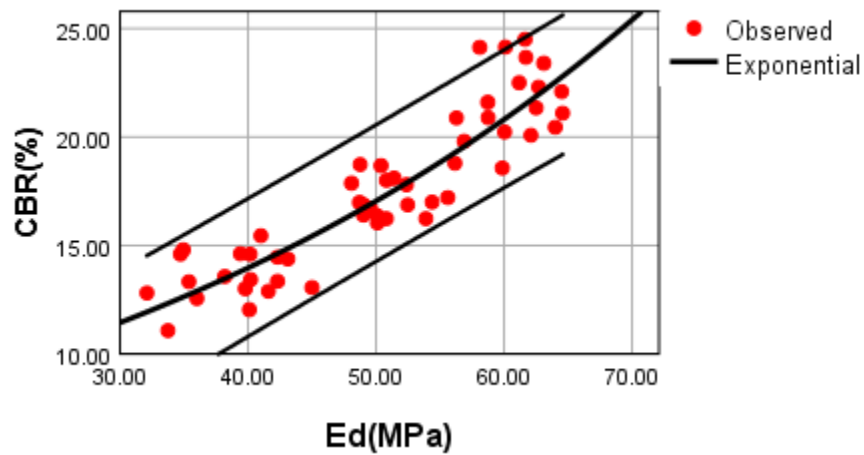
Three simple non-linear regression models were developed to predict dry density (CBR) as a function of LWD parameters. Three nonlinear correlations were developed using the principles of selected regression model where this model



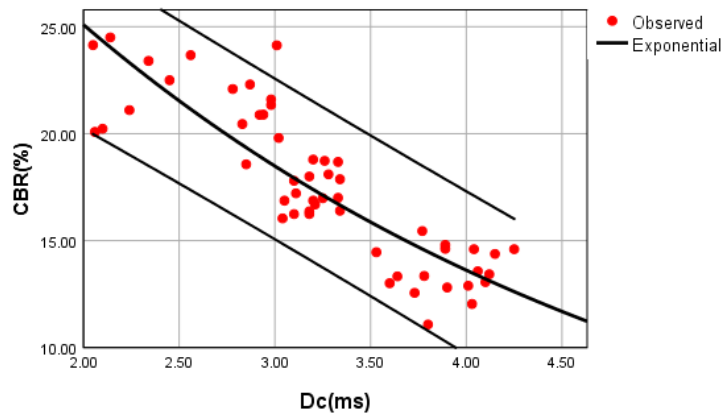
represented higher  $R^2$  value among other models such as (linear, inverse, logarithmic, quadratic, cubic, exponential, power, ... etc.) as shown in Table (5.7) and models' expression for these relations were shown in Figure (5.13).

Table 5-7: Summary of statistical models based on LWD parameters.

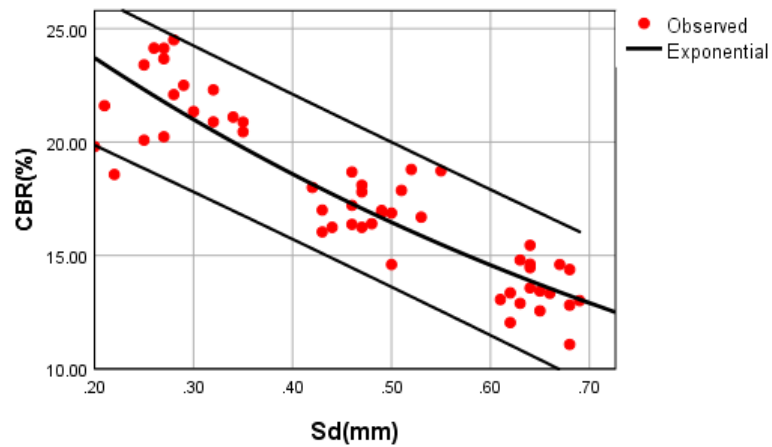
Ind. Variable	D. variable	Models expression	$R^2$	Std. Error	Estimated parameters
CBR	Ed	$CBR = B_1 e^{B_0 Ed}$	0.837	0.085	$B_0 = 0.02$ $B_1 = 6.295$
	Sd	$CBR = B_1 e^{B_0 Sd}$	0.741	0.107	$B_0 = -0.306$ $B_1 = 46.234$
	Dc	$CBR = B_1 e^{B_0 Dc}$	0.817	0.09	$B_0 = -1.216$ $B_1 = 30.239$



(A) Exponential relationship between CBR- Ed



(B) Exponential relationship between CBR- Dc



( C )Exponential relationship between CBR-  $S_d$

Figure 5-13: Correlations between CBR parameters and LWD

A multiple non-linear regression model was developed to predict the dry density (DD) as a function of LWD parameters, Table (5.8) presents the statistical model with  $R^2 = 89.01\%$ , which indicate a strong correlation between DD and LWD parameters.

For ensuring the accuracy of information entered, the results of models were validated using previous experimental data.

Figure (5.14) explains the adequacy of the model and the acceptability of scattered between the predicted and measured dry density (DD). From the figure it can be recognized that all values are within the significant level boundaries with  $R^2 = 0.986$ . A figure (5.15) shows the scatter of residual points around the mean zero. In this Figure the residuals are plotted against the dependent variable dry density (DD) to check the normality assumption.

Table 5-8: Summary of statistical models based on CBR-LWD data

Predictors	Model	$R^2$	Adjusted $R^2$	Std. Error
Ed	CBR=6.3-8.55 $S_d$ +0.353 Ed+1.96 Dc-0.0565 Ed Dc	89.01%	89.1%	0.053
$S_d$				
Dc				

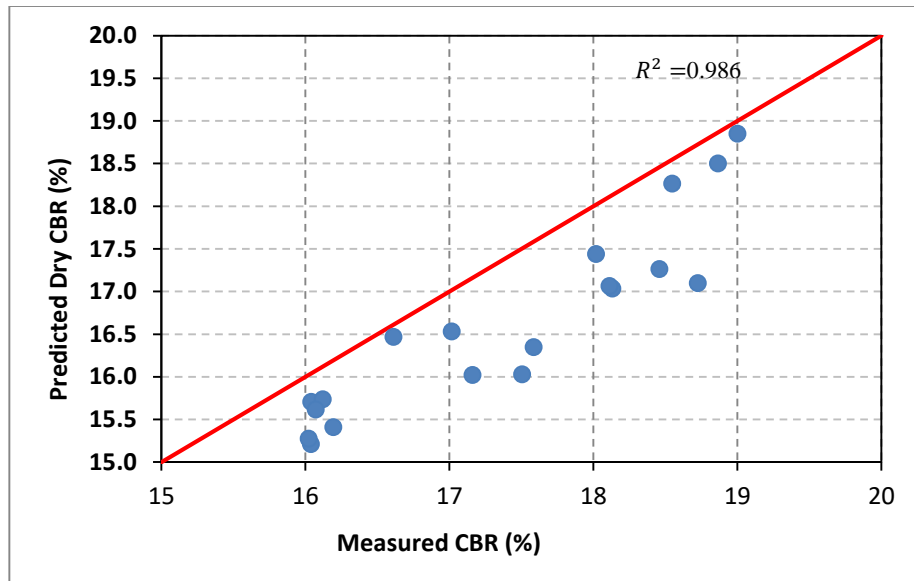


Figure 0-14: Predicted CBR verse measured CBR (CBR-LWD) Model

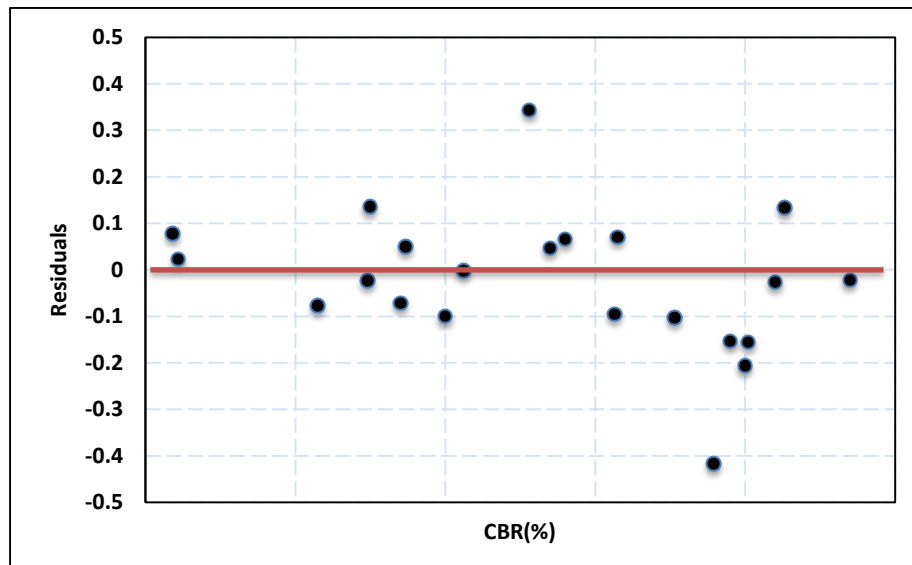


Figure 5-15: Residuals verse CBR model

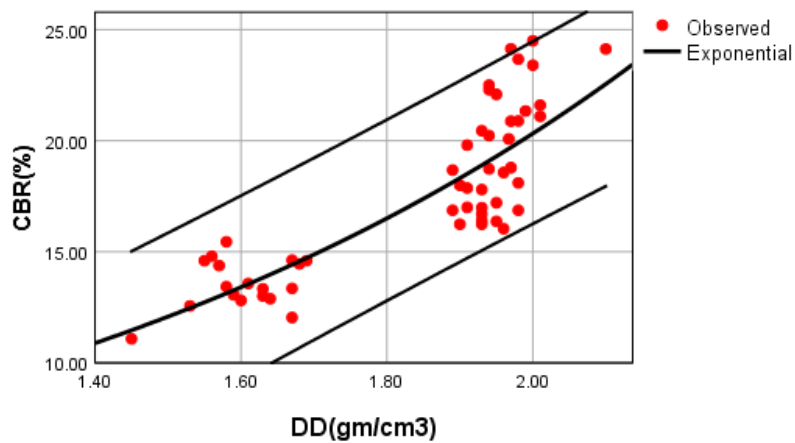
### 5.3.2.2 Developing CBR-Basic soil properties Model

Three simple non-linear regression models were developed to predict dry density (CBR) as a function of basic soil properties parameters. Three nonlinear correlations were developed using the principles of selected regression model where this model represented higher  $R^2$  value among other models such as (linear, inverse, logarithmic, quadratic, cubic, exponential, power, ... etc.) as shown in Table (5.13)

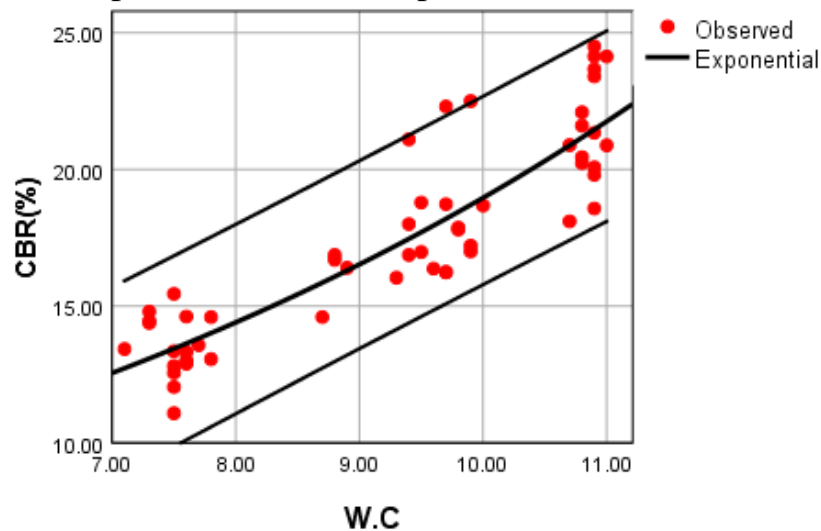
and models' expression for these relations were shown in Figure (5.18).

Table 5-9: Summary of models and coefficients for Nonlinear CBR, LWD parameter

Ind. Variable	D. variable	Models expression	$R^2$	Std. Error	Estimated parameters
CBR	DD	$CBR = B_1 e^{B_0 DD}$	0.756	0.104	$B_0 = 0.617$ $B_1 = 5.152$
	W.C	$CBR = B_1 e^{B_0 w.c}$	0.809	0.092	$B_0 = 0.137$ $B_1 = 4.827$



(A) Exponential relationship between CBR- DD



(B) Exponential relationship between CBR- W.C

Figure 5-16: Correlation between CBR parameters and Basic soil properties

A multiple non-linear regression model was developed to predict the dry density (DD) as a function of LWD parameters, Table (5.14) presents the statistical model with  $R^2 = 90.1\%$ , which indicate a strong correlation between DD and LWD parameters.

For ensuring the accuracy of information entered, the results of models were validated using previous experimental data.

Figure (5.17) explains the adequacy of the model and the acceptability of scattered between the predicted and measured dry density (DD). From the figure it can be recognized that all values are within the significant level boundaries with  $R^2 = 0.9105$ . A figure (5.18) shows the scatter of residual points around the mean zero. In this Figure the residuals are plotted against the dependent variable dry density (DD) to check the normality assumption.

Table 5-10: Summary of statistical models based on CBR-Basic soil properties parameters.

Predictors	Model	$R^2$	Adjusted $R^2$	Std. Error
DD W.C	$CBR = 5.13 + 5.29 * DD + 1.399 * M.C$	90.1%	90.03%	0.058

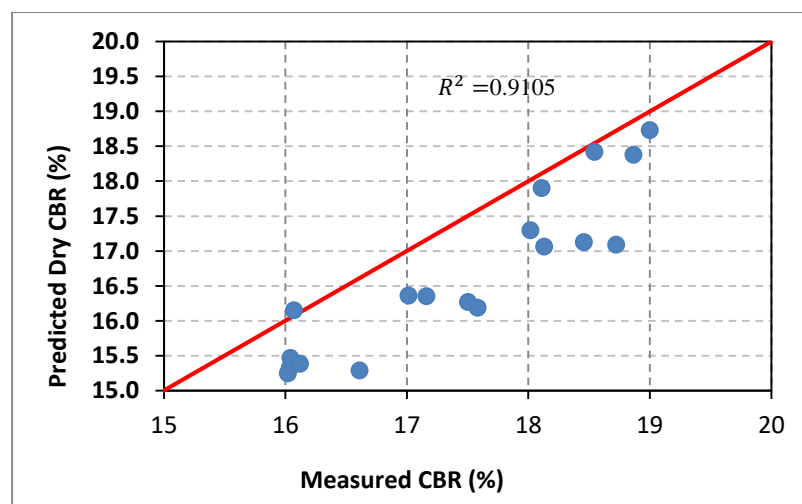


Figure 5-17: Predicted CBR verse measured CBR (LWD-basic soil properties)

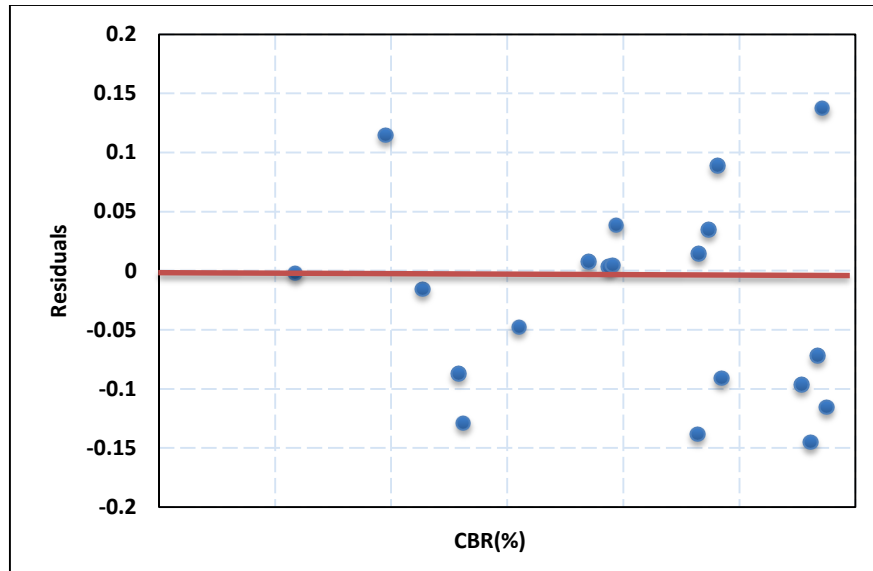


Figure 5-18: Residuals verse CBR model

### 5.3.2.3 Developing CBR with (LWD and Basic soil properties) Model

A multiple non-linear regression model was developed to predict the CBR as a function of LWD parameter ( $E_d$ ) and basic soil properties (dry density), Table (5.11) presents the statistical model with  $R^2 = 85.5\%$ , which indicate a strong correlation between DD and LWD parameters.

For ensuring the accuracy of information entered, the results of models were validated using previous experimental data.

Figure (5.19) explains the adequacy of the model and the acceptability of scattered between the predicted and measured dry density (DD). From the figure it can be recognized that all values are within the significant level boundaries with  $R^2 = 0.976$ . A figure (5.20) shows the scatter of residual points around the mean zero. In this Figure the residuals are plotted against the dependent variable dry density (DD) to check the normality assumption.

Table 5-11: Summary of statistical models based on CBR-LWD-Basic soil properties parameters.

Predictors	Model	$R^2$	Adjusted $R^2$	Std. Error
DD	$\text{CBR} = -8 + 25.1\text{DD} - 0.378 \text{Ed} + 0.01296 (\text{Ed})^2 - 0.381 \text{DD Ed}$	85.5%	86.00%	0.065
Ed				

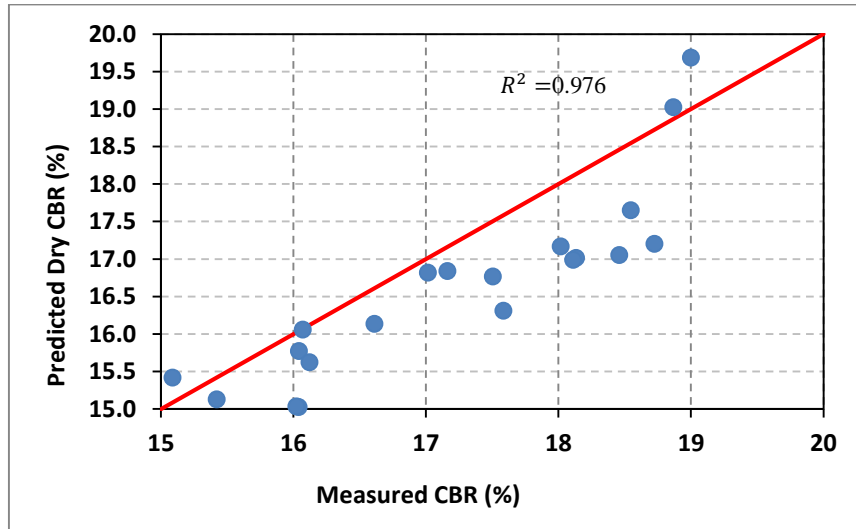


Figure 5-19: Predicted CBR verse measured CBR (CBR- (LWD. Basic soil properties)) Model

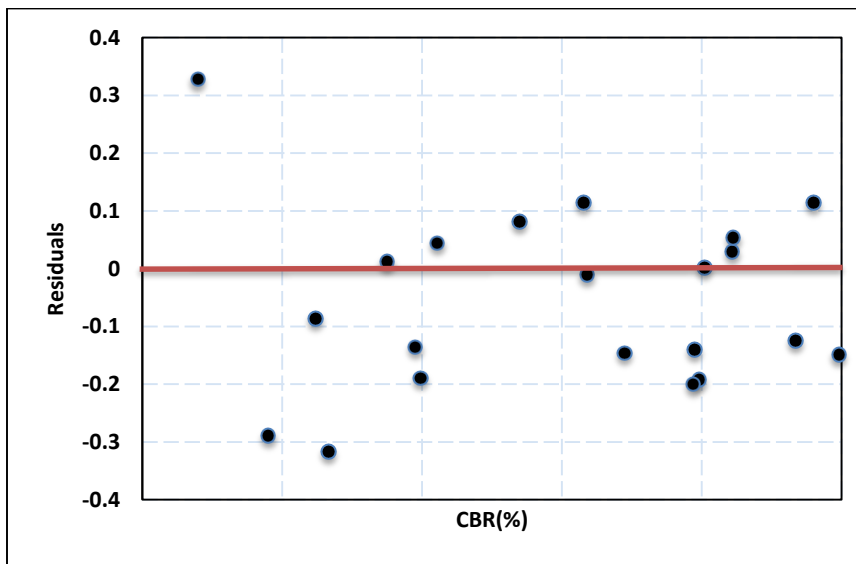


Figure 5-20: Residuals verse CBR model

## Chapter Six

### Conclusions and Recommendations

#### 6.1 Summary and Conclusions

The following conclusions are derived supported the experimental and theoretical summary:

1. The predominant subgrade soils at Karbala city is A-3 soils which is classified as a poorly graded sand soil with a high gypsum content.
  2. It was found that increasing the dry density of soils leads to an increase in CBR and LWD dynamic modulus. However, increasing dry density results in a decrease in both surface deflection, and degree of compatibility.
  3. It was concluded that exponential statistical models provide a best dry density prediction based on LWD measurements. The results showed that the dynamic modulus is the most significant correlating parameter in determining dry density with  $R^2=80\%$ .
  4. It was concluded that exponential statistical models provide a best dry density prediction based on DCP measurements. The results showed that the dynamic cone penetration index is the most significant correlating parameter in estimating dry density with  $R^2=87\%$ .
  5. It was concluded that exponential statistical models provide a best CBR prediction based on LWD measurements ( $E_d$ ,  $\delta_d$ ,  $D_c$ ). The results showed that the dynamic modulus is the most significant correlating parameter in estimating CBR with  $R^2=87\%$ .
-



6. The results of statistical analysis show that exponential models provide a best CBR prediction based on basic soil properties measurements (w.c, dry density) and found that the w.c is the most significant correlating parameter in estimating CBR with  $R^2=80\%$ .
7. As a result, the regression of dry density models based on a combination of LWD measurements and DCP measurements give higher value of  $R^2 = 85\%$ , whereas the regression of CBR models based on a combination of LWD measurements and basic soil properties measurements give higher value of  $R^2 = 86\%$ .
8. This study indicate that the values of LWD measurements ( $E_d$ ,  $S_d$ ,  $D_c$ ) for soil samples of different sites were (64.57MPa, 0.36 mm, 2.05 ms) respectively, and the values of DCP measurements (CBR, DCPI) for soil samples of different sites were (18.34, 12.214).

## 6.2 Recommendations and Further Works

1. It is recommended to evaluate properties of subgrade soils using chemical stabilization method to improve the strength.
2. It is also recommended to conduct theoretical work using finite element to evaluate the strength and stiffness of subgrade.
3. It is recommended to select more types of subgrade soils like clay soils to develop other statistical models.
4. It is recommended to determine measured dry density by using nuclear density gauge device instead of using the conventional method (i.e., SRM) which was adopted in this research to ensure the accuracy for validated results.

5. It is recommended to comparison between light weight deflectometer and nuclear density gauge to assess compaction quality for subgrade soils.
6. The light weight deflectometer serves as an effective tool for construction inspection of any roadway project because of its simplicity, portability, and shortens the times (i.e., testing operation less than 2 minutes).
7. The dynamic cone penetrometer is a simple field test equipment that saves time and requires less maintenance, when comparing with traditional CBR test.

## *References*

---

AASHTO M145-91, "Standard Specification for Classification of Soils and Soil Aggregate Mixtures for Highway Construction Purposes," American Association of State and Highway Transportation Officials, Washington, DC. 2012

Abbas Mohajeran. (2017, june 8). Prediction of subgrade resilient modulus for flexible pavement. *Scientific Research and Essays*, 6(21), pp.4567-4576.

Ahela. (2017). *Assessment of Modulus of Subgrade Reaction of Stabilized Soils Using Light Weight Deflectometer*, Department of Civil Engineering.

Ahmet. (2005). *Geoenvironmental behavior of foundry sand amended mixtures for highway subbases*, Eleviser, pp. 932-945.

Ahsan, A. N. (2014). *Pavement performance monitoring using Dynamic Cone Penetrometer and Geogauge during construction*. The University of Texas at Arlington.

Akmaz, E., Ullah, S., Tanyu, B. F., & Guler, E. F. (2020). Construction quality control of unbound base course using light weight deflectometer where reclaimed asphalt pavement aggregate is used as an example. *Transportation Research Record*, 2674(10), pp. 989-1002.

Allersma . (1988). *Optical Analysis of Stress and Strain Around the Tip of a Penetration Probe*, *Proceedings, 1st International Symposium on Penetration Testing*, pp. 615-620.

Alshibli, K. A., Abu-Farsakh, M., & Seyman, E. (2005). Laboratory evaluation of the geogauge and light falling weight deflectometer as construction control tools. *Journal of materials in civil engineering*, 17(5), 560-569.

Andrew, (2012, May25). Comparative evaluation of compacting process for base materials using lab compaction methods. *Transportation Research Record*, 2673(4), pp.558-567.

## *References*

---

*ASTM 1557 research designation. Standard Test Methods for Laboratory Compaction Characteristics of Soil Using Modified Effort.*

*ASTM D 6951-03. (2009). Test method for use of the dynamic cone penetrometer in shallow pavement applications', ASTM International, West Conshohocken, PA.*

*ASTM D1556. (2015). 'Standard Test Method for Density and Unit Weight of Soil in Place by Sand-Cone', ASTM International, West Conshohocken, PA., pp. 1–8.*

*ASTM D1557–12. (2012). "Standard Test Methods for Laboratory Compaction Characteristics of Soil Using Modified Effort," American Society for Testing and Materials .*

*ASTM D1883. (2014). Standard Test Method for CBR (California Bearing Ratio) of Laboratory-Compacted Soils', ASTM International, West Conshohocken, PA, 263(9), , pp. 4095-4063.*

*ASTM D1883–07. (2007). "Standard Test Method for CBR (California Bearing Ratio) of Laboratory-Compacted Soils," American Society for Testing and Materials (ASTM), West .*

*ASTM D2011, " Standard Test Method for Density and Unit Weight of Soil in Place by Sand Cone," American Society for Testing and Materials (ASTM), West Conshohocken, PA. 201.*

*ASTM D2487 – 11, "Standard Practice for Classification of Soils for Engineering Purposes (Unified Soil Classification System)," American Society for Testing and Materials (ASTM), West Conshohocken, PA. 2005.*

*ASTM D854 – 14. (2014). " Standard Test Methods for Specific Gravity of Soil Solids by Water Pycnometer", American Society for Testing and Materials (ASTM), West .*

*bin Arshad, A. K. (2007). Flexible pavement design: Transitioning from empirical to mechanistic-based design methods.*

## *References*

---

Coonse, J. W. (1999). *Estimating California bearing ration of cohesive Piedmont residual soil using the Scala dynamic cone penetrometer (Doctoral dissertation, North Carolina State University)*

Das, N. (2009). *A comparison study of three non-parametric control charts to detect shift in location parameters. The International Journal of Advanced Manufacturing Technology, 41(7), 799-807.*

Dr. van Vuuren . (2015, June 5). *Assessment of Material Strength Using Dynamic Cone Penetrometer Test for Pavement Applications, Airfield and Highway Pavement.*

Ebrahimi, A., & Edil, T. B. (2013). *Light-weight deflectometer for mechanistic quality control of base course materials. Proceedings of the Institution of Civil Engineers-Geotechnical Engineering, 166(5), 441-450.*

Emre AKmaz. (2020, August 27). *Construction Quality Control of Unbound Base Course using Light Weight Deflectometer where Reclaimed Asphalt Pavement Aggregate is Used as an Example, Transportation Research Record,, pp. 989-1002.*

Fleming, P. R., Frost, M. W., & Lambert, J. P. (2007). *Review of lightweight deflectometer for routine in situ assessment of pavement material stiffness. Transportation Research Record, 2004(1), 80-87.*

Gabr. (2000, July 12). *PFWD, DCP and CBR correlations for evaluation of lateritic subgrades, International Journal of Pavement Engineering . pp.189.199.*

George, D., & Mallery, P. (2019). *IBM SPSS statistics 26 step by step: A simple guide and reference. Routledge.*

Günaydın, O. (2009). *Estimation of soil compaction parameters by using statistical analyses and artificial neural networks. Environmental Geology, 57(1), 203.*

## *References*

---

*Harison, J. A. (1989). In situ CBR determination by DCP testing using a laboratory-based correlation. Australian Road Research, 19(4).*

*Harison, J. A. (1989). In situ CBR determination by DCP testing using a laboratory-based correlation. Australian Road Research, 19(4).*

*Hossain, M. S., & Apeageyi, A. K. (2010). Evaluation of the lightweight deflectometer for in-situ determination of pavement layer moduli (No. VTRC 10-R6). Virginia Transportation Research Council.*

*John Bilyeu. (2001, March 4). Application of Dynamic Cone Penetrometer in Evaluation of Base and Subgrade Layers ,Transportation Research Record, pp. 1-10.*

*Kleyn, E. G. (1975). The use of the dynamic cone penetrometer (DCP). Transvaal Provincial Administration.*

*Lee, P. Y., & Suedkamp, R. J. (1972). Characteristics of irregularly shaped compaction curves of soils. Highway Research Record, 381, 1-9.*

*lin . (2006, March 4). Influence Of Falling Height And Plate Size On Surface Stiffness Evaluated By LWD, Department of Civil Engineering, King Mongkut's University of Technology Thonburi, Thailand.*

*Livneh M. and Livneh N. A., 1994, "Subgrade Strength Evaluation with the Extended Dynamic Cone Penetrometer," Proc., 7th Int., Congress Int., Association of Engineering Geology, Vol. 1, Lisbon.*

*Livneh, A., & Langevitz, P. (2000). Diagnostic and treatment concerns in familial Mediterranean fever. Best Practice & Research Clinical Rheumatology, 14(3), 477-498.*

*Louay et al. (2009). Estimation of Subgrade Soils Resilient Modulus from In-Situ Devices Test Results." Journal of Testing and Evaluation (ASTM), 37(3),PP. 1-9.*

## *References*

---

*Madhira, M., Abhishek, S. V., & Rajyalakshmi, K. (2015). Modelling ground–foundation interactions. In Hyderabad, India: International Conference on Innovations in Structural Engineering, At Osmania University, December.*

*Meier and Baladi. (1988). Cone Index Based Estimates of Soil Strength, Theory and Computer Code CIBESS”, Technical Report No. SL-88-11.*

*MJ Thomas. (2007, October 10). Relationships between In Situ and Roller-Integrated Compaction Measurements for Granular Soils ,Asia Pacific Disability Rehabilitation Journal.pp.60-75.*

*Moony. (2013, March 1). nfluence of Lightweight Deflectometer Characteristics on Deflection Measurement,Geotechnical Testing Journal , pp. 216-226.*

*Mujtaba, H., Farooq, K., Sivakugan, N., & Das, B. M. (2013). Correlation between gradational parameters and compaction characteristics of sandy soils. International Journal of Geotechnical Engineering, 7(4),pp. 395-401.*

*Nazzal, M. (2003). Field evaluation of in-situ test technology for QC/QA procedures during construction of pavement layers and embankments. Louisiana State University, Master of Science, Baton Rouge.*

*Nazzal, M., Abu-Farsakh, M., Alshibli, K., & Mohammad, L. (2004). Evaluating the potential use of a portable LFWD for characterizing pavement layers and subgrades. In Geotechnical Engineering for Transportation Projects (pp. 915-924).*

*Patel, A. (2019). Geotechnical investigations and improvement of ground conditions. Woodhead Publishing.*

*Ramaswami Sridharan. (2004, July). Dynamic Compaction of Granular Soils ,International Journal of Physical, pp. 44-62.*

## *References*

---

Rao et al. (2008). "PFWD, CBR and DCP Evaluation of Lateritic Subgrades of Dakshina Kannada, India." *The 12th International Conference of International Association for Computer Methods and Advances in Geotechnics IACMAG*, National Institute of Technology Karnataka, Mangalore , pp. 4417-4423.

Reyn. (2005, December). *Correlation of Resistance Value with California Bearing Ratio for use in design of flexible pavements*. SAGE Journal. pp.80-85.

Richard Ji. (2013, November 17). *Evaluation of Resilient Modulus of Subgrade and Base Materials in Indiana and Its Implementation in MEPDGNDOT Office of Research and Development, 1205 Montgomery Street, West Lafayette, IN 47906, USA*, pp. 1-15.

Rodrigo, S.R., & Yoon, S. (2003). *Dynamic cone penetration test (DCPT) for subgrade assessment*. Joint Transportation Research Program, 73.

Roy. (2013, March 22). *Influence of pavement moisture content on the load-bearing capacity of forest road*, researchgate. SAGE Journals. pp. 1-8.

Salgado, R., Mitchell, J. K., & Jamiolkowski, M. (1997). *Cavity expansion and penetration resistance in sand*. *Journal of Geotechnical and Geoenvironmental Engineering*, 123(4), 344-354.

Sanjeev. (2020, November 16). *Development of structural condition assessment model for flexible pavement based on LWD and GPR measurements*, pp. 570-578.

Santner, T. J., Williams, B. J., Notz, W. I., & Williams, B. J. (2003). *The design and analysis of computer experiments (Vol. 1)*. New York: Springer.

Savage . (2012, September). *Optimum Design Of Sustainable Sealed Low Volume Roads Using the Dynamic Cone Penetrometer (DCP)*. SAGE Journals. pp.10.25.



## *References*

---

*Scala, S. M., & Baulknight, C. W. (1959). Transport and thermodynamic properties in a hypersonic laminar boundary layer part i properties of the pure species. ARS Journal, 29(1), 39-45.*

*Shaban, A. M., & Cosentino, P. J. (2016). Comparative analyses of granular pavement moduli measured from lightweight deflectometer and miniaturized pressuremeter tests. Transportation Research Record, 2579(1), pp.48-58.*

*Shaban. (2016, December). Comparative Analyses of Granular Pavement Moduli Measured from Lightweight Deflectometer and Miniaturized Pressuremeter Tests, Transportation Research Board, Washington,, pp. 48-58.*

*Shen, Y., Tang, T., Zuo, R., Tian, Y., Zhang, Z., & Wang, Y. (2020). The effect and parameter analysis of stress release holes on decreasing frost heaves in seasonal frost areas. Cold Regions Science and Technology, 169, 102898.*

*Shipley, B. (2016). Cause and correlation in biology: a user's guide to path analysis, structural equations and causal inference with R. Cambridge University Press.*

*Shirur and hirematth. (2014, September). Establishing Relationship between CBR Value and Physical Properties of, IOSR journal of mechanical and civil, pp. 26-30.*

*Stamp, D. H., & Mooney, M. A. (2013). Influence of lightweight deflectometer characteristics on deflection measurement. Geotechnical Testing Journal, 36(2), pp.216-226.*

*Talukdar, D. K. (2014). A study of correlation between California Bearing Ratio (CBR) value with other properties of soil. International Journal of Emerging Technology and Advanced Engineering, 4(1), 559-562.*

*Tascon, A. (2011). Effective depth of soil compaction under a controlled compactive effort at laboratory scale.*

## *References*

---

Vennapusa and White.(2016). Compaction quality control of pavement layers using LWD. *Journal of Materials in Civil engineering*, 28(2), 04015111.

Verma, G., & Kumar, B. (2020). *Prediction of compaction parameters for fine-grained and coarse-grained soils: a review. International Journal of Geotechnical Engineering*, 14(8), 970-977.

Williams, G. W., Sehn, A. L., & Seed, R. B. (1991). *Estimation earth pressures due to compaction. Journal of geotechnical engineering*, 117(12), 1833-1847.

Xiaoyang Jia. (2019, July). *Field density testing by using a nuclear density gauge. Construction and Building Materials*.pp.229.

Yavuz Güll. (2020, May 11). *Prediction of the California bearing ratio from some field measurements of soils,1Department of Mining Engineering, Faculty of Engineering, Sivas Cumhuriyet*, pp. 1-26.

Zhang, Y., Meratnia, N., & Havinga, P. (2007). *A taxonomy framework for unsupervised outlier detection techniques for multi-type data sets. Computer*, 49(3), 355-363.

## Appendix A: LWD Testing Curves

### A-3: Al-Fares district

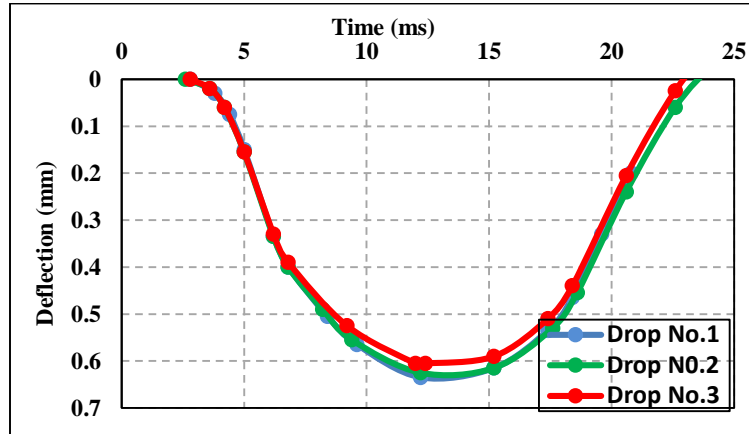


Figure (1.1): Point one time-deflection curve of LWD (No. of passing 10)

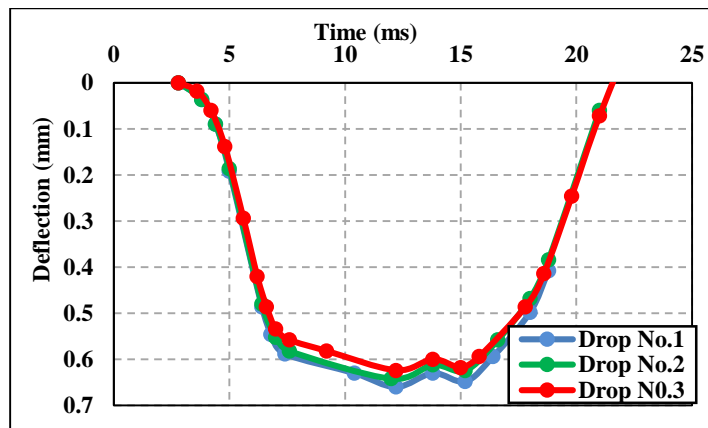


Figure (1.2): Point two time-deflection curve of LWD (No. of passing 10)

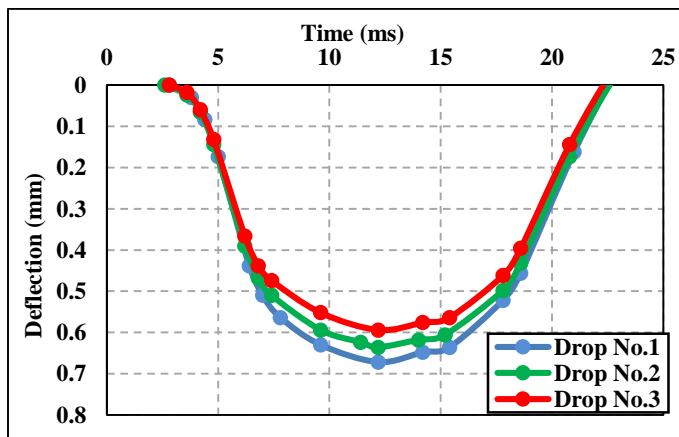


Figure (1.3): Point three time-deflection curve of LWD (No. of passing 10)

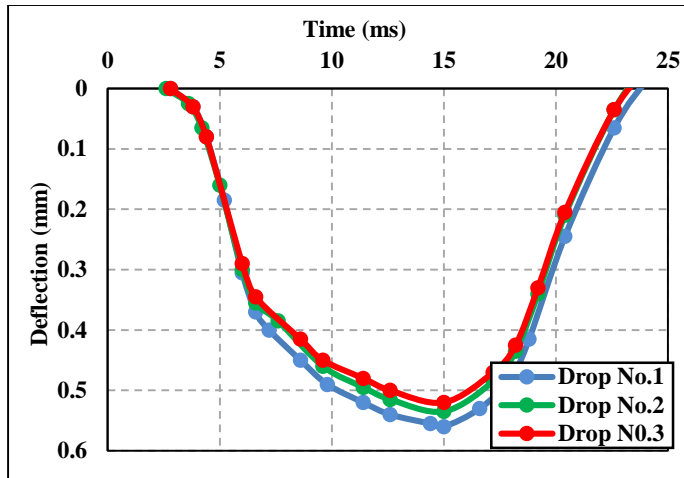


Figure (1.4): Point four time-deflection curve of LWD (No. of passing 10)

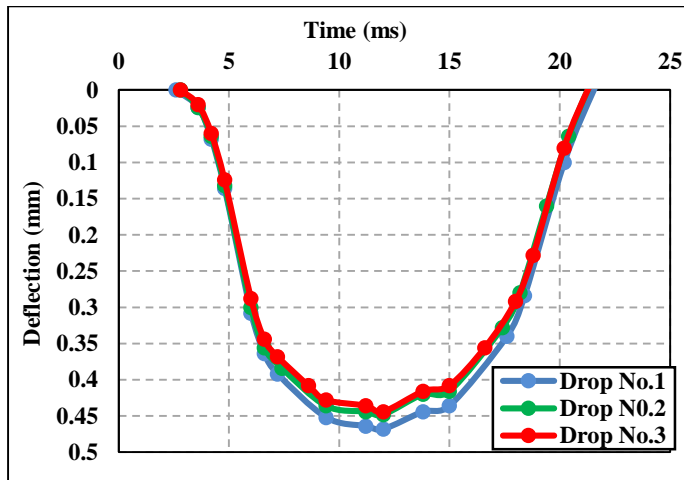


Figure (1.5): Point five time-deflection curve of LWD (No. of passing 10)

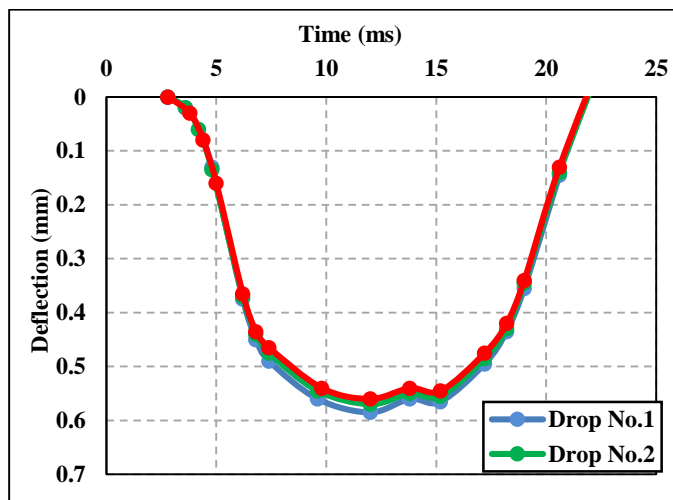


Figure (1.6): Point six time-deflection curve of LWD (No. of passing 10)

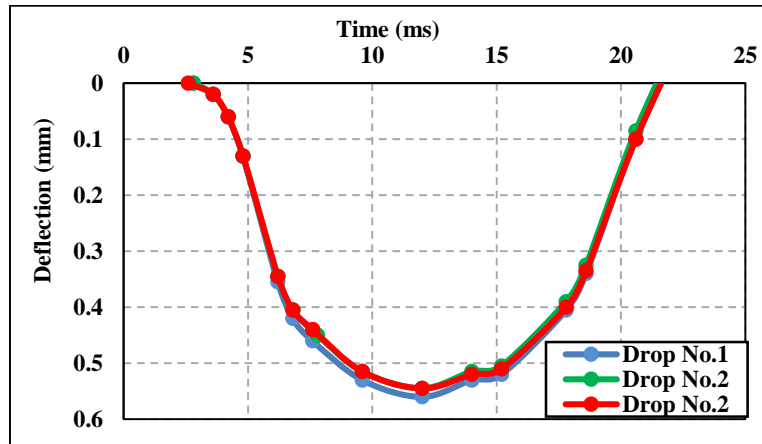


Figure (2.1): Point one time-deflection curve of LWD (No. of passing 14)

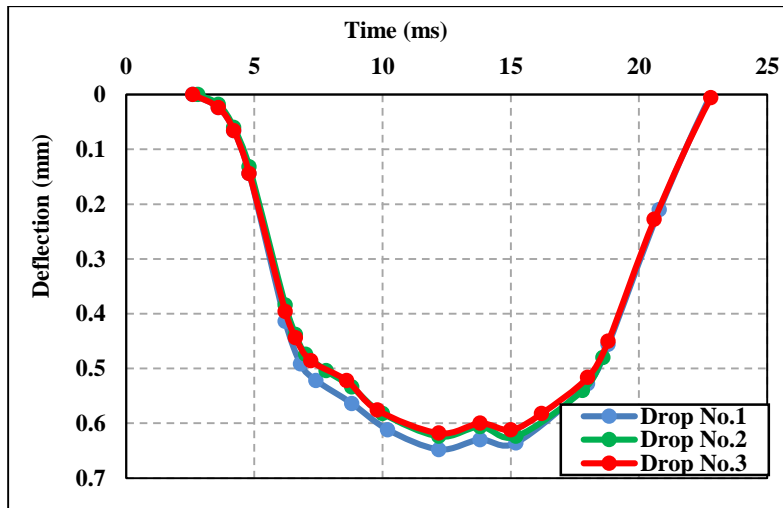


Figure (2.2): Point two time-deflection curve of LWD (No. of passing 14)

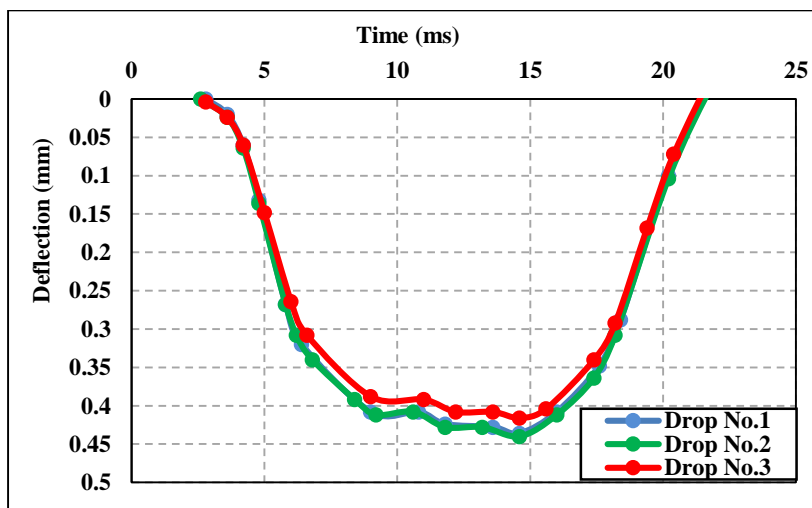


Figure (2.3): Point three time-deflection curve of LWD (No. of passing 14)

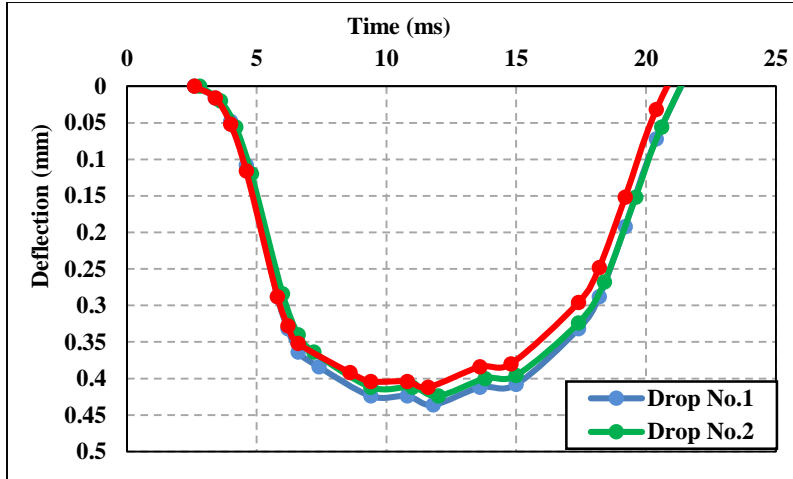


Figure (2.4): Point four time-deflection curve of LWD (No. of passing 14)

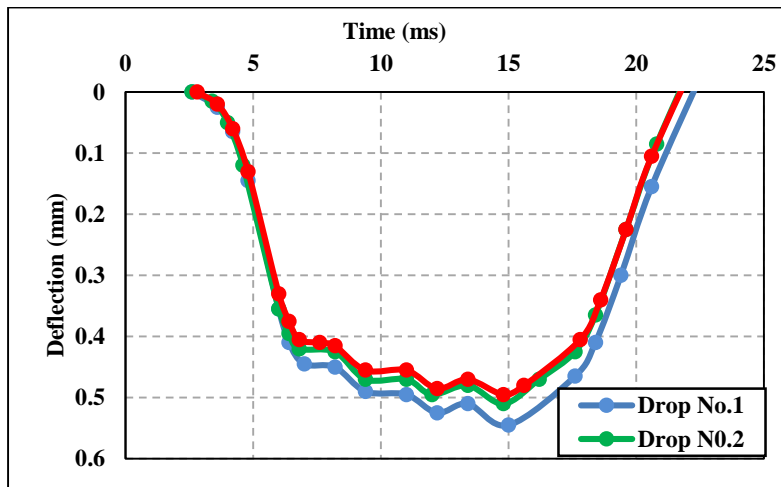


Figure (2.5): Point five time-deflection curve of LWD (No. of passing 14)

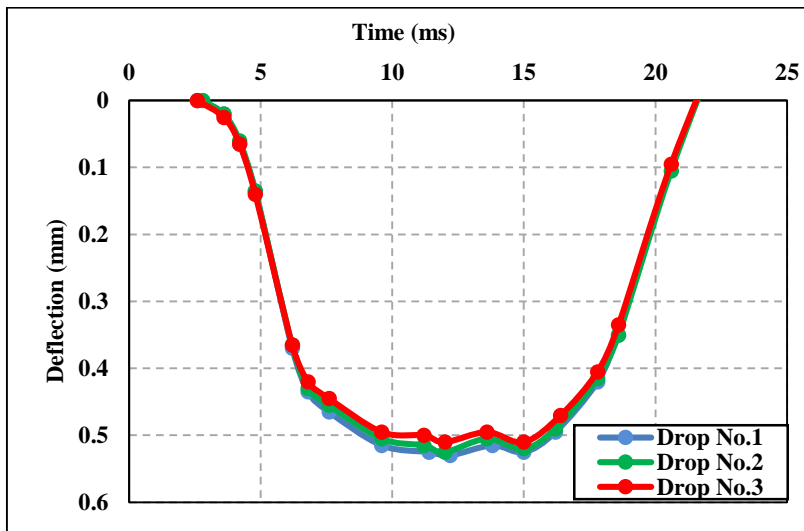


Figure (2.6): Point six time-deflection curve of LWD (No. of passing 14)

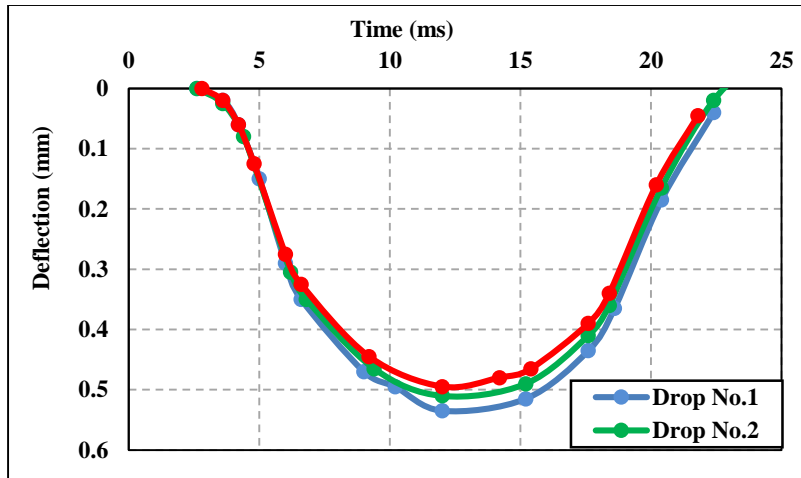


Figure (3.1): Point one time-deflection curve of LWD (No. of passing 18)

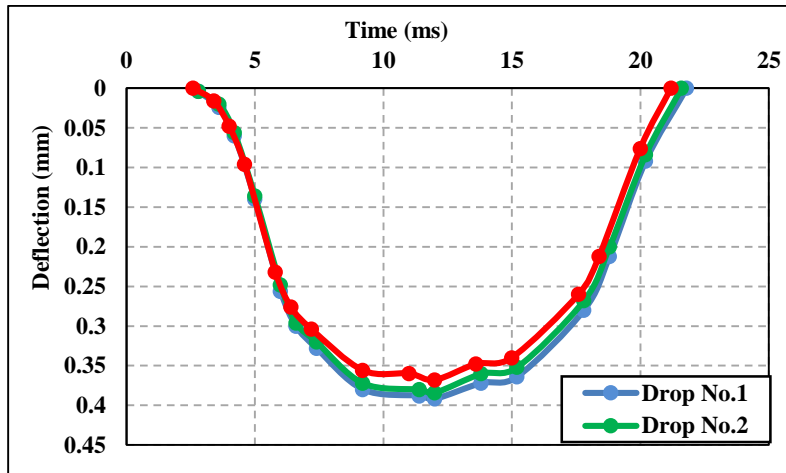


Figure (3.2): Point two time-deflection curve of LWD (No. of passing 18)

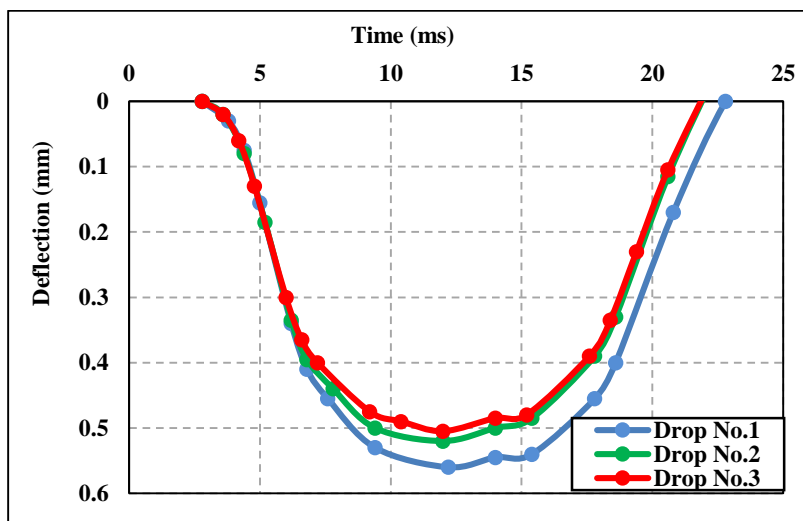


Figure (3.3): Point three time-deflection curve of LWD (No. of passing 18)

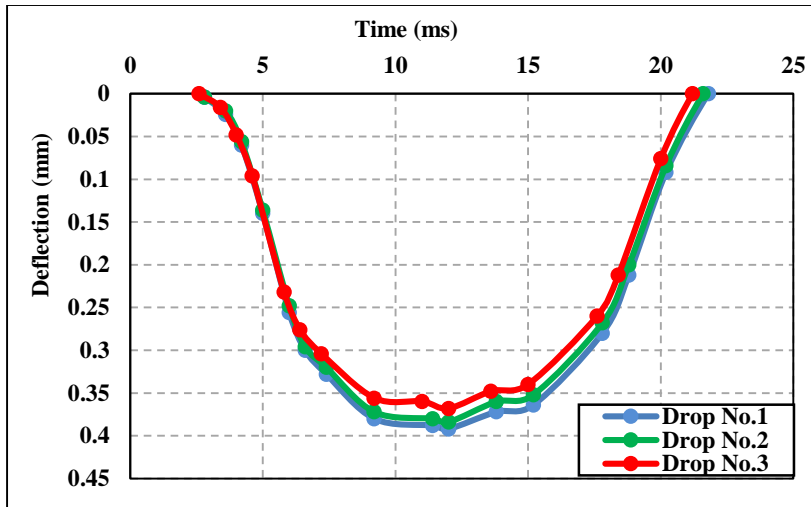


Figure (3.4): Point four time-deflection curve of LWD (No. of passing 18)

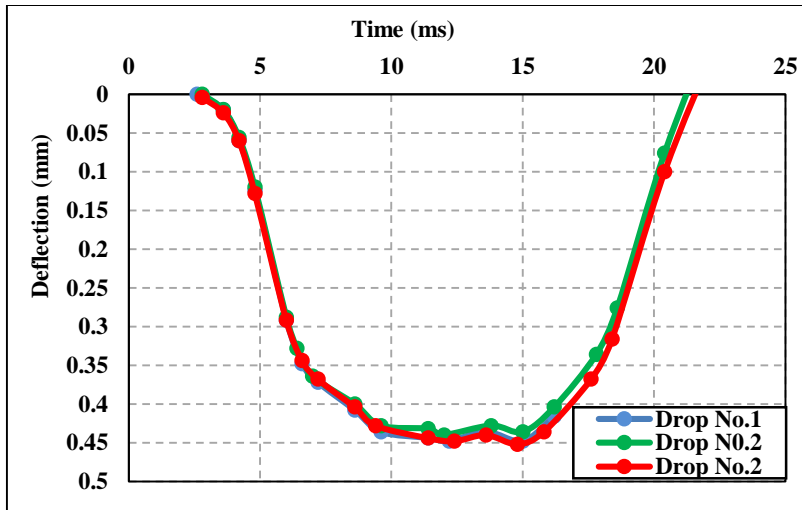


Figure (3.5): Point five time-deflection curve of LWD (No. of passing 18)

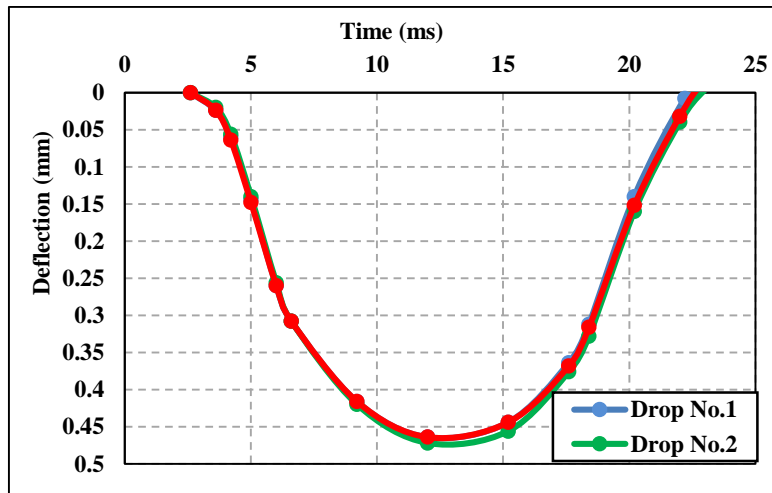


Figure (3.6): Point six time-deflection curve of LWD (No. of passing 18)



**A-3: Al-Intifada district**

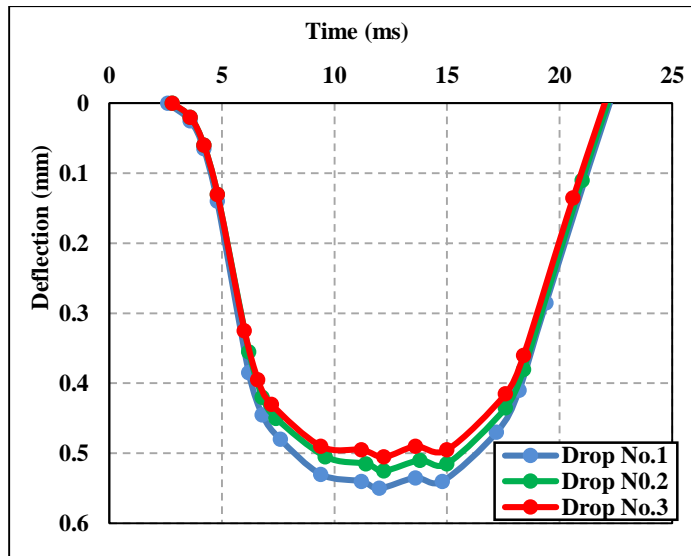


Figure (1.1): Point one time-deflection curve of LWD (No. of passing 10)

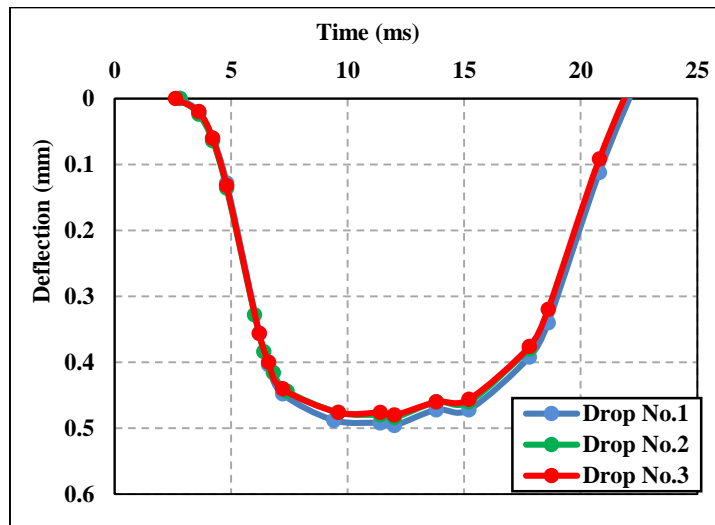


Figure (1.2): Point two time-deflection curve of LWD (No. of passing 10)

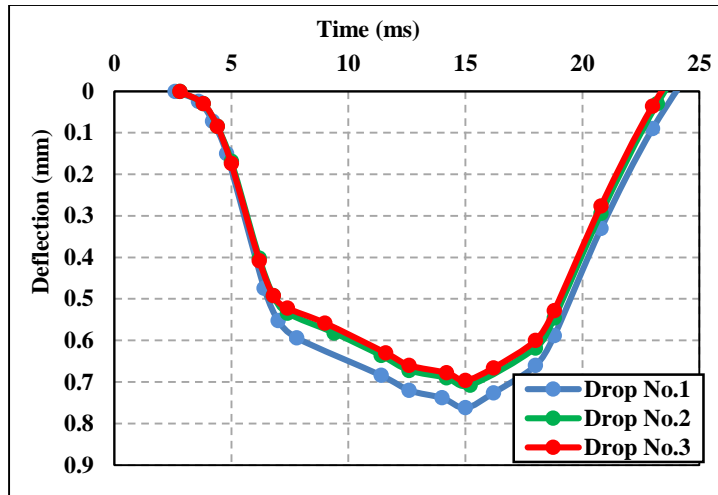


Figure (1.3): Point three time-deflection curve of LWD (No. of passing 10)

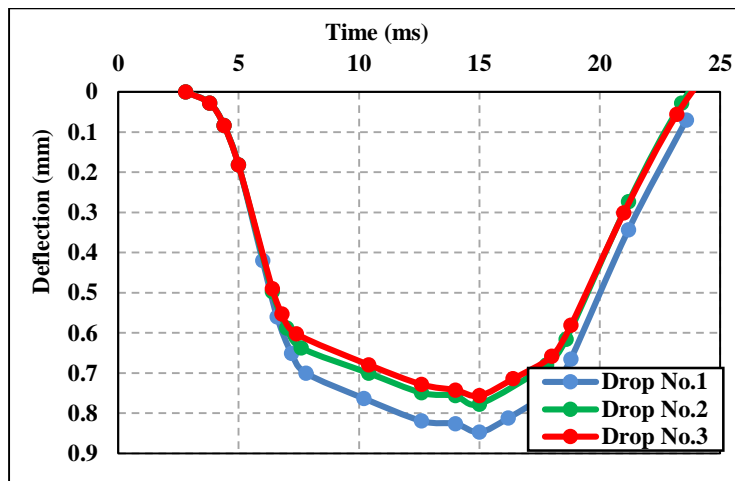


Figure (1.4): Point four time-deflection curve of LWD (No. of passing 10)

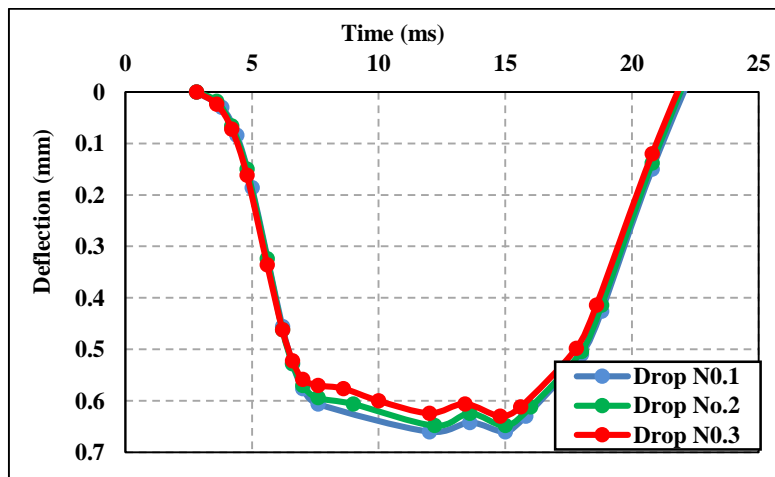


Figure (1.5): Point five time-deflection curve of LWD (No. of passing 10)

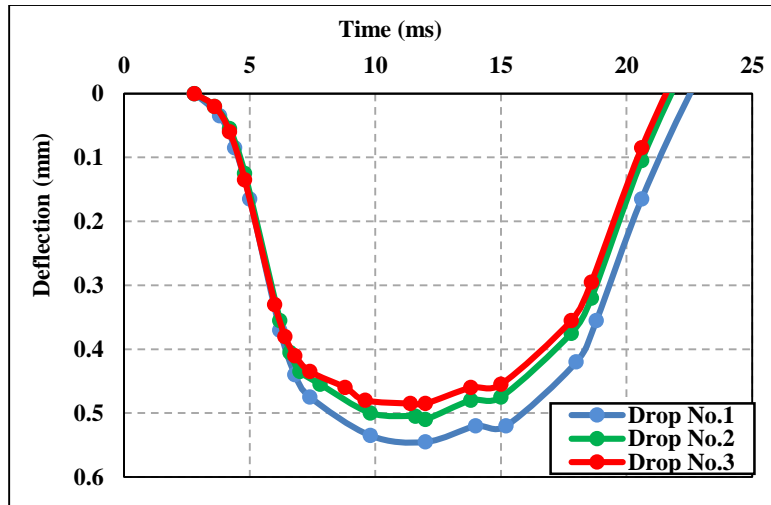


Figure (1.6): Point six time-deflection curve of LWD (No. of passing 10)

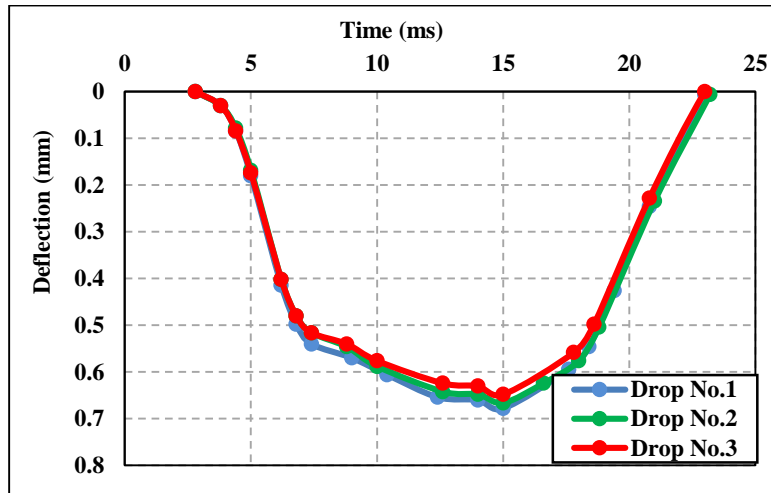


Figure (2.1): Point one time-deflection curve of LWD (No. of passing 14)

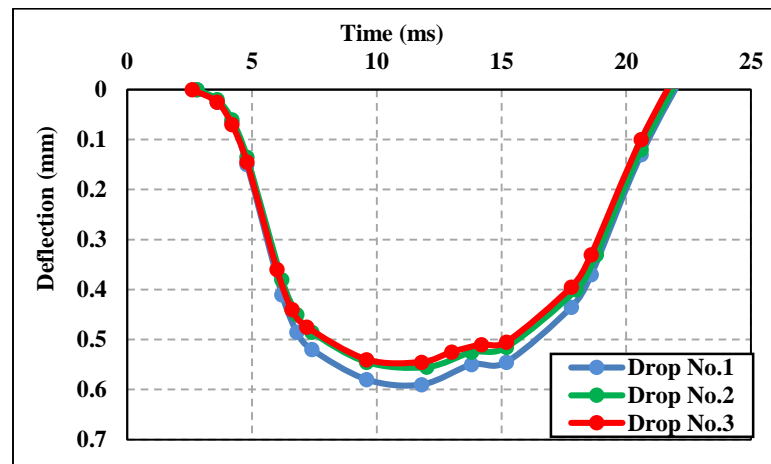


Figure (2.2): Point two time-deflection curve of LWD (No. of passing 14)

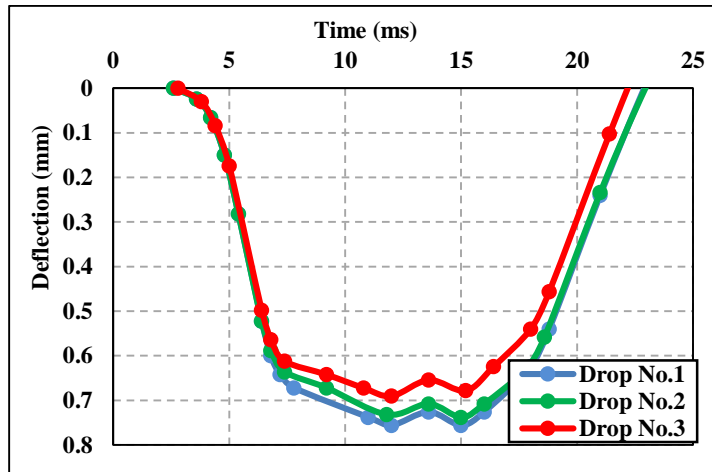


Figure (2.3): Point three time-deflection curve of LWD (No. of passing 14)

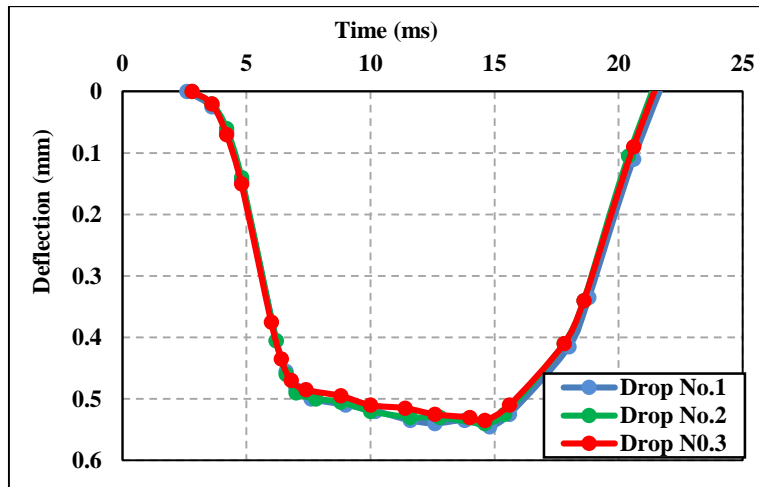


Figure (2.4): Point four time-deflection curve of LWD (No. of passing 14)

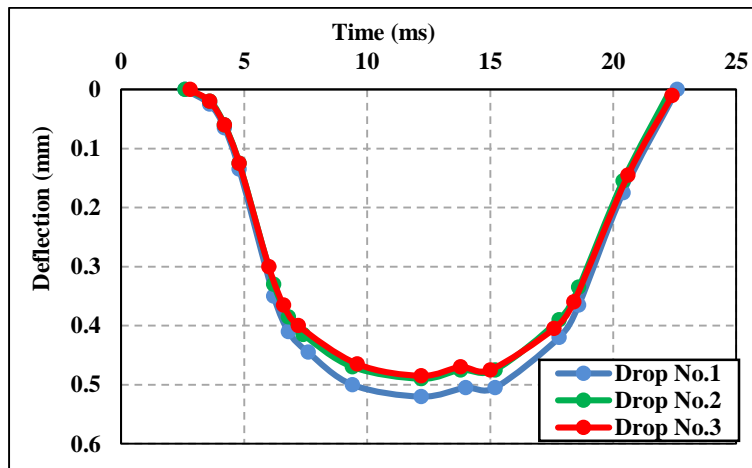


Figure (2.5): Point five time-deflection curve of LWD (No. of passing 14)

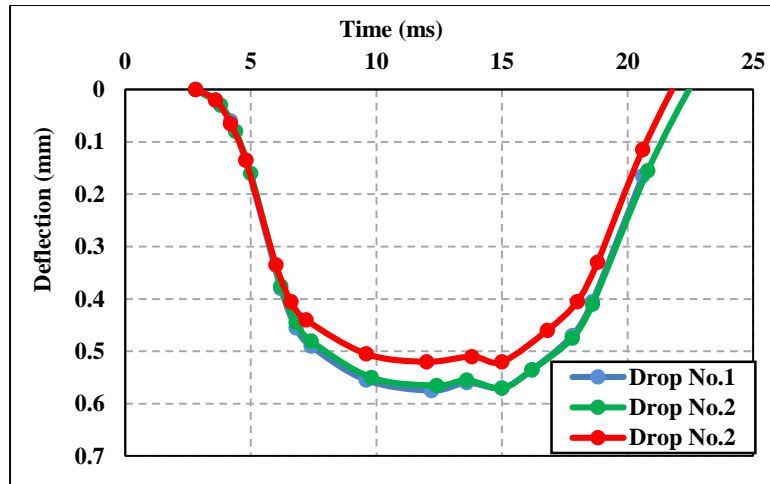


Figure (2.6): Point six time-deflection curve of LWD (No. of passing 14)

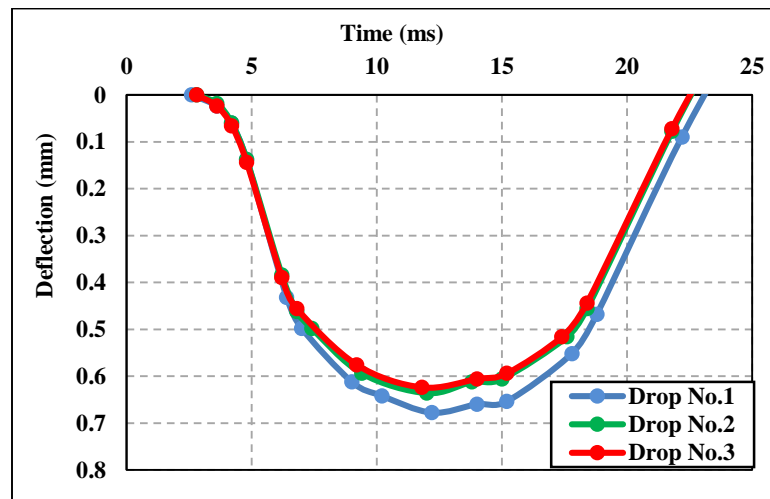


Figure (3.1): Point one time-deflection curve of LWD (No. of passing 18)

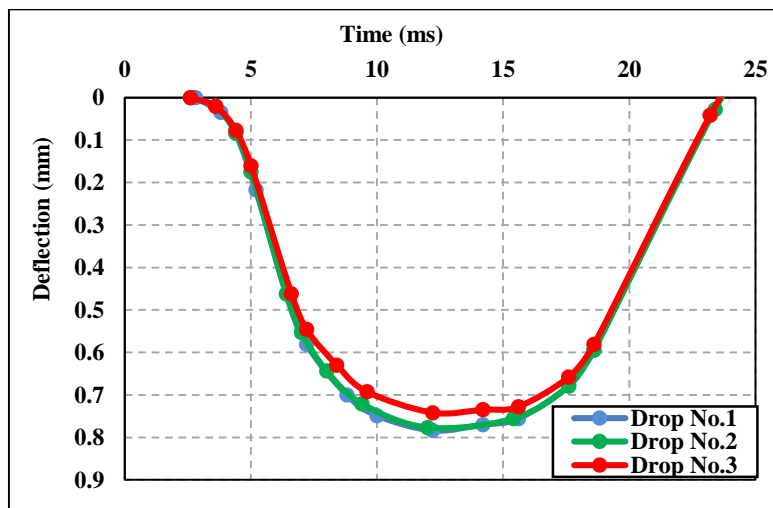


Figure (3.2): Point two time-deflection curve of LWD (No. of passing 18)

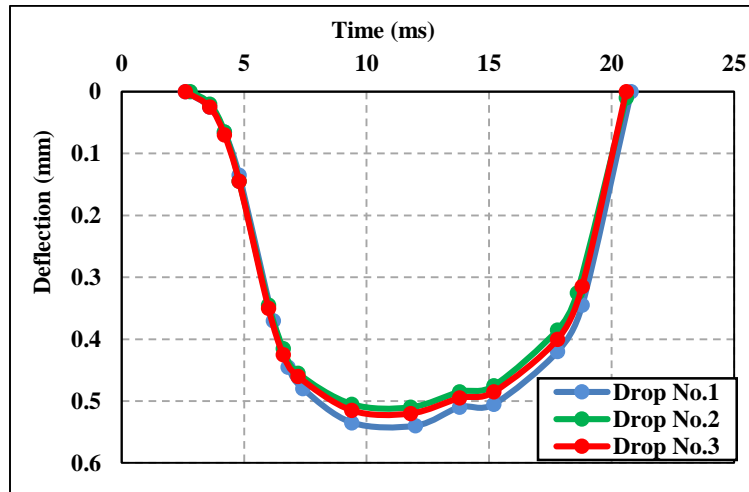


Figure (3.3): Point three time-deflection curve of LWD (No. of passing 18)

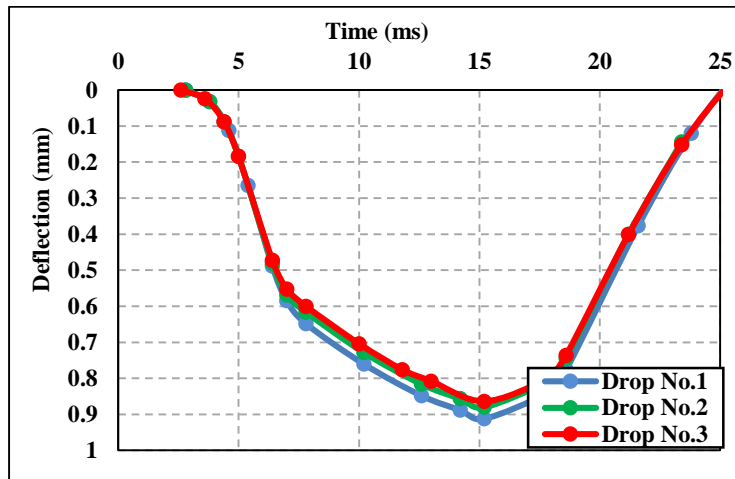


Figure (3.4): Point four time-deflection curve of LWD (No. of passing 18)

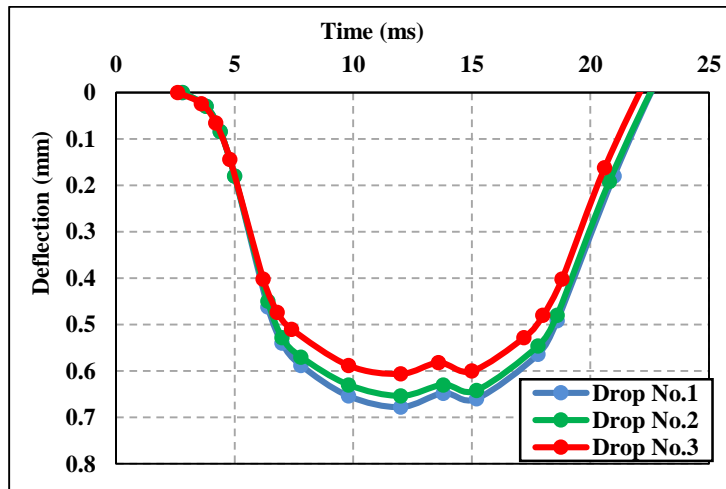


Figure (3.5): Point five time-deflection curve of LWD (No. of passing 18)

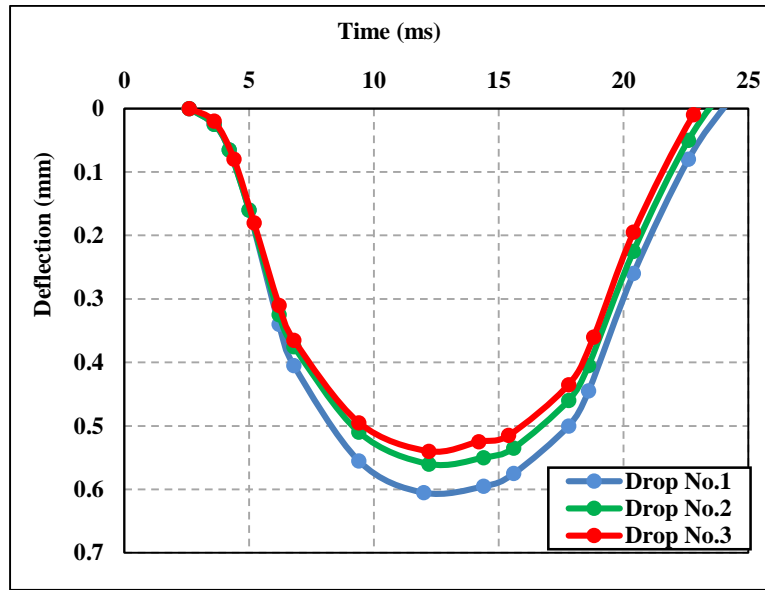


Figure (3.6): Point six time-deflection curve of LWD (No. of passing 18)

### A-3: Al-Tahady district

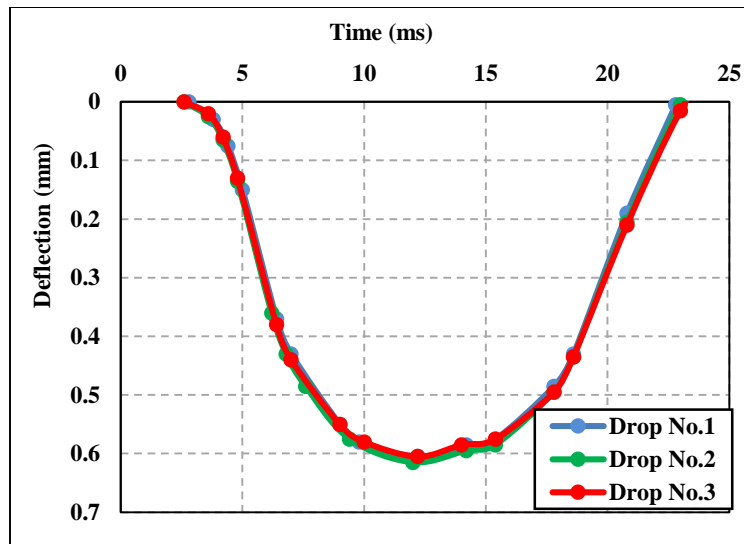


Figure (1.1): Point one time-deflection curve of LWD (No. of passing 10)

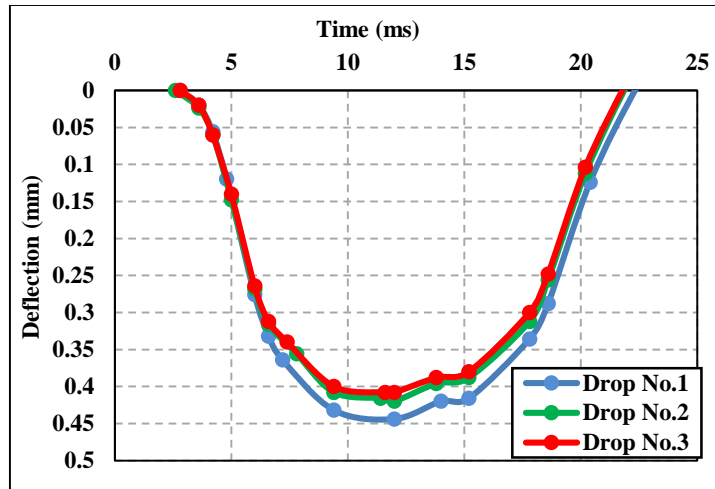


Figure (1.2): Point two time-deflection curve of LWD (No. of passing 10)

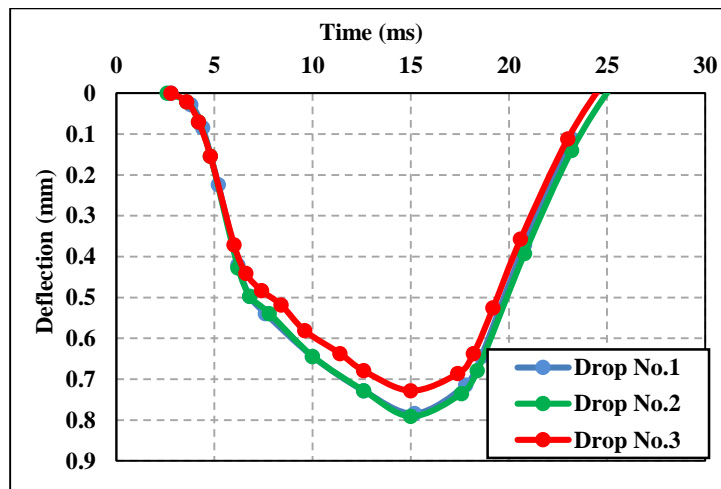


Figure (1.3): Point three time-deflection curve of LWD (No. of passing 10)

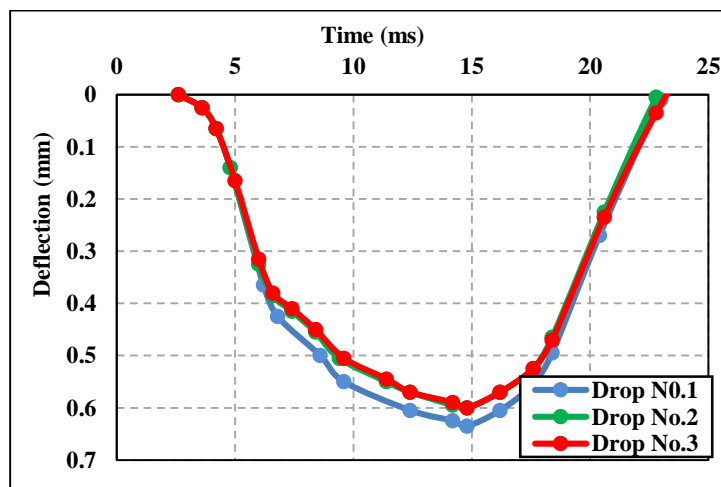


Figure (1.4): Point four time-deflection curve of LWD (No. of passing 10)



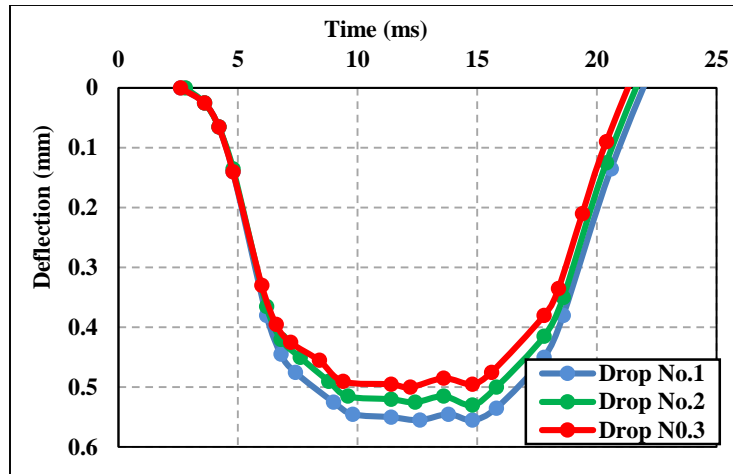


Figure (1.5): Point five time-deflection curve of LWD (No. of passing 10)

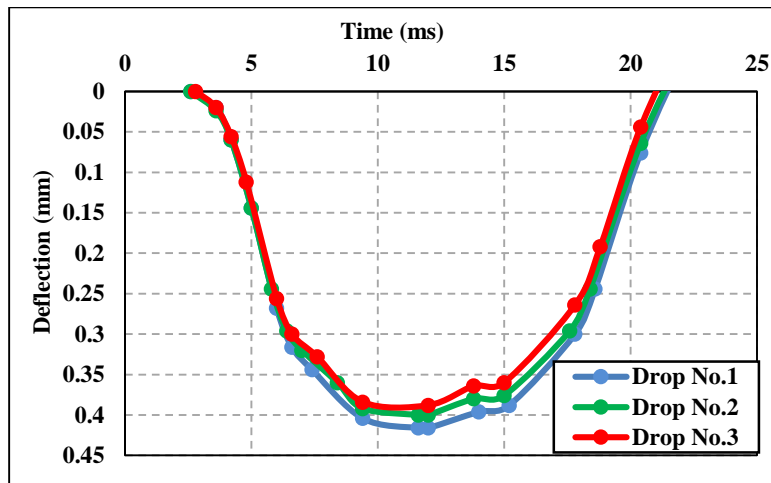


Figure (1.6): Point six time-deflection curve of LWD (No. of passing 10)

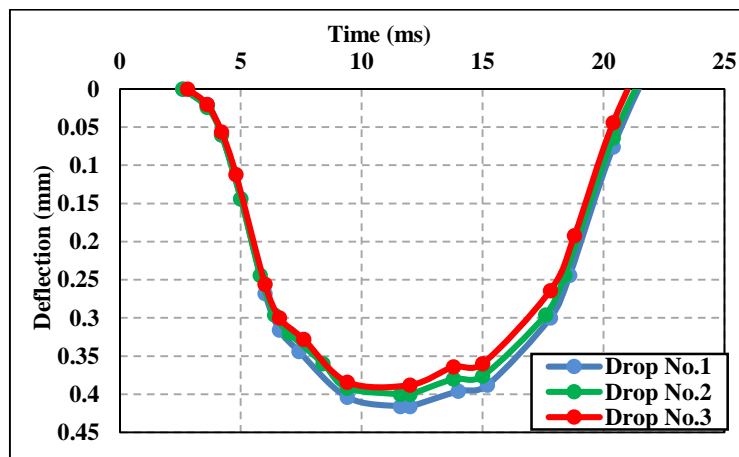


Figure (2.1): Point one time-deflection curve of LWD (No. of passing 14)

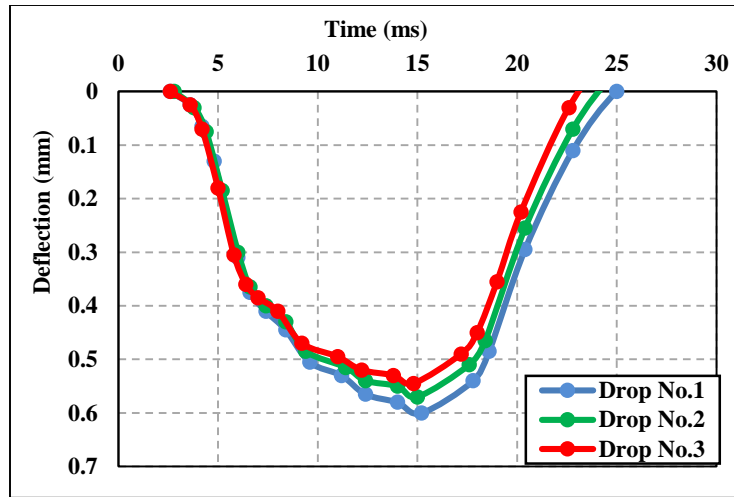


Figure (2.2): Point two time-deflection curve of LWD (No. of passing 14)

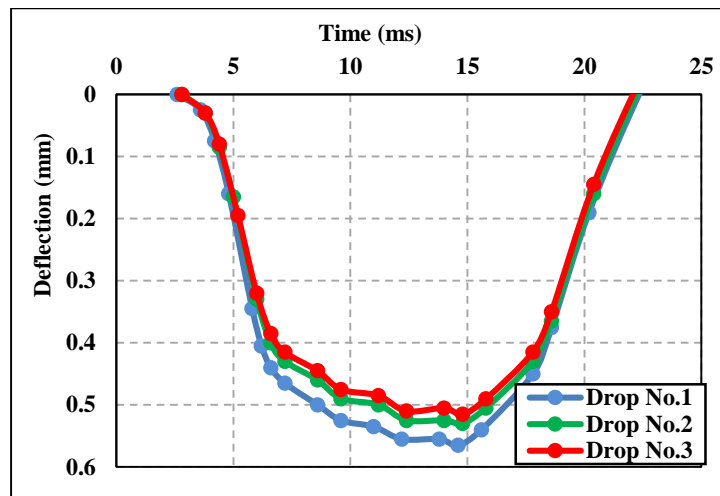


Figure (2.3): Point three time-deflection curve of LWD (No. of passing 14)

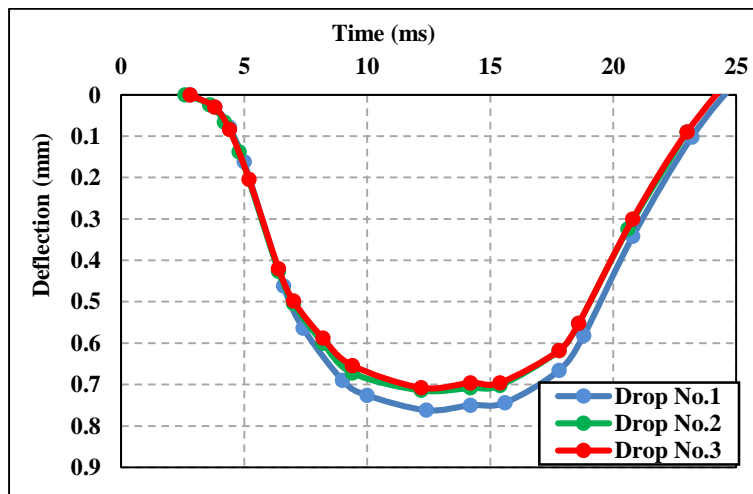


Figure (2.4): Point four time-deflection curve of LWD (No. of passing 14)

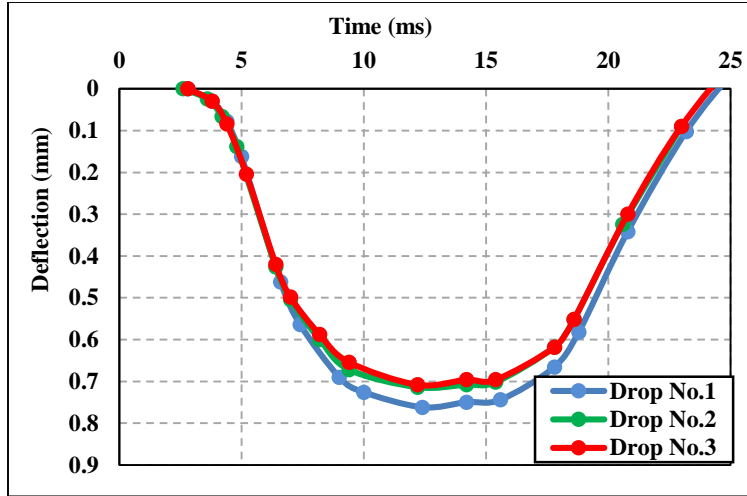


Figure (2.5): Point five time-deflection curve of LWD (No. of passing 14)

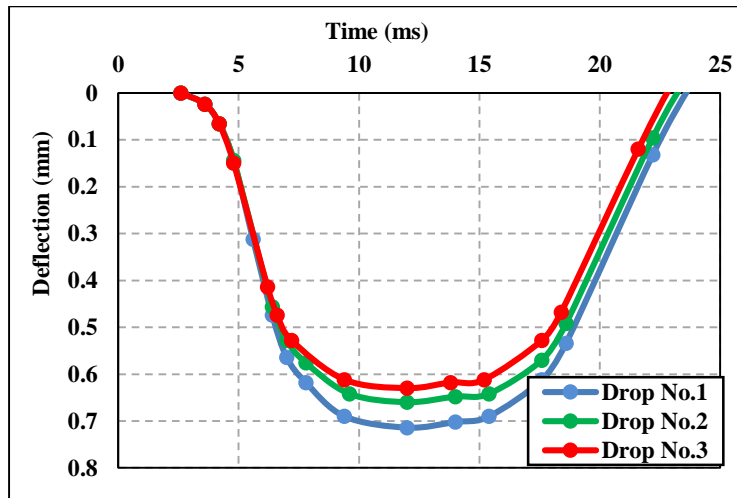


Figure (2.6): Point six time-deflection curve of LWD (No. of passing 14)

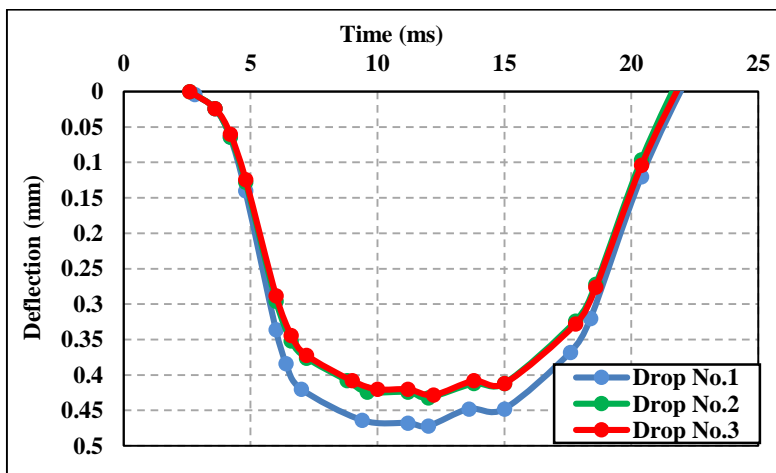


Figure (3.1): Point one time-deflection curve of LWD (No. of passing 18)

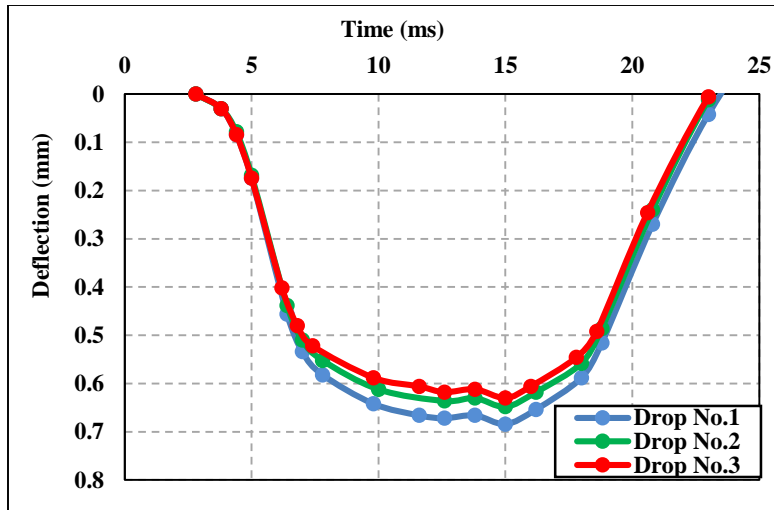


Figure (3.2): Point two time-deflection curve of LWD (No. of passing 18)

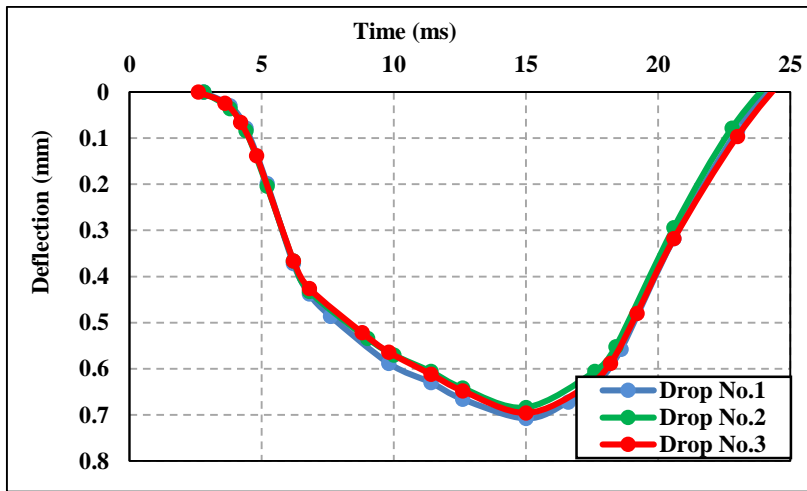


Figure (3.3): Point three time-deflection curve of LWD (No. of passing 18)

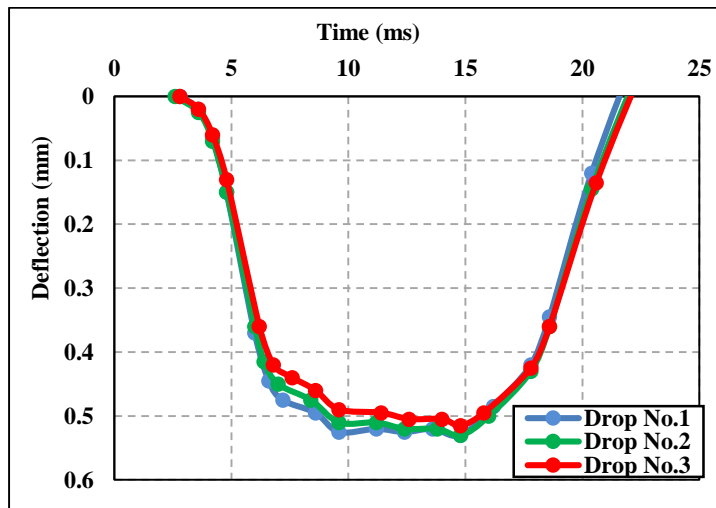


Figure (3.4): Point four time-deflection curve of LWD (No. of passing 18)

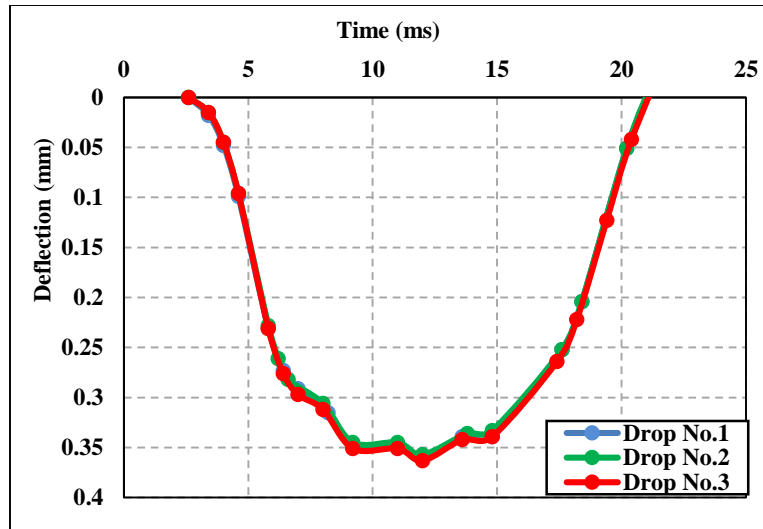


Figure (3.5): Point five time-deflection curve of LWD (No. of passing 18)

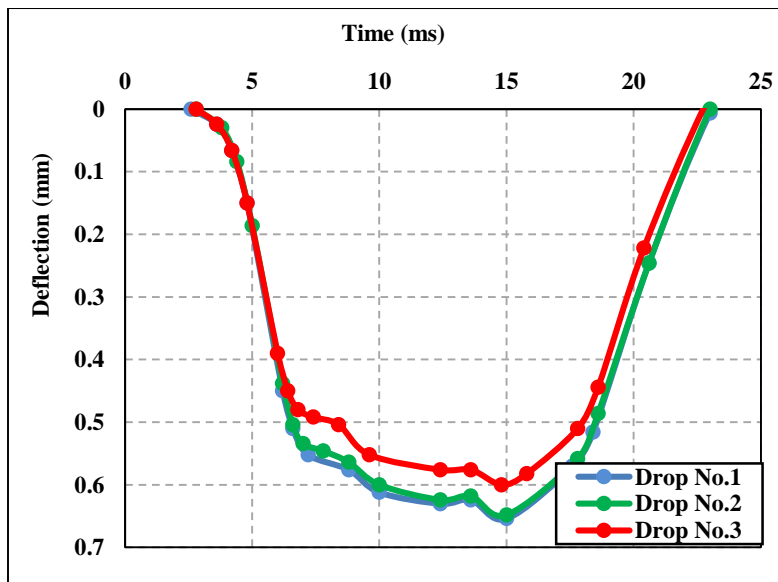


Figure (3.6): Point six time-deflection curve of LWD (No. of passing 18)

## Appendix A: DCP Testing Curves

### A-3: Al-Faris district

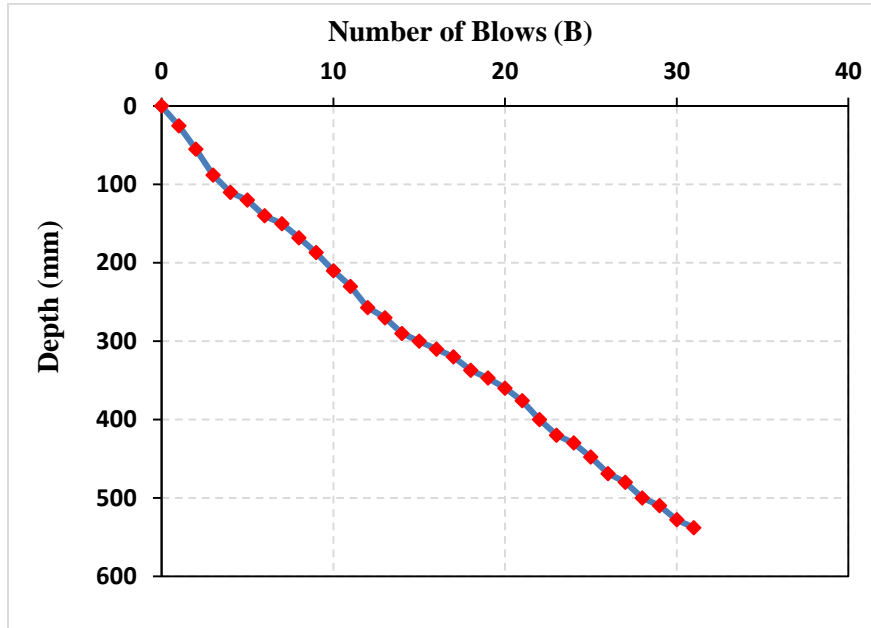


Figure (1.1): Number of blows verse the depth of DCP (No. of passing 10)

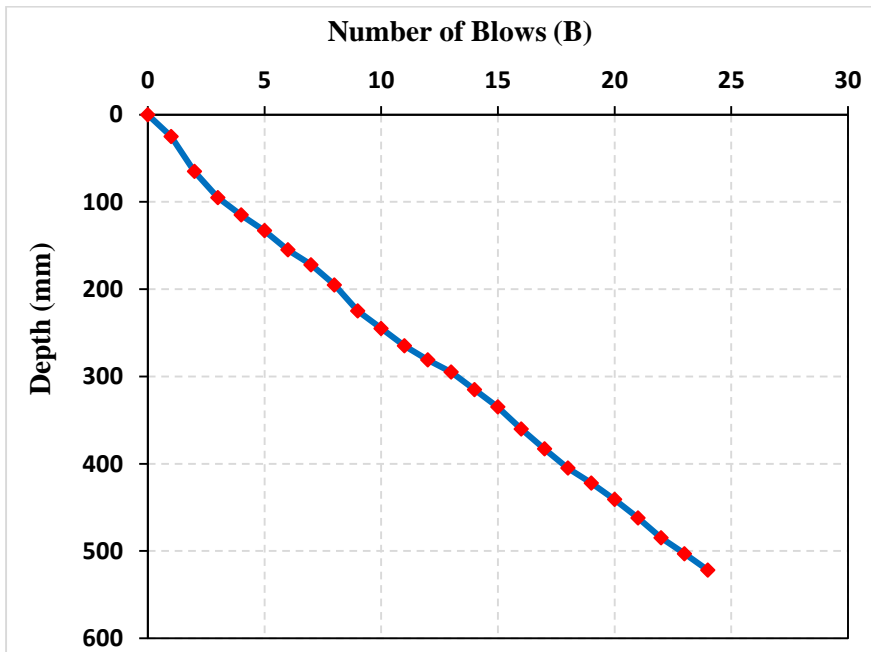


Figure (1.2): Number of blows verse the depth of DCP (No. of passing 10)

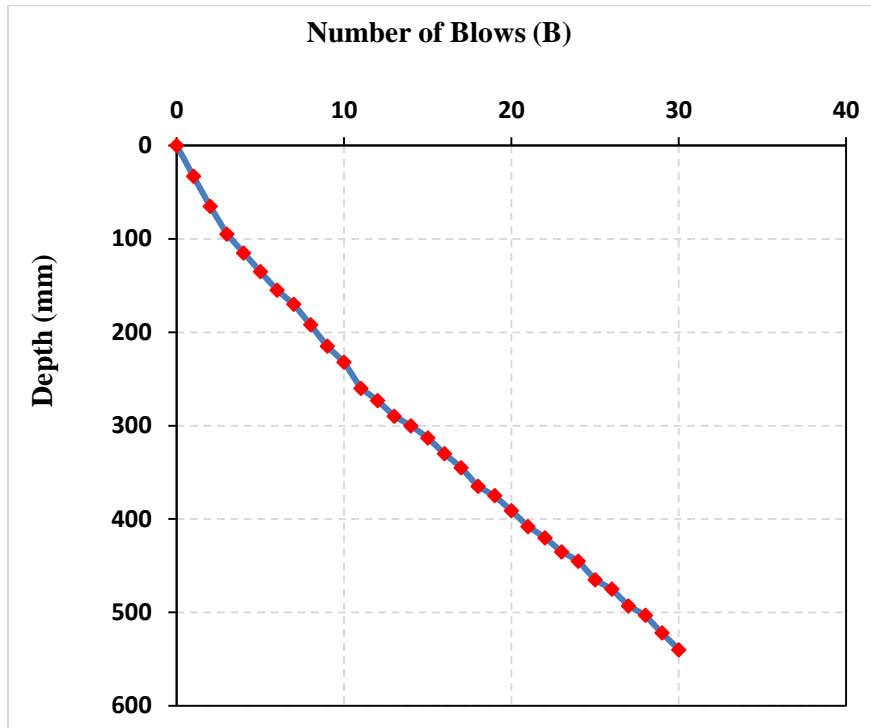


Figure (1.3): Number of blows verse the depth of DCP (No. of passing 10)

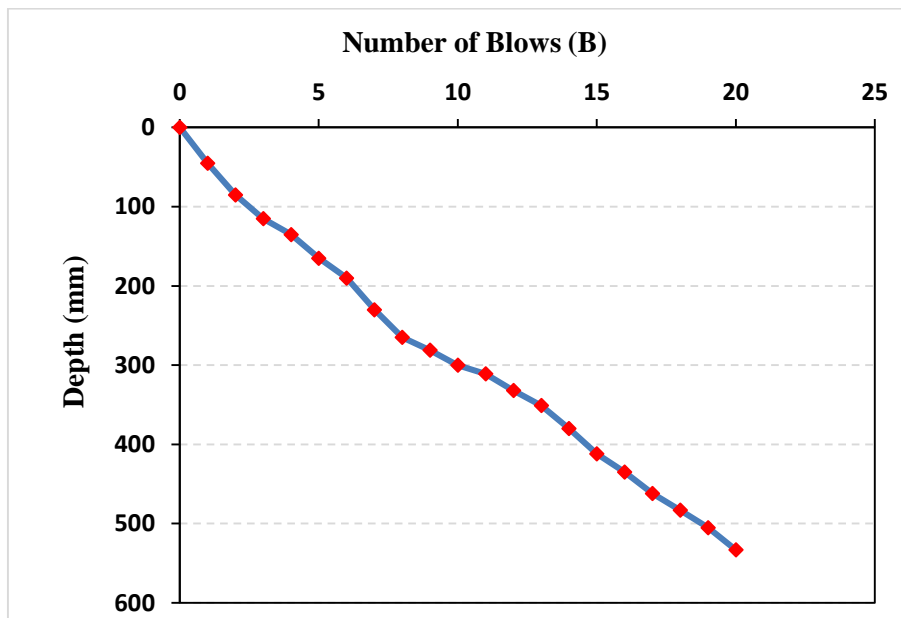


Figure (1.4): Number of blows verse the depth of DCP (No. of passing 10)

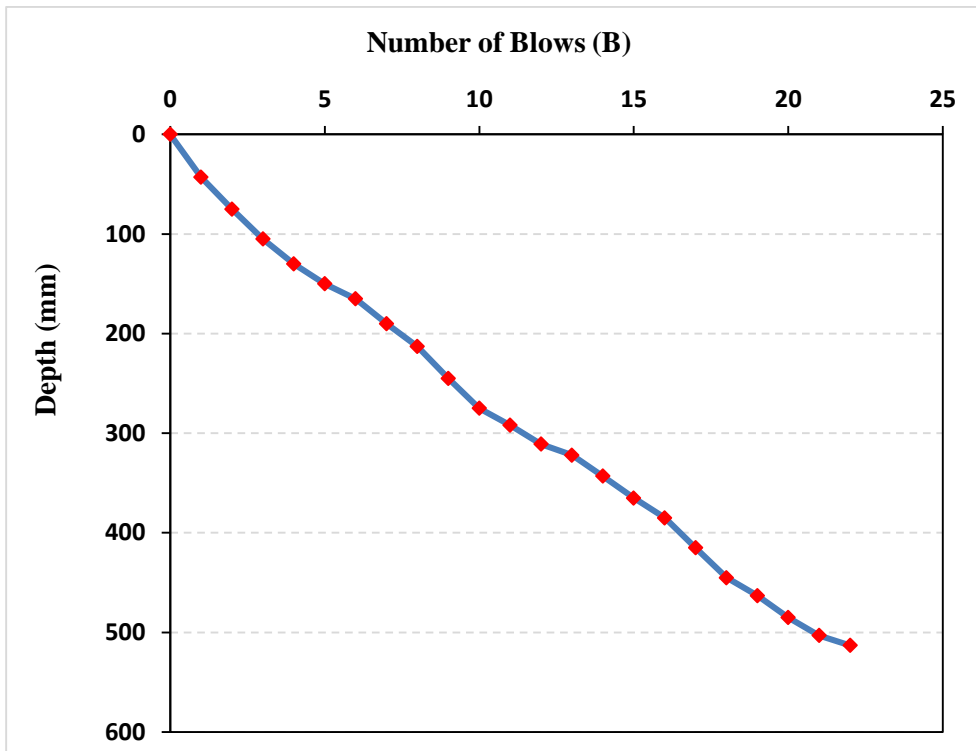


Figure (1.5): Number of blows verse the depth of DCP (No. of passing 10)

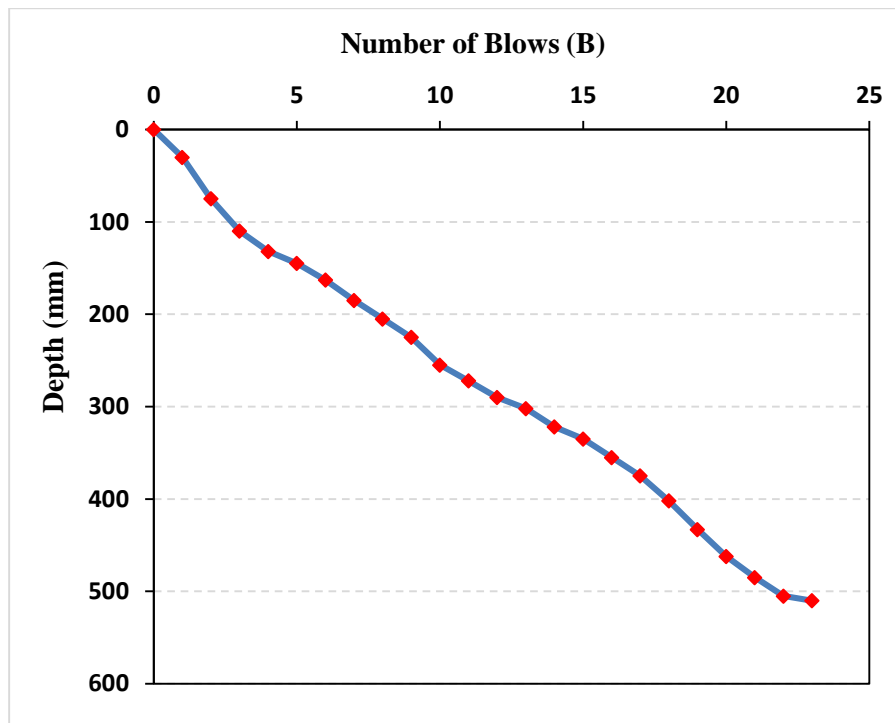




Figure (1.6): Number of blows verse the depth of DCP (No. of passing 10)

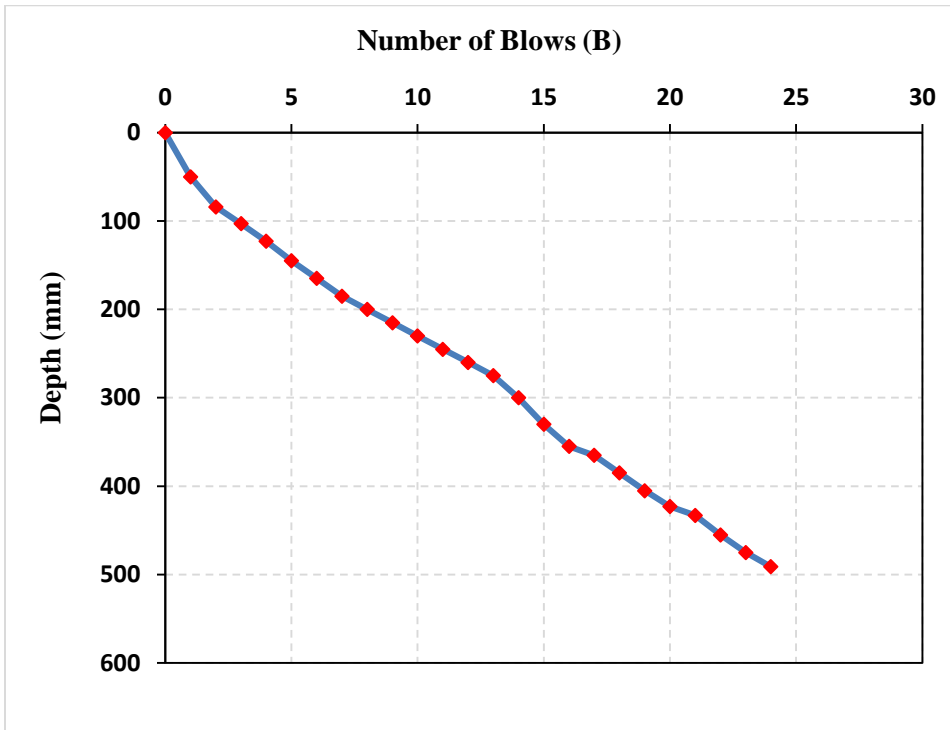


Figure (2.1): Number of blows verse the depth of DCP (No. of passing 14)

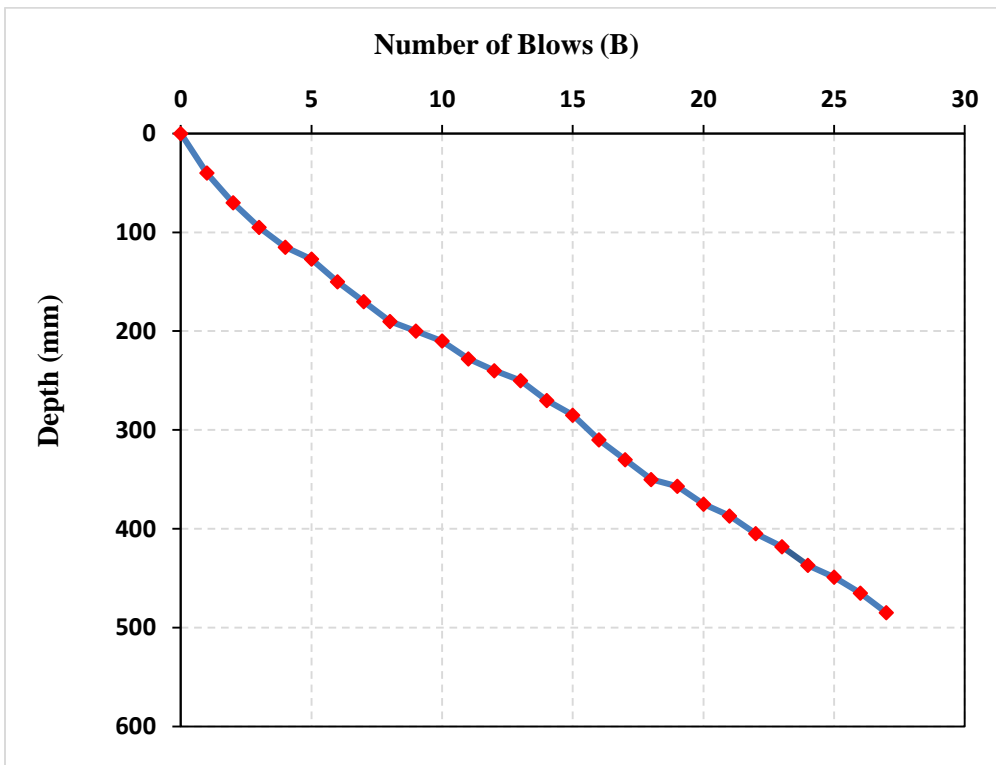


Figure (2.2): Number of blows verse the depth of DCP (No. of passing 14)

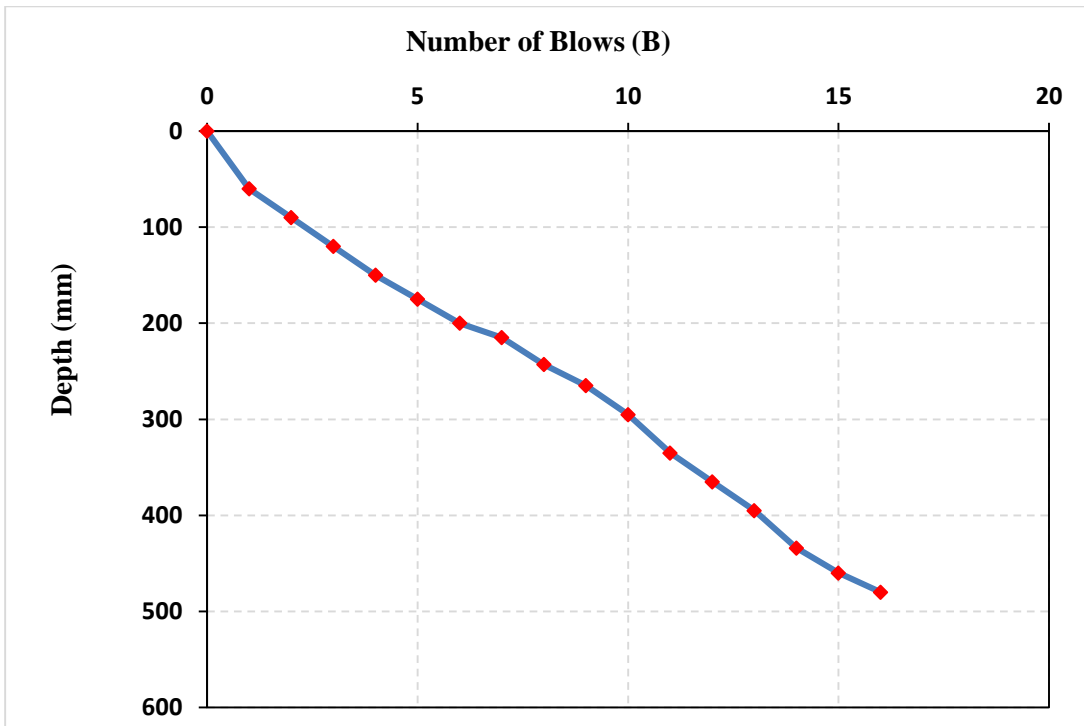


Figure (2.3): Number of blows verse the depth of DCP (No. of passing 14)

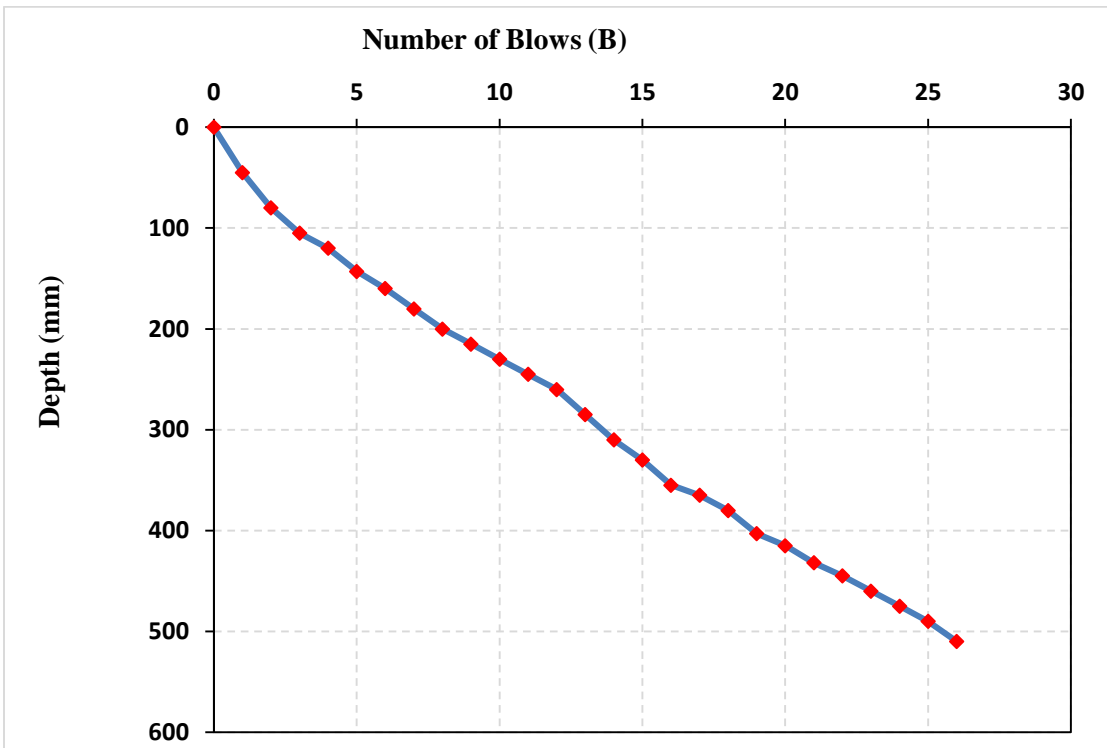


Figure (2.4): Number of blows verse the depth of DCP (No. of passing 14)

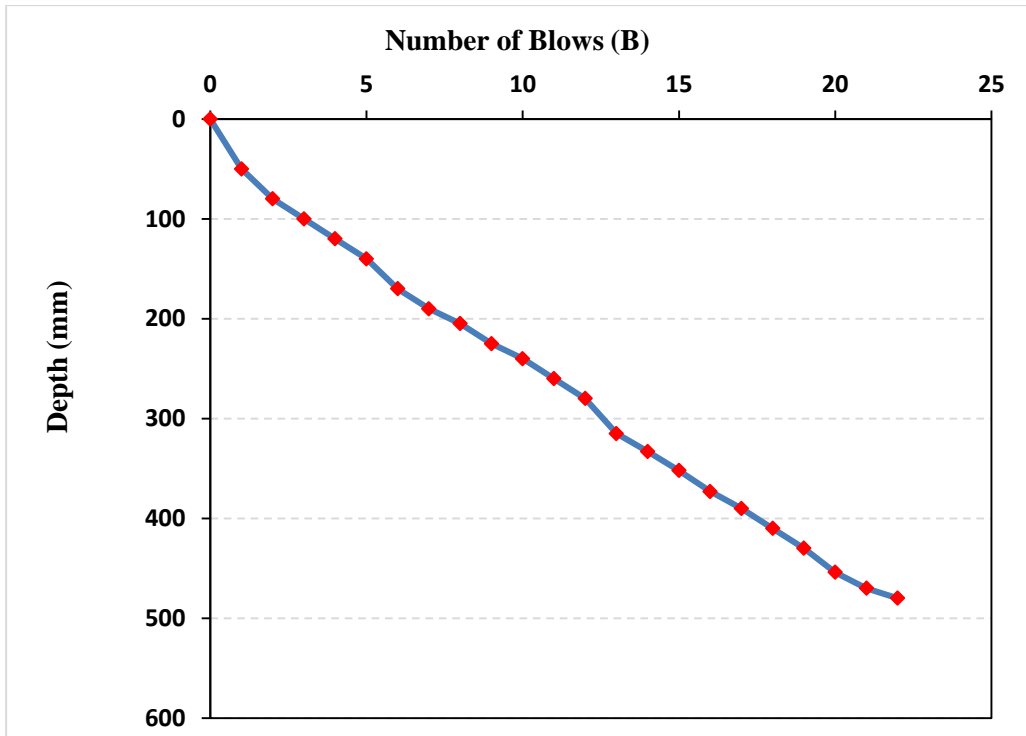


Figure (2.5): Number of blows verse the depth of DCP (No. of passing 14)

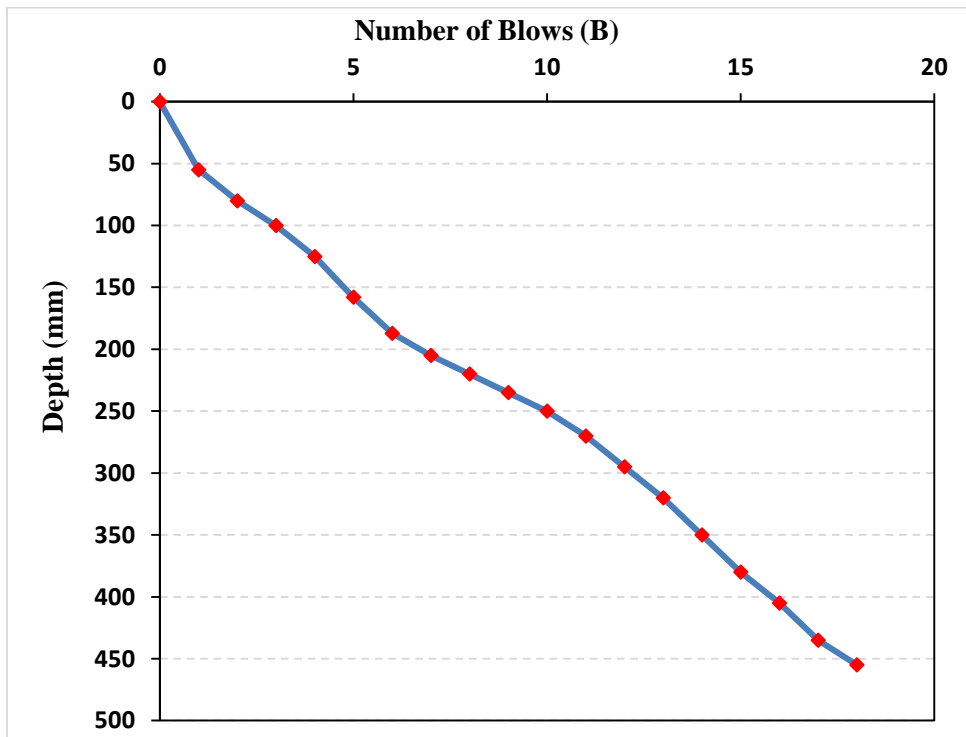


Figure (2.6): Number of blows verse the depth of DCP (No. of passing 14)

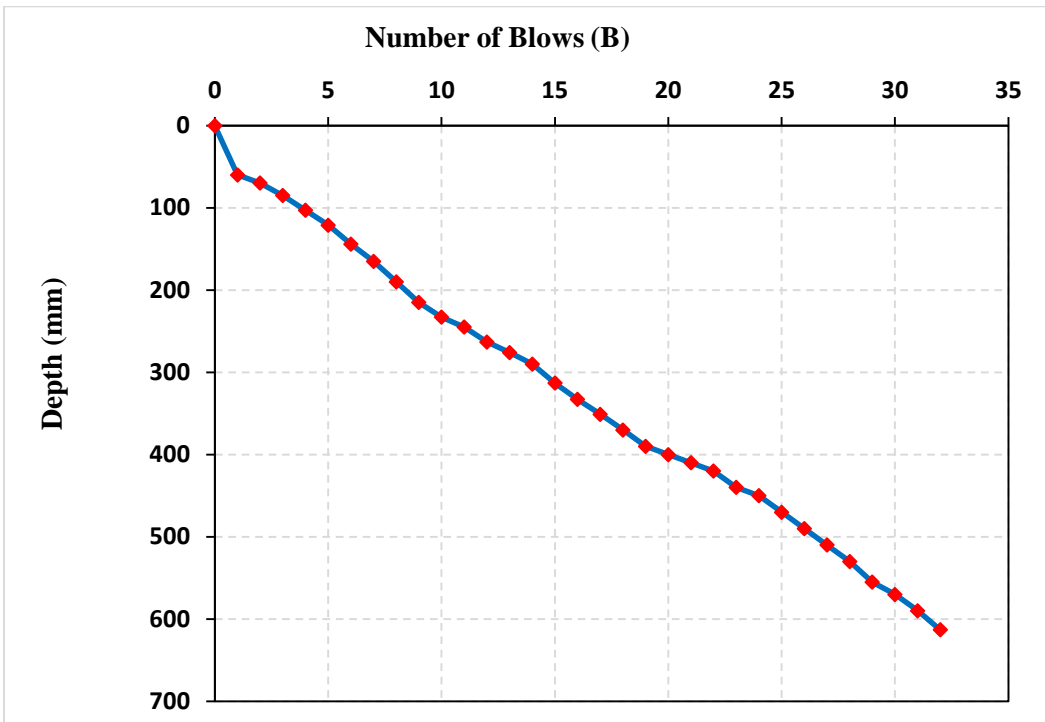


Figure (3.1): Number of blows verse the depth of DCP (No. of passing 18)

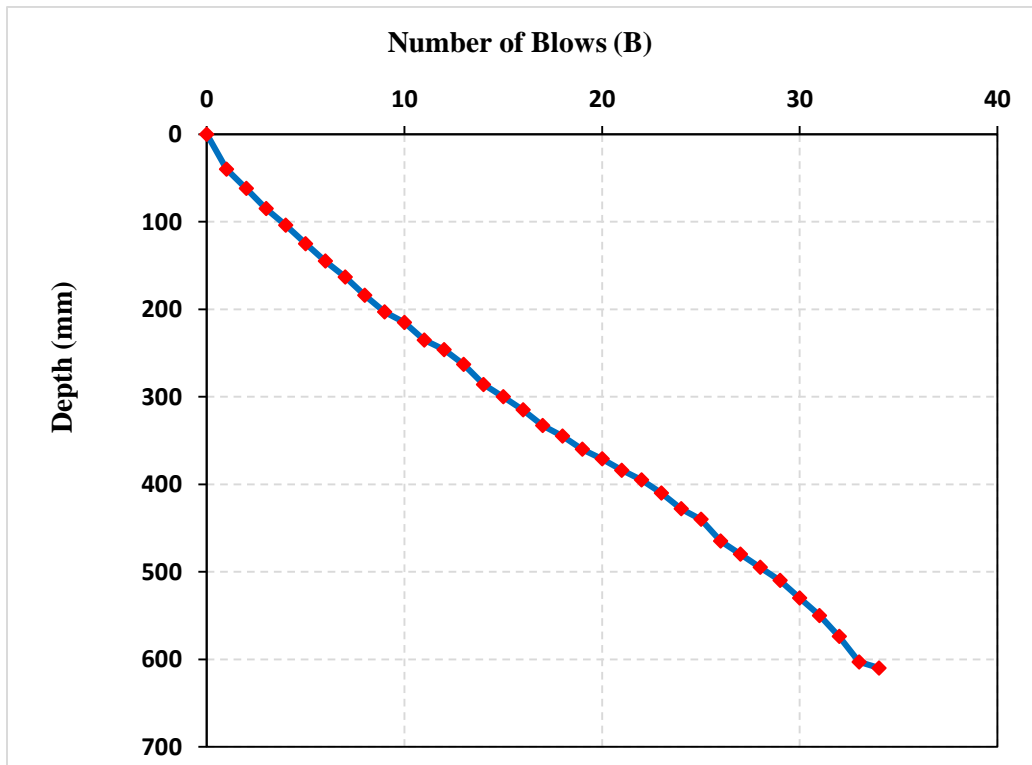


Figure (3.2): Number of blows verse the depth of DCP (No. of passing 18)

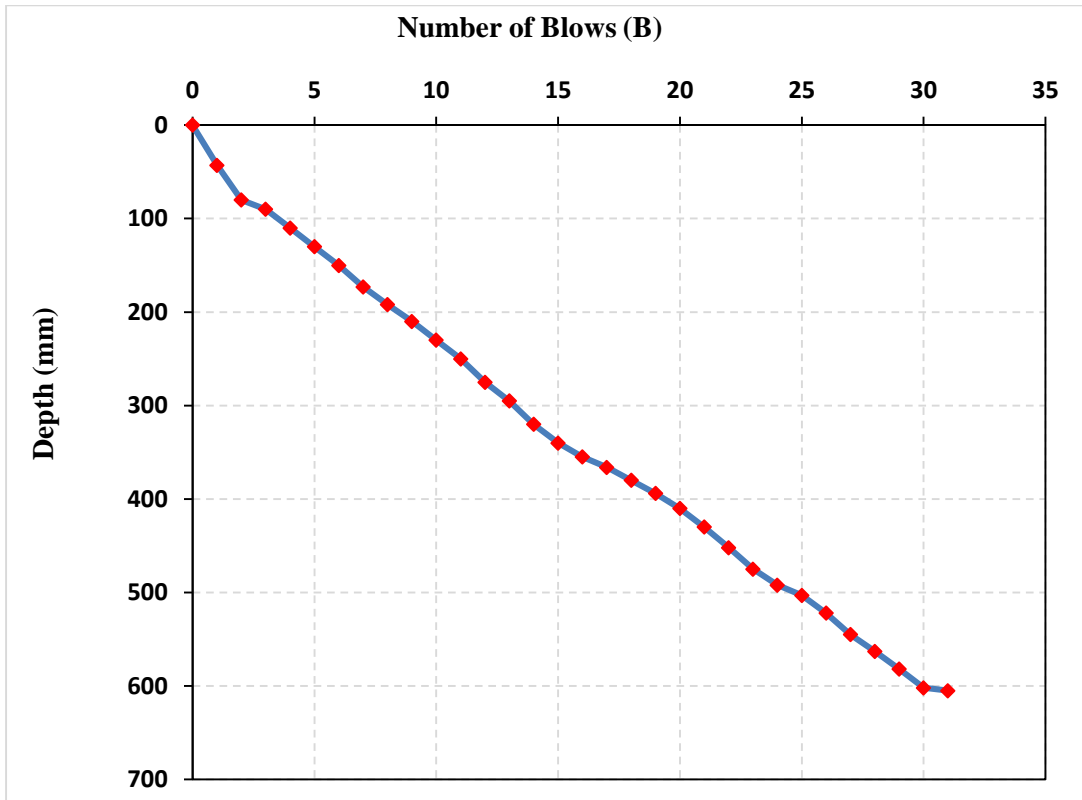


Figure (3.3): Number of blows verse the depth of DCP (No. of passing 18)

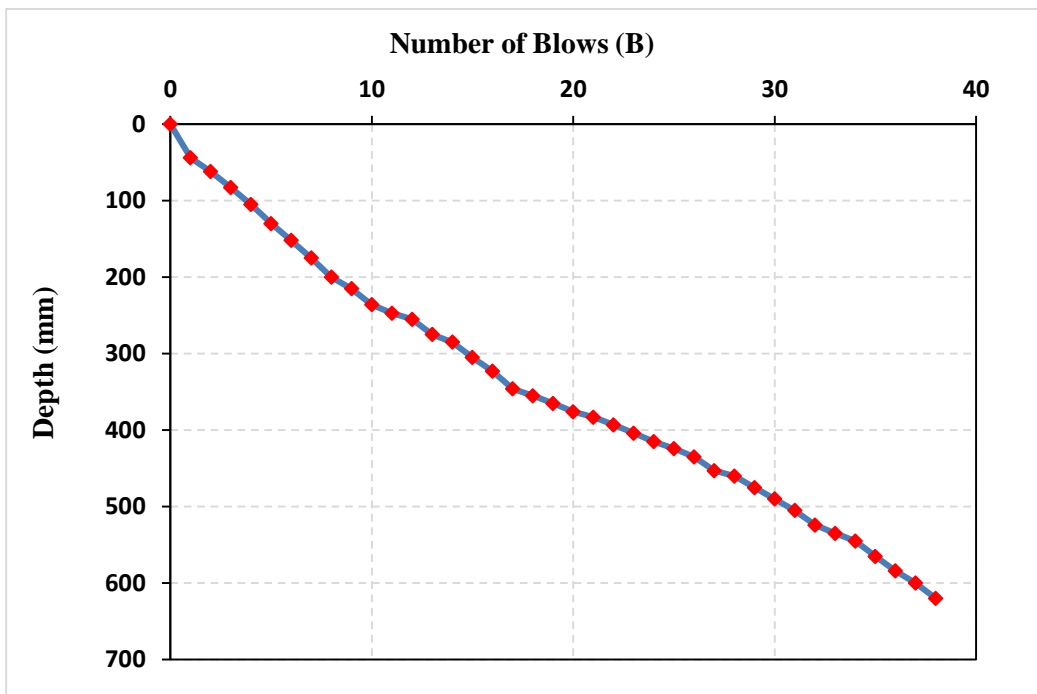


Figure (3.4): Number of blows verse the depth of DCP (No. of passing 18)

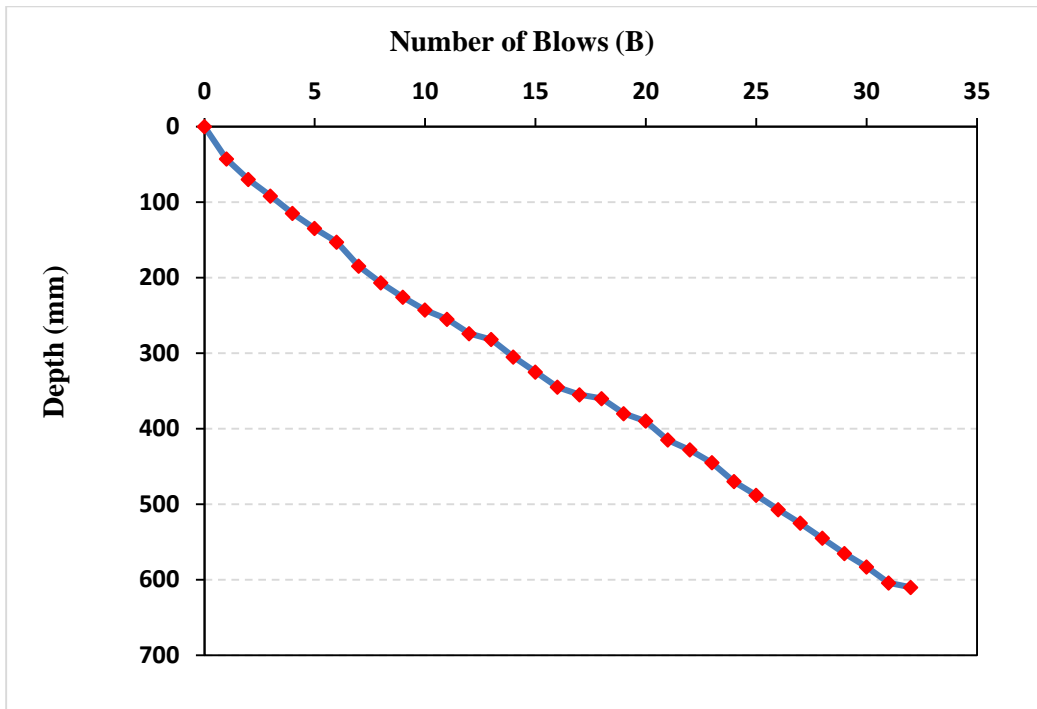


Figure (3.5): Number of blows verse the depth of DCP (No. of passing 18)

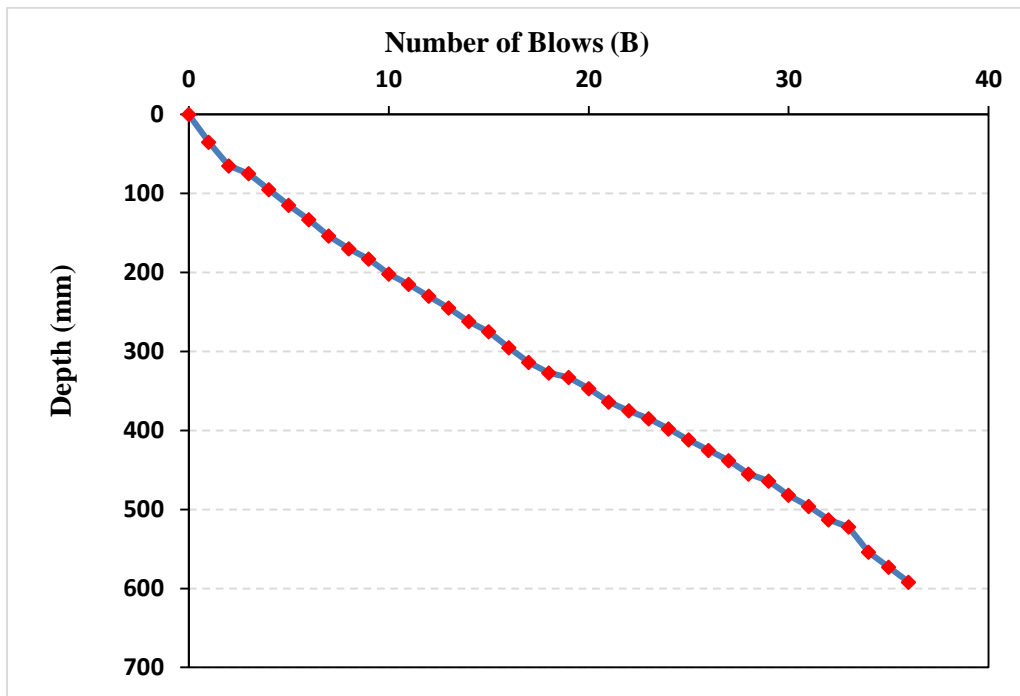


Figure (3.6): Number of blows verse the depth of DCP (No. of passing 18)

### A-3: Al-Intifada district

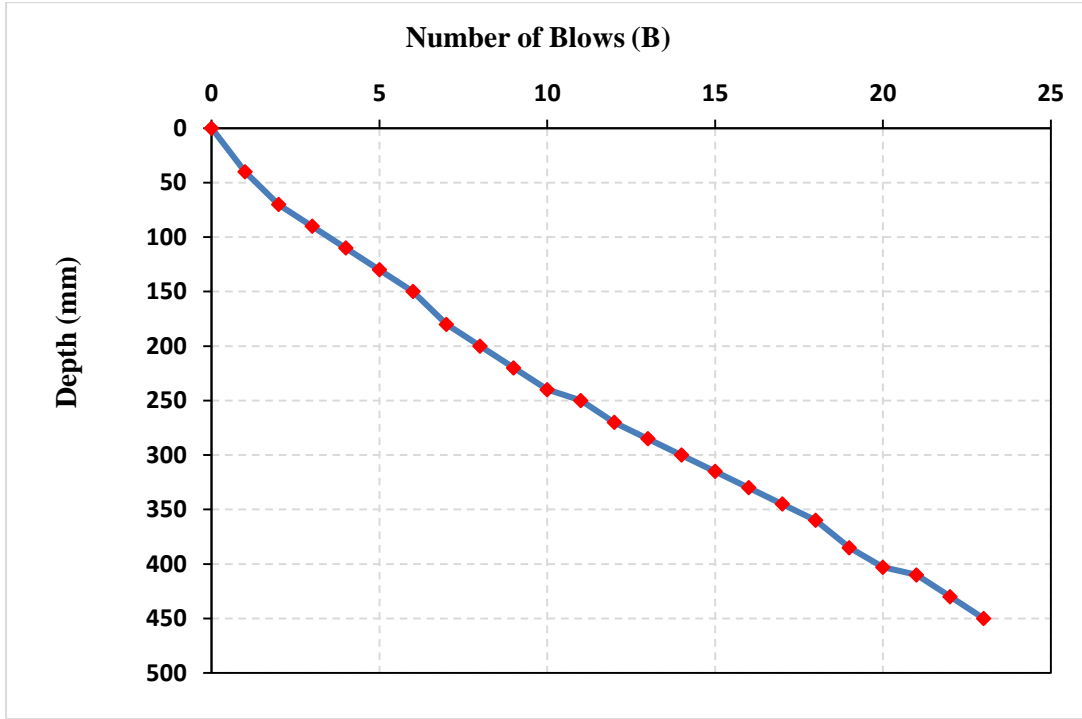


Figure (1.1): Number of blows verse the depth of DCP (No. of passing 10)

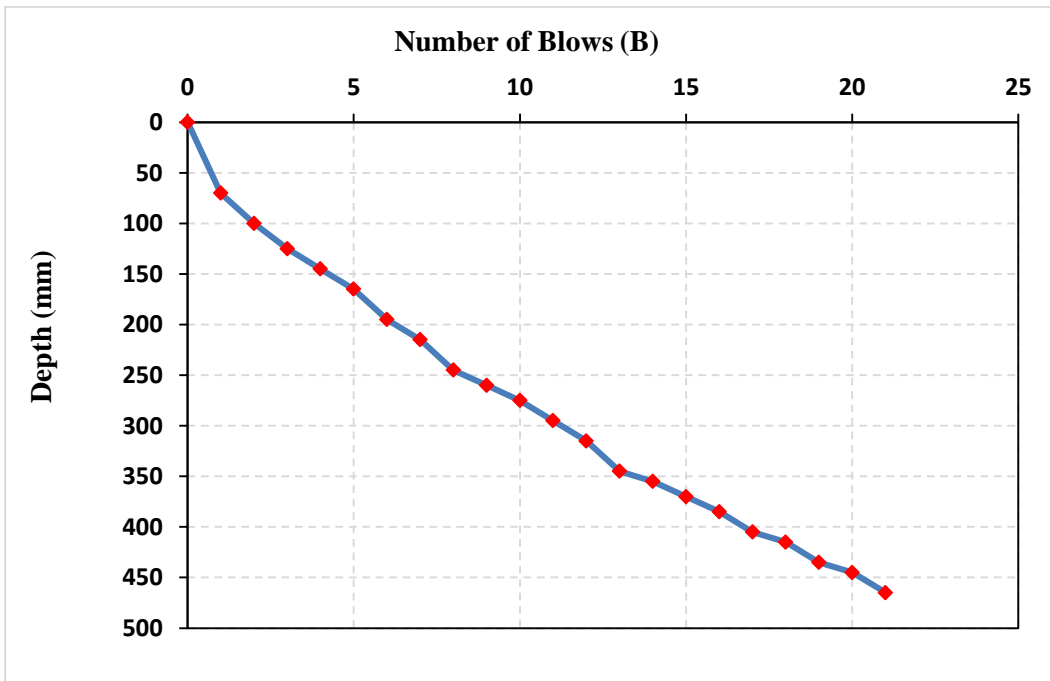


Figure (1.2): Number of blows verse the depth of DCP (No. of passing 10)

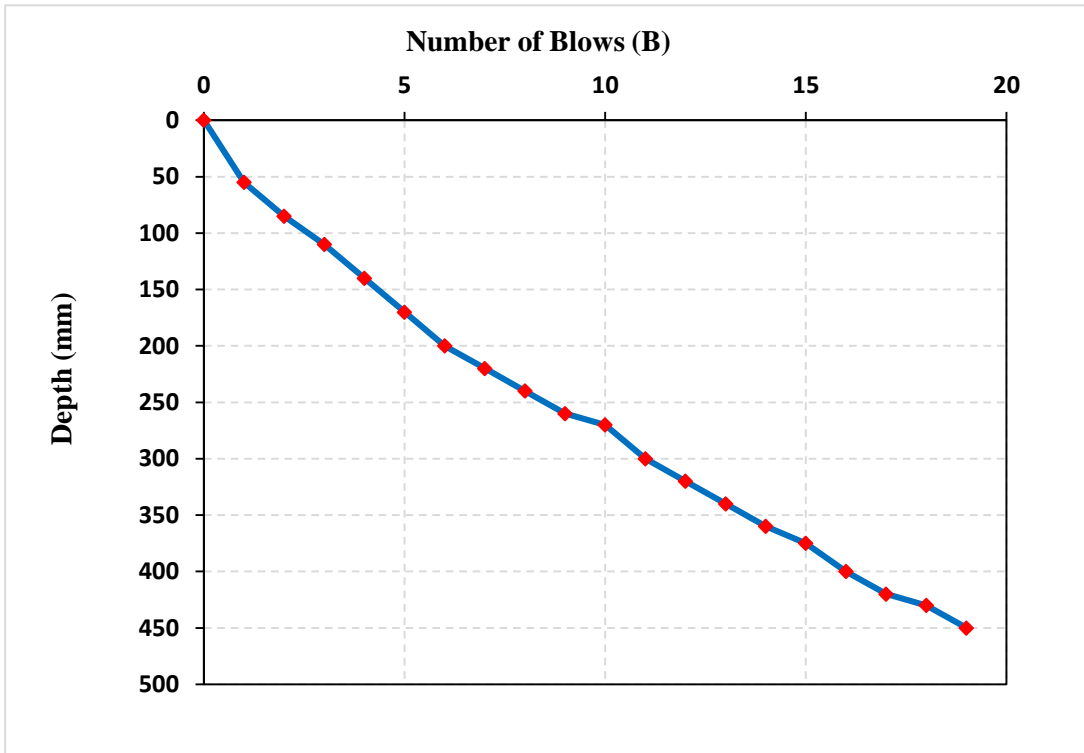


Figure (1.3): Number of blows verse the depth of DCP (No. of passing 10)

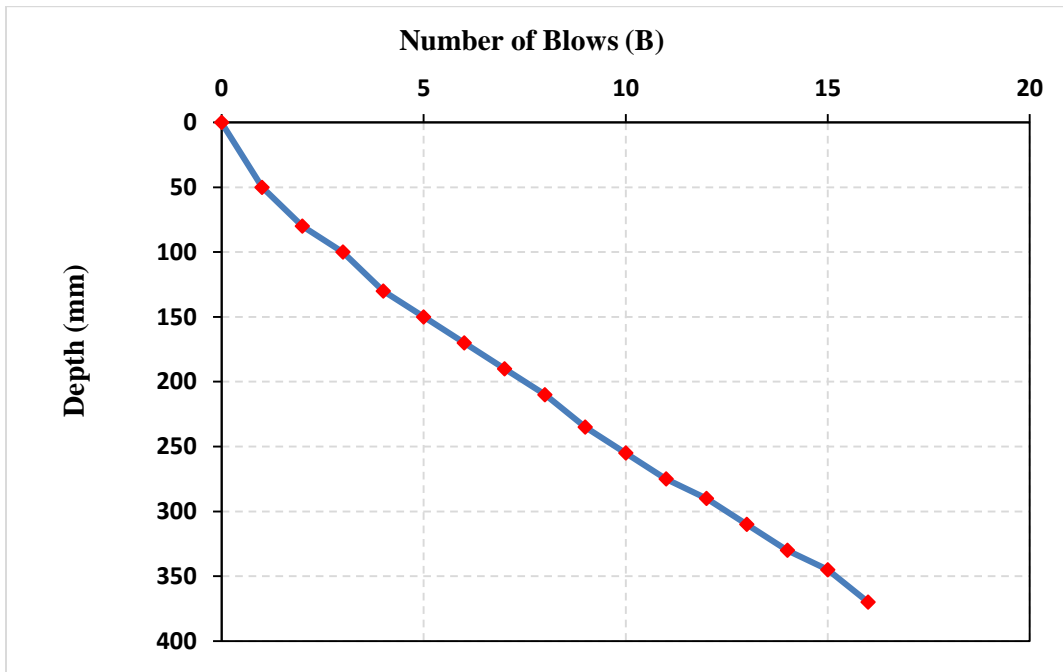


Figure (1.4): Number of blows verse the depth of DCP (No. of passing 10)



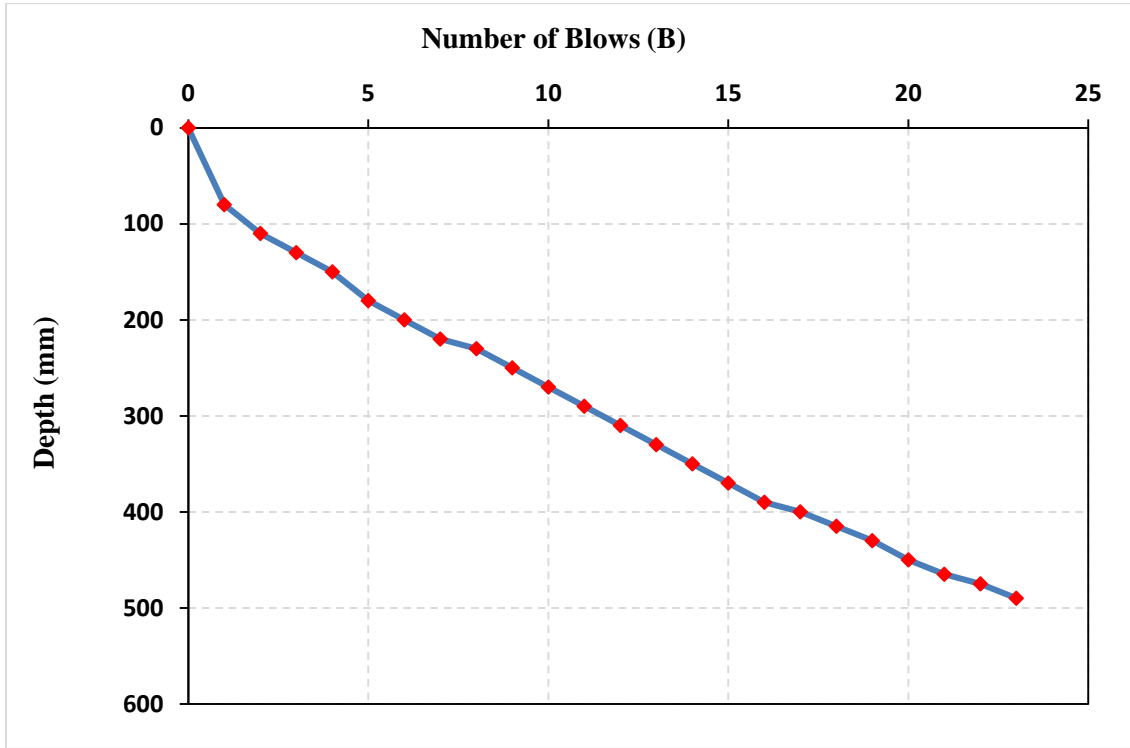


Figure (1.5): Number of blows verse the depth of DCP (No. of passing 10)

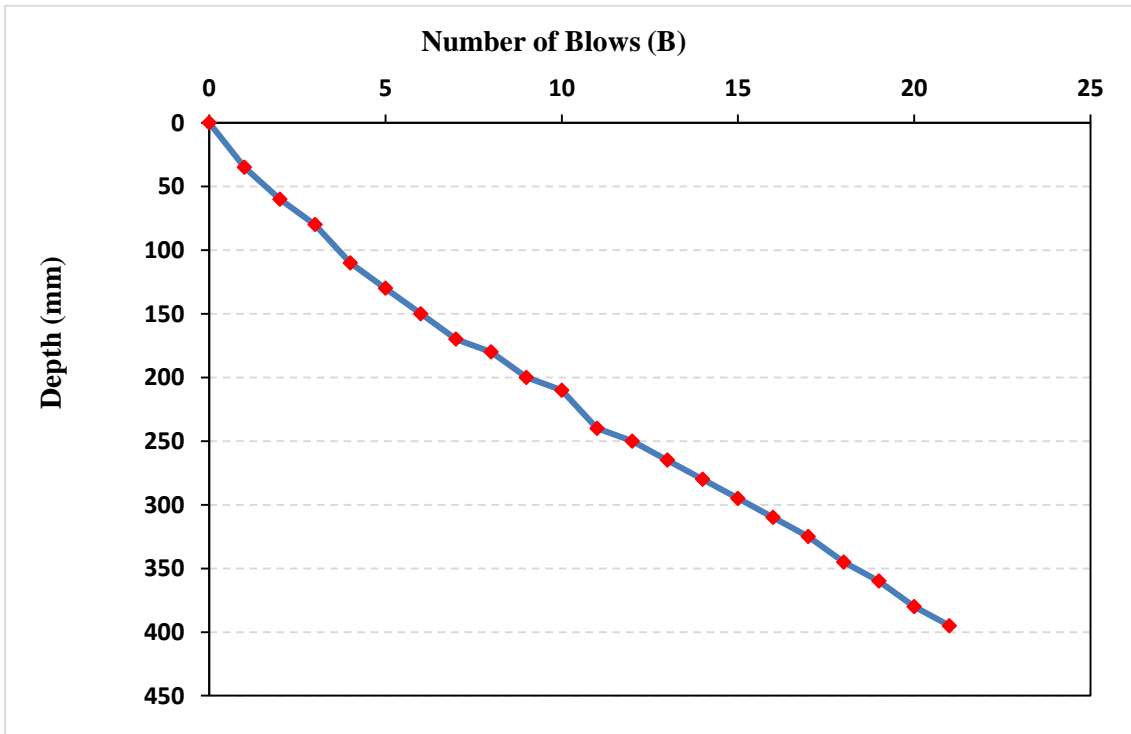


Figure (1.6): Number of blows verse the depth of DCP (No. of passing 10)

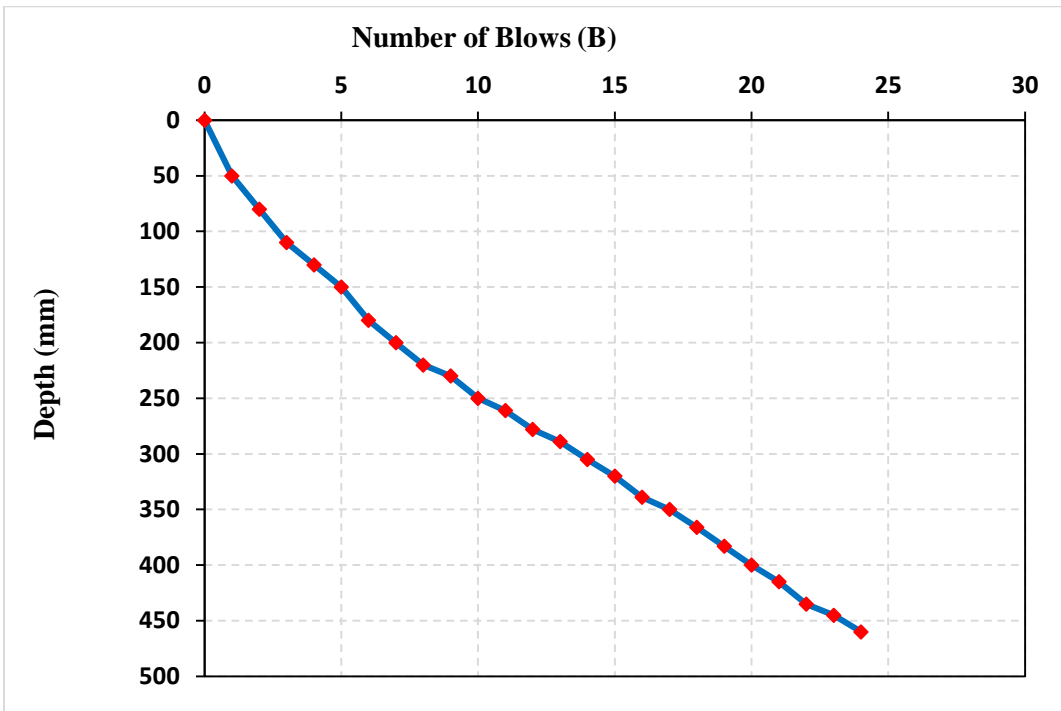


Figure (2.1): Number of blows verse the depth of DCP (No. of passing 10)

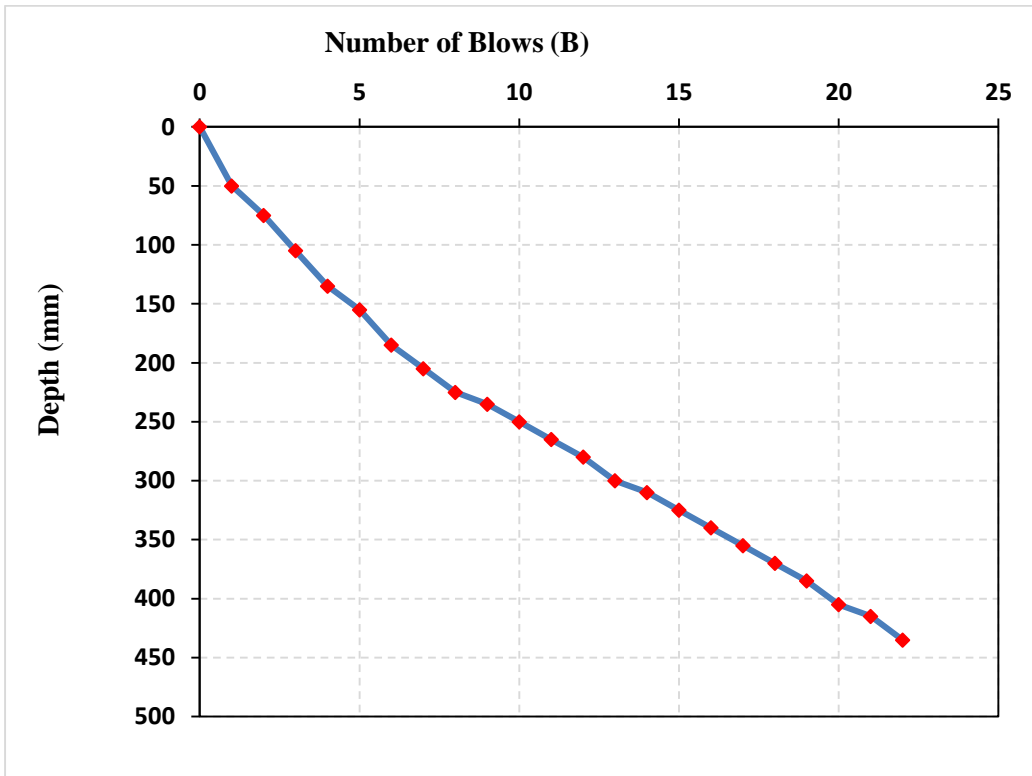


Figure (2.2): Number of blows verse the depth of DCP (No. of passing 14)

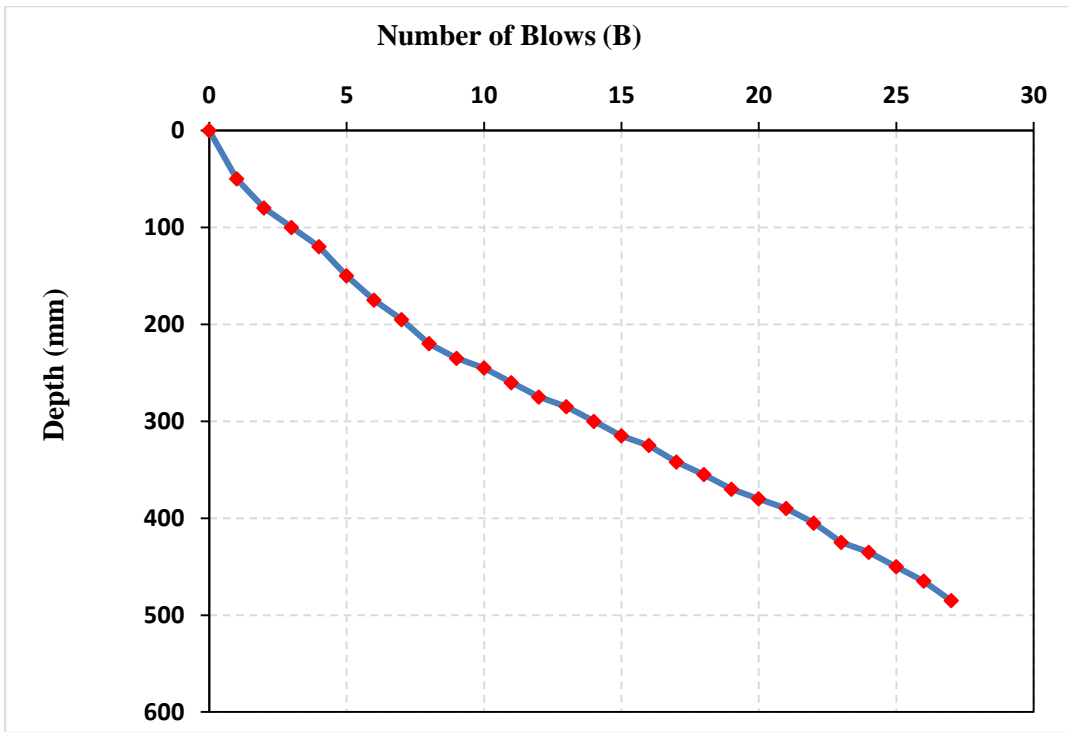


Figure (2.3): Number of blows verse the depth of DCP (No. of passing 14)

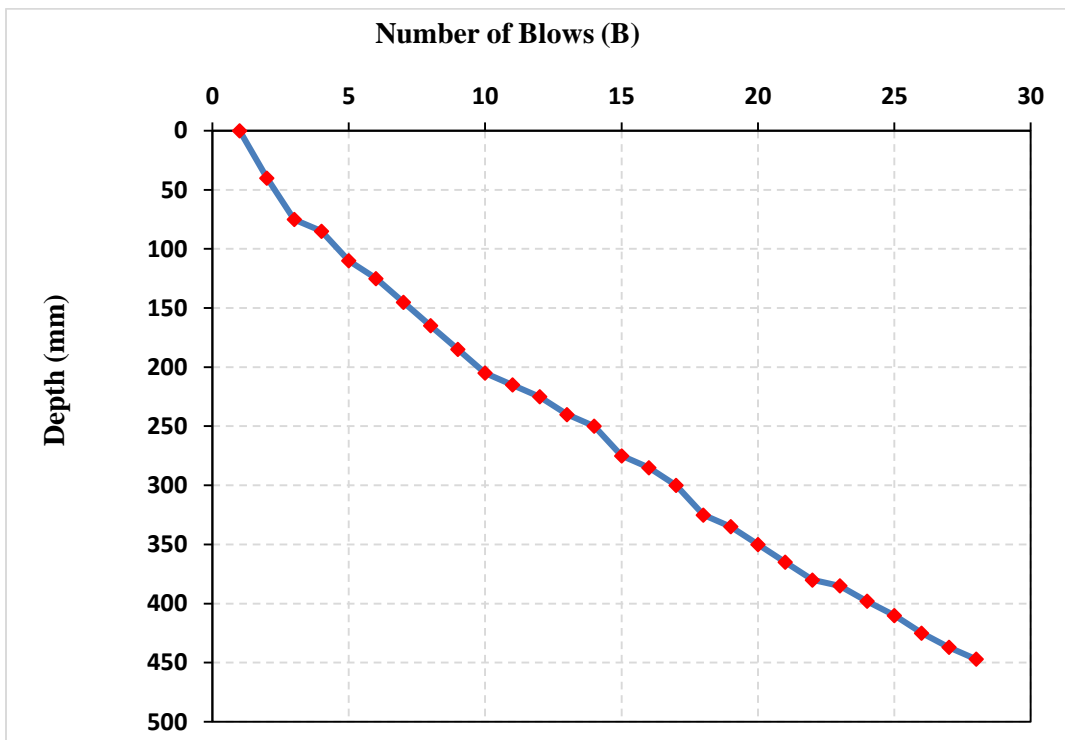


Figure (2.4): Number of blows verse the depth of DCP (No. of passing 14)

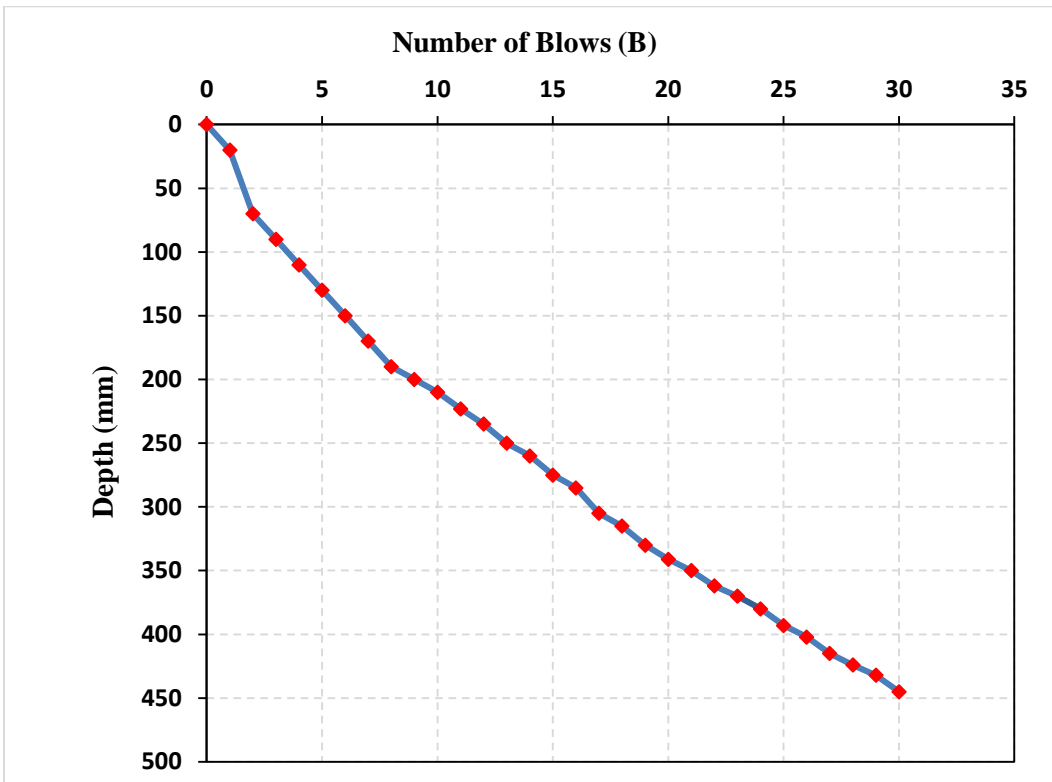


Figure (2.5): Number of blows verse the depth of DCP (No. of passing 14)

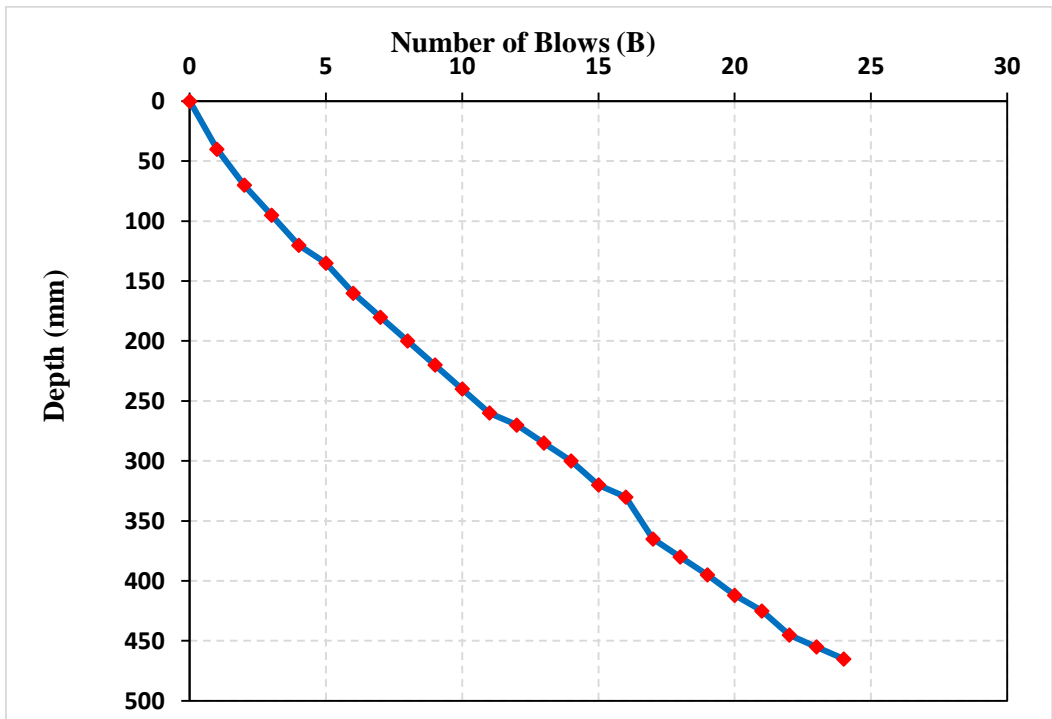


Figure (2.6): Number of blows verse the depth of DCP (No. of passing 14)

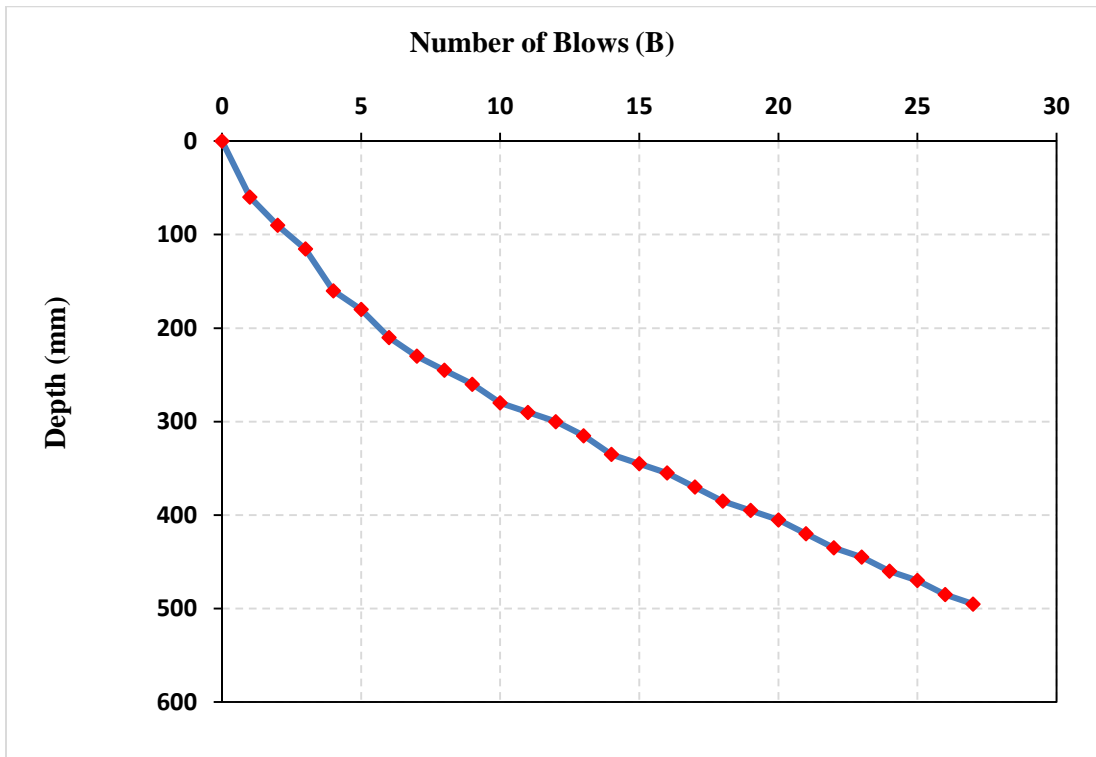


Figure (3.1): Number of blows verse the depth of DCP (No. of passing 18)

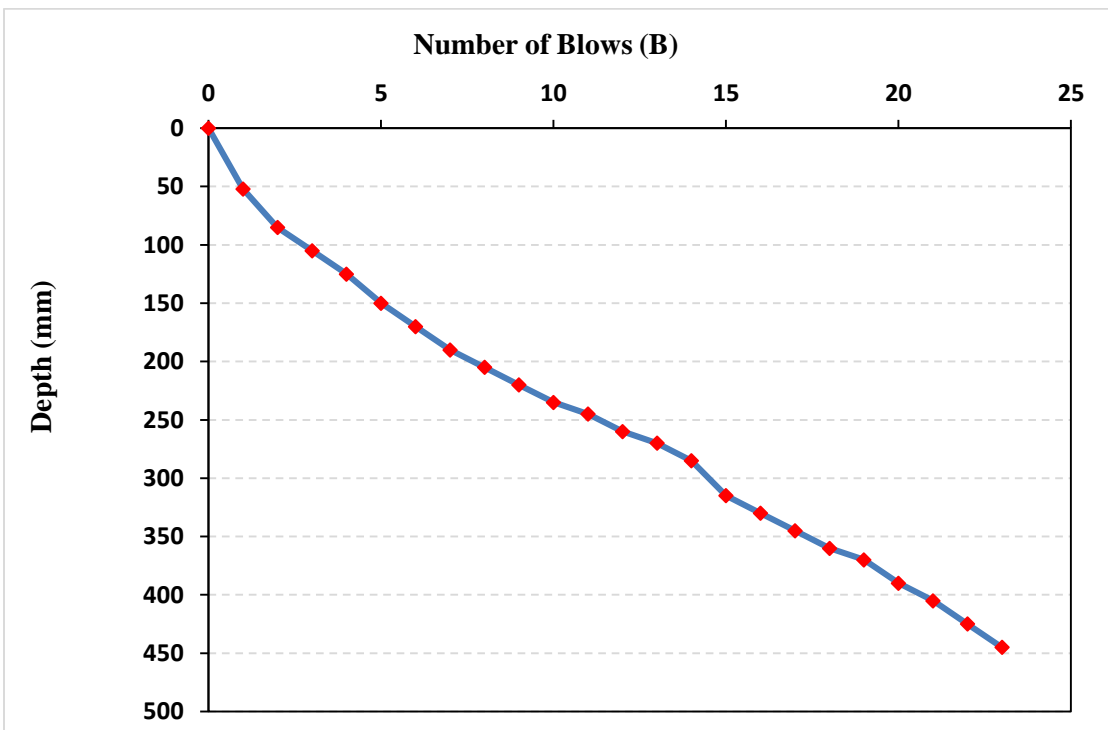


Figure (3.2): Number of blows verse the depth of DCP (No. of passing 18)

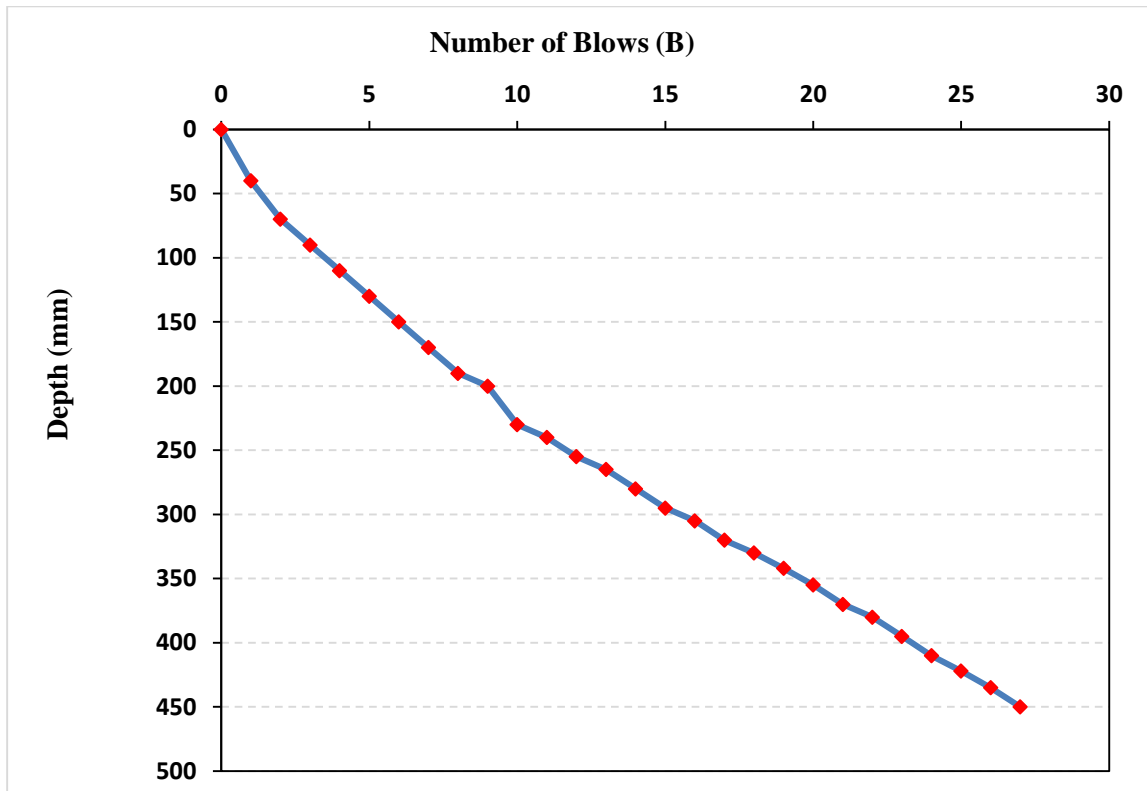


Figure (3.3): Number of blows verse the depth of DCP (No. of passing 18)

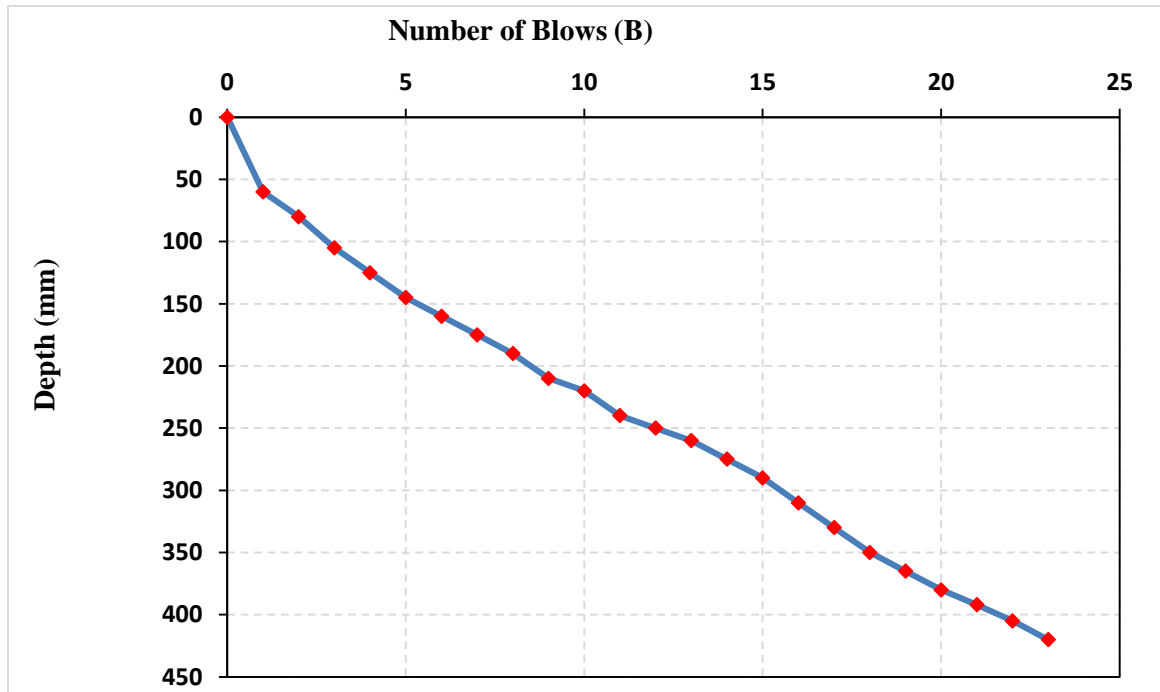


Figure (3.4): Number of blows verse the depth of DCP (No. of passing 18)

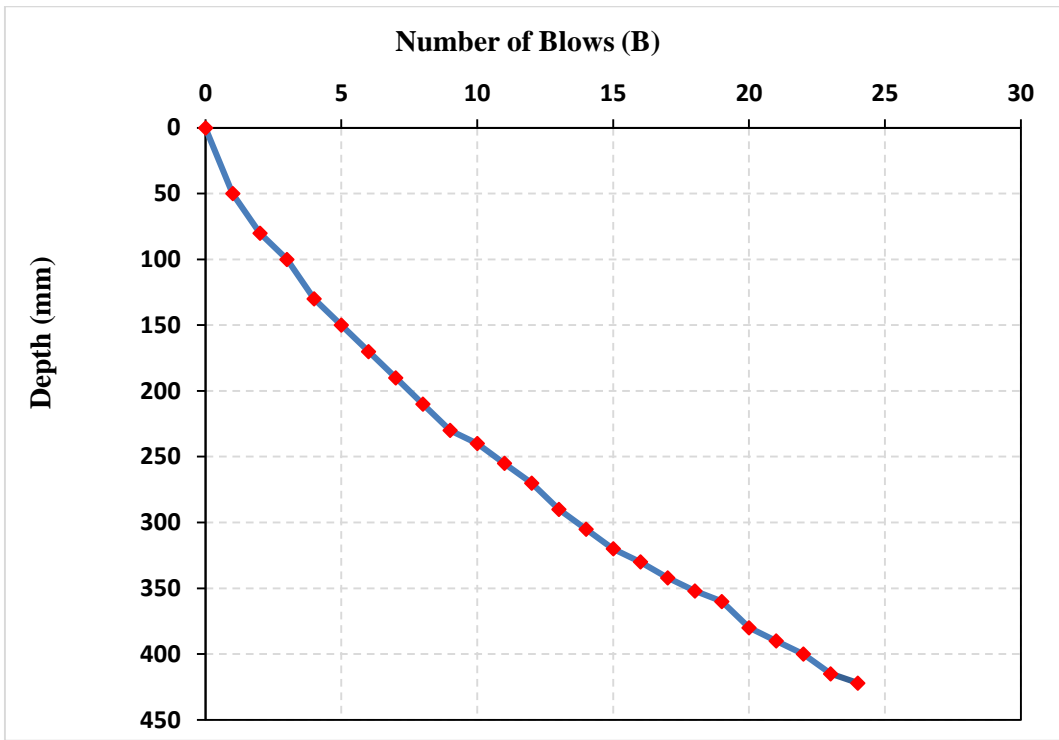


Figure (3.5): Number of blows verse the depth of DCP (No. of passing 18)

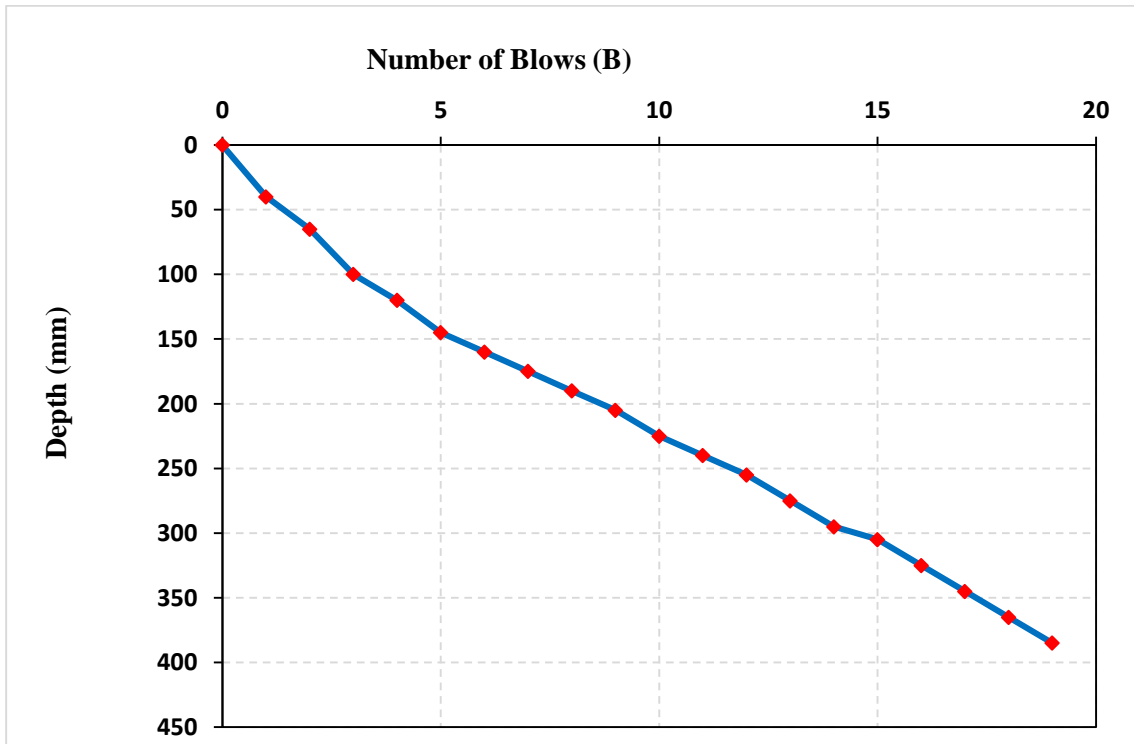


Figure (3.6): Number of blows verse the depth of DCP (No. of passing 18)

**Al-Tahady district**



Figure (1.1): Number of blows verse the depth of DCP (No. of passing 10)

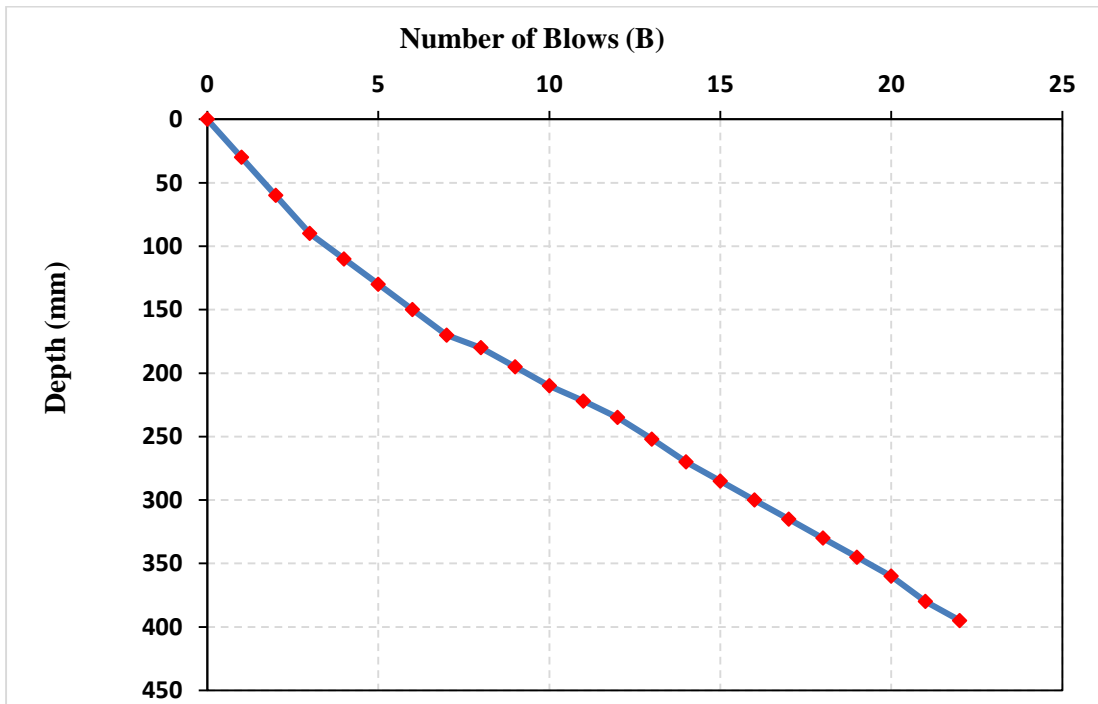




Figure (1.2): Number of blows verse the depth of DCP (No. of passing 10)

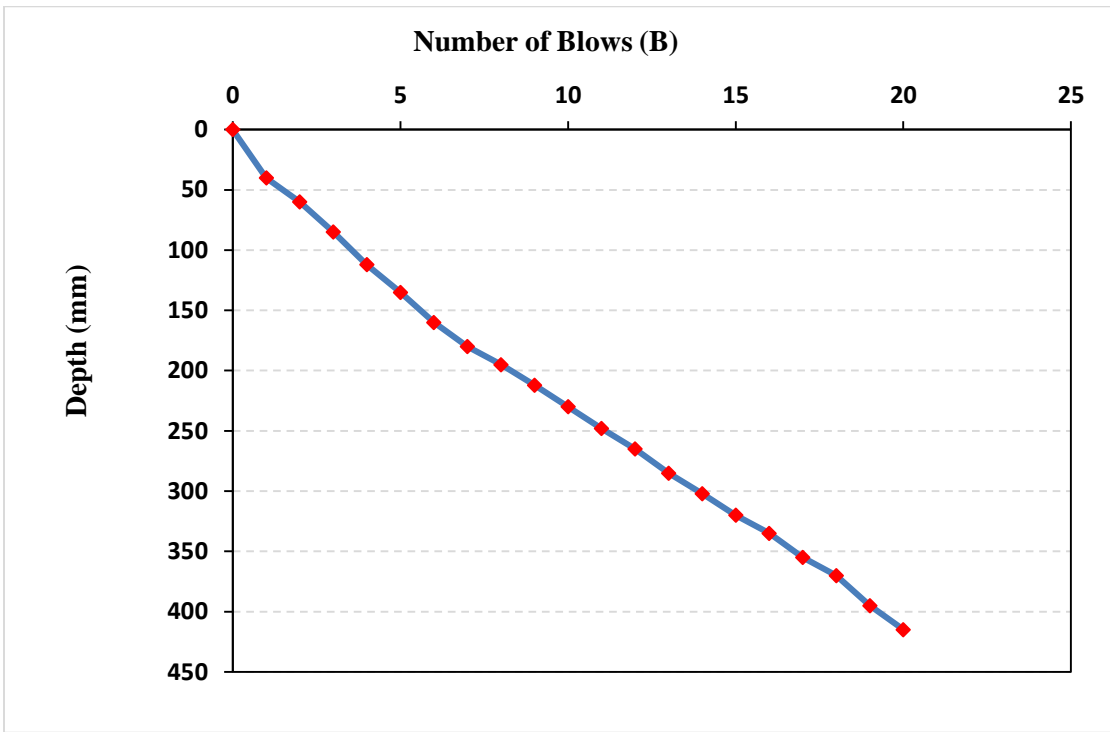


Figure (1.3): Number of blows verse the depth of DCP (No. of passing 10)

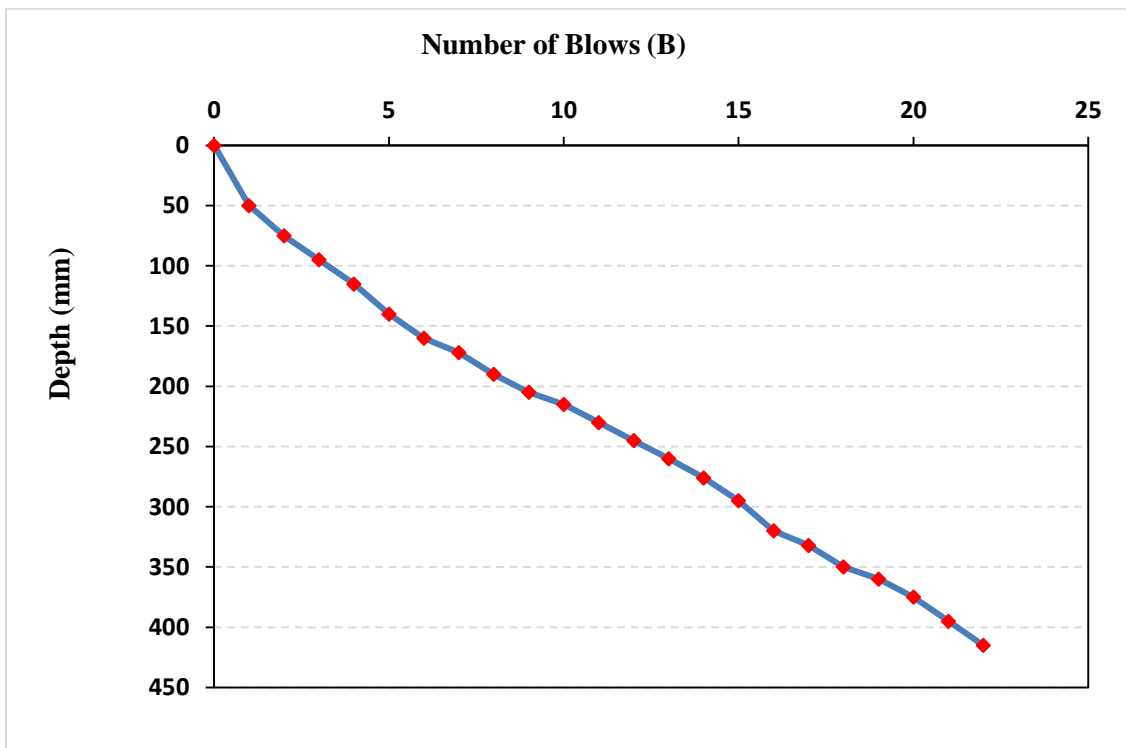


Figure (1.4): Number of blows verse the depth of DCP (No. of passing 10)

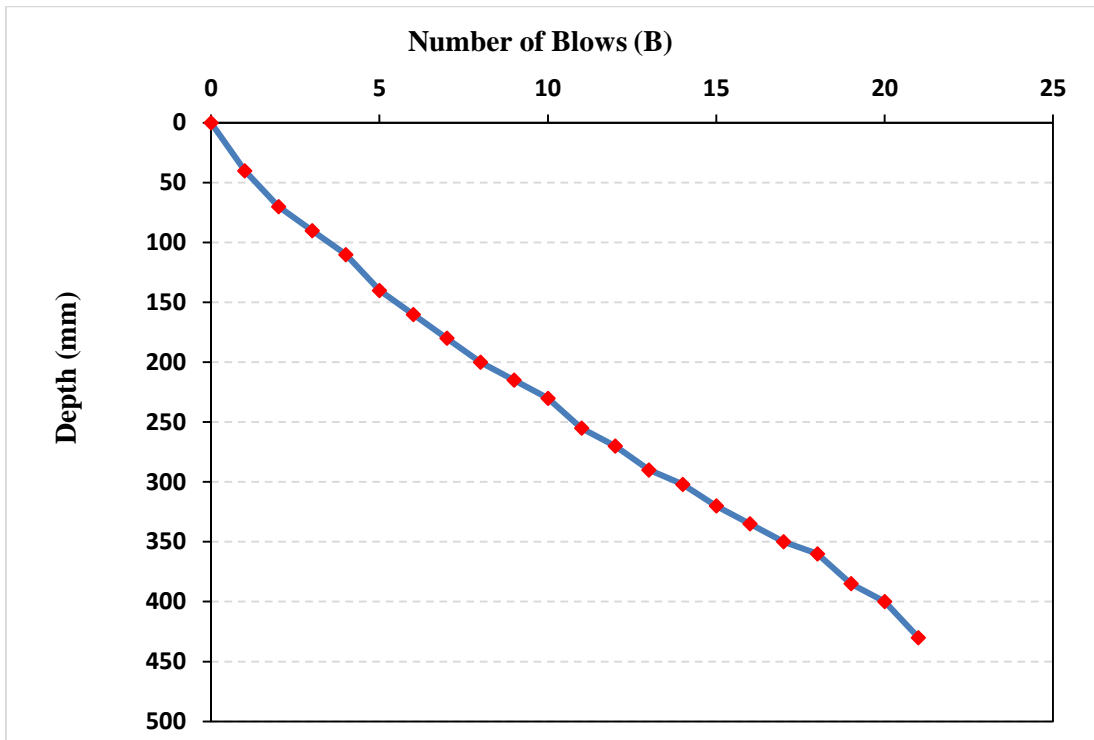


Figure (1.5): Number of blows verse the depth of DCP (No. of passing 10)

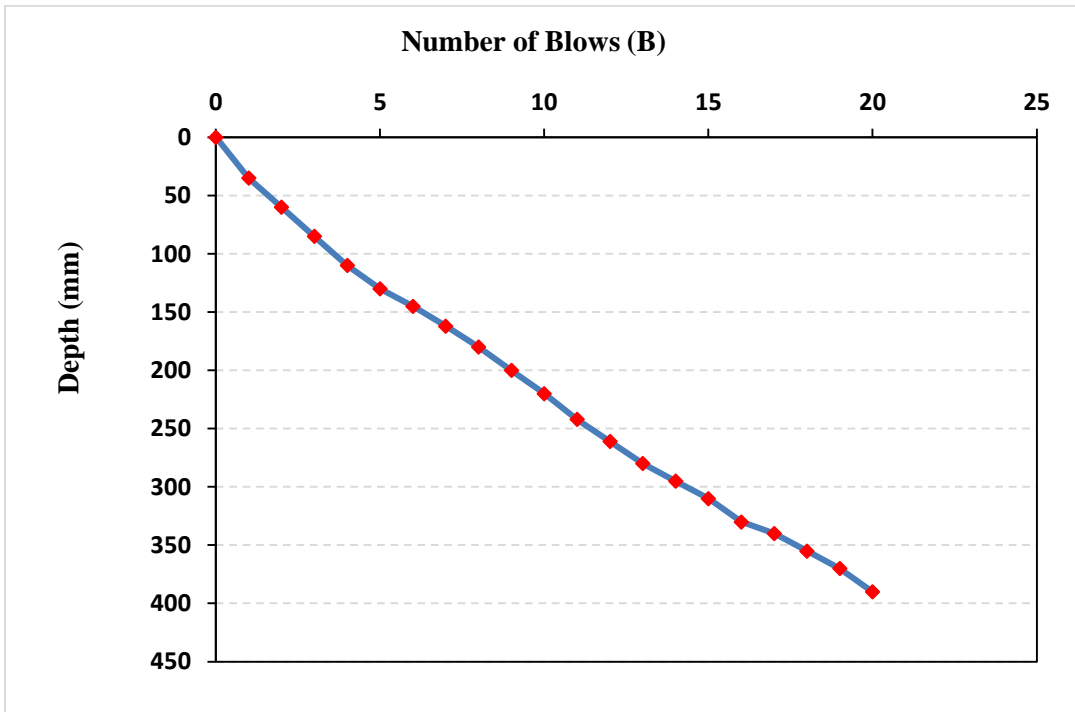


Figure (1.6): Number of blows verse the depth of DCP (No. of passing 10)

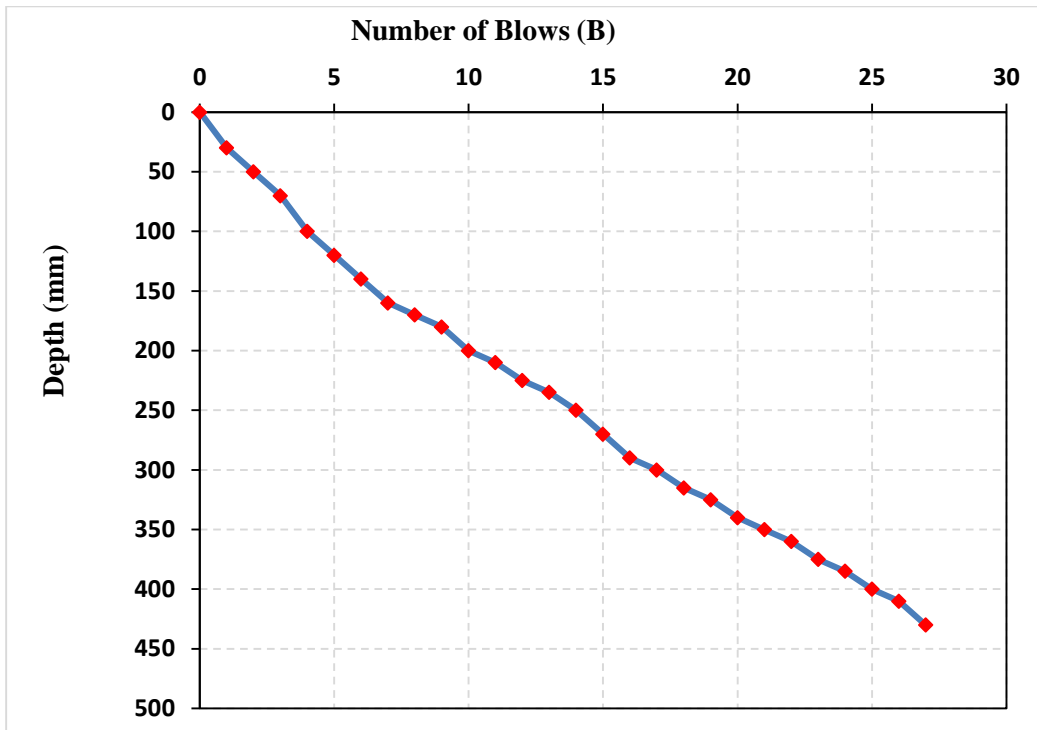


Figure (2.1): Number of blows verse the depth of DCP (No. of passing 14)

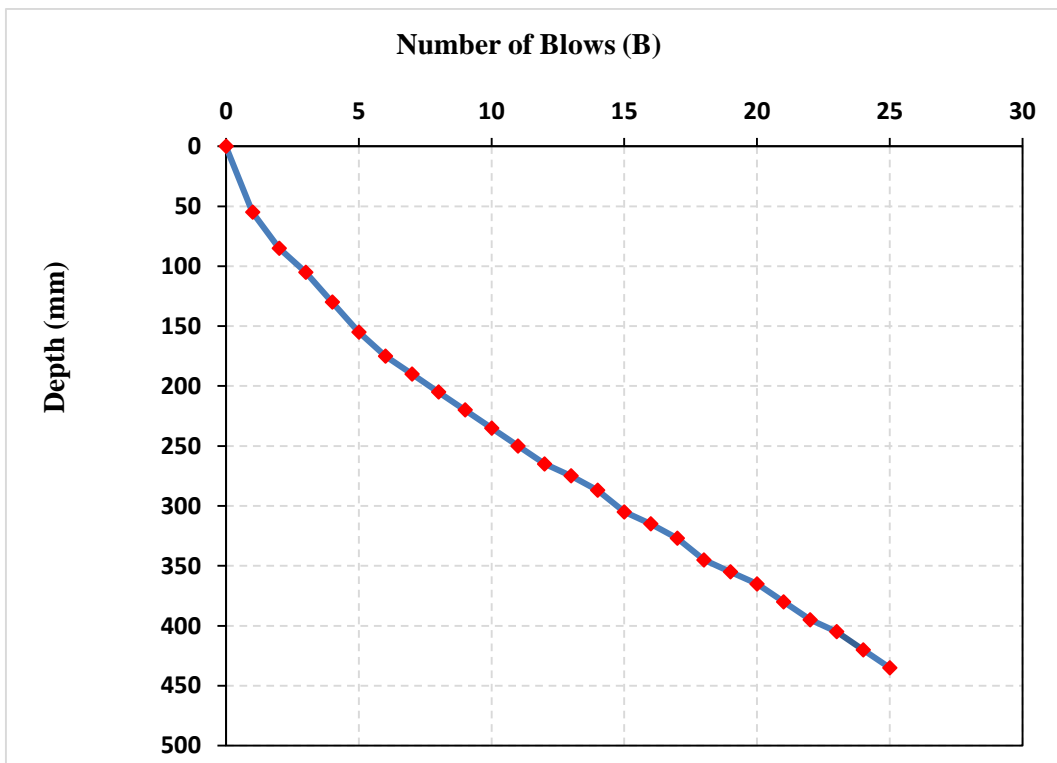


Figure (2.2): Number of blows verse the depth of DCP (No. of passing 14)

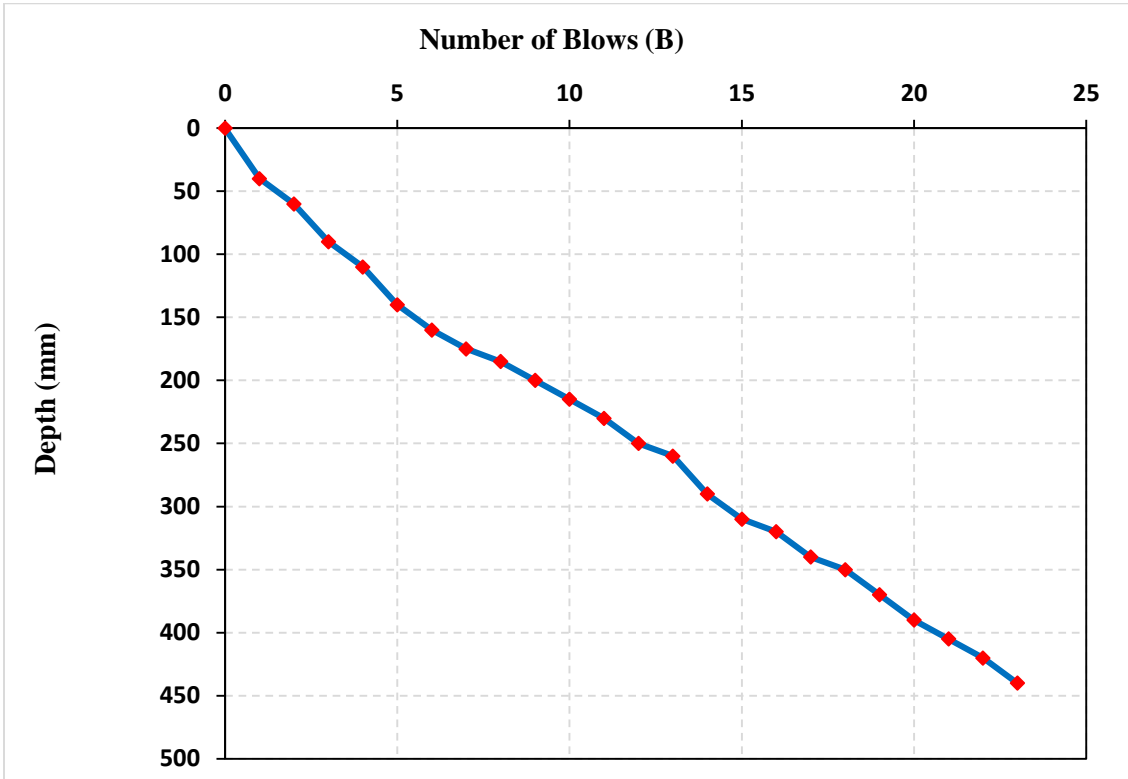


Figure (2.3): Number of blows verse the depth of DCP (No. of passing 14)

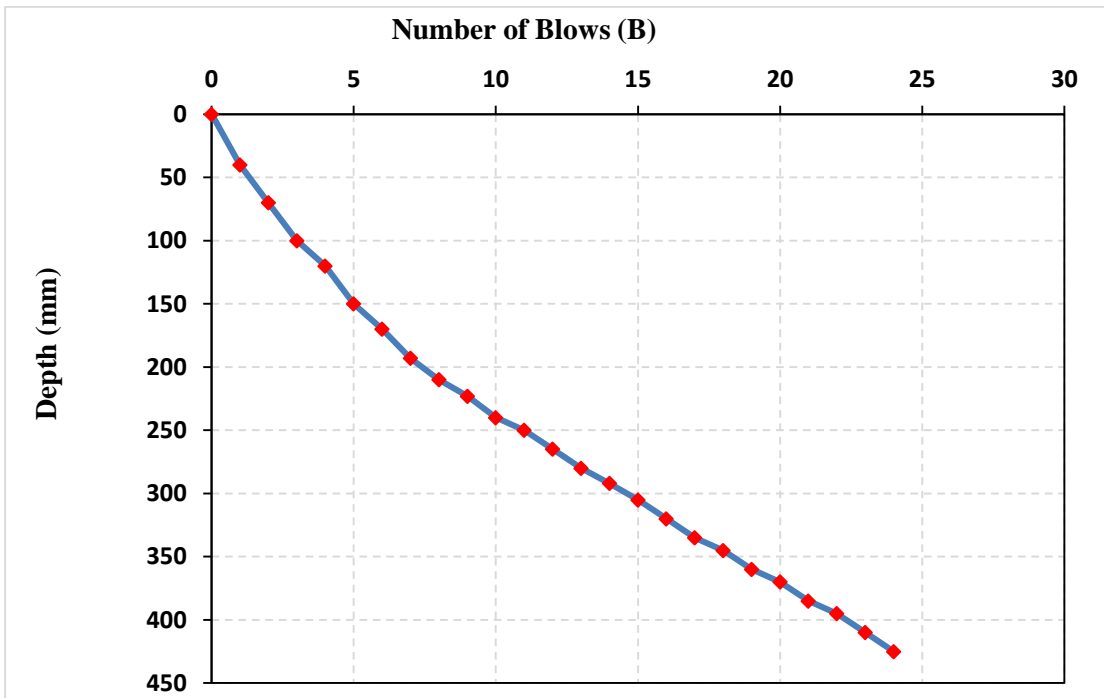


Figure (2.4): Number of blows verse the depth of DCP (No. of passing 14)

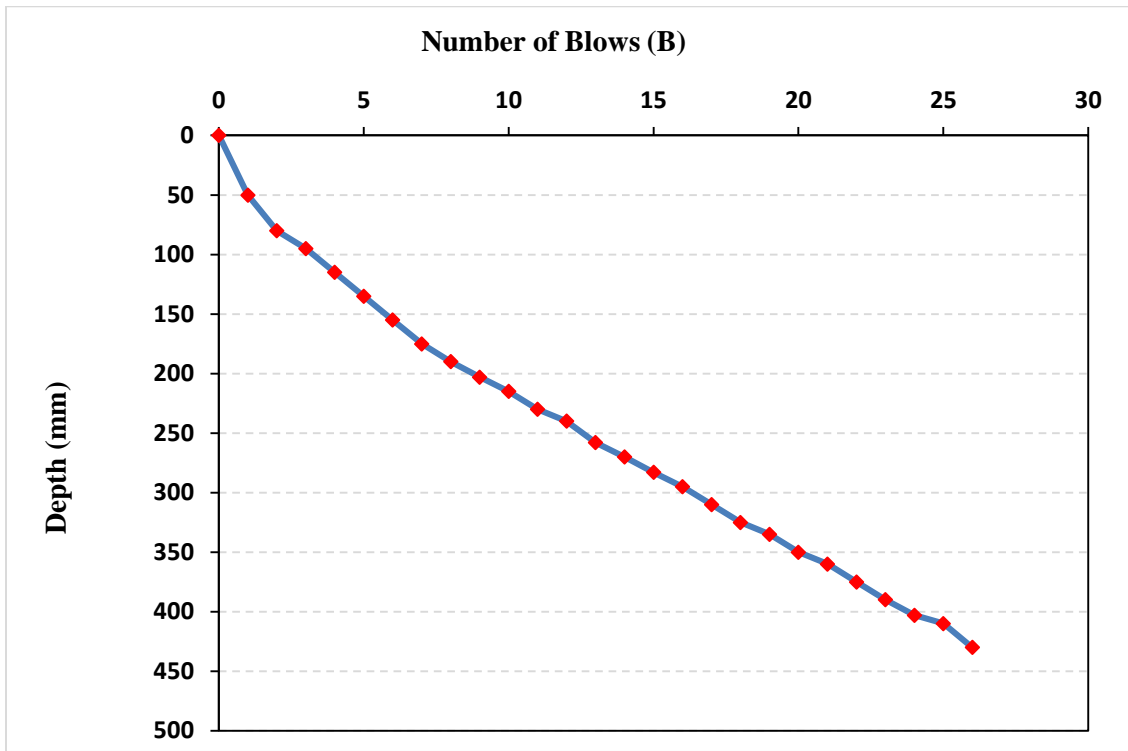


Figure (2.5): Number of blows verse the depth of DCP (No. of passing 14)

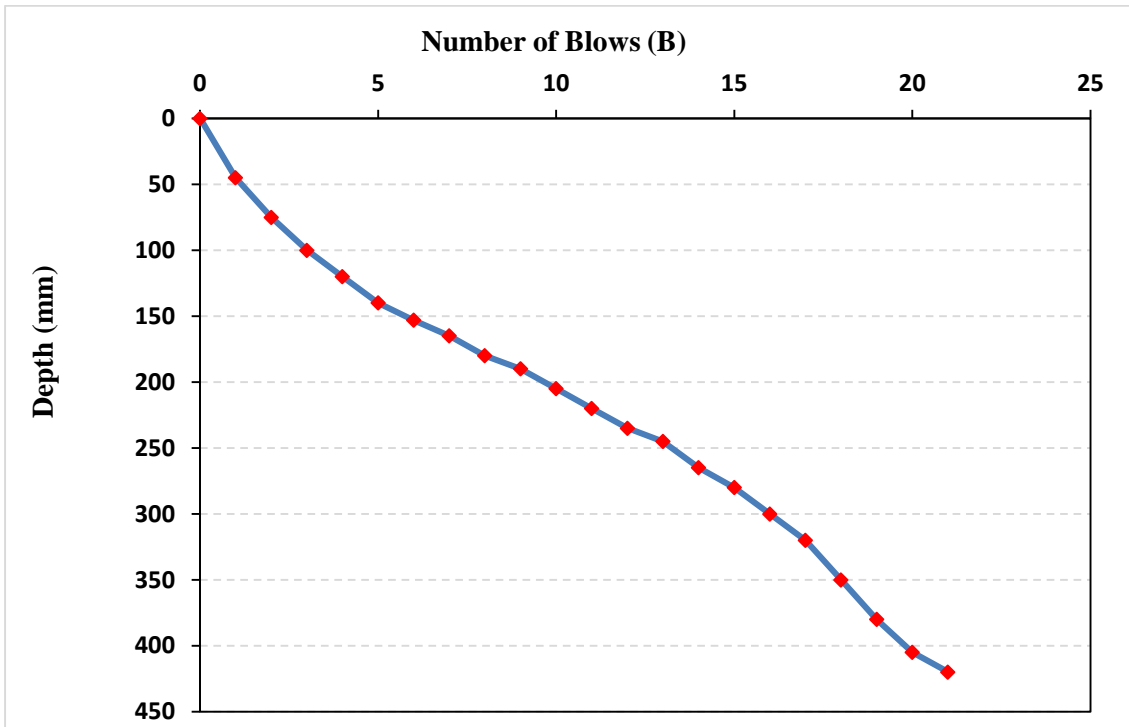


Figure (2.6): Number of blows verse the depth of DCP (No. of passing 14)

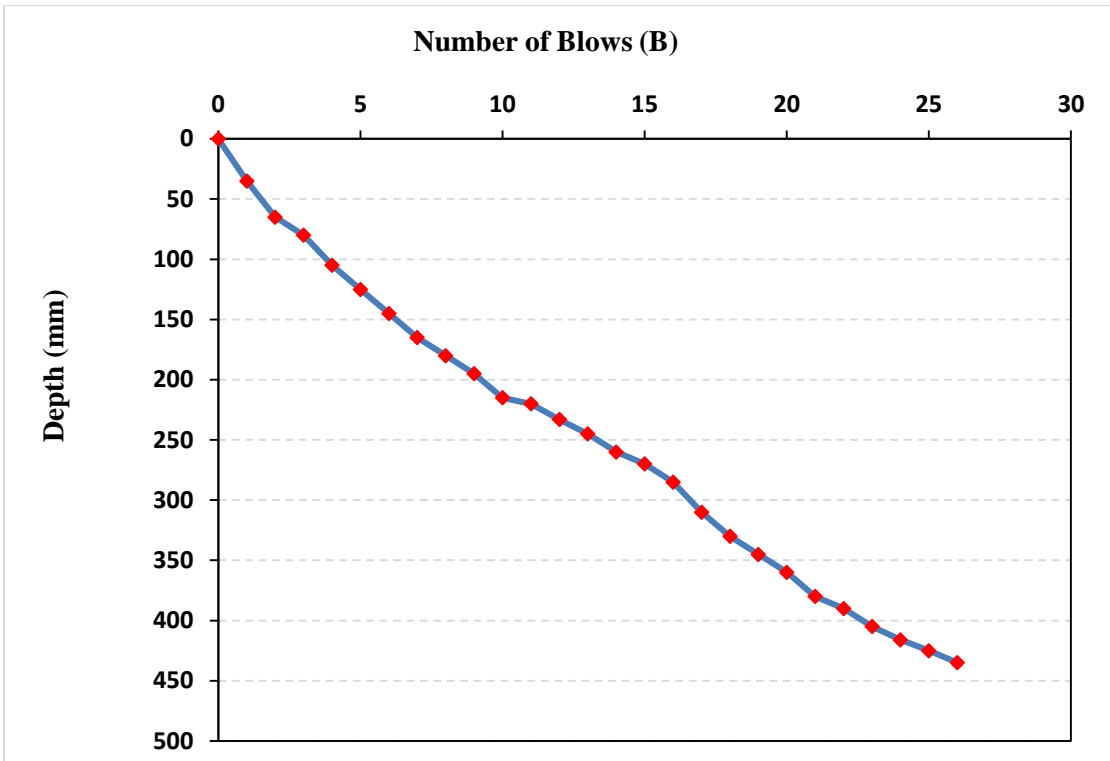


Figure (3.1): Number of blows verse the depth of DCP (No. of passing 18)

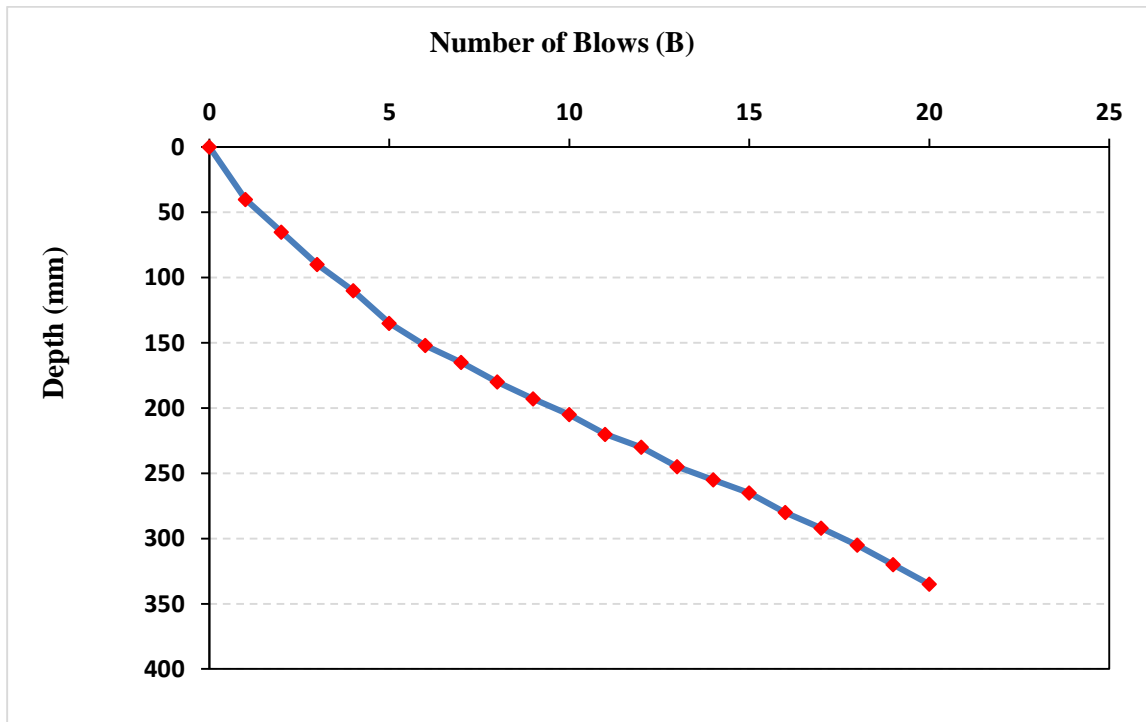


Figure (3.2): Number of blows verse the depth of DCP (No. of passing 18)

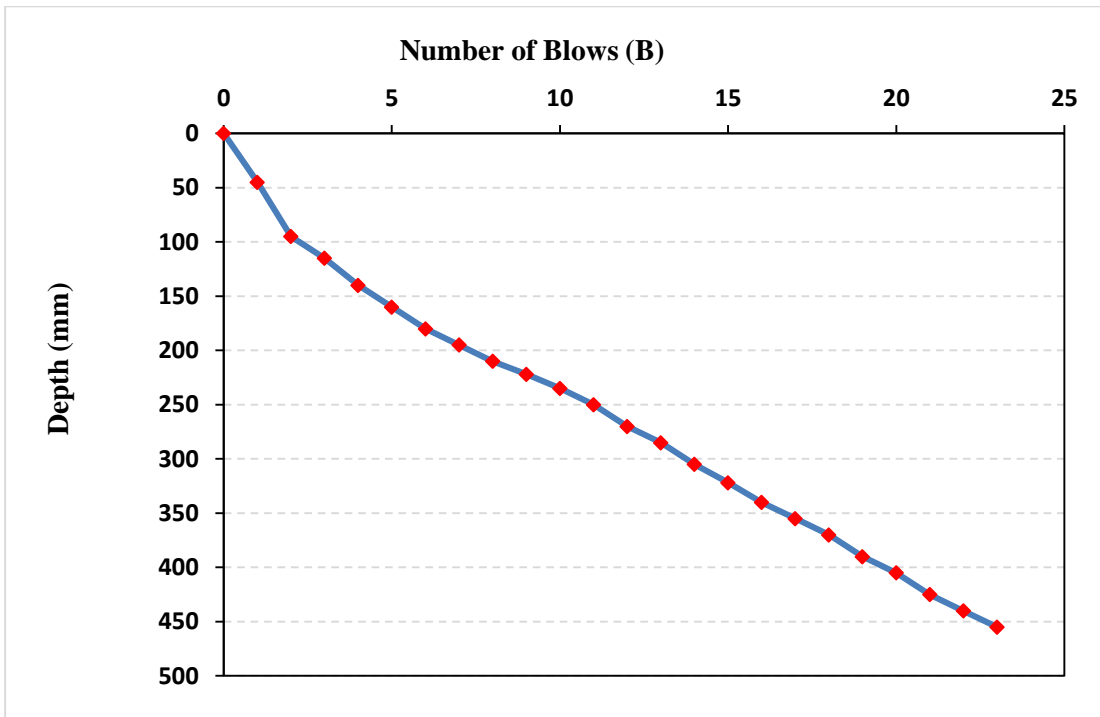


Figure (3.3): Number of blows verse the depth of DCP (No. of passing 18)

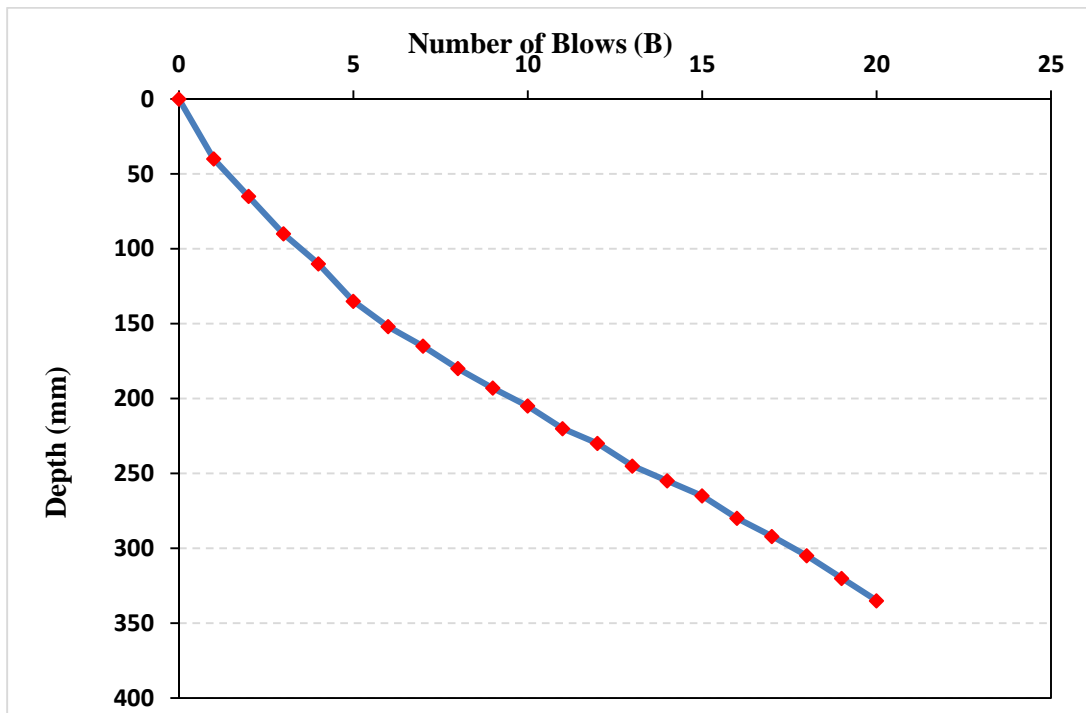


Figure (3.4): Number of blows verse the depth of DCP (No. of passing 18)

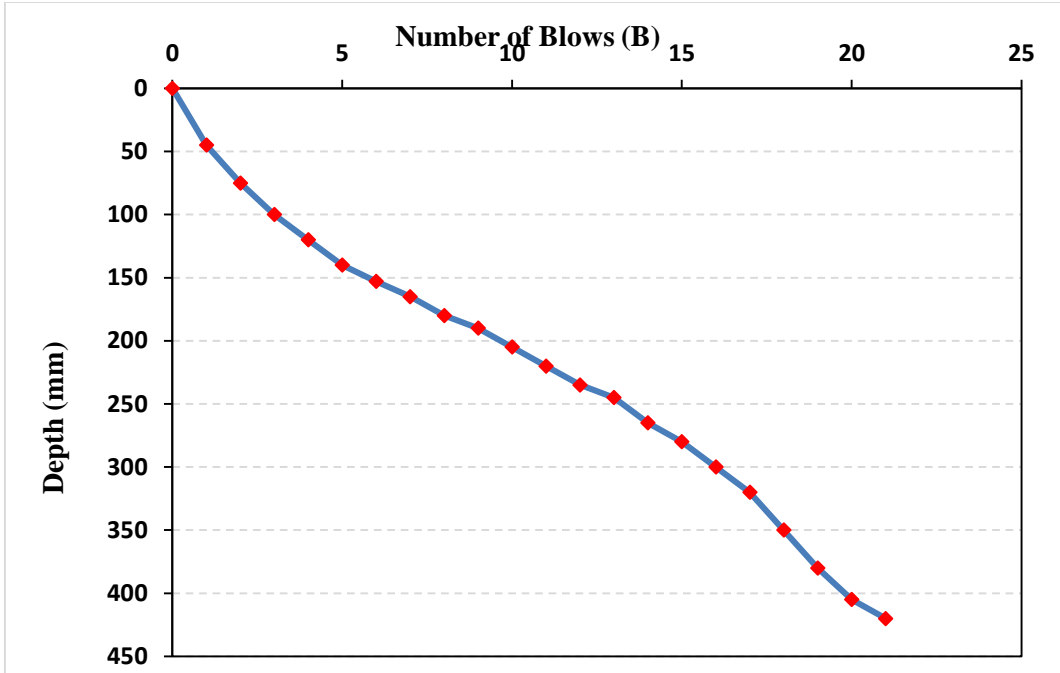


Figure (3.5): Number of blows verse the depth of DCP (No. of passing 18)

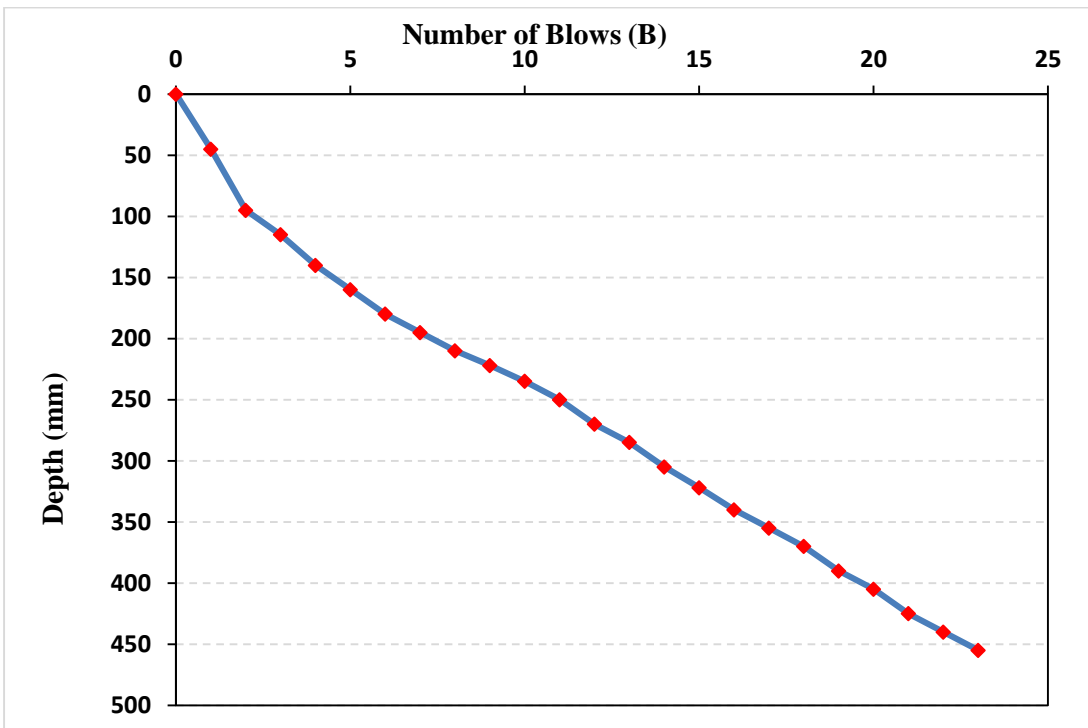


Figure (3.6): Number of blows verse the depth of DCP (No. of passing 18)



## الخلاصة

تعتبر طبقات التربة السفلية جزء مهم في طبقات رصف الطرق، حيث تنتقل جميع الأحمال المرورية عبر التربة من خلال طبقات التربة السفلية. إضافة الى إنه توفر دعماً رئيسياً لهياكل الأساسات واستقرار والتعليقات الترابية. في الوقت الحاضر، تلجأ معظم وكالات الطرق السريعة الدولية إلى استخدام تقنيات الفحص الائتلافية الموقعية لتحديد خصائص طبقات رصف الطرق. ومع ذلك، لا تزال تقنيات الاختبار هذه لا تحظى بشعبية في العراق، في حين أن جميع الهيئات ودوائر الطرق في المحلية تعتمد فقط على الفحوصات المخبرية التقليدية لتقييم جودة مواد الرصف.

لذلك، هناك ضرورة لاستخدام فحوصات أكثر فاعلية يمكن اعتبارها بمثابة اختبار مراقبة الجودة لقوة مواد الرصف. الهدف الرئيسي من هذه الرسالة هو تطوير بروتوكول اختبار بديل يتضمن استخدام القياسات الديناميكية لتقييم مستوى الحدل في الموقع وقوة طبقات الرصيف لطبقة التربة السفلية من خلال حساب الكثافة الجافة نسبة التحمل الكاليفورني.

في هذا العمل، تم استخدام ثلاثة طرق للاختبار لثلاثة أنواع مختلفة من تربة الاساس: اختبار فحص الهطول خفيف الوزن لتقدير الخصائص الديناميكية لتربة طبقة الاساس، ومقياس الاختراق المخروطي الديناميكي لحساب مقاومة الاختراق الديناميكي للتربة واختبار فحص الكثافة الجافة ومحتوى الرطوبة. حيث تم اختيار ثلاثة مشاريع للطرق السريعة في كربلاء لاختبار تربة الاساس.

موقع الانتفاضة، وموقع الفارس، وموقع التحدي حيث كانت التربة في هذه المواقع الثلاث عبارة عن تربة رملية) نوع (A-3). تم الحصول على ثلاثة قياسات ديناميكية من فحص الهطول خفيف الوزن: الهبوط السطحي بقيم تتراوح بين (0,383-0,701) ملم، ودرجة الحدل مع قيم تتراوح بين (2,936-4,25) مللي ثانية، ومعامل المرونة الديناميكي بقيم تتراوح (60,04-38,18) ميجا باسكال. أيضاً، تم الحصول على متغيرين من فحص الاختراق المخروطي الديناميكي: مؤشر اختراق الديناميكي بقيم تتراوح بين (15,89-25,833) ملم / ضربة، نسبة التحمل الكاليفورني في الموقع بقيم تتراوح (19,206-8,77) % . بالإضافة إلى ذلك ، الكثافة الجافة بقيم تتراوح بين (1,698-1,01) جم / سم<sup>3</sup>، ومحتوى الرطوبة بقيم تتراوح بين (7.514-7.887) %.

تم إجراء التحليل الإحصائي في مجموعتين: الكثافة الجافة ونسبة التحمل الكاليفورني بالنسبة لمجموعة الكثافة الجافة، تم تطوير ثلاث مجموعات من معادلات الارتباط الرياضية بناءً على المتغيرات المستقلة: بيانات قياسات اختبار فحص الهطول خفيف الوزن وبيانات قياسات الاختراق المخروطي الديناميكي وبيانات قياسات كل من اختبار فحص الهطول خفيف الوزن مقياس الاختراق المخروطي الديناميكي.

في المجموعة الأولى، تم إجراء العديد من معادلات ارتباط غير خطية للتنبؤ بالكثافة الجافة كدالة للاختبار فحص الهطول خفيف الوزن. أظهرت النتائج أن هناك علاقة جيدة بين الكثافة الجافة وقياسات فحص الهطول خفيف الوزن في المجموعة الثانية، تم تطوير مجموعة من معادلات ارتباط غير الخطي وكان معامل الارتباط 0,88 للتنبؤ بالكثافة الجافة كدالة لقياسات الاختراق المخروطي الديناميكي في المجموعة الثالثة تم استخدام كل من معامل اختبار فحص الهطول خفيف الوزن ومؤشر المخروط الديناميكي وكان معامل الارتباط لهما 0,84.

بالإضافة إلى ذلك، في المجموعة الثانية؛ تم تطوير ثلاث مجموعات من نماذج الانحدار بناءً على متغيرات مستقلة: بيانات قياسات فحص الهطول خفيف الوزن، وخصائص التربة الأساسية، وكلا من فحص الهطول خفيف الوزن وخصائص التربة الأساسية. في المجموعة الأولى، تم إجراء العديد من نماذج الانحدار غير الخطي للتنبؤ بالقوة كدالة لقياسات فحص الهطول خفيف الوزن وكان معامل الارتباط بقيمة 0,89. أظهرت النتائج أيضاً علاقة مقبولة بين قياسات القوة وقياسات فحص الهطول خفيف الوزن في المجموعة الثانية، تم تطوير نموذج الانحدار غير الخطي وكان معامل الارتباط بقيمة 0,90 للتنبؤ بالقوة كدالة لخصائص التربة الأساسية (الكثافة الجافة، محتوى الماء). في المجموعة الثالثة، تم استخدام كل من معامل فحص الهطول خفيف الوزن والكثافة الجافة لتطوير النموذج النظري غير الخطي وكان معامل الارتباط بقيمة 0,86.

أخيراً، أظهرت نتائج هذه الدراسة كفاءة وإمكانية استخدام القياسات الديناميكية (جهاز اختبار فحص الهطول خفيف الوزن وجهاز مقياس الاختراق الديناميكي) بسرعة وسهولة للتنبؤ بكثافة وقوة تربة الاساس.



جمهورية العراق  
وزارة التعليم العالي والبحث العلمي  
جامعة كربلاء  
كلية الهندسة  
قسم الهندسة المدنية

## استخدام القياسات الديناميكية لتقييم قوة ودرجة حدل طبقات التربة تحت الطرق

رسالة مقدمة الى قسم الهندسة المدنية جامعة كربلاء وهي جزء من متطلبات الحصول على درجة الماجستير في الهندسة المدنية (الهندسة المدنية)

من قبل:

ندى عامر يوسف

بكالوريوس في علوم الهندسة المدنية لسنة (٢٠١٧ - ٢٠١٨)  
بإشراف

أ.م.د. علاء محمد جواد هادي  
م.د. رائد رحمان المحنا